



The molecular interplay of proteins expressed in the sexual stages and the induction of gamete formation in the malaria parasite *Plasmodium falciparum*

Molekulare Wechselwirkungen in den Sexualstadien exprimierter Proteine und die Induktion der Gametenbildung im Malariaerreger *Plasmodium falciparum*

Doctoral thesis
for a doctoral degree at the Graduate School of Life Sciences,
Julius-Maximilians-Universität Würzburg
Section “Infection and Immunity”

submitted by
Andrea Kühn

from
Schwerin

Würzburg 2013

Supervisory Committee

Chairperson: Prof. Dr. Thomas Hünig
Primary supervisor: PD Dr. Gabriele Pradel
Second supervisor: Prof. Dr. Klaus Brehm
Third supervisor: Dr. Oliver Billker

Date of Thesis Submission:

Affidavit

I hereby confirm that my thesis entitled "The molecular interplay of proteins expressed in the sexual stages and the induction of gamete formation in the malaria parasite *Plasmodium falciparum*" is the result of my own work. I did not receive any help or support from commercial consultants. All sources and / or materials applied are listed and specified in the thesis.

Furthermore, I confirm that this thesis has not been submitted as part of another examination process neither in identical nor in similar form.

Place, Date

Signature

Eidesstattliche Erklärung

Hiermit erkläre ich an Eides statt, die Dissertation "Molekulare Wechselwirkungen in den Sexualstadien exprimierter Proteine und die Induktion der Gametenbildung im Malariaerreger *Plasmodium falciparum*" eigenständig, d.h. insbesondere selbständig und ohne Hilfe eines kommerziellen Promotionsberaters angefertigt und keine anderen als die von mir angegebenen Quellen und Hilfsmittel verwendet zu haben.

Ich erkläre außerdem, dass die Dissertation weder in gleicher noch in ähnlicher Form bereits in einem anderen Prüfungsverfahren vorgelegen hat.

Ort, Datum

Unterschrift

Table of contents

1	Introduction	1
1.1	The tropical disease malaria	1
1.1.1	Epidemiology of malaria	1
1.1.2	Pathogenesis and symptomatology	2
1.2	<i>Plasmodium falciparum</i> , transmitting agent of malaria tropica	3
1.2.1	Systematics	3
1.2.2	The life cycle of <i>P. falciparum</i>	3
1.3	The sexual phase of the life cycle	5
1.3.1	Gametocyte formation	5
1.3.2	Gametocyte morphology	7
1.3.3	Gametogenesis	7
1.3.4	Signal transduction during gametogenesis	8
1.4	Sexual stage-specific proteins	9
1.4.1	Adhesion proteins of the sexual parasite stages	9
1.4.2	Multimeric protein complexes of the sexual stages of <i>P. falciparum</i>	15
1.4.3	Transmission blocking vaccines	16
1.5	WD40-motif proteins	18
1.5.1	The WD40-motif	18
1.5.2	The WD40 motif-containing protein PfWLP1	18
1.6	Invasion and motility of <i>P. falciparum</i>	19
1.6.1	Morphology of invasion stages	19
1.6.2	Motility of invasive stages is mediated by an actin-myosin motor complex	20
1.7	Transport across the red blood cell membrane	23
1.7.1	Red blood cell-owned transporter systems	23
1.7.2	Parasite induced modifications to the red blood cell	25
1.8	Aim of the PhD thesis	26

2	Materials and Methods	28
2.1	Materials	28
2.1.1	Technical equipment	28
2.1.2	Consumable supplies	30
2.1.3	Chemicals	31
2.1.4	Enzymes and Kits	37
2.1.5	Media and buffers for cell biological methods	38
2.1.6	Media and buffers for molecular biological methods	40
2.1.7	Media and buffers for protein biochemical methods	42
2.1.8	Bacteria strains and cell lines	44
2.1.9	Antibodies and antisera	45
2.1.10	Oligonucleotides	48
2.1.11	PlasmoDB gene identifiers	55
2.1.12	Plasmids	56
2.1.13	DNA- and protein ladders	56
2.1.14	Computer programs and online tools	57
2.2	Cell biological methods	57
2.2.1	Culturing of <i>Plasmodium falciparum</i>	57
2.2.2	Monitoring parasite growth via Giemsa-stained blood smears and test for exflagellation	59
2.2.3	Gametocyte purification	60
2.2.4	Transfection of <i>Plasmodium falciparum</i>	60
2.2.5	Obtaining clones via limiting dilution and detection of clones by Malstat assay	61
2.2.6	Indirect Immunofluorescence Assay	62
2.2.7	Transmission electron microscopy	63
2.2.8	Exflagellation assays	64
2.3	Molecular biological methods	65
2.3.1	Polymerase chain reaction	65
2.3.2	Agarose gel electrophoresis	67

2.3.3	Subcloning of PCR products	68
2.3.4	Purification of PCR products and gel purification of vectors	68
2.3.5	Preparative restriction digest	69
2.3.6	Ligation	69
2.3.7	Transformation of <i>E. coli</i>	69
2.3.8	Analysis of transformants	70
2.3.9	Isolation of plasmid DNA	70
2.3.10	Determination of DNA concentration	71
2.3.11	DNA Sequencing	71
2.3.12	RNA isolation	73
2.3.13	cDNA synthesis and RT-PCR	74
2.3.14	Southern Blot	76
2.3.15	Isolation of genomic DNA	78
2.3.16	Cultivation and storage of bacteria	78
2.4	Protein biochemical Methods	79
2.4.1	Expression of recombinant proteins	79
2.4.2	Isolation of inclusion bodies	80
2.4.3	SDS-PAGE	81
2.4.4	Co-immunoprecipitation	81
2.4.5	Western Blot analysis	82
2.4.6	Generation of antisera via immunization of mice	83
2.5	Entomological methods	83
2.5.1	Rearing of <i>Anopheles stephensi</i>	83
2.5.2	Infection of <i>Anopheles stephensi</i>	84
2.6	Mass spectrometry	84
3	Results	85
3.1	Reverse genetics studies on PfCCp5 and PFFNPA	85
3.1.1	Verification of modified gene loci	85
3.1.2	Phenotype analyses of genetically modified parasites	88
3.2	Co-dependent expression of sexual stage-specific proteins	91

3.2.1	Analysis of co-dependent expression via indirect IFA	91
3.2.2	Analysis of co-dependent expression via RT-PCR	93
3.3	Studies on the IMC of <i>P. falciparum</i> gametocytes	94
3.3.1	Transcript analysis of genes encoding components of the IMC	94
3.3.2	Ultrastructural study on IMC composition	95
3.3.3	Generation of anti-PfmyoA antiserum	96
3.3.4	Indirect IFAs investigating presence of PV and IMC	97
3.4	Characterization of PfactinII	98
3.4.1	Expression of PfactinII throughout the life cycle of <i>P. falciparum</i>	99
3.4.2	Co-dependent expression of PfactinII and Pfs230	101
3.4.3	Modifications of the pfactinII locus via single crossing-over homologous recombination	105
3.5	Characterization of the WD domain containing protein PfWLP1	108
3.5.1	Generation of anti-PfWLP1 antiserum	108
3.5.2	Expression of PfWLP1 throughout the life cycle of <i>P. falciparum</i>	110
3.5.3	Modifications of the pfwlp1 locus via single crossing-over homologous recombination	112
3.6	Induction of gametogenesis	114
3.6.1	Interaction of XA with non-infected RBCs	114
3.6.2	Uptake of XA by non-infected RBCs	115
3.6.3	Inhibitors of RBC transport pathways	119
3.6.4	Effect of alterations of RBC membrane composition on XA uptake and gametogenesis	126
3.6.5	Influence of ionophores on induction of gamete formation	129
3.6.6	Reverse genetics study on XA receptor candidate genes	131
3.6.7	Ultrastructural investigations of gametocyte activation	133
4	Discussion	139
4.1	Surface proteins of sexual stages of <i>Plasmodium falciparum</i>	139
4.1.1	Expression of PfCCp proteins	139
4.1.2	Co-dependent expression of PfCCp proteins and other sexual stage-specific proteins	141

4.1.3	Interactions of sexual-stage adhesion proteins	142
4.1.4	Potential role of PfCCp-based multimeric protein complexes	144
4.2	The inner membrane complex of gametocytes and cytoskeleton proteins	145
4.2.1	Molecular composition of the inner membrane complex of gametocytes	145
4.2.2	Expression of myosin isoforms in <i>P. falciparum</i> gametocytes	147
4.3	Characterization of PfactinII	148
4.3.1	Expression of PfactinII	148
4.3.2	Interaction of Pfs230 and PfactinII	149
4.3.3	Possible functions of PfactinII	150
4.4	Gametocyte activation and egress	151
4.4.1	Induction of gametogenesis by xanthurenic acid	151
4.4.2	Reverse genetics study on XA receptor candidate genes	153
4.4.3	Influence of ionophores on gametocyte activation	154
4.4.4	Ultrastructural investigations of gametocyte activation	155
4.4.5	Conclusions	156
5	Summary	158
6	Zusammenfassung	160
7	References	162
8	Appendix	196
8.1	Vector maps	196
8.2	Substances employed in exflagellation assays	198
8.3	Parameters used in LC/ESI/MS/MS analyses	200
8.4	Indirect IFAs investigating co-dependent expression	202
8.5	Abbreviations	206
8.6	Curriculum Vitae	210
8.7	Acknowledgements	212

1 Introduction

1.1 The tropical disease malaria

1.1.1 Epidemiology of malaria

The tropical disease malaria represents one of the most devastating infectious diseases of the world. Despite partial success in combating malaria there are still more than 3.3 billion people living at risk of an infection which accounts to almost half of the world's population. According to the latest World Malaria Report of the World Health Organization (WHO, 2012a), an estimated 219 million clinical cases occurred in 2010 and 660 000 people died. More than 100 countries are endemic for malaria, however more than 80% of reported cases occurred in sub-Saharan Africa (Fig. 1.1). Young children are most vulnerable for the disease. Malaria has been reported to be the third most frequent cause of death in children younger than five years world-wide (Liu *et al.*, 2012; Black *et al.*, 2010). About 86% of malaria-caused death cases were found in this age group in 2010 (WHO, 2012a). The causative agents of malaria are protozoan parasites of the genus *Plasmodium*. There are five different species infecting man: *Plasmodium falciparum*, *Plasmodium vivax*, *Plasmodium ovale*, *Plasmodium malariae* and *Plasmodium knowlesi*. The latter was known to infect monkeys and was only recently identified as a human pathogen (White, 2008; reviewed in Cox-Singh, 2012). Most malaria cases are due to infection with *P. falciparum* and/or *P. vivax*.

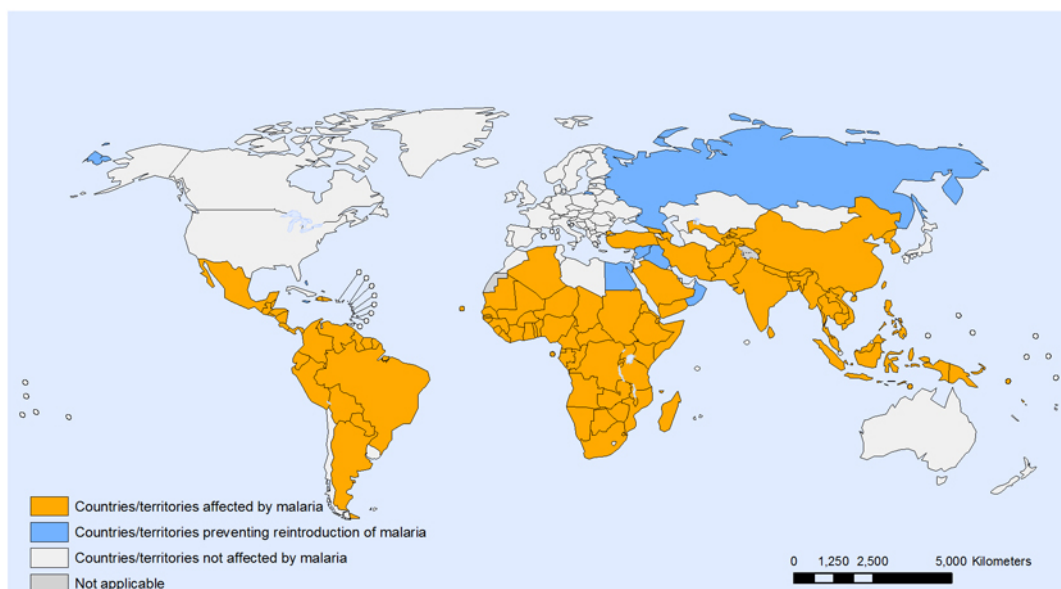


Fig. 1.1: Countries and territories affected by malaria in 2010 (WHO, 2012b).

In the past six years the goal shifted from malaria control to malaria elimination and eradication (Roberts and Enserink, 2007; Feachem *et al.*, 2010; Moonen *et al.*, 2010; Tanner and Hommel, 2010; Tatem *et al.*, 2010; reviewed in Alonso *et al.*, 2011). Thus, funding committed to malaria prevention, treatment and research increased (Roll Back Malaria Partnership, 2008; Alonso and Tanner, 2013). However, from 2010 onwards, a stagnation was observed (Alonso and Tanner, 2013). Beside the human burden of malaria in endemic countries, malaria also represents an enormous economical burden (reviewed in Kokwaro, 2009). It is estimated that African countries spend up to 40% of their health budget on malaria control and treatment. Families of highly endemic regions lose up to 25% of their income due to sickness of malaria (reviewed in Kokwaro, 2009). Thus, it is of uttermost importance to further improve malaria prevention and control to continue approaching the goal of malaria eradication.

1.1.2 Pathogenesis and symptomatology

Upon infection with a malaria parasite, the first symptoms can be observed after a minimum of seven days for *P. falciparum*, nine days for *P. vivax*, ten days for *P. ovale* and 15 days for *P. malariae*. At the beginning of an infection unspecific symptoms like headache, myalgia or faintness dominate. In general, symptoms associated with malaria are for instance fever, chills, sweating, dyspnea, arthralgia, headache, myalgia, abdominal pain, dizziness, diarrhea, nausea, and vomiting (da Silva-Nunes and Ferreira, 2007; Karunaweera *et al.*, 1998). If untreated, the infection will commonly result in anemia, thrombocytopenia, splenomegalie and mild icterus. In the case of severe malaria organ dysfunctions, respiratory distress, pulmonary edema and coma can be observed (WHO, 2000). Originally only described in *P. falciparum*, the number of cases of severe malaria in *P. knowlesi* and *P. vivax* is increasing (Daneshvar *et al.*, 2009; Singh *et al.*, 2011; Lacerda *et al.*, 2012; Willmann *et al.*, 2012).

A key player during infection of *P. falciparum* is the protein PfEMP1 (*P. falciparum* erythrocyte membrane protein 1) which is expressed on the surface of the infected erythrocyte. PfEMP1 locates to knob-like electron dense structures. It mediates adherence of the parasite-infected red blood cell (RBC) to the vascular endothelium via endothelial receptors such as ICAM1 (intercellular adhesion molecule 1) and CD36 (cluster of differentiation 36) (reviewed in Miller *et al.*, 2002 and Miller *et al.*, 2013). Binding of PfEMP1 to CD36 and other receptor proteins expressed on uninfected RBCs results in rosetting, the formation of aggregates of parasitized and uninfected RBCs. Aggregate formation between infected RBCs and platelets mediated via binding of PfEMP1 to C36 is referred to as clumping (reviewed in Miller *et al.*, 2002). Sequestration of infected RBCs to the endothelium, aggregate formation as well as induction of coagulation and thrombosis via adhering infected RBCs block the blood flow in the microvasculature resulting in limited oxygen supply to organs. The consequences are organ damage and

failure in heart, lung, brain, liver, kidney and subcutaneous tissues that can result in coma and deaths of the patient (reviewed in Miller *et al.*, 2002). In pregnant woman sequestration of parasitized RBCs to the placenta is a major risk factor to the unborn child. Adherence is mediated mainly via chondroitin sulfate A and often results in premature delivery, low birth weight and an increased risk of death of the newborn, (reviewed in Miller *et al.*, 2002).

1.2 *Plasmodium falciparum*, transmitting agent of malaria tropica

1.2.1 Systematics

Plasmodium spp. are unicellular eukaryotes. They belong to the phylum Alveolata. The organisms of this taxum possess a pellicle of trilaminar appearance consisting of the plasma membrane and cortical vesicles (alveoli). The taxum is divided into three subgroups, Dinoflagellata, Ciliophora and Apicomplexa, the latter comprising the family of Plasmodiidae. Apicomplexa are characterized by the apical complex which is located at the anterior cell pole and is formed by several organelles. The five *Plasmodium* spp. infecting humans belong to different clades (Ayala *et al.*, 1999). Whilst *P. falciparum* belongs to the subgenus *Lavaranina*, the other four species have been assigned to the sub-genus *Plasmodium* (Bray, 1963; Garnham, 1964).

1.2.2 The life cycle of *P. falciparum*

The malaria parasite is transmitted by female mosquitoes of the genus *Anopheles*. More than 30 different vector species are known (Kiszewski *et al.*, 2004). The infectious sporozoites reside in the salivary glands of the mosquito. During a blood meal of the mosquito sporozoites are injected with the saliva into the human host. The parasites migrate through the avascular skin and finally invade a blood vessel (Matsuoka *et al.*, 2002; Vanderberg and Frevert, 2004; Amino *et al.*, 2008). Via the blood system the sporozoites reach the liver where they leave the sinusoid capillaries. They glide along the sinusoidal epithelium and traverse Kupfer cells or fenestrated endothelial cells to cross the space of Disse (Pradel und Frevert, 2001; Frevert *et al.*, 2005; Baer *et al.*, 2007; Taveres *et al.*, 2013). After reaching the liver parenchyma parasites traverse several hepatocytes before they finally invade a hepatocyte (Mota *et al.*, 2001; Frevert *et al.*, 2005). During invasion a parasitophorous vacuole (PV) is formed, which separates the parasite from the host cytosol. Subsequently the parasites multiply via exo-erythrocytic schizogony. From one liver schizont up to 30 000 merozoites are derived (Meis and Verhave, 1988). Upon parasite-induced rupture of the PV membrane (PVM) merozoites are released into the liver sinusoid within merozoites, vesicles derived from the host cell

plasma membrane (Sturm *et al.*, 2006; reviewed in Wirth and Pradel, 2012). After the merozoites were liberated from the merozoite membrane they invade RBCs. Within the RBC the parasites are again surrounded by a PV which is formed during invasion. The parasites first develop into ring stages. Thereafter, parasites enter a metabolically highly active phase, the trophozoite stage, in which parasites rapidly increase in size (Gabay and Ginsburg, 1993). Via erythrocytic schizogony the parasites multiply again and up to 32 merozoites evolve from one schizont (Fig. 1.2). Already few hours after invasion of the RBC the parasites synthesize adhesion proteins which are expressed on the RBC surface. These proteins mediate cytoadhesion. The parasitized cells attach to endothelial walls, to other parasitized cells (autocoagulation) as well as to non-parasitized RBCs (rosetting). This so-called sequestration of elder trophozoites and schizonts results in perturbation of circulation and finally may lead to a severe outcome of the disease due to organ damage (see 1.1.2). Beside sequestration another important factor contributing to pathogenesis is the release of inflammatory substances. This occurs during parasite-induced rupture of a mature schizont.

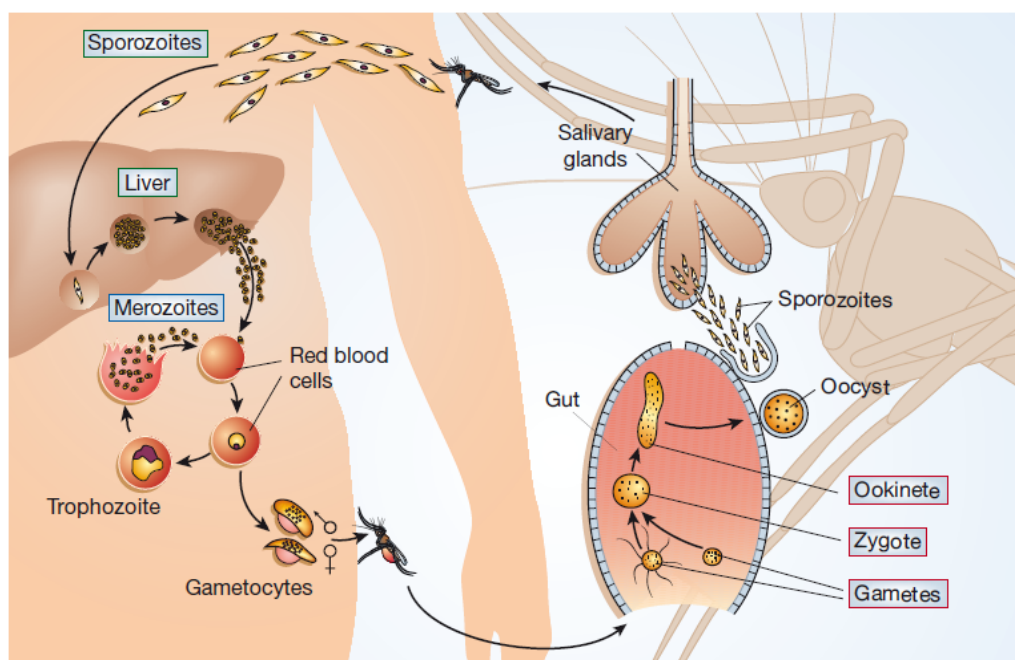


Fig. 1.2: Schematic of the life cycle of *P. falciparum* (Ménard, 2005).

The merozoites that are released into the blood subsequently invade a new RBC. After several rounds of asexual replication a proportion of parasites will differentiate and enter the sexual phase of the life cycle (see 1.3). The sexual development starts with the formation of male and female gametocytes within the RBC. When these are taken up by a mosquito during its blood meal, the gametocytes are able to percept the change of surrounding conditions (see 1.3.3). This will trigger them to form male and female gametes that subsequently undergo fertilization. The resulting diploid zygote undergoes meiotic

division and becomes tetraploid. It further develops into a motile ookinete (Janse *et al.*, 1986). The ookinete passes the peritrophic matrix which surrounds the blood meal and also traverses the midgut epithelium. Between midgut epithelium and basal lamina the ookinete settles down to form an oocyst. Within the oocyst up to 10 000 haploid sporozoites develop. These then make their way to the salivary glands. The sporozoites invade the distal lateral lobes and the median lobes (Carter and Graves, 1988). During the next blood meal of the mosquitoes the sporozoites are prepared to infect another human when they are injected with the saliva.

1.3 The sexual phase of the life cycle

1.3.1 Gametocyte formation

Gametocytes are the parasite stage that enables transmission of the parasites from human host to the insect vector. The formation of gametocytes is thus crucial for ensuring the continuation of the life cycle in the mosquito. At the same time, parasites pass through a population bottleneck during the sexual phase of the life cycle. Of approximately 10 000 gametocytes taken up during a blood meal, only 1 000 ookinetes are formed and only 1 to 5 parasites develop into oocysts (Fig. 1.3) (Sinden, 1999; Sinden and Billingsley, 2001; Sinden, 2010). In the past years gametocytes raised the interest of malaria research due to their importance for transmission of the disease. The comparably small parasite numbers of gametocytes as compared to the billions of asexual blood stage parasites rendered them an attractive target for intervention strategies (see 1.4.3).

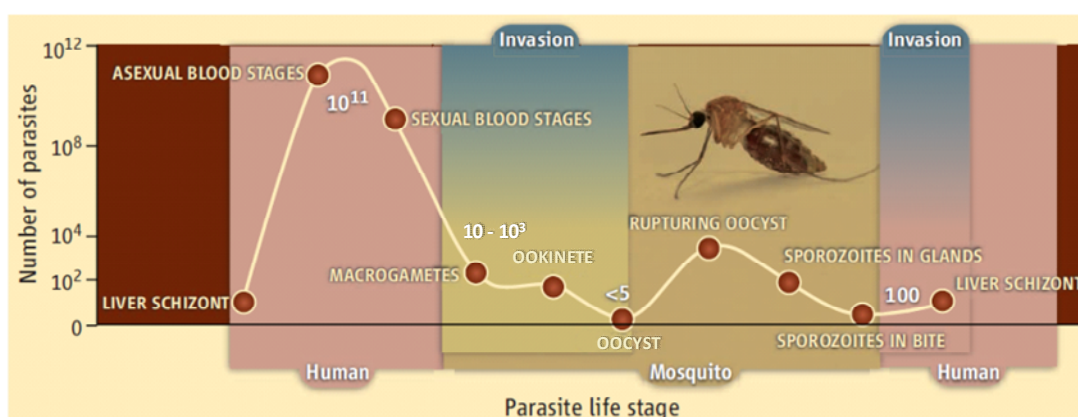


Fig. 1.3: Dynamics of parasite population in the course of the life cycle. Both the development from gametocyte to oocyst and the transmission of sporozoites to the human host during a mosquito's bite are considered life cycle bottlenecks (adapted from Vogel, 2010; Sinden, 2010).

In *P. falciparum*, the formation of sexual parasite stages is induced only after several cycles of asexual replication. Several factors have been discussed to induce the formation of gametocytes, the sexual precursor cells. These factors have in common that they

would negatively influence the development of the parasites within the human host (Stephens and Christophers, 1908). Examples for such stress factors are for instance high parasitaemia, drug treatment, anemia or immune response of the host (reviewed in Talman *et al.*, 2004; Baker, 2010). The molecular background of induction of gametocytogenesis remains unsolved, however some genes that seem to influence gametocyte formation have been reported (Eksi *et al.*, 2012; reviewed in Guttery *et al.*, 2012).

The determination of parasites to enter sexual development has been postulated to occur in the schizont stage (Bruce *et al.*, 1990). All merozoites released from such schizont will develop into gametocytes of the same gender (Smith *et al.*, 2000; Silvestrini *et al.*, 2000; reviewed in Dixon *et al.*, 2008). Male and female gametocytes undergo five stages of sexual development (Field and Shute, 1956; Hawking *et al.*, 1971). The development of gametocytes of *P. falciparum* into mature stage V gametocytes takes approximately 8 to 12 days (Fig. 1.4) (Sinden, 1982; Sinden, 1998; reviewed in Liu *et al.*, 2011). Only from stage IV onwards genders can be discriminated (reviewed in Talman *et al.*, 2004). Stage I–IV gametocytes are not circulating in the blood vessel, but instead are sequestered. In early studies bone-marrow and spleen had been discussed as site of gametocyte sequestration (Thompson, 1935; Smalley *et al.*, 1981). A recent study suggested the sequestration of stage II–IV gametocytes in the extravascular space of the bone marrow (Farfour *et al.*, 2012). After approximately 10 days of maturation the mature stage V gametocytes leave the bone marrow and circulate in the peripheral blood where they can be taken up by a mosquito during its blood meal (Eichner *et al.*, 2001; reviewed in Bousema and Drakeley, 2011).

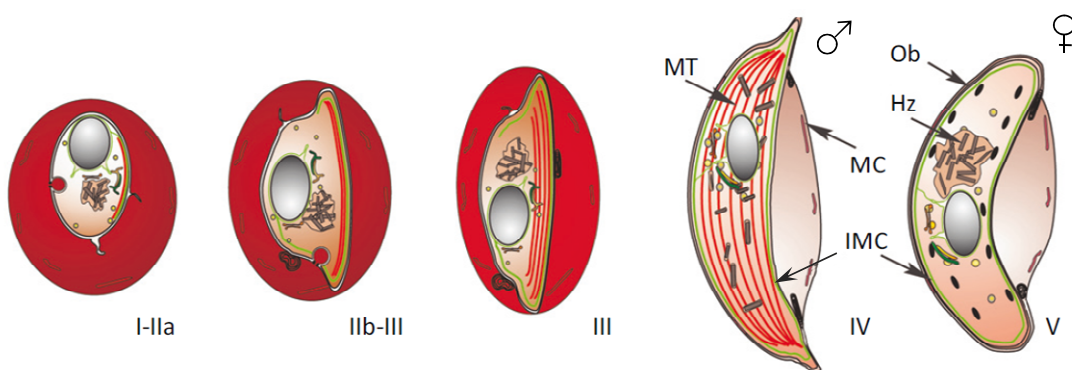


Fig. 1.4: Schematic of gametocyte morphogenesis in *P. falciparum*. The young stage I–IIa gametocyte is spherical and difficult to distinguish from asexual parasites via light microscopy. Stage IIB gametocytes elongate and exhibit a D-shape. Stage IV gametocytes have undergone further elongation and appear spindle-like. Stage V gametocytes show the typical crescent-like shape. Hz, hemozoin, IMC, inner membrane complex (subpellicular membrane complex), MC, Maurer's clefts, MT longitudinal microtubules; Ob, osmiophilic bodies (adapted from Dixon *et al.*, 2012).

1.3.2 Gametocyte morphology

Gametocytes of *P. falciparum* show the typical crescent shape, of which the name of this species was derived from (Lavaran, 1880). On the contrary, gametocytes of all other malaria parasites infecting humans are spherical. After Giemsa staining female gametocytes appear blue whilst male gametocytes turn pink. The female macrogametocyte shows a small nucleus with a nucleolus and concentrated malaria pigment. Microgametocytes on the other hand possess a larger nucleus with no visible nucleolus. The hemozoin is distributed more diffusely in the male gametocyte. Female stage V gametocytes contain a network of rough endoplasmatic reticulum (ER) and numerous ribosomes – prerequisite for protein biosynthesis upon gametocyte activation (Sinden, 1982). Numerous oval shaped electron dense vesicles can be found underneath the surface of macrogametocytes (Fig. 1.4) (Severini *et al.*, 1999). These organelles are termed osmiophilic bodies and can be found in male gametocytes as well, however in much lower abundance (Sinden, 1982). Osmiophilic bodies play a crucial role in egress of the macrogametocytes (see 1.4.1) (de Koning-Ward *et al.*, 2008). Microgametocytes possess a microtubule organizing center and kinetochores attached to the chromosomes, thus being prepared for rapid mitosis upon gametocyte activation (reviewed in Liu *et al.*, 2011). Gametocytes of both genders possess one branched mitochondrion and one apicoplast (Okamoto *et al.*, 2009). Gametocytes possess a pellicule comprising three layers of membrane: the plasma membrane and the flattened subpellicular membrane vacuoles, which are lined by longitudinally oriented microtubules (Fig. 1.4) (Sinden, 1982).

1.3.3 Gametogenesis

In the mosquito midgut two factors are perceived by the gametocytes that lead to induction of gamete formation within 15 seconds (Billker *et al.*, 1998). The first factor is the drop in temperature by at least 5 degrees (Sinden; 1983, Carter and Graves, 1988; Sinden *et al.*, 1996). The second triggering factor is the mosquito-derived molecule xanthurenic acid (XA) (Billker *et al.*, 1998, Garcia *et al.*, 1998) which is a byproduct of the ommochrome synthesis pathway (Beard *et al.*, 1995) and can be found ubiquitously in the mosquito body. *In vitro*, XA can be replaced by a pH of 8.0-8.2 in the surrounding medium, instead of the physiological pH of 7.4 found in the blood (Sinden, 1983, Nijhout and Carter, 1978).

After induction of gametogenesis gametocytes round up and egress from their host cells. Male gametocytes undergo three rounds of DNA replication and endomitotic division (Janse *et al.*, 1988) followed by exflagellation of the newly developed microgametes. During this process eight flagella-shaped microgametes detach from the residual body of the microgametocyte by means of fast pulsating movements. The moving microgametes adhere to neighboring infected and uninfected erythrocytes, as well as to macro-

gametes (Templeton *et al.*, 1998). Approximately 10 min after gametocyte activation the formation of microgametes is completed (Billker *et al.*, 1998). The process of exflagellation is believed to promote egress of microgametes. The mechanisms underlying egress of the amotile macrogamete in contrast are so far widely unknown. Within approximately 20 min after gametocyte activation fertilization has been completed and development of the zygote has started (Carter *et al.*, 1979).

1.3.4 Signal transduction during gametogenesis

Several signal molecules and enzymes have been identified that are involved in signal transduction controlling gamete formation (Fig. 1.5). Most information has been gained on the formation of male gametes due to the fact, that the formation of the motile microgametes can be investigated microscopically more easily as compared to formation of macrogametes. Three secondary messengers are involved in the signaling cascade resulting in gamete formation: cGMP (Kawamoto *et al.*, 1990; Kawamoto *et al.*, 1993), Ca^{2+} (Kawamoto *et al.*, 1990) and inositol 1,4,5-triphosphate (IP_3 , Ogwan'g *et al.*, 1993; Martin *et al.*, 1994). Upon gametocyte activation the cytosolic Ca^{2+} concentration increases as early as 10 sec after activation (Billker *et al.*, 2004). Recently, ryanodine receptors have been reported to be involved in the increase of Ca^{2+} concentration (Raabe *et al.*, 2011). Furthermore, the activation of gametocytes results in hydrolysis of phosphatidylinositol 4,5-bisphosphate (PIP_2) into diacylglycerol (DAG) and IP_3 by a membrane-associated phosphoinositide phospholipase C (PI-PLC) (Martin *et al.*, 1994). The activation of PI-PLC occurs both via Ca^{2+} and upstream of the Ca^{2+} signal (Elabbadi *et al.*, 1994; Raabe *et al.*, 2011). Thus, a positive feedback loop is probable. In response to the increase of cytosolic Ca^{2+} concentration the Calcium-dependent protein kinase CDPK4 is activated (Billker *et al.*, 2004; Ranjan *et al.*, 2004). In the rodent malaria agent *P. berghei* CDPK4 has been shown to mediate genome replication and mitosis in microgametocytes (Billker *et al.*, 2004). As a possible substrate of CDPK4 the mitogen-activated protein kinase Map-2 has been suggested. Map-2 is essential for axoneme motility, DNA condensation and cytokinesis in the developing microgametes (Tewari *et al.*, 2005). Independently of the Ca^{2+} signal a membrane-associated guanylate cyclase is activated upon induction of gametogenesis via XA and the temperature drop (Muhia *et al.*, 2001). The guanylate cyclase mediates the formation of cGMP. Increased cytosolic cGMP levels activate the protein kinase G which induces rounding up of gametes of both sexes (McRobert *et al.*, 2008). The cGMP signal is terminated by the PDE δ in *P. falciparum*, which returns the cGMP levels to the basal level. After gamete formation and fertilization two protein kinases, Pbnk-2 and Pbnk-4, have been described to induce genome replication in the zygote, resulting in a tetraploid genome (Khan *et al.*, 2005; Reininger *et al.*, 2005; Reininger *et al.*, 2009). Despite the knowledge of several

components of the XA-induced signal pathway the molecular details on how XA and the reduction of temperature are perceived by the parasite remain elusive.

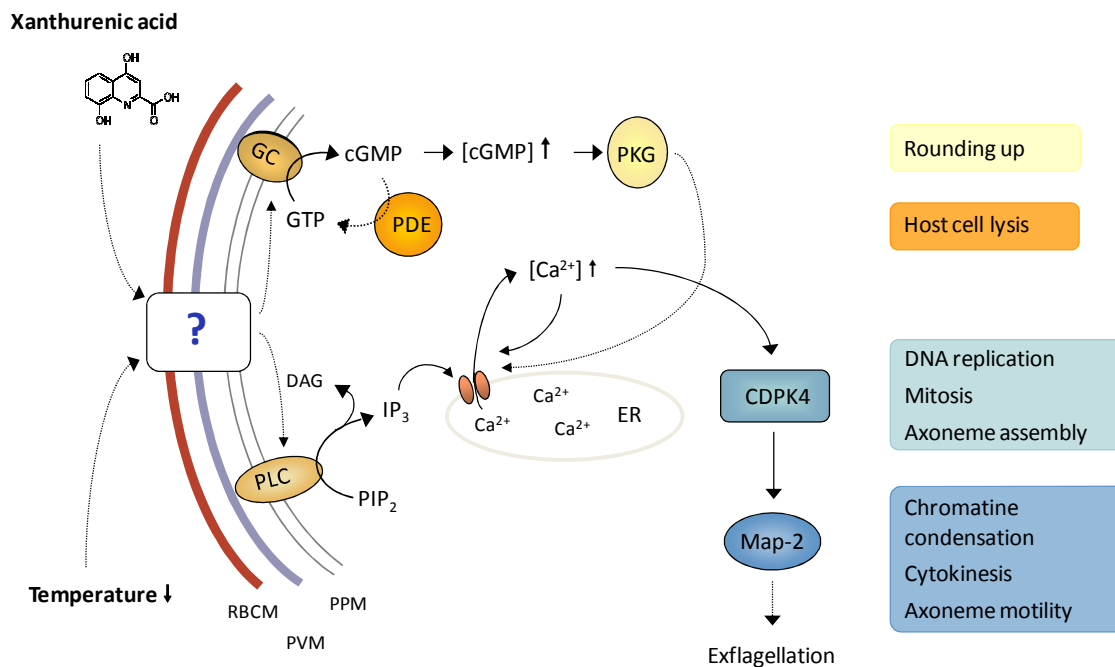


Fig. 1.5: Schematics of the signaling pathway culminating in gametogenesis. Activation of male gametocytes is initiated in the mosquito midgut by xanthurenic acid and the decreased temperature. It leads to formation of male gametes via exflagellation. The signal mediated by XA has to cross three membranes from the exterior to the gametocyte cytosol. GC, guanylate cyclase; PDE, phosphodiesterase; PKG, protein kinase G; PLC, phospholipase C; PPM, parasite plasma membrane; PVM, parasitophorous vacuole membrane; RBCM, red blood cell membrane (Adapted from Tewari *et al.*, 2005; Kuehn and Pradel, 2010).

1.4 Sexual stage-specific proteins

1.4.1 Adhesion proteins of the sexual parasite stages

In order to prepare for the switch from the human to the mosquito host the malaria parasite expresses a large number of genes specifically during the sexual phase (reviewed in Pradel, 2007). More than 40% of blood stage proteins are present exclusively in gametocytes (Khan *et al.*, 2005). Above several regulatory proteins governing developmental processes during the sexual phase were described (see 1.3.4). Adhesion proteins are another group of proteins of great importance for the sexual stages as they ensure communication with the changing environment. Sequencing of the genome of *P. falciparum* (Gardner *et al.*, 2002) as well as analyses of the proteome (Florens *et al.*, 2002; Lasond-er *et al.*, 2002) enabled the identification of so far uncharacterized proteins comprising putative adhesion motifs and signal peptides. These tools of the postgenomic era for

instance revealed the PfCCp protein family (Pradel *et al.*, 2004). These and other sexual-stage adhesion proteins are described in the following:

The PfCCp protein family

The members of the PfCCp protein family are characterized by their protein structure comprising multiple adhesion domains. Five of the proteins, PfCCp1 to PfCCp5 possess an LCCL (Limulus coagulation factor C-like) domain which gave rise to the name of the protein family (Fig. 1.6) (Pradel *et al.*, 2004). A sixth protein was included, despite lacking the LCCL domain, due to its structural similarity to PfCCp5. In *P. berghei* the protein family was described under the term PbLAP protein family (LCCL-lectin adhesive-like proteins) (Trueman *et al.*, 2004; Raine *et al.*, 2007). Beside the LCCL domain the proteins contain multiple protein motifs the adhesive properties of which have been well described in other organisms (reviewed in Kuehn *et al.*, 2010).

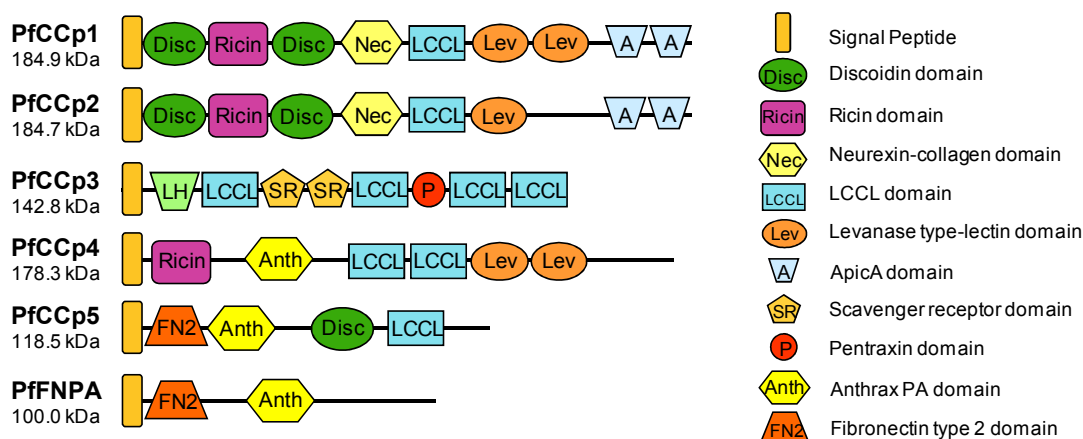


Fig. 1.6: Schematic depicting the domain structure of the PfCCp proteins that comprise multiple adhesion domains (modified from Kuehn *et al.*, 2010).

The expression of the *pfccp* genes is restricted to sexual parasite stages. It starts in gametocytes of stage II and increases with gametocyte maturation. Upon gametogenesis and zygote formation the expression ceases (Pradel *et al.*, 2004; Scholz *et al.*, 2008). PfCCp1, PfCCp2 and PfCCp3 show a punctuate expression pattern and localize to the gametocyte surface in association with the plasma membrane (Fig. 1.7) (Pradel *et al.*, 2004). PfCCp5 and PffFNPA are localized at the cell poles (Scholz *et al.*, 2008). In contrast to all other PfCCp proteins, *pfccp5* is not only expressed in sexual parasite stages, but also in schizonts (Pradel *et al.*, 2004; Scholz *et al.*, 2008). PfCCp4 is already present in gametocytes of stage I. It is distributed homogeneously and remains associated with the gamete surface after gametogenesis (Fig. 1.7) (Scholz *et al.*, 2008). On the contrary, for PfCCp1 to PfCCp3 it has been shown that they are shed to some extent during gamete formation (Pradel *et al.*, 2004). The study of PfCCp2- and PfCCp3-deficient parasites suggested a role of the proteins in parasite development in the mosquito vector.

Whilst development of the mutant parasites until formation of oocyst sporozoites was comparable to wild-type parasites, the transition of sporozoites from the oocyst to the salivary glands was disturbed (Pradel *et al.*, 2004). PfCCp4 on the other hand seems to be dispensable for the development in the mosquito (Scholz *et al.*, 2008).

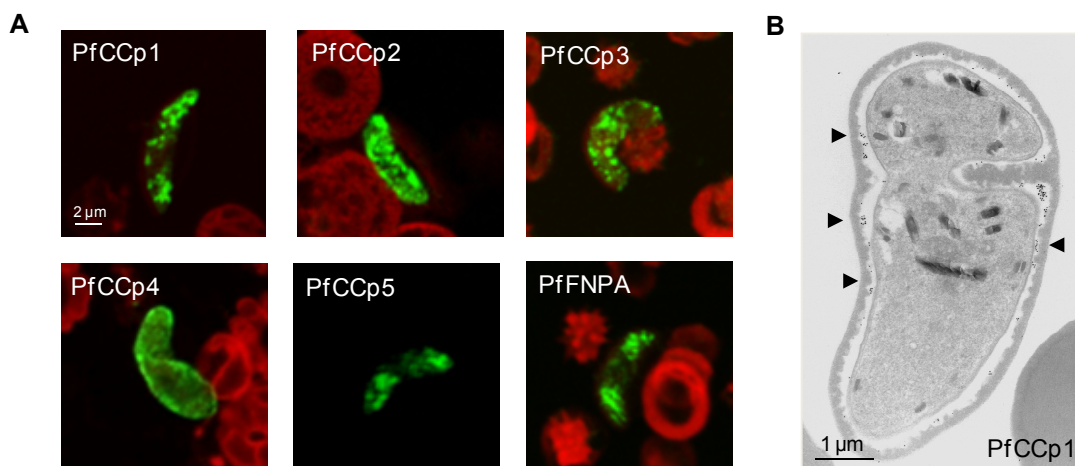


Fig. 1.7: **A.** Expression pattern of PfCCp proteins in mature gametocytes. Erythrocytes were counterstained with Evans Blue. **B.** Electron micrograph of immunogold-labeled PfCCp1 (arrow heads). (Panel B from Pradel *et al.*, 2004).

The 6-Cys protein family

The 6-Cys protein family comprises ten proteins characterized by the possession of one to seven cysteine-rich double domains (Templeton und Kaslow, 1999; Gerloff *et al.*, 2005). Eight of the genes encoding the 6-Cys proteins are arranged in tandems on the same chromosome, respectively. It is assumed that the paralogs were formed via gene duplication events (Thompson, J. *et al.*, 2001). The protein family is unique to and well conserved in *Plasmodium* spp. (Templeton and Kaslow, 1999; Thompson, J. *et al.*, 2001). All proteins comprise a signal peptide (Templeton and Kaslow, 1999; Sanders *et al.*, 2005; Ishino *et al.*, 2005; Gerloff and al., 2005). Four genes encoding members of the protein family are exclusively transcribed in gametocytes. These genes encode the proteins Pfs48/45, Pfs47, Pfs230 and Pfs230p (also termed PfsMR5) (summarized in van Dijk *et al.*, 2010). The most prominent proteins of this protein family are Pfs48/45 and Pfs230 which have been described as candidates for the generation of transmission blocking vaccines almost three decades ago (see 1.4.3) (Rener *et al.*, 1983; Vermeulen *et al.*, 1985).

Pfs230 is the largest protein of the 6-Cys protein family. It possesses 7 cysteine-rich double domains and has a molecular weight of 360 kDa. It is present in gametocytes from stage II onwards and localizes to the outer leaflet of the gametocyte plasma membrane (Vermeulen *et al.*, 1986). Expression persists until the gamete stage. During gametocyte activation the protein is proteolytically cleaved (Williamson *et al.*, 1996; Brooks and Williamson, 2000). Pfs230 is a hydrophilic, secreted protein. It forms a sta-

ble complex with Pfs48/45 which is covalently bound to the gametocyte surface via a glycosyl-phosphatidyl inositol (GPI) anchor (Kumar, 1987; Kumar and Wize, 1992). Pfs230-deficient parasite mutants form gametocytes and gametes comparably to wild-type parasites. However, male gametocytes are not able to attach to RBCs, thus the formation of exflagellation centers is dramatically reduced. The formation of oocysts in the midgut is also strongly impeded (Eksi *et al.*, 2006). In the rodent parasite *P. berghei* on the contrary, exflagellation center formation is not affected in the absence of Pfs230. There, reduced binding of microgametes to female gametes was observed resulting in a dramatically reduced fertilization rate (van Dijk *et al.*, 2010).

PfsMR5 (also called Pfs230p) is located on chromosome 2 upstream of its paralog Pfs230. With a molecular weight of 293 kDa and only 6.5 cysteine-rich double domains it is smaller than Pfs230 (Fig. 1.8). Highest transcript levels of *pfsmr5* were detected in gametocytes of stage III and IV. The protein is present exclusively in male stage V gametocytes (Eksi and Williamson, 2002). Expression ceases rapidly after gametocyte activation. Only three minutes after induction of gametogenesis the protein is not detectable anymore. In contrast to Pfs230 PfsMR5 does not show an obvious peripheral expression pattern, although it possesses a signal for secretion of the protein. It has thus been suggested that it might locate to intracellular vesicles (Eksi and Williamson, 2002). The gene encoding the *P. berghei* ortholog of PfsMR5, termed P230p, was disrupted and the P230p deficient mutants did not show alterations in gametocyte formation, gametogenesis or fertilization rate as compared to wild-type parasites (van Dijk *et al.*, 2010).

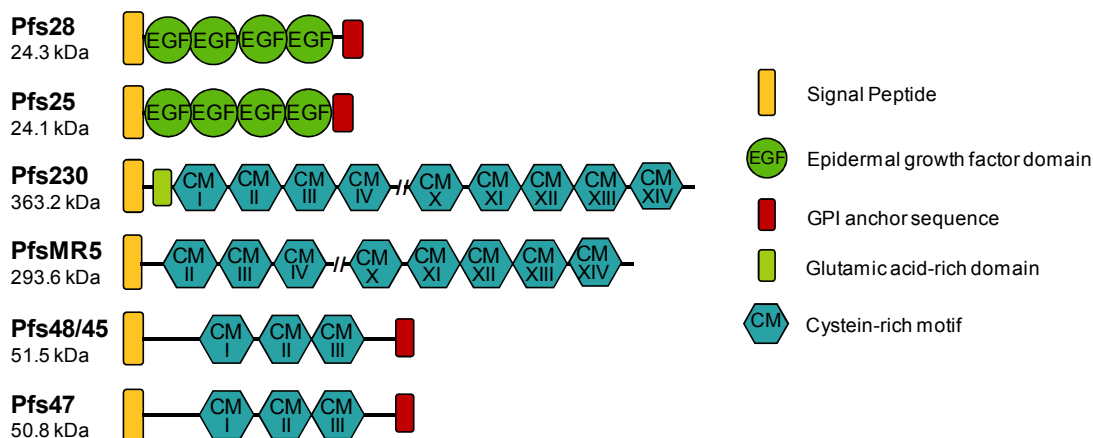


Fig. 1.8: Schematic of the EGF-like domain containing proteins Pfs25 and Pfs28 and the cysteine-rich motif proteins Pfs230, PfsMR5, Pfs48/45 and Pfs47 (modified from Kuehn *et al.*, 2010).

Pfs48/45 possesses 1.5 cysteine-rich double domains (van Dijk *et al.*, 2001). Its expression starts in gametocytes of stage II and persists until the gamete stage. Pfs48/45 is covalently bound to the parasite surface via a GPI anchor (Vermeulen *et al.*, 1986;

Kocken *et al.*, 1993). The study of Pfs48/45-deficient parasites showed that Pfs48/45 is important for fertility of male gametes. While the protein is dispensable for gametocyte and gamete formation, the microgametocytes are unable to attach to and fuse with macrogametes (van Dijk *et al.*, 2001). The orthologous protein in *P. berghei* seems to have the same function (van Dijk *et al.*, 2001). The lack of Pfs48/45 and Pbs45/48 resulted in a dramatically reduced infectivity to the mosquito, respectively (van Dijk *et al.*, 2001).

In contrast to its paralog, Pfs47 is expressed exclusively in female gametocytes. Its transcription starts between gametocyte stage II and III and increases from stage IV onwards (van Schaijk *et al.*, 2006). After gamete formation it can be found on the surface of the macrogamete. In parasites deficient for Pfs47 gametocyte formation, sex ratio and gametogenesis were comparable to wild-type parasites (van Schaijk *et al.*, 2006). In *P. falciparum* the protein does not play a role during fertilization, ookinete development or oocyst development (van Schaijk *et al.*, 2006). In contrast, in *P. berghei* female gametes are infertile. It has been suggested that Pbs47 is essential for attachment of microgametes (van Dijk *et al.*, 2010).

The EGF-like domain containing proteins Pfs25 and Pfs28

Likewise the proteins of the protein family around Pfs230, Pfs25 and Pfs28 are arranged as tandem on chromosome 10 (Duffy and Kaslow, 1997). Both paralogous proteins possess four epidermal growth factor (EGF)-like domains, an N-terminal signal peptide and a GPI anchor sequence, respectively, that links the proteins to the parasite plasma membrane (Kaslow *et al.*, 1988). The EGF-like domain can be found in many proteins of animals, in particular in the extracellular parts of membrane proteins. In many cases it has been reported to play important roles in protein-protein interactions (reviewed in Appella *et al.*, 1988). Both Pfs25 and Pfs28 are conserved in *Plasmodium* spp. For better inter-species comparisons they are termed P25 and P28 as suggested by Tomas *et al.* (2001).

Pfs25 is located on the surface of gametes, zygotes and ookinetes and can also be detected in lower abundance in mature gametocytes (Vermeulen *et al.*, 1985; 1986). In gametocytes the protein is concentrated in intracellular vesicles (Scholz *et al.*, 2008). Only after gametocyte activation the protein is transported to the gamete cell surface as shown for the rodent parasite *P. berghei* (Billker *et al.*, 1997). After fertilization the expression is dramatically increased (Vermeulen *et al.*, 1985). Pfs28 is also present on zygote stages, however it is mainly found on retort stages and ookinetes (Duffy and Kaslow, 1997). Expression of both Pfs25 and Pfs28 is transcriptionally regulated. The mRNA of the proteins is already present in gametocytes, however translation is only initiated upon gametocyte activation (Paton *et al.*, 1993; Mair *et al.*, 2006). Translational repression is mediated by the binding of mRNAs by the RNA helicase DOZI (development of zygote inhibited) and CITH (CAR-I/Trailer Hitch Homolog) which are part

of a messenger ribonucleoprotein particle located in the cytoplasm (Mair *et al.*, 2006; 2010).

The crystal structure of Pvs25, the Pfs25 ortholog in *P. vivax*, was determined to have a triangular shape. It is assumed that P25 covers the parasite surface in a tile-like manner (Saxena *et al.*, 2006). This is in agreement with the study of P25/P28 double knockout in *P. berghei* which suggested a role in protection from hostile midgut factors (Tomas *et al.*, 2001). Furthermore, a role in oocyst formation (Sidén-Kiamos *et al.*, 2000; Tomas *et al.*, 2001) and in crossing of the midgut epithelium has been postulated for P25 and P28 (reviewed in Baton and Randford-Cartwright., 2005). Yeast two hybrid assays revealed both the formation of P25 homodimers and the formation of P25-P28 heterodimers (Sidén-Kiamos *et al.*, 2000). P25 proteins of *P. vivax* and *P. berghei* interact with midgut proteins (Arrighi *et al.*, 2002; Rodriguez *et al.*, 2007; reviewed in Saxena *et al.*, 2007).

Pfg377

Pfg377 is a gametocyte-specific protein which is associated with the osmiophilic bodies in a membrane-bound form (Alano *et al.*, 1995). The osmiophilic bodies are characteristic for maturing macrogametocytes (see 1.3.2), and thus, Pfg377 is found predominantly in female gametocytes of stage III–V (Severini *et al.*, 1999). As the osmiophilic bodies are detectable only from stage IV onwards, a role of Pfg377 in formation or maturation of these organelles has been proposed (Rudzinska und Trager, 1968; Severini *et al.*, 1999). The study of Pfg377-deficient parasites provided evidence, that the protein is critical for the formation of osmiophilic bodies (de Koning-Ward, 2008). It is anticipated that osmiophilic bodies secrete their content upon gametocyte activation (Aikawa *et al.*, 1984; Alano *et al.*, 1995) and the presence of osmiophilic bodies is important for egress of macrogametocytes and macrogamete formation (de Koning-Ward *et al.*, 2008). Pfg377 possesses a signal peptide, which together with the subsequent 60 amino acids is sufficient to target the protein to the osmiophilic bodies (Sannella *et al.*, 2012).

Pfpeg3/Pfmdv-1

As for reported for Pfg377, the expression of Pfpeg3 (*P. falciparum* protein of early gametocytes), also referred to as Pfmdv-1, (*P. falciparum* male development gene 1) is restricted to gametocytes. The expression of Pfpeg3, however starts in gametocytes of stage I already, at approximately 30–40 h upon invasion of the RBC (Carter *et al.*, 1989; Alano *et al.*, 1991; Silvestrini *et al.*, 2005). Pfpeg3 locates to the PVM and membrane systems derived from the PVM like the food vacuole and cleft like structures in the RBC cytosol (Silvestrini *et al.*, 2005; Furuya *et al.*, 2005; Lanfrancotti *et al.*, 2007). In Pfpeg3-deficient parasites several membrane structures showed a disturbed appearance (Furuya *et al.*, 2005). In *P. berghei* the protein was shown to localize to osmiophil-

ic bodies of macrogametocytes (Ponzi *et al.*, 2009). The protein plays an important role in egress of both macro- and microgametocytes, however detailed information on its mechanism of action is missing (Furaya *et al.*, 2005; Lal *et al.*, 2009; Ponzi *et al.*, 2009).

Pfs16

Pfs16 is expressed in gametocytes of stage I–V and its expression starts approximately six hours earlier than Pfpeg3 (Bruce *et al.*, 1994). It is a transmembrane protein of the PVM (Baker *et al.*, 1994; Bruce *et al.*, 1994). It co-localizes with Pfpeg3 in the PVM and PVM-derived membranes as well as in cleft-like membrane structures of the gametocyte-infected RBC (Lanfrancotti *et al.*, 2007).

1.4.2 Multimeric protein complexes of the sexual stages of *P. falciparum*

The gametocyte proteome contains a vast number of secreted proteins as assumed from the prediction of signal peptides from their amino acid sequence. Only few of them possess a GPI anchor sequence that would ensure retention of the proteins to the parasite surface. This observation as well as the fact that several of the supposedly secreted proteins possess predicted adhesion domains, lead to the assumption that various protein-protein interactions occur at the sexual stage parasite surface.

Likewise to the proteins of the PfCCp protein family Pfs230 is a hydrophilic secreted protein. Hence, it was assumed that it is retained to the parasite surface via interacting with other proteins attached to the parasite plasma membrane (Kumar, 1985). Indeed, a stable protein complex is formed between Pfs230 and the GPI-anchored Pfs48/45 (Kumar, 1987; Kumar and Wizek, 1992). In Pfs48/45-deficient gametocytes Pfs230 localizes to the parasite surface as it is the case in wild-type parasites. However, in Pfs48/45-deficient gametes Pfs230 was detected in low abundance in a rather vesicular distribution (Eksi *et al.*, 2006). The presence of Pfs48/45 therefore seems to be essential for correct localization of Pfs230 after gametocyte egress.

It has been shown that almost all proteins of the PfCCp protein family are interacting with each other (Wagner *et al.*, 2006; Simon *et al.*, 2009). Furthermore, select proteins interact with the sexual stage-specific proteins Pfs25, Pfs230 and Pfs48/45 (Scholz *et al.*, 2008; reviewed in Kuehn *et al.*, 2010). PfCCp1 to PfCCp3 are co-localizing at the plasma membrane of gametocytes (Pradel *et al.*, 2006). Interestingly, the proteins of the PfCCp protein family are expressed in a co-dependent manner. This is reflected in such way, that in mutants with a single *pfccp* gene disrupted, all PfCCp proteins are absent or detectable only in low amounts. As the transcription of *pfccp* genes is not affected in these mutants, an interdependency on translational or post-translational level is assumed (Pradel *et al.*, 2006; Simon *et al.*, 2009).

Recently, a so far uncharacterized protein has been identified as potential component of the multi-protein complex comprising the PfCCp proteins. In co-immunoprecipitation assays on gametocyte lysate followed by mass spectrometry a WD40-domain containing protein has been detected as interaction partner of PfCCp1 (see 1.5.2) (Simon, 2012).

1.4.3 Transmission blocking vaccines

The transmission of the malaria parasites from the human host to insect vector occurs via sexual precursor cells, the gametocytes. However, it is the asexual parasite stages, which are responsible for pathogenesis of malaria. As a consequence antimalarial drugs are targeting asexual blood stage parasites. Gametocytes on the contrary, are rather insensitive to these drugs (Lang-Unnasch and Murphy, 1998; Peatey *et al.*, 2009). Due to this peculiarity of the malaria parasite it is essential to include intervention strategies targeting parasite transmission, when aiming at eradication of malaria. Transmission blocking vaccines (TBV) are considered as a potential tool for malaria elimination. TBVs would induce the production of antibodies in the human that are directed against surface proteins of the mosquito stages gametes, zygotes and ookinetes (reviewed in Stowers and Carter, 2001; Sauerwein 2007; Saul, 2007). Taken up together with the blood meal of the mosquito the antibodies would inhibit parasite development via complement-mediated lysis of parasites or via blocking of essential parasite receptors (reviewed in Stowers and Carter, 2001; Dinglasan and Jacobs-Lorena, 2008). Transmission blocking antibodies have already been described more than three decades ago (Carter and Chen, 1976; Gwadz, 1976). The proteins that were identified first as potential candidates for TBV generation are Pfs230, Pfs48/45 and Pfs25 (Rener *et al.*, 1983; Vermeulen *et al.*, 1985; Quakyi *et al.*, 1987). For antibodies directed against Pfs230 a complement-mediated killing of parasites has been suggested as mechanism responsible for inhibiting parasite development in the mosquito (Read *et al.*, 1994; Williamson *et al.*, 1995). One advantage of the pre-fertilization surface proteins Pfs230 and Pfs48/45 is that they are expressed already in gametocytes in the human host. Therefore, a boosting of the antibody response is possible (reviewed in Cater *et al.*, 2000). Indeed, antibodies directed against Pfs230 and Pfs48/45 are produced during natural infections (Graves *et al.*, 1988; Ong *et al.*, 1990; Mulder *et al.*, 1993, 1994; Premawansa *et al.*, 1994; Healer *et al.*, 1997; Ouédraogo *et al.*, 2011). However, the expression of correctly folded recombinant variants of Pfs230 and Pfs48/45 seems to be difficult. Recently, a wheat germ cell-free system and plant-produced Pfs230 recombinant protein provided new approaches (Williamson *et al.*, 1995; Tachibana *et al.*, 2011; Farrance *et al.*, 2011). The wheat-germ expressed fragment of Pfs230 showed transmission blocking activity even in absence of complement, suggesting an alternative mechanisms of action. For Pfs48/45 expression of a correctly folded recombinant protein has been improved re-

cently by codon-harmonized expression in *Escherichia coli* and the green algae *Chlamydomonas reinhardtii* (Chowdhury *et al.* 2009; Jones *et al.*, 2013).

Most progress has been made with the TBV candidate P25, as yeast expression systems have been shown to be well suited for production of the immunogen. The derived antibodies showed good transmission-blocking activity (Hisaeda *et al.*, 2000, reviewed in Carter 2001). P25 of *P. falciparum* and *P. vivax* have been tested in phase I clinical trials already. Both transmission blocking efficacy and antibody titers were promising (Malkin *et al.*, 2005; Wu *et al.*, 2008; reviewed in Kaslow, 2002). As P25 and P28 have been shown to complement for each other in gene-disruptant parasites a combined vaccine targeting both proteins has been suggested. Membrane feeding assays testing a mixture of antisera directed against both P25 and P28 significantly reduced the oocyst production in the mosquito (reviewed in Stowers and Carter, 2001). One disadvantage of P25 and P28 is that as post-fertilization surface proteins they are only expressed in the mosquito midgut, therefore a boosting of the human antibody response during natural infections is not possible.

More recently, several new candidate proteins have been identified as targets for transmission blocking vaccines. These include the proteins of the above described PfCCp protein family (see 1.4.1). The suitability of the PfCCp proteins has been anticipated as for PfCCp2 and PfCCp3 an essential role for the development in the mosquito had been shown (Pradel *et al.*, 2004). Anti-PfCCp antisera caused a complement-mediated inhibition of microgamete formation *in vitro* (Scholz *et al.*, 2008). The efficacy of anti-PfCCp antibodies on the development in the mosquito remains to be investigated. As PfCCp proteins are expressed on the gametocyte surface in the human host, the formation of natural antibodies boosting the immune response upon vaccination is possible. Further recently discovered *Plasmodium* spp. candidate proteins are the chitinase expressed in ookinetes which is essential for traversal of the peritrophic matrix that surrounds the blood meal. A transmission-blocking efficacy of chitinase-neutralizing antibodies has been shown (Langer *et al.*, 2002; Li *et al.*, 2005). Another protein with an essential role for parasite development in the mosquito is CTRP (circumsporozoite and TRAP related protein) (Dessens *et al.*, 1999; Yuda *et al.*, 1999). The microneme proteins SOAP (secreted ookinete adhesive protein) and MOAP (membrane attack ookinete protein) are essential for invasion of the midgut epithelium (Dessens *et al.*, 2003; Kadota *et al.*, 2004). As the for the PfCCp proteins, the essential function of these surface expressed or secreted proteins renders them attractive as targets of transmission blocking antibodies.

1.5 WD40-motif proteins

1.5.1 The WD40-motif

The WD40 protein domain is one of the ten most abundant types of protein motifs found in eukaryotes (reviewed in Li and Roberts, 2001; Stirnimann *et al.*, 2010; Xu and Min, 2011). It was first described in 1986 in the bovine β -transducin, as part of the trimeric G protein transducin complex (Fong *et al.*, 1986). Typical characteristics of the WD40 motif are a length of 44–60 amino acids, glycine and histidine residues at positions 11–24 of the protein motif and the eponymous tryptophan-aspartic acid (WD) dipeptide at the C-terminus (Fong *et al.* 1986; Neer *et al.*, 1994; Smith *et al.*, 1999). Each WD40 motif folds into a four-stranded antiparallel β -sheet (Wu *et al.*, 2010). The beta-sheets of generally seven neighboring WD40 motifs form a circularized so-called propeller fold that is stabilized via a network of hydrogen bonds (Wu *et al.*, 2010; reviewed in Li and Roberts, 2001; Stirnimann *et al.*, 2010). As there are usually seven or a multiple of seven WD40 domains per protein, they are also referred to as WD40 repeats. WD40 propeller folds are quite large domains providing three surfaces for interactions with other proteins, peptides or DNA: The top region of the propeller, the bottom and the circumference (reviewed in Stirnimann *et al.*, 2010). These multiple interaction sites render the WD40 domain a scaffold for large protein complexes comprising multiple interaction partners. The functions of WD40 domain-containing proteins are manifold and include for instance signal transduction, regulation of transcription, cell division, organization of cytoskeleton and apoptosis (Neer *et al.*, 1994; Smith *et al.*, 1999; Yu *et al.*, 2000; reviewed in Stirnimann *et al.*, 2010; Xu and Min, 2011). Until now, no WD40 protein has been described to possess catalytic function (reviewed in Stirnimann *et al.*, 2010).

1.5.2 The WD40 motif-containing protein PfwLp1

The sexual stages of *P. falciparum* form multimeric protein complexes at the parasite plasma membrane (see 1.4.2). During the search for further components of these protein complexes a so far uncharacterized protein was discovered. Co-immunoprecipitation assays followed by mass spectrometry identified the protein with the PlasmoDB identifier PF3D7_1443400 (formerly PF14_0412) as interaction partner of PfCCp1 and consequently as potential component of the multi-protein complex assembled around PfCCp proteins (Simon, 2012). The protein sequence comprises 819 amino acids and the protein possesses a molecular weight of 95.8 kDa. The search for protein domains with the SMART database revealed that the protein contains 5 WD40 repeat domains (see Fig. 1.9). However, one of them comprises 120 amino acids, thus it is likely that this domain forms three propeller blades consisting of approximately 40 amino acids each. This would result in seven propeller blades in total, as observed in most WD40

motif-containing proteins. Another probability for formation of the stable propeller fold is the supplementation with a propeller blade of an interacting protein (reviewed in Xu and Min, 2011). Due to the possession of the WD40 repeats the so far undescribed protein was named PfWLP1 (WD repeat protein-like protein 1) (Nkwouano Ngongang, 2012).

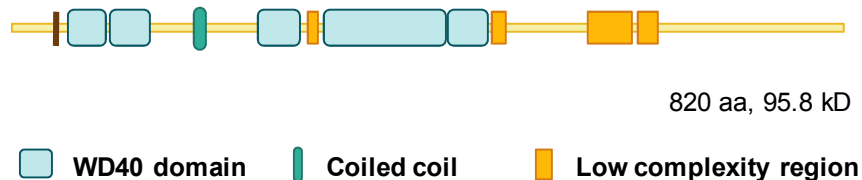


Fig. 1.9: Domain structure of the uncharacterized WD40 repeat-containing protein PfWLP1. The WD40 domains were depicted according to the SMART protein domain database (<http://smart.embl-heidelberg.de/>).

1.6 Invasion and motility of *P. falciparum*

1.6.1 Morphology of invasion stages

During the complex life cycle of *P. falciparum*, the parasites egress from host cells and subsequently invade a next host cell several times. There are three different invasive stages that share most of the morphological features: Merozoites, ookinetes and sporozoites. The invasive parasite stages share with gametocytes in common the possession of the trilaminar pellicle comprising the plasma membrane and flat membrane cisternae. The more or less elongated shape of the invasive stages is determined by an array of microtubules subtending the pellicle. The microtubules emanate from the apical polar rings, representing the microtubule-organizing center (Russel and Burns, 1984). They confer polarity and stability to the parasite, important prerequisites for motility and invasion (Hepler *et al.*, 1966; Stokkermans *et al.*, 1996). Beside the trilaminar pellicle another feature common to all invasive stages of Apicomplexan parasites is the apical complex. It comprises several organelles that play important roles during invasion processes (reviewed in Preiser *et al.*, 2000; Cowman and Crabb, 2006; Baum *et al.*, 2008). The cigar-shaped micronemes secrete their contents including proteases like PfSUB2 and adhesions like PfAMA-1 during host cell invasion (Healer *et al.*, 2002; Harris *et al.*, 2005). The larger club-shaped rhoptries release adhesion proteins like RON4 that are needed for attachment to the host cell and proteins that are important for PV formation like ROM1 (Fig. 1.10) (Richard *et al.*, 2010; Vera *et al.*, 2011). The spherical dense granules secrete their content into the PV, thereby contributing to the establishment of the PV (Culvenor *et al.*, 1991). Another group of vesicles, the exoemes have so far only been described in merozoites. They secrete proteases like PfSUB1, resulting in host cell rupture (Yeoh *et al.*, 2007).

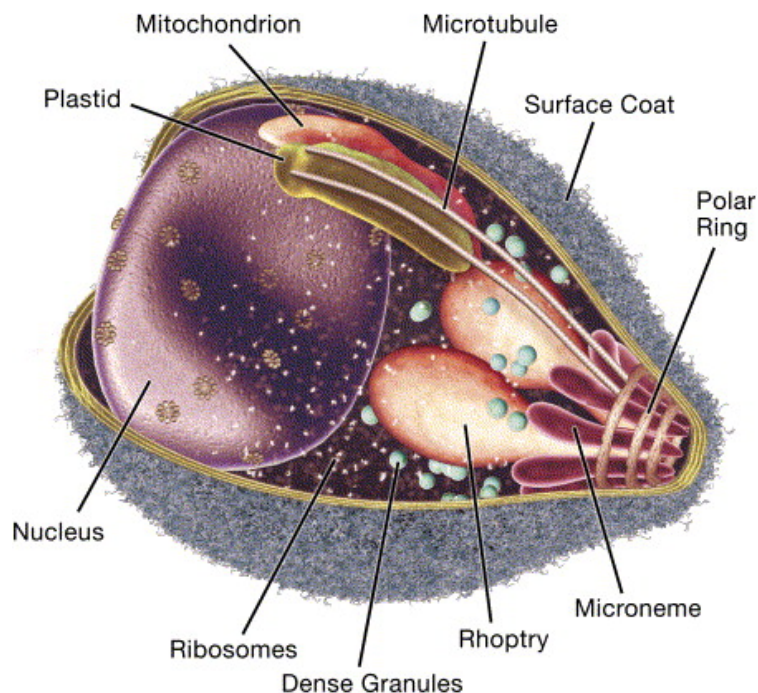


Fig. 1.10: Schematic of a merozoite of *P. falciparum* depicting the most important organelles and cellular structures (Cowman and Crabb, 2006).

Like other Apicomplexan parasites all stages of *P. falciparum* except microgametes possess an apicoplast (Okamoto *et al.*, 2009). This organelle is a relict of a chloroplast, which was achieved via endosymbiosis of a red or green algae (Köhler *et al.*, 1997; McFadden and Waller, 1997; Blanchard and Hicks, 1999; Fast *et al.*, 2001; Funes *et al.*, 2002; Waller *et al.*, 2003). The apicoplast is surrounded by four plasma membranes and possess a circular genome (Lemgruber *et al.*, 2013). The apicoplast genome encodes genes involved in fatty acid and isoprenoid precursor synthesis and is thus indispensable for parasite replication (reviewed in Ralph *et al.*, 2004; McFadden, 2011).

Furthermore, the invasive stages possess the typical eukaryotic cellular organelles, mitochondrion, nucleus and ribosomes (Fig. 1.10). The ER is associated with the nucleus and the Golgi apparatus. Contrary to Golgi apparatuses of higher eukaryotes, in *Plasmodium* spp. it is rather rudimentary consisting of only one or few membrane cisternae and associated vesicles (reviewed in Cooke *et al.*, 2004). The trafficking of proteins via ER and Golgi ensures that secreted proteins and proteins of intracellular organelles are transported to their correct destinations.

1.6.2 Motility of invasive stages is mediated by an actin-myosin motor complex

Gliding on surfaces and host cell invasion are mediated by a molecular motor which is conserved in invasive parasite stages of Apicomplexan parasites. It has been described in detail in sporozoites and merozoites of *Plasmodium* spp. and tachzoites of *T. gondii* (Baum *et al.*, 2006). In ookinetes only few components of the so-called glideosome

have been described so far. The motor complex is located underneath the parasite plasma membrane where it is anchored to the inner membrane complex (IMC), the basis of which are the flat membrane cisternae that are part of the parasite's pellicule. The key components are filamentous actin and class XIV myosin, PfMyoA. Anchoring of PfMyoA to the IMC is mediated by PfMTIP (myosin A tail domain interacting protein) and the glideosome-associated proteins PfGAP45 and PfGAP50 (Fig. 1.11) (Bergman *et al.*, 2003; Baum *et al.*, 2006; Green *et al.*, 2006). The small transmembrane protein family PfGAPM (glideosome-associated protein with multiple membrane spans) has been postulated to connect the membrane cisternae to the cytoskeleton of the parasite via alveolins (Gould *et al.*, 2008; Bullen *et al.*, 2009; Volkmann *et al.*, 2012). The actin filaments are connected via Pfaldo to a transmembrane protein, referred to as invasin, which links the intracellular actin-myosin motor to ligands of the surface of the host cell (Jewett and Sibley, 2003). Several invasins have been described with stage-specific expression. Sporozoites possess both the micronemal proteins PfTRAP (TRAP-like protein) and PFTLP (TRAP-like protein) and PFTREP (TRAP-related protein) (Heiss *et al.*, 2008; Moreira *et al.*, 2008; Combe *et al.*, 2009). The respective protein in merozoites is PfMTRAP and in ookinetes the same role is carried out by PfCTRP (circumsporozoite protein and TRAP related protein) (Baum *et al.*, 2006; Templeton *et al.*, 2000). The forward moving of the parasites is caused by the interaction of MyoA with actin, similar to the sliding-filament model of the skeletal muscles. Upon ATP hydrolysis the head domain of MyoA moves the actin filament which is connected to the host cell receptor rearwards, thereby driving the parasite forward in respect to the host cell surface (reviewed in Baum *et al.*, 2008). Select components of the actin-myosin motor complex are described in more detail:

Actins and actin regulatory proteins of *Plasmodium* spp.

Actin is a globular protein which can form polarized filaments upon polymerization. Actin filament assembly and disassembly is highly dynamic and depends both on ATP binding and hydrolysis as well as on actin regulatory proteins (reviewed in Engel *et al.*, 1977; Carlier, 1990). Several of the regulatory proteins encoded in the genome of *Plasmodium* spp. are orthologous to those of other eukaryotes. Amongst these are for instance the capping protein, which regulates growth of actin filaments and coronin, a WD40-repeat domain protein, which mediates bundling of actin filaments (Tardieux *et al.*, 1998; Gardner *et al.*, 2002; reviewed in Morrissette and Sibley, 2002; Gandhi and Goode, 2008; Cooper and Sept, 2008; Sattler *et al.*, 2011). Several of classical actin regulating proteins are absent in *Plasmodium* parasites, like the Arp2/3 complex which enables branching of actin filaments (Gordon and Sibley, 2005; Mullins *et al.*, 1998). Compared to other eukaryotic organisms actin filaments of *Plasmodium* spp. are rather short, only measuring 150 nm in length (Schmitz *et al.*, 2005, 2010; Schüler *et al.*,

2005). It has been suggested that low polymerizability and short persistence of actin polymers are intrinsic properties of actin proteins of *Plasmodium* spp. (reviewed in Sattler *et al.*, 2011). In contrast to other Apicomplexan parasites *Plasmodium* spp. encode two actin isoforms, termed actinI and actinII (Gordon and Sibley 2005; Wesseling *et al.*, 1988; Gardner *et al.*, 2002). Whilst actinI is expressed in all blood stages (and all invasive stages), expression of actinII is restricted to sexual parasite stages (Wesseling *et al.*, 1989; Rupp *et al.* 2010).

Myosins of *P. falciparum*

Myosin proteins are commonly comprised of three different domains, the head domain, which interacts with actin filaments and possess ATPase activity, a hinge domain, functioning as lever arm and the tail domain. According to sequence comparisons of the head domain, myosins are divided into several classes (Hodge and Cope 2000; Thompson and Langford 2002). Almost all Apicomplexan myosins, including all *P. falciparum* myosins have been allocated to myosin class XIV (Heintzelman and Schwartzman, 1997; Chaparro-Olaya *et al.*, 2005). “Conventional” myosins as found in the skeleton muscles of vertebrates cluster in class II. The genome of *P. falciparum* contains six myosin genes termed *myoA–myoF* (Chaparro-Olaya *et al.*, 2003; reviewed in Vale, 2003). Semi-quantitative RT-PCR showed that all six genes are expressed in asexual blood stages (Chaparro-Olaya *et al.*, 2005).

Pfaldo

Pfaldo belongs to class I aldolases which can be found in all living organisms with the amino acid sequences largely conserved (reviewed in Gefflaut *et al.*, 1995). It catalyses the cleavage of Fructose-1,6-diphosphate into dihydroxyacetone phosphate and glyceraldehyde-3-phosphate and its reverse reaction. As all aldolases Pfaldo is present as tetramer. Both its multimeric nature and its molecular flexibility are important features for its interaction with both actin and the cytoplasmic tail of TRAP-like proteins (Bosch *et al.*, 2007). Carrying out two completely unrelated functions Pfaldo can be considered as moonlighting protein (reviewed in Jeffery, 1999; Huberts and van der Klei, 2010).

PfGAP50, PfGAP45 and PfMTIP

PfGAP50 is another example for a multifunctional protein of *P. falciparum*. In addition to its structural role in the glideosome, PfGAP50 has been described as a secreted acid phosphatase expressed in asexual blood stages. A role in uptake of nutrients from the host cell upon dephosphorylation has been proposed (Müller *et al.*, 2010). PfGAP50 possesses an N-terminal signal peptide which leads to translation of the protein into the ER. The C-terminal transmembrane domain and the cytoplasmic domain are responsible for the correct localization with the IMC (Yeoman *et al.*, 2011). PfGAP45 forms a

ternary complex with the myosin light chain PfMTIP and PfMyoA in the parasite cytosol (Fig. 1.11). PfGAP45 is acylated at its N-terminus and phosphorylated, however it seems to be mainly the interaction with PfGAP50 that ensures anchoring of the protein complex at the IMC (Rees-Channer *et al.*, 2006; Green *et al.*, 2008; Ridzuan *et al.*, 2012).

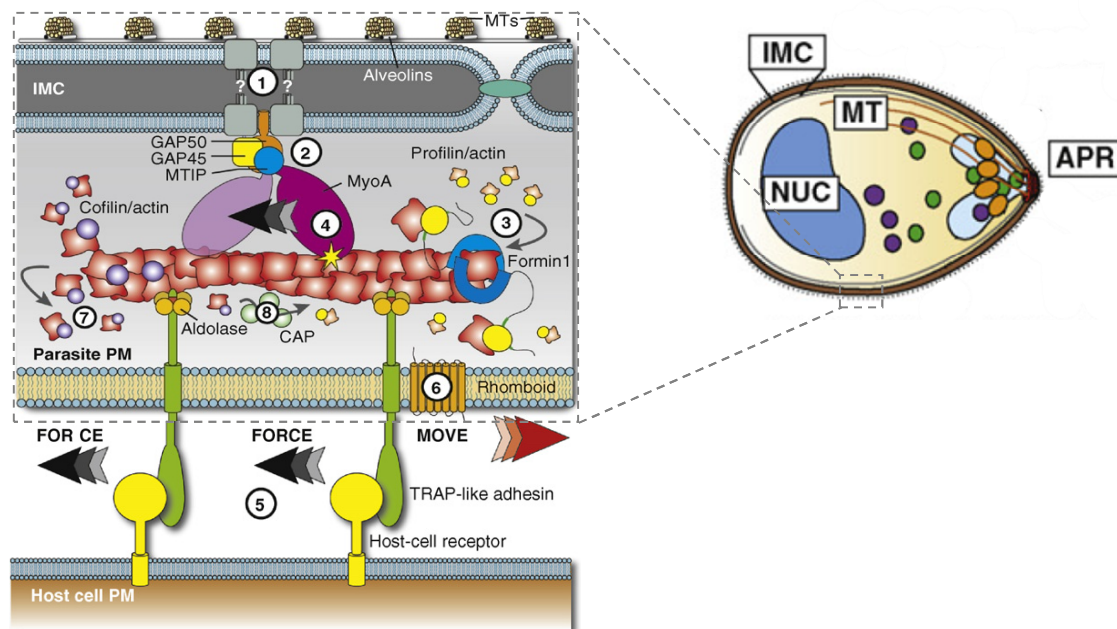


Fig 1.11: Schematic depicting the molecular motor complex mediating gliding motility and invasion in the invasive stages of *Plasmodium* spp. The right panel illustrates the location of the magnified schematic of the left panel within a merozoite. APR, apical polar rings, IMC, inner membrane complex, MT, subpellicular microtubules, NUC, nucleus (modified from Baum *et al.*, 2008).

1.7 Transport across the red blood cell membrane

1.7.1 Red blood cell-owned transporter systems

RBCs (also known as erythrocytes) are the most abundant type of blood cells. They are disc-shaped, biconcave cells that mediate the transport of oxygen from lung to tissue cells and the transport of carbon dioxide from cells of the human body to the lung. The metalloprotein hemoglobin accounts for approximately 35% of the erythrocytes mass. It is responsible for oxygen binding and the hem group gives the cells their red color. RBCs are highly deformable which allows their passage through capillaries that are much smaller (2–3 μm diameter) than the diameter of the RBC (6–8 μm). Flexibility is enabled due to the complex cytoskeleton located underneath the plasma membrane. The most prominent parts of the 2D meshwork are spectrin tetramers. They are connected via ankyrin to the band 3 protein (anion exchanger protein, AE1) or via the protein band 4.1 to glycophorin C (GpC). Both band 3 and GpC are transmembrane proteins of the RBC membrane, thus mediating the attachment of the cytoskeleton meshwork to the plasma membrane of the RBC.

Despite the fact that erythrocytes lack a nucleus and cell organelles like ribosomes or mitochondria and despite their inability to synthesize proteins (Gronowicz *et al.*, 1984; Germinard *et al.*, 2002) they are far more than a “hapless sack of hemoglobin” (Greenwalt, 1993). They have a “sophisticated and focused metabolism” that allows to respond to alterations in their surroundings and that includes programmed cell death (reviewed in Hess and Beyer, 2006). RBCs use glycolysis for energy production. Both glucose and fructose are used as substrates.

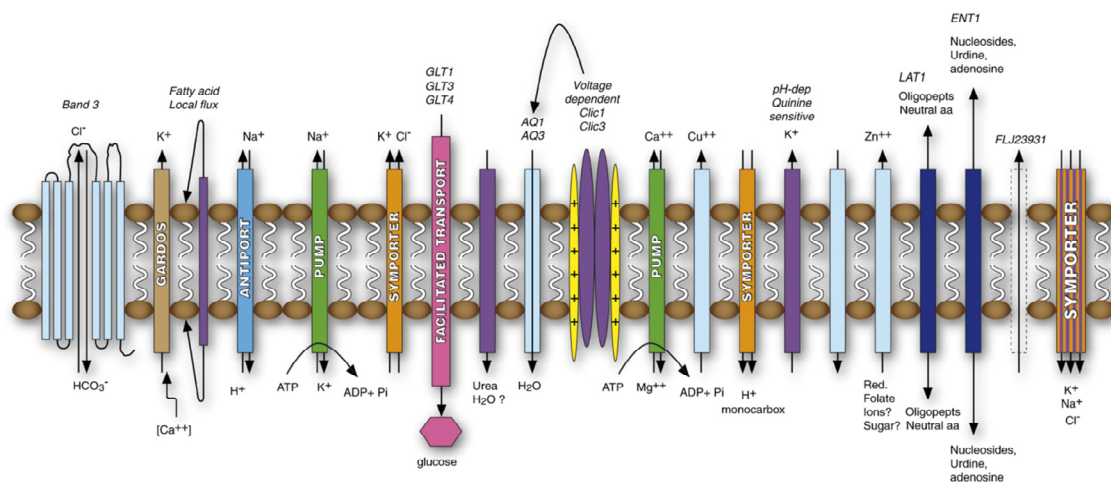


Fig. 1.12: Schematic of transport proteins of the RBC membrane that have been identified via mass spectrometry. GLT1, GLT3, GLT4, facilitated glucose transporters, AQ1, AQ3, Aquaporins, LAT1, System L amino acid transporter 1, ENT1, equilibrative nucleoside transporters ENT-1 (Pasini *et al.*, 2010).

The proteome of the RBC has been studied intensively in the past years (Low *et al.*, 2002; Kakhniashvilli *et al.*, 2004; Tyan *et al.*, 2005; Pasini *et al.*, 2006; reviewed in Goodman *et al.*, 2007; Pasini *et al.*, 2010). Mass spectrometric analyses identified 592 RBC proteins, amongst these 252 membrane-associated proteins (Pasini *et al.*, 2006). The latter include 47 proteins involved in transport responsible for osmoregulation and uptake of nutrients (see Fig. 1.12) (Pasini *et al.*, 2006). The most prominent transport protein is the anion exchanger band 3 (Fujinaga *et al.*, 1999) which mediates exchange of bicarbonate and chloride anions (Tanner, 1993; reviewed in Pasini *et al.*, 2010). Other anions like, phosphate, phosphoenolpyruvate, and superoxide are transported less efficiently. A Na^+/K^+ -ATPase and a Ca^{2+} -ATPase maintain the concentration of these cations at concentrations typical for mammalian cells (Kaplan, 1989; Mercer *et al.*, 1989; Vincenzi *et al.*, 1989). Examples for secondary active transport across the RBC membrane are a K^+/Cl^- -co-transporter and the Na^+/H^+ -exchanger (Gunn *et al.*, 1989; Parker and Dunham, 1989). Three proteins have been implicated to regulate the RBC volume in response to changes in osmolarity via transport of water: Aquaporin-1, aquaporin-3 and the urea transporter UT-B (Roudier *et al.*, 1998; Agre, 2006; reviewed in Pasini *et al.*, 2010). Furthermore, the amino acid transporter protein XK has been proposed to be involved in osmoregulation (reviewed in Pasini *et al.*, 2010). Further ami-

no acid transporters of the RBC have been described: Member 1 and member 2 of the solute carrier family 43, as well as the System L amino acid transporter 1 (LAT-1), and a glutamate transporter (Li and Whorton, 2007; reviewed in Pasinin *et al.*, 2010). Uptake of glucose, the main energy source of RBCs, is mediated by the facilitated glucose transporters GLUT1, GLUT3 and GLUT 4 (Mueckler *et al.*, 1985; reviewed in Thorens and Mueckler, 2010; Pilch, 1990). Nucleosides uridine and adenosine are supposedly taken up by the RBC via the equilibrative nucleoside transporters ENT-1 (reviewed in King *et al.*, 2006). RBCs also possess a transporter for the uptake of nucleobases, the human facilitative nucleobase transporter (hFNT1) (Griffith and Jarvis, 1993; Quashie *et al.*, 2010).

1.7.2 Parasite induced modifications to the red blood cell

Like the RBC the intra-erythrocytic parasite utilizes glucose as main energy source. RBC-owned transport proteins are sufficient to supply the amount of glucose metabolized by the parasite (Kirk *et al.*, 1996; Kirk und Saliba, 2006). However, nutrient requirements of the parasite are much more complex as compared to those of the RBC. The parasite solves this problem by modifying the host cell according to its needs. A number of parasite-derived proteins are inserted into the RBC membrane. They are referred to as “new permeability pathways” (NPP) (Ginsburg *et al.*, 1983; Elford *et al.*, 1985) and mediate uptake of amino acids, peptides, sugars, vitamins, choline and other molecules (reviewed in Cabantchik, 1990; Kirk, 2001; Ginsburg und Stein, 2004). As mature erythrocytes do not possess a secretion system for trafficking of proteins to the RBC membrane, the parasite itself establishes a continuous network of membranes within the RBC cytosol. It comprises the Maurer’s clefts, which consist of flat membrane cisternae and vesicles, as well as the tubovesicular network emanating from the PVM into the RBC cytosol (Atkinson und Aikawa, 1990; Behari und Halder, 1994; Lanzer *et al.*, 2006). These membrane structures are postulated to play an essential role for protein trafficking to the RBC (for review see Przyborski *et al.*, 2003; Lanzer *et al.*, 2006; Epp und Deitsch, 2006). Transport to the RBC membrane via Maurer’s clefts has for instance been shown for the immune variant cell surface antigens PfEMP1, RIFIN (repetitive interspersed gene encoded protein) and SURFIN (surface-associated interspersed gene encoded protein) (Fernandez *et al.*, 1999; Kriek *et al.*, 2003; Haeggström *et al.*, 2004; Winter *et al.*, 2005; Khattab und Klinkert, 2006). The modifications of the host cell by the parasite are manifold and in great part not characterized in detail, yet. It is thus an important objective to further study the interface between parasite and host cell, as it is of great importance for parasite survival, and thus represents an attractive target for intervention studies.

1.8 Aim of the PhD thesis

The sexual phase is a crucial and at the same time critical part of the life cycle of *P. falciparum*. Only a minor fraction of asexual blood stage parasites will develop into gametocytes, the precursor cells of gametes. After their uptake into the mosquito midgut only a small proportion of gametocytes will successfully undergo gametogenesis and fertilization followed by formation of an oocyst. Thus, the sexual stages are considered bottle neck stages presenting an attractive target for intervention strategies. During the sexual development processes in the mosquito midgut a number of essential intercellular interactions occur that are mediated via cell surface-expressed adhesion proteins. Details on the molecular interplay, however are rare and the exact function of most sexual stage-specific adhesion proteins remains elusive.

The proteins of the PfCCp protein family are expressed specifically in sexual parasite stages. All members of this protein family possess multiple adhesion domains. Protein-protein interactions were described both amongst members of the protein family as well as between PfCCp proteins and the sexual-stage proteins Pfs25, Pfs48/45 and Pfs230. In view of the manifold interactions of the PfCCp proteins the formation of a multimeric protein complex is anticipated. Additionally, the PfCCp proteins show a co-dependent expression manifesting at post-translational level. The loss of one member of the protein family thus results in diminished or abrogated expression of the other proteins of the PfCCp protein family.

The first main objective of this PhD thesis was to study expression and potential protein-protein interactions of sexual stage proteins to obtain information about protein function. The specific aims are described below:

- ❖ Knock-out (KO) parasite lines expressing truncated forms of PfCCp1, PfCCp4, PfCCp5, PfFNPA, Pfs230, Pfs48/45 and Pfg377 were investigated, in order to reveal interdependencies in protein expression. Via indirect immunofluorescence assays (IFAs) the expression of 20 proteins was investigated in sexual parasite stages of the KO parasite lines.
- ❖ A parasite line expressing a truncated version of the sexual stage-specific protein PfactinII as well as a parasite line expressing PfactinII as hemagglutinin (HA) fusion protein were generated. Mutants were studied with the aim of gaining information on the function of the protein. Indirect IFAs were carried out to investigate the expression profile of PfactinII. In addition, co-immunoprecipitation assays (co-IPs) and indirect IFAs were carried out to examine its relation with other sexual stage proteins.
- ❖ The expression of the so far uncharacterized protein PfWLP1 was studied in several parasite stages via indirect IFA in order to gain information on its spatial

and temporal expression pattern. Both a KO mutant and a mutant expressing PfwLP1 fused to an HA tag were generated.

- ❖ Via reverse transcriptase PCR (RT-PCR) and indirect IFA the expression of IMC proteins was investigated in gametocytes. The objective of this study was to better understand the composition of the subpellicular membrane complex of gametocytes and to compare it to the composition of the IMC of asexual parasites.

The second main objective was to study the molecular background of gametocyte activation and the mode of action of XA. Inhibitor studies were carried out with both uninfected and gametocyte-infected RBCs in order to check for interference with XA-induced gametocyte activation. In addition, gametocyte activation was studied on the ultrastructural level in order to better understand the sequential processes of gametocyte activation on cellular level.

2 Materials and Methods

2.1 Materials

2.1.1 Technical equipment

Tab. 2.1: Utilized technical devices and respective manufacturer.

Technical device	Manufacturer
Universal oven	Memmert GmbH + Co. KG (Schwabach)
Bunsen burner schuett flammy S	schuett-biotec GmbH (Göttingen)
Centrifuge Avanti® J-26 XP	Beckman Coulter GmbH (Krefeld)
Clean bench HERAsafe®	Heraeus Holding GmbH (Hanau)
Confocal laser scanning microscope LSM 510	Carl Zeiss AG (Oberkochen)
Confocal laser scanning microscope TCS SP1	Leica Microsystems GmbH (Wetzlar)
Developing machine CURIX 60	Agfa HealthCare GmbH (Bonn)
Dispenser Multipette® plus	Eppendorf AG (Hamburg)
Dry block thermostats TBD-100, TBD-120	LAB4YOU GmbH (Berlin)
Electrophoresis chambers MIDI, MAXI	Carl Roth GmbH & Co. KG (Karlsruhe)
Electrophoresis power supply Consort E835	Consort via A. Hartenstein GmbH (Würzburg)
Electrophoresis power supply PowerPac™ HC	Bio-Rad Laboratories GmbH (München)
Electroporation System Gene Pulser Xcell™	Bio-Rad Laboratories GmbH (München)
French® Press	G. Heinemann (Schwäbisch Gmünd)

Tab. 2.1 (continued)

Technical device	Manufacturer
Gel documentation system GelDoc™ 2000	Bio-Rad Laboratories GmbH (München)
Hemocytometer (Neubauer chamber)	Paul Marienfeld GmbH (Lauda-Königshofen)
Incubator HERAccl®	Heraeus Holding GmbH (Hanau)
Light microscope Leitz Laborlux 11	Leitz (Wetzlar)
Light microscope Leica DMLS	Leica Microsystems GmbH (Wetzlar)
Luminescent Image Analyzer LAS-1000	Fujifilm (Vila Nova de Gaia, Portugal)
Mini-gel drying frame	Carl Roth GmbH & Co. KG (Karlsruhe)
Mini-rocker shaker MR-1	LAB4YOU GmbH (Berlin)
Mini-shaker for PSU-2T	LAB4YOU GmbH (Berlin)
Multichannel micropipette Calibra® 852	Socorex via A. Hartenstein GmbH (Würzburg)
PCR thermocycler PTC-100™	MJ Research Inc. (St. Bruno, Canada)
PCR thermocycler Primus 25 advanced®	PEQLAB (Erlangen)
pH meter inoLab® pH Level1	WTW GmbH (Weilheim)
Pipetter accu-jet®	Brand GmbH & Co. KG (Wertheim)
Pipette set Research®	Eppendorf AG (Hamburg)
Precision scales 440-47N and 440-33	Kern und Sohn GmbH (Balingen-Frommern)
Protein gel electrophoresis chamber Mini-PROTEAN® 3	Bio-Rad Laboratories GmbH (München)
Refrigerated centrifuge Avanti® J-26 XP	Beckmann (München)
Roller mixer	Karl Hecht KG (Sondheim)
Roller mixer	Labinco BV (DG Breda, The Netherlands)
Slide stretching table OTS 40	Medite GmbH (Hannover)
Spectrophotometer BioPhotometer plus	Eppendorf AG (Hamburg)

Tab. 2.1 (continued)

Technical device	Manufacturer
Spectrophotometer Nanodrop® 1000	PEQLAB (Erlangen)
Thermo Scientific TKA water purification system	Thermo Electron LED GmbH (Niederelbert)
Transmission electron microscope EM10	Carl Zeiss AG (Oberkochen)
Microcentrifuge Biofuge pico	Heraeus Holding GmbH (Hanau)
Ultrasound device Sonoplus HD70	Bandelin (Berlin)
Universal shaker SM 30 A control and incubation hood TH 30	Edmund Bühler GmbH (Tübingen)
UV Stratalinker® 1800	Stratagene (Amsterdam, The Netherlands)
Vacuum blotter VacuGene XL	Pharmacia Biotech (Freiburg)
Vortex mixer	Labinco BV (DG Breda, The Netherlands)
Water bath WB-20	P-D Industriegesellschaft mbH (Wilsdruff)
Water bath incubator WTE var 3185	Karl Hecht KG (Sondheim)
Western Blot transfer cell Mini Trans-Blot	Bio-Rad Laboratories GmbH (München)

2.1.2 Consumable supplies

Consumable material used during this thesis was purchased from Becton Dickinson GmbH (Heidelberg), Sarstedt AG & Co. (Nümbrecht), Eppendorf AG (Hamburg) and Greiner Bio-One GmbH (Frickenhausen). Further manufacturers are listed in Tab. 2.2.

Tab. 2.2: Utilized consumable material and the respective manufacturer.

Consumable material	Manufacturer
Bottle top filter 0.22 µm PES membrane	Biochrom AG (Berlin)
Centrifugal filter unit Vivaspin 6 (5 kDa cut-off)	Sigma-Aldrich Chemie GmbH (München)

Tab. 2.2 (continued)

Consumable material	Manufacturer
Cover slips	A. Hartenstein GmbH (Würzburg)
Disposable syringes	B. Braun Melsungen AG (Melsungen)
Electroporation cuvette, gap width 2 mm	VWR International GmbH (Darmstadt)
Fuji Medical X-Ray Film Super X	Fujifilm via A. Hartenstein GmbH (Würzburg)
Hybond ECL nitrocellulose membrane	GE Healthcare Europe GmbH (Freiburg)
Hybond N+ nylon membrane	GE Healthcare Europe GmbH (Freiburg)
Syringe filter Rotilabo® (PVDF membran, pore size 0.22 µm)	Carl Roth GmbH & Co. KG (Karlsruhe)
Microscope slides, double frosted	Glaswarenfabrik Karl Hecht GmbH & Co. KG (Sondheim) via A. Hartenstein GmbH (Würzburg)
Pasteur pipettes	A. Hartenstein GmbH (Würzburg)
Pasteur pipettes with cotton-wool plug	A. Hartenstein GmbH (Würzburg)
Poly-Prep Chromatography Columns	Bio-Rad Laboratories GmbH (München)
Teflon coated diagnostic microscope slides	Gerhard Menzel, Glasbearbeitungswerk GmbH & Co. KG (Braunschweig) via Carl Roth GmbH & Co. KG (Karlsruhe)
96-well plates F96 MicroWell™	Nunc GmbH & Co. KG via A. Hartenstein GmbH (Würzburg)

2.1.3 Chemicals

Tab. 2.3: Utilized chemicals and the respective manufacturer.

Chemical	Manufacturer
N-Acetyl-D-glucosamin (GlcNAc)	Carl Roth GmbH & Co. KG (Karlsruhe)
Acrylamid/ Bisacrylamid stock solution (37.5: 1) Protogel	Biozym Scientific GmbH (Hessisch Oidendorf)

Tab. 2.3 (continued)

Chemical	Manufacturer
Adenine	Sigma-Aldrich Chemie GmbH (München)
Difco™ Agar	BD GmbH (Heidelberg)
Agarose NEEO ultra quality	Carl Roth GmbH & Co. KG (Karlsruhe)
Albumin fraction V (BSA)	Carl Roth GmbH & Co. KG (Karlsruhe)
para-Aminobenzoic acid	Sigma-Aldrich Chemie GmbH (München)
AminoLink Coupling Resin	Pierce (Thermo Fisher Scientific, Bonn)
Ammonium hydroxide (5.0 N solution)	Fluka®, Sigma-Aldrich Chemie GmbH (München)
Ammonium peroxodisulfate	Carl Roth GmbH & Co. KG (Karlsruhe)
Ampicillin	Carl Roth GmbH & Co. KG (Karlsruhe)
3-Acetylpyridine adenine dinucleotide (APAD)	Sigma-Aldrich Chemie GmbH (München)
BAPTA-AM	Sigma-Aldrich Chemie GmbH (München)
Blue Stain protein staining solution	Pierce (Thermo Fisher Scientific, Bonn)
BCIP/NBT tablets	Sigma-Aldrich Chemie GmbH (München)
Blasticidin S HCl	Invitrogen™ (Life Technologies GmbH, Darmstadt)
β-Mercaptoethanol	Sigma-Aldrich Chemie GmbH (München)
Bromophenol blue solution	AppliChem GmbH (Darmstadt)
100x BSA	New England Biolabs GmbH (Frankfurt)
Chloramphenicol	Carl Roth GmbH & Co. KG (Karlsruhe)
Citifluor	Citifluor Ltd. (London, UK)
Cyanoborohydride Solution	Pierce (Thermo Fisher Scientific, Bonn)

Tab. 2.3 (continued)

Chemical	Manufacturer
Cytochalasin B	Sigma-Aldrich Chemie GmbH (München)
Deoxynucleotide Set, 100 mM	Sigma-Aldrich Chemie GmbH (München)
Chloroform	Carl Roth GmbH & Co. KG (Karlsruhe)
Diaphorase	Sigma-Aldrich Chemie GmbH (München)
Diethylpyrocarbonate (DEPC) ($\leq 97\%$ solution)	Carl Roth GmbH & Co. KG (Karlsruhe)
1,4-Dithiothreitol (DTT)	Carl Roth GmbH & Co. KG (Karlsruhe)
Ethanol, <i>p.a.</i>	Carl Roth GmbH & Co. KG (Karlsruhe)
EDTA disodium salt $\times 2\text{H}_2\text{O}$	AppliChem GmbH (Darmstadt)
EGTA	AppliChem GmbH (Darmstadt)
Erythromycin	Kindly provided by Prof. T. Schirmeister, University of Wuerzburg
Ethanol, denatured	Carl Roth GmbH & Co. KG (Karlsruhe)
Evans Blue	Sigma-Aldrich Chemie GmbH (München)
Ethidium bromide (10 mg/ml solution)	Carl Roth GmbH & Co. KG (Karlsruhe)
Gentamicin (10 mg/ml)	Gibco® (Life Technologies GmbH, Darmstadt)
Gel Blue Stain Solution	Carl Roth GmbH & Co. KG (Karlsruhe)
Giemsa stock solution	Carl Roth GmbH + Co. KG (Karlsruhe)
D-(+) Glucose	Sigma-Aldrich Chemie GmbH (München)
Glutaraldehyde, 25 %	Fluka®, Sigma-Aldrich Chemie GmbH (München)
Glutathione sepharose	GE Healthcare Europe GmbH (Freiburg)
Glycerol, anhydrous, <i>p.a.</i>	Carl Roth GmbH + Co. KG (Karlsruhe)

Tab. 2.3 (continued)

Chemical	Manufacturer
Goat serum (Neutral goat serum)	Sigma-Aldrich Chemie GmbH (München)
HEPES	Carl Roth GmbH + Co. KG (Karlsruhe)
HCl 32%, <i>p.a.</i>	AppliChem GmbH (Darmstadt)
HCl 37% fuming, <i>p.a.</i>	AppliChem GmbH (Darmstadt)
Hoechst stain 33342	Molecular Probes® (Life Technologies GmbH, Darmstadt)
Hypoxanthine	Sigma-Aldrich Chemie GmbH (München)
Immersion oil	Carl Roth GmbH + Co. KG (Karlsruhe)
Isopropanol, <i>p.a.</i>	Carl Roth GmbH + Co. KG (Karlsruhe)
Isopropyl- β -D-thiogalactopyranoside (IPTG)	Invitrogen™ (Life Technologies GmbH, Darmstadt)
KCl	Carl Roth GmbH + Co. KG (Karlsruhe)
Ketamine	Sigma-Aldrich Chemie GmbH (München)
K ₂ HPO ₄	AppliChem GmbH (Darmstadt)
Kynurenic acid	Sigma-Aldrich Chemie GmbH (München)
DL-Lactic acid sodium solution 60 %	Sigma-Aldrich Chemie GmbH (München)
L(+)-Lactic acid	Sigma-Aldrich Chemie GmbH (München)
L-Leucine	Carl Roth GmbH + Co. KG (Karlsruhe)
Maleic acid	Carl Roth GmbH + Co. KG (Karlsruhe)
MgCl ₂ x 6H ₂ O	Carl Roth GmbH + Co. KG (Karlsruhe)
MgSO ₄ x 7H ₂ O	AppliChem GmbH (Darmstadt)
Methanol, <i>p.a.</i>	Carl Roth GmbH + Co. KG (Karlsruhe)

Tab. 2.3 (continued)

Chemical	Manufacturer
Milk powder, blotting grade	Carl Roth GmbH + Co. KG (Karlsruhe)
NaCl	Carl Roth GmbH + Co. KG (Karlsruhe)
Na ₂ HPO ₄ , anhydrous	AppliChem GmbH (Darmstadt)
NaH ₂ PO ₄ x 2 H ₂ O	Carl Roth GmbH + Co. KG (Karlsruhe)
NaOH	Carl Roth GmbH + Co. KG (Karlsruhe)
NBTI (NBMPR)	Sigma-Aldrich Chemie GmbH (München)
Nigericin	Sigma-Aldrich Chemie GmbH (München)
Nitroblue tetrazolium (NBT)	Carl Roth GmbH + Co. KG (Karlsruhe)
Nonidet® P-40 (NP-40)	Fluka®, Sigma-Aldrich Chemie GmbH (München)
Paraformaldehyde	Sigma-Aldrich Chemie GmbH (München)
Percoll®	Sigma-Aldrich Chemie GmbH (München)
Phenol	Carl Roth GmbH + Co. KG (Karlsruhe)
L-Phenylalanine	Carl Roth GmbH + Co. KG (Karlsruhe)
Poly-L-Lysine	Sigma-Aldrich Chemie GmbH (München)
Potassium hexacyanoferrate (III)	Sigma-Aldrich Chemie GmbH (München)
Propylene oxide	Sigma-Aldrich Chemie GmbH (München)
Protein G PLUS-Agarose	Santa Cruz Biotechnology, Inc. (Heidelberg)
Pyrimethamine	Sigma-Aldrich Chemie GmbH (München)

Tab. 2.3 (continued)

Chemical	Manufacturer
Rifampicin	DUCHEFA Biochemie B.V. (Haarlem, Netherlands)
RPMI 1640 medium (containing 25 mM HEPES, 2.05 mM L-Glutamine, Phenol Red)	Gibco®, Life Technologies GmbH, Darmstadt
RPMI 1640 powder	Gibco®, Life Technologies GmbH, Darmstadt
Saponin from quillaja bark	Sigma-Aldrich Chemie GmbH (München)
Sea salt	Alnatura GmbH (Bickenbach)
Sodium hypochlorite solution 13 %	AppliChem GmbH (Darmstadt)
D(-)-Sorbitol	AppliChem GmbH (Darmstadt)
SDS, ultra pure for electrophoresis	Carl Roth GmbH + Co. KG (Karlsruhe)
TEMED for electrophoresis	Carl Roth GmbH + Co. KG (Karlsruhe)
Tris PUFFERAN® ultra quality	Carl Roth GmbH + Co. KG (Karlsruhe)
Triton® X-100	Carl Roth GmbH + Co. KG (Karlsruhe)
TRIzol® Reagent	Life Technologies GmbH (Darmstadt)
Trypton/pepton from casein	Carl Roth GmbH + Co. KG (Karlsruhe)
L-Tryptophan	Carl Roth GmbH + Co. KG (Karlsruhe)
Tween® 20	Carl Roth GmbH + Co. KG (Karlsruhe)
Valinomycin	Sigma-Aldrich Chemie GmbH (München)
Water, double-distilled (ddH ₂ O) for cell culture	Carl Roth GmbH + Co. KG (Karlsruhe)
Yeast extract, pulverized, for bacteriology	Carl Roth GmbH + Co. KG (Karlsruhe)
Xanthurenic acid	Fluka®, Sigma-Aldrich Chemie GmbH (Munich)
Xylazine	Sigma-Aldrich Chemie GmbH (München)

2.1.4 Enzymes and Kits

Tab. 2.4: Enzymes used and the respective manufacturer.

Enzyme	Manufacturer
Antarctic Phosphatase	NEB GmbH (Frankfurt/Main)
Calve Intestinal Phosphatase (CIP)	NEB GmbH (Frankfurt/Main)
Chymotrypsin	Sigma-Aldrich Chemie GmbH (München)
DNaseI	QUIAGEN GmbH (Hilden)
GoTaq® DNA Polymerase	Promega GmbH (Mannheim)
Phusion® High-Fidelity DNA Polymerase	New England Biolabs GmbH (NEB) (Frankfurt/Main)
Polynucleotide Kinase	NEB GmbH (Frankfurt/Main)
Proteinase K	Sigma-Aldrich Chemie GmbH (München)
Restriction endonucleases	NEB GmbH (Frankfurt/Main)
T4 DNA Ligase	NEB GmbH (Frankfurt/Main)

Tab. 2.4 summarizes enzymes that were used. The following laboratory kits were utilized in the course of this work:

- NucleoSpin® Plasmid kit (Macherey & Nagel GmbH & Co. KG, Düren)
- Midi kit NucleoBond® Xtra Midi (Macherey & Nagel)
- NucleoSpin® Gel and PCR Clean-up kit (Macherey & Nagel)
- NucleoSpin® Blood kit (Macherey & Nagel)
- innuPREP RNA Mini Kit (Analytik Jena AG)
- BigDye™ Terminator Cycle Sequencing Kit (Applied Biosystems™, Life Technologies GmbH, Darmstadt)
- SuperScript® III First-Strand Synthesis System for RT-PCR (Life Technologies GmbH, formerly Invitrogen GmbH, Darmstadt)
- DIG High Prime DNA Labeling and Detection Starter Kit II (Roche Diagnostics Deutschland GmbH, Mannheim)
- MasterPure™ DNA Purification Kit (Epicentre®, via Biozym Scientific GmbH, Hessisch Oldendorf)
- Epoxy Embedding Medium Kit (Sigma-Aldrich Chemie GmbH, München)

2.1.5 Media and buffers for cell biological methods

All solutions were prepared using Milli-Q water (MQH₂O). Solutions and media used for culturing of *P. falciparum* were prepared from cell culture-grade ddH₂O and were sterile filtered using syringe filter or a bottle-top filter.

2000x Blasticidin S stock solution

- 5 mg/ml Blasticidin S dissolved in ddH₂O, stored in aliquots at -20°C

Cytomix buffer (Wu *et al.* 1995)

120 mM	KCl
0.15 mM	CaCl ₂
2 mM	EGTA
5 mM	MgCl ₂
10 mM	K ₂ HPO ₄ /KH ₂ PO ₄
25 mM	HEPES
ddH ₂ O ad 500 ml, pH 7.6	

Erythrocyte concentrate (Hematocrit 50%)

- purchased erythrocyte concentrate (blood type A Rh⁺, Bavarian Red Cross, Augsburg) was mixed 1:1 with RPMI incomplete medium, centrifuged at 3220 x g for 10 min
- supernatant was removed, cells were washed two more times with RPMI incomplete medium
- storage of cells in RPMI incomplete medium at 50% hematocrit at 4°C for up to four weeks

Fresh erythrocytes for transfection experiments

- 16 ml of human whole blood (blood type A Rh⁺) were taken into a syringe containing 4 ml 106 mM disodium citrate
- inversion of syringe, blood was centrifuged
- serum and buffy coat were removed
- red blood cells were washed three times with RPMI incomplete medium, stored at a hematocrit of 50%, used within one week

10x Giemsa buffer

51.4 mM	KH ₂ PO ₄
37.3 mM	Na ₂ HPO ₄

Glycerolyte

13.33 g	DL-Lactic acid sodium (60% solution, final concentration 1.6%)
285 g	Glycerol (45% [v/v])
4 mM	KCl
3.77 mM	NaH ₂ PO ₄
8.75 mM	Na ₂ HPO ₄
ddH ₂ O ad 500 ml	

Human serum (blood type A Rh⁺)

- sera from different donors (Bavarian Red Cross, Würzburg) were pooled
- sterile filtered, aliquoted and heat-inactivated at 55°C for 50 min
- storage at -20°C

1000x Hypoxanthine stock solution

- 50 mg/ml in 1 M NaOH

IFA incubation solution

0.5 % BSA
0.01 % Saponin
in 1 x PBS, pH 7.4

Malstat reagent

0.5 ml 10% Triton X-100 solution
0.5 g L-Lactic acid
0.165 g Tris-Base
• Dissolved in ddH₂O, cooled
0.0165 g APAD
• Dissolved, ddH₂O ad 50 ml, pH 9.0

10x PBS (Phosphate-buffered saline)

75 mM Na₂HPO₄
75 mM NaH₂PO₄
1.45 M NaCl
MQH₂O ad 1 l, pH 7.4

4% PFA/ PBS

- heating of 90 ml dH₂O to 60°C
- addition of 4 g paraformaldehyde, covering of glass beaker, maintained at 60°C
- addition of ~50 µl of 2 M NaOH, solution will clear
- addition of 10 ml 10x PBS, pH to 7.2
- filtered and kept on ice
- storage light-protected in aliquots at -20°C

250x Pyrimethamine stock solution

- 15 mg/ml dissolved in DMSO at 37°C
- diluted in RPMI incomplete medium to a final concentration of 125 µg/ml

RPMI 1640 complete A⁺ medium (RPMI complete medium)

500 ml RPMI 1640
50 ml Humane serum A Rh⁺
550 µl 1000 x Hypoxanthine
550 µl 1000 x Gentamicin

RPMI 1640 complete GlcNAc (N-Acetyl glucosamin) medium

- 6.08 g of GlcNAc were dissolved in 550 ml RPMI 1640 complete A⁺ medium (final concentration of 50 mM) followed filtration through a bottle-top filter to sterilize

RPMI 1640 complete pyrimethamine medium

- 2.2 ml of the 250x Pyrimethamine stock solution were added to 550 ml of RPMI 1640 complete A⁺ medium

RPMI 1640 complete blasticidin medium

- 275 µl of the 2000x Blasticidin S stock solution were added to 550 ml of RPMI 1640 complete A⁺ medium

1 x RPMI 1640 incomplete medium (ICM)

- 0.05 g hypoxanthine (final concentration 0.36 mM) were heated 2 x 2 min in 200 ml ddH₂O until dissolved
- 5.94 g HEPES (final concentration 25 mM) were added and stirred for 30 min
- 1 package RPMI 1640 powder (10.43 g) was added followed by stirring for 30 min
- ddH₂O added to a volume of 1 l, sterile filtered

10 x RPMI 1640 incomplete medium

- preparation as for 1 x RPMI 1640 incomplete medium
- ddH₂O added to a final volume of 100 ml

1 mM Xanthurenic acid

- 25 mg/ml dissolved in 0.5 M NH₄OH
- diluted in MQH₂O to final concentration

2.1.6 Media and buffers for molecular biological methods

Buffers and stock solutions were prepared with deionised water (dH₂O) from the on-site desalting plant. Buffers and solutions for Southern blot were prepared with MQH₂O.

1000x Ampicillin

- 100 mg/ml dissolved in dH₂O, shelf life at 4°C: four weeks
- Long term storage of aliquots at -20°C

Bacteria freezing solution

- 65% (v/v) glycerol
- 100 mM MgSO₄
- 25 mM Tris-HCl pH 8.0
- autoclaved to sterilize

Blocking buffer Southern Blot

- 10x Blocking solution (vial 6, DIG High Prime DNA Labeling and Detection Starter Kit II, Roche) in Maleic acid buffer

Chloramphenicol

- 50 mg/ml dissolved in Ethanol, storage at -20°C

DEPC-H₂O

- 0.1% (v/v) DEPC in MQH₂O, stirring
- incubation at 37°C overnight
- autoclaved to inactivate DEPC

10mM dNTP mix

- 10 ml each of 100 mM dATP, dCTP, dGTP and dTTP
- sterile MQH₂O ad 100 µl

Detection buffer Southern Blot

100 mM	Tris-HCl, pH9.5
100 mM	NaCl

LB medium

10 g/l	Tryptone
5 g/l	Yeast extract
5 g/l	NaCl

LB agar

10 g/l	Tryptone
5 g/l	Yeast extract
5 g/l	NaCl
15 g/l	Agar

Maleic acid buffer

100 mM	Maleic acid
150 mM	NaCl

adjust pH to 7.5 with solid NaOH

Plasmid DNA isolation resuspension buffer P1

50 mM	Tris-HCl pH 8.0
10 mM	EDTA
100 µg/ml	RNase A

Plasmid DNA isolation lysis buffer P2

200 mM	NaOH
1 %	SDS

SOC medium

20 g/l	Tryptone
5 g/l	Yeast extract
0.5 g/l	NaCl
10 ml	250 mM KCl
5 ml	2 M MgCl ₂
20 ml	1 M Glucose

20x SSC

300 mM	Trisodium citrate 2 x H ₂ O
3.0 M	NaCl

50x TAE (Tris-acetate-EDTA) buffer

2.0 M	Tris
2.0 M	Acetic acid
50 mM	EDTA (100 ml 0.5 M EDTA, pH 8.0)
dH ₂ O ad 1 l	

TSE buffer

20 mM	Tris, pH 8.0
100 mM	NaCl
50 mM	EDTA

Washing buffer Southern Blot

- 3 % Tween 20 in Maleic acid buffer

2.1.7 Media and buffers for protein biochemical methodsBlocking solution Western Blot

1 x TBS	
5 % (w/v)	Milk powder
1 % (w/v)	BSA

Co-immunoprecipitation (Co-IP) lysis buffer

0.2 %	Saponin
0.8 %	NP-40
1 %	Protease inhibitor cocktail (PIC)
5 μM	EDTA
in 1 x PBS, pH 7.4	

Detergent buffer inclusion bodies

20 mM	Tris-Base
2 mM	EDTA
0.20 M	NaCl
1 % (w/v)	Deoxycholic acid
1 % (v/v)	NP-40
pH 7.5	

Equilibration buffer Western Blot

100 mM	Tris
100 mM	NaCl
110 mM	MgCl ₂
dH ₂ O ad 1 l, pH 9.5	

GST Elution buffer

50 mM Tris
10 mM glutathione
pH 8.0

Lysis buffer inclusion bodies

50 mM Tris-Base
0.25 % (w/v) Sucrose
1 mM EDTA
pH8.0

10x SDS-PAGE running buffer

240 mM Tris
1.92 M Glycine
1 % (w/v) SDS
dH₂O ad 1 l

5% SDS Polyacrylamide stacking gel (for 2 mini gels)

0.6 ml 30% Acrylamid
1 ml 500 mM Tris pH 6.8
12 µl 10% SDS
30 µl 10% APS
4 µl TEMED
2.4 ml dH₂O

12% SDS Polyacrylamide separating gel (for 2 mini gels)

4 ml 30% Acrylamid
2.5 ml 1.5 M Tris pH 8.8
100 µl 10% SDS
100 µl 10% APS
4 µl TEMED
3.3 ml dH₂O

2x SDS-PAGE sample buffer

2.5 ml 500 mM Tris pH 6.8
2 ml Glycerine
4 ml 10% SDS
0.5 ml 0.1% Bromophenol blue
dH₂O ad 10 ml

Stop buffer Western Blot

10 mM Tris
1.4 mM EDTA
dH₂O ad 1 l, pH 8.0

10x TBS (Tris-buffered saline)

100 mM Tris
 1.49 M NaCl
 dH₂O ad 1 l, pH 7.5

Transfer buffer Western Blot

25 mM Tris
 192 mM Glycin
 20% (v/v) Methanol
 dH₂O ad 1 l

TBSM

1 x TBS
 3% (w/v) Milk powder

Washing buffer

0.5% Triton X-100
 1 mM EDTA

2.1.8 Bacteria strains and cell lines

The following *E. coli* strains were used for recombinant DNA techniques:

E. coli Nova Blue (originally from Life Technologies GmbH, Darmstadt): chemical competent cells (generation according to Inoue *et al.* 1990)

E. coli BL21 CodonPlus®(DE3)-RIL-Zellen (Agilent Technologies Sales & Services GmbH & Co.KG, Waldbronn) competent cells for protein expression

P. falciparum strains and KO cell lines investigated in this work are listed in Tab. 2.5.

Tab. 2.5: *P. falciparum* cell lines and clones investigated. Plasmids used for genetically manipulation of parasites and the respective selection marker are listed.

Cell line	Clones	Plasmid	Selection marker	Reference
Wild-type NF54	-	-	-	-
3D7 (clone of NF54)	F12	-	-	Alano <i>et al.</i> , 1995
NF54, PfCCp1-KO	5YE2	pHHT-TK	Pyrimethamine	Simon <i>et al.</i> , 2009
NF54, PfCCp4-KO	L4C	pDT.Tg23	Pyrimethamine	Scholz <i>et al.</i> , 2008

Tab. 2.5 (continued)

Cell line	Clones	Plasmid	Selection marker	Reference
NF54, PffNPA-KO	1H4	pCAM-BSD	Blasdicidin S	Simon <i>et al.</i> , 2009
NF54, Pfs230-KOd1	12-1	pDT.Tg23	Pyrimethamine	Eksi <i>et al.</i> , 2002
NF54, Pfs230-KOd2	15-4	pDT.Tg23	Pyrimethamine	Eksi <i>et al.</i> , 2002
NF54, Pfs48/45-KO		pDT.Tg23	Pyrimethamine	van Dijk <i>et al.</i> , 2001
3D7, Pfg377-KO	E4	pHH1	WR99210	de Koning-Ward <i>et al.</i> , 2008

2.1.9 Antibodies and antisera

Antibodies and antisera used for this work are listed in Tab. 2.6. Antisera generated in the Pradel laboratory are polyclonal antisera derived from female NMRI mice (Charles River Laboratories Germany GmbH, Sulzfeld). Some of the non-commercially obtained antisera were friendly provided by Dr. Jude Przyborski (Marburg), Prof. Kim Williamson (Chicago, USA), Dr. Pietro Alano (Rome, Italy) und Prof. Tom Templeton (New York, USA).

Tab. 2.6: Primary and secondary antibodies and antisera utilized.

Antibody/Antiserum	Animal of origin	Dilution		Source
		Western Blot	IFA	
Primary antibodies/ antisera				
anti-Glycophorin A	mouse	1:500	–	Sigma-Aldrich (clone E4, G7900)
anti-MYO1C (human)	rabbit	–	1:50–1:100	Sigma-Aldrich (SAB2104382)
anti-PfactinI rp1	mouse	–	1:100	Pradel Lab

Tab. 2.6 (continued)

Antibody/Antiserum	Animal of origin	Dilution		Source
		Western Blot	IFA	
anti-PfactinII rp1	mouse	1:50–1:200	1:50–1:200	Pradel Lab
anti-PfCCp1 rp1	mouse	–	1:100	Pradel Lab
anti-PfCCp2 rp3	mouse	1:100	1:50	Pradel Lab
anti-PfCCp3 rp3	mouse	–	1:50	Pradel Lab
anti-PfCCp3 SR1	mouse	–	1:50	Tom Templeton
anti-PfCCp4 rp1	mouse	–	1:25–1:50	Pradel Lab
anti-PfCCp5 rp4	mouse	1:200	1:50	Pradel Lab
anti-PfFNPA rp2	mouse	–	1:50	Pradel Lab
anti-PfFNPA rp1	mouse	1:200	–	Pradel Lab
anti-PfExp-1	rabbit	–	1:50	Jude Przyborski
anti-Pfg377	rat	–	1:50	Pietro Alano
anti-PfGAP50 rp1	mouse	–	1:50	Pradel Lab
anti-PfMR5	mouse	–	1:50	Pradel Lab
anti-Pfpeg3	rat	–	1:50	Pietro Alano
anti-Pfpeg4	rat	–	1:50	Pietro Alano
anti-Pfs16	mouse	–	1:200	Pradel Lab (Plasmid by Kim Williamson)
anti-Pfs16	rabbit	–	1:100	Biogenes (Plasmid by Kim Williamson)
anti-Pfs25	rabbit	1:200	1:500–1:1000	ATCC (Manassas, USA)
anti-Pfs28	rabbit	–	1:100	ATCC (MRA-18) (Manassas, USA)
anti-Pfs230-C	mouse	1:500	1:100–1:200	Pradel Lab (Plasmid by Kim Williamson)

Tab. 2.6 (continued)

Antibody/Antiserum	Animal of origin	Dilution		Source
		Western Blot	IFA	
anti-Pfs230-C	rabbit	–	1:100–1:200	Biogenes (Plasmid by Kim Williamson)
anti-Pfs47.1	rat	–	1:50	Robert Sauerwein
anti-Tubulin (<i>Strongylacentrotus purpuratus</i>)	mouse	–	1:100	Sigma-Aldrich (T5168)
anti- α -tubulin II rp1	mouse	–	1:20	Pradel Lab
anti- α -tubulin II	rabbit	–	1:500	ATCC (Manassas, USA)
anti-Pf39 (PfERC)	mouse	1:100	–	Pradel Lab
anti-PfMSP1	rabbit	–	1:1000	ATCC (Manassas, USA)
anti-PfWLP1 rp2	mouse	–	1:50	Pradel Lab
anti-HA tag	mouse	1:1000	–	Roche (11583816001)
anti-HA tag	mouse	1:100	1:50	Santa Cruz (sc-805)
anti-PfCCp1-1rp1	mouse	1:200	1:100	AG Pradel
anti-PfCCp1-1rp5	mouse	1:200	1:100	AG Pradel
anti-PfCCp2-2rp3	mouse	1:200	1:100	AG Pradel
anti-PfCCp3-SR1	mouse	1:100	1:100	Tom Templeton
anti-PfCCp4-4rp1	mouse	–	1:50	AG Pradel
Secondary antibodies				
anti-mouse alkaline phosphatase conjugated antibody	goat	1:6000	–	Molecular Probes, Invitrogen, Karlsruhe

Tab. 2.6 (continued)

Antibody/Antiserum	Animal of origin	Dilution		Source
		Western Blot	IFA	
anti-rabbit alkaline phosphatase conjugated antibody	goat	1:6000	–	Molecular Probes, Invitrogen, Karlsruhe
anti-mouse Alexa Fluor® 488 antibody	goat	–	1:1000	Sigma-Aldrich
anti-rabbit Alexa Fluor® 488 antibody	goat	–	1:1000	Sigma-Aldrich
anti-rat Alexa Fluor® 488 antibody	goat	–	1:1000	Sigma-Aldrich
anti-mouse Alexa Fluor® 594 antibody	goat	–	1:1000	Sigma-Aldrich
anti-rabbit Alexa Fluor® 594 antibody	goat	–	1:1000	Sigma-Aldrich

2.1.10 Oligonucleotides

Oligonucleotides used in this work were purchased from biomers.net (Ulm). Oligonucleotides used for the generation of transfection plasmids are listed in Tab. 2.7, oligonucleotides employed in diagnostic PCRs investigating manipulated gene loci of transfected parasites are listed in Tab. 2.8. All other oligonucleotides are listed in Tab. 2.9.

Tab. 2.7: Sequence of oligonucleotides (5'–3' orientation) used for generation of genetically modified parasites. Recognition sites of restriction endonucleases are shown as capitals, stop codons are underlined.

Oligonucleotide	Sequence	Product length
CCp5-KO-S	atGGATCCggttcgcgcgattgggat	507 bp
CCp5-KO-AS	taGCGGCCGC <u>tatt</u> tctaatggtcctctact	
CCp5-HA1-S	atCTGCAGctccaataattaatccaaac	569 bp
CCp5-HA-AS	taGGATCCaattttcaatattgaagtgcc	
CCp5-HA2-S	atCTGCAGccaaatagtattccattgta	525 bp
CCp5-HA-AS	taGGATCCaattttcaatattgaagtgcc	

Tab. 2.7 (continued)

Oligonucleotide	Sequence	Product length
FNPA-KO-S	atGGATCCggggtacatgcatttatg	568 bp
FNPA-KO-AS	taGCGGCCGCttacgtattgaccagtgatt	
PfactinII-HA-S1	atCTGCAGgaacattcagatgaaatagaaga	435 bp
PfactinII-HA-AS1	taGGATCCgaaacattttctatgaacaatactag	
PfactinII-KO2-S1	atGGATCCgtgaagtctggttgctgga	381 bp
PfactinII-KO2-AS1	taGCGGCCGCttaatataggataagatggcttgat	
PfWLP1-HA-S1	atCTGCAGtatgtcaaatcatactttaacat	417 bp
PfWLP1-HA-AS1	taGGATCCaaaagccacaaacgceca	
PfWLP1-KO-S1	atGGATCCccgatataaataacataagctac	404 bp
PfWLP1-KO-AS1	taCGGCCGCttacatattatcactctctgaacagtt	
PfSR1-KO-S1	atGGATCCccaatttttaatgatggaatgtt	489 bp
PfSR1-KO-AS1	taGCGGCCGCttacctctttgtatcacaaccgt	
PFE1265w-KO-S1	atGGATCCaaagaaagaagaatagtattacc	513 bp
PFE1265w-KO-AS1	taGCGGCCGCttattcctttgattcttcggtgt	

Tab. 2.8: Primer pair combinations used for diagnostic PCR investigating the genotype of transfected parasites and the expected lengths of PCR products. 5' integr - 5' region of gene locus modified by vector integration, 3' integr. - 3' region of modified locus, episome - detection of transfection plasmid, WT - detection of WT gene locus.

Region of interest	Oligonucleotid	Sequence	Product length
PfCCp5-KO			
5' integr.	CCp5-KO-Integ5-S	ggtgttatgtcgaagtcaatt	598 bp
	pCAM-BSD/R	caattaaccctcactaaag	
3' integr.	pCAM-BSD/F	tattcctaatacatgtaaatcttaa	656 bp
	CCp5-KO-Integ3-AS	atacccttcataacgaataga	
Episome	pCAM-BSD/F	tattcctaatacatgtaaatcttaa	773 bp
	pCAM-BSD/R	caattaaccctcactaaag	
WT	CCp5-KO-Integ5-S	ggtgttatgtcgaagtcaatt	581 bp
	CCp5-KO-Integ3-AS	atacccttcataacgaataga	

Tab. 2.8 (continued)

Region of interest	Oligonucleotid	Sequence	Product length
PfCCp5-HA1			
5' integr.	CCp5-HA-Integ5-S	gcttctattcatgcaggt	821 bp
	pCAM-comp-AS2	aacattaagctgccatatcc	
3' integr.	pCAM-BSD/F	tattcctaatacatgtaaatcttaaa	748 bp
	CCp5-HA-Integ3-AS	ttctatatgacgttggtg	
Episome	pCAM-BSD/F	tattcctaatacatgtaaatcttaaa	760 bp
	pCAM-comp-AS2	aacattaagctgccatatcc	
WT	CCp5-HA-Integ5-S	gcttctattcatgcaggt	815 bp
	CCp5-HA-Integ3-AS	ttctatatgacgttggtg	
PfCCp5-HA2			
5' integr.	CCp5-HA-Integ5-S	gcttctattcatgcaggt	821 bp
	pCAM-comp-AS2	aacattaagctgccatatcc	
3' integr.	pCAM-BSD/F	tattcctaatacatgtaaatcttaaa	703 bp
	CCp5-HA-Integ3-AS	ttctatatgacgttggtg	
Episome	pCAM-BSD/F	tattcctaatacatgtaaatcttaaa	715 bp
	pCAM-comp-AS2	aacattaagctgccatatcc	
WT	CCp5-HA-Integ5-S	gcttctattcatgcaggt	815 bp
	CCp5-HA-Integ3-AS	ttctatatgacgttggtg	
PfFNPA-KO			
5' integr.	FNPA-KO-Integ5-S	ggtaatgtatctacgcct	699 bp
	pCAM-BSD/R	caattaaccctcactaaag	
3' integr.	pCAM-BSD/F	tattcctaatacatgtaaatcttaaa	828 bp
	FNPA-KO-Integ3-AS	aatgatgatgccaggag	
Episome	pCAM-BSD/F	tattcctaatacatgtaaatcttaaa	734 bp
	pCAM-BSD/R	caattaaccctcactaaag	
WT	FNPA-KO-Integ5-S	ggtaatgtatctacgcct	792 bp
	FNPA-KO-Integ3-AS	aatgatgatgccaggag	

Tab. 2.8 (continued)

Region of interest	Oligonucleotid	Sequence	Product length
PfactII-KO			
5' integr.	actIIKO-Integ5-S	aatgtataaatactatggtagatt	833 bp
	pCAM-BSD/R	caattaaccctcactaaag	
3' integr.	pCAM-BSD/F	tattcctaatacatgtaaatcttaa	509 bp
	actIIKO-Integ3-AS	acctgtgttcttctgatg	
Episome	pCAM-BSD/F	tattcctaatacatgtaaatcttaa	547 bp
	pCAM-BSD/R	caattaaccctcactaaag	
WT	actIIKO-Integ5-S	aatgtataaatactatggtagatt	795 bp
	actIIKO-Integ3-AS	acctgtgttcttctgatg	
PfactII-HA			
5' integr.	actIIHA-Integ5-S	ttgcatgattaatttatctga	830 bp
	pCAM-comp-AS2	aacattaagctgccatatcc	
3' integr.	pCAM-BSD/F	tattcctaatacatgtaaatcttaa	614 bp
	actIIHA-Integ3-AS	aacatgaattagccaaatatac	
Episome	pCAM-BSD/F	tattcctaatacatgtaaatcttaa	625 bp
	pCAM-comp-AS2	aacattaagctgccatatcc	
WT	actIIHA-Integ5-S	ttgcatgattaatttatctga	819 bp
	actIIHA-Integ3-AS	aacatgaattagccaaatatac	
PfWLP1-KO			
5' integr.	PfWLP1-KO-Integ5-S	gggtccaagaagtacatcaa	693 bp
	pCAM-BSD/R	caattaaccctcactaaag	
3' integr.	pCAM-BSD/F	tattcctaatacatgtaaatcttaa	813 bp
	PfWLP1-KO-Integ3-AS	acaccatctctccacctga	
Episome	pCAM-BSD/F	tattcctaatacatgtaaatcttaa	570 bp
	pCAM-BSD/R	caattaaccctcactaaag	
WT	PfWLP1-KO-Integ5-S	gggtccaagaagtacatcaa	939 bp
	PfWLP1-KO-Integ3-AS	acaccatctctccacctga	

Tab. 2.8 (continued)

Region of interest	Oligonucleotid	Sequence	Product length
PfWLP1-HA			
5' integr.	PfWLP1-HA-Integ5-S	aacaaattagaacccacatggtc	614 bp
	pCAM-comp-AS2	aacattaagctgccatatcc	
3' integr.	pCAM-BSD/F	tattcctaatacatgtaaatcttaaa	875 bp
	PfWLP1-HA-Integ3-AS	ttcaggaggaactccagt	
Episome	pCAM-BSD/F	tattcctaatacatgtaaatcttaaa	607 bp
	pCAM-comp-AS2	aacattaagctgccatatcc	
WT	PfWLP1-HA-Integ5-S	aacaaattagaacccacatggtc	822 bp
	PfWLP1-HA-Integ3-AS	ttcaggaggaactccagt	
PfSR1-KO			
5' integr.	SR1-KO-Integ5-S	acatacacagattgccttg	650 bp
	pCAM-BSD/R	caattaaccctcactaaag	
3' integr.	pCAM-BSD/F	tattcctaatacatgtaaatcttaaa	746 bp
	SR1-KO-Integ3-AS	ctcttctctctctcc	
Episome	pCAM-BSD/F	tattcctaatacatgtaaatcttaaa	655 bp
	pCAM-BSD/R	caattaaccctcactaaag	
WT	SR1-KO-Integ5-S	acatacacagattgccttg	784 bp
	SR1-KO-Integ3-AS	ctcttctctctctcc	
PFE1265w-KO			
5' integr.	1265wKO-Integ5-S	tctttacgatgggtgatg	838 bp
	pCAM-BSD/R	caattaaccctcactaaag	
3' integr.	pCAM-BSD/F	tattcctaatacatgtaaatcttaaa	1218 bp
	1265wKO-Integ3-AS	gagctgggaaatagactagat	
Episome	pCAM-BSD/F	tattcctaatacatgtaaatcttaaa	679 bp
	pCAM-BSD/R	caattaaccctcactaaag	
WT	1265wKO-Integ5-S	tctttacgatgggtgat	1377 bp
	1265wKO-Integ3-AS	gagctgggaaatagactagat	

Tab. 2.9: Sequence of oligonucleotides (5'–3' orientation). Recognition sites of restriction endonucleases are shown as capitals, stop codons are underlined.

Oligonucleotide	Sequence
Oligonucleotides for generation of recombinant proteins	
PfWLP1-rp2-S1	atGGATCCatgatagacctaaattatgttaaattg
PfWLP1-rp2-Not-AS	taGCGGCCGC <u>t</u> tatcgtattagtggttgtttaagca
PfWLP1-rp2-Pst-AS	taCTGCAG <u>t</u> tatcgtattagtggttgtttaagca
Oligonucleotides for RT-PCR	
PfactinI-RT2-S	aatgtaaagcaggagtgc
PfactinI-RT2-AS	catcctcaccagattccttttg
PfactinII-RT2-S	gcatcaggaagaacaacag
PfactinII-RT2-AS	atttcttctatttcactcgaatg
PfCCp1-RT3-S	ctggtatggaccattatgttggg
PfCCp1-RT3-AS	cgaattacagaagaatcaacaccatg
PfCCp2-RT2-S	tcggatggagaatccgtt
PfCCp2-RT2-AS	gtatcccatgtcttga
PfCCp3-RT2-S	gccctcatgaaacacatgatg
PfCCp3-RT2-AS	cacatcctctgttgcgc
PfCCp4-RT1-S	atgcccgaacaaatcatt
PfCCp4-RT1-AS	tgctgaggcgcataact
PfCCp5-RT1-S	ggttcgcgcgattgggat
PfCCp5-RT1-AS	tttccgcacacagaatc
PfFNPA-RT3-S	cgctggattcagtggaataacc
PfFNPA-RT3-AS	ccgattggctctttattggag
Pf39-RTPCR-1S	cttgaacaccatgatga
Pf39-RTPCR-1AS	tccacttcatgagcagg
Pfmyo-A-RT1-S	cgtattcagacagcaataatggc*
Pfmyo-A-RT1-AS	tcctccttctggttcaattcttg*
Pfmyo-B-RT1-S	gggtggtaaatctaattgtagt*g
Pfmyo-B-RT1-AS	ctgattcaattataattccttc*
PfmyoC-RT1-S	ggtaataatacgcgatgatgc*c
PfmyoC-RT1-AS	gagtaacaacttattcgacatcg*
PfmyoD-RT1-S	agcacaacaagggtcagggtattag

Tab. 2.9 (continued)

Oligonucleotide	Sequence
PfmyoD-RT1-AS	gtttataacttaatTTTgttccttcc
PfmyoE-RT1-S	atatctataagcaagaaggattgg
PfmyoE-RT1-AS	ttcccatttgatcataatcataag
PfmyoF-RT1-S	aaatataataaattcggcaaagt
PfmyoF-RT1-AS	ttacattgTTTgttcctatcac
GAP45-RT1-S	attatgcaactcaagaaaataaatc
GAP45-RT1-AS	tcaataaagggtgatcggataaatc
GAP50-RT1-S	taaggatacaaaagggtcagatattg
GAP50-RT1-AS	ggtcacttgatactgtaaaatg
Pfaldo-RT1-S	tagatggattagcagaaagatgc
Pfaldo-RT1-AS	agaaaccaacatcttgagtagtgg
MTIP-RT1-S	tagtggTgggaaaataagtatagac
MTIP-RT1-AS	aaggcattaagagcatctatgg
PfAMA1-RT-1S	ggattatgggtc gatgga
PfAMA1-RT-1AS	gatcactactagcgttctt
Oligonucleodites for generation of Southern blot probes	
CCp5-SB-S	atCTGCAGccaaatagttattccattgta
CCp5-SB-AS	atCTGCAGccaaatagttattccattgta
FNPA-SB-S	gcaacatctctaagtatactgg
FNPA-SB-AS	tggtatccctgtgtccca
Vector-specific oligonucleotides	
pGEX-S	tggaccaaatgtgcctgg
pGEX-AS	acgtgactgggtcatggc
pIH-S	ggtcgtcagactgtcgatgaagcc
pIH-AS2	cctcttcgctattacgccagc
pCAM-BSD/F	tattcctaatacatgtaaatcttaa
pCAM-BSD/R	caattaaccctcactaaag
pCAM-comp-AS2	aacattaagctgcatatcc

*Oligonucleotides as in Chaparro-Olaya *et al.* 2005

2.1.11 PlasmoDB gene identifiers

The proteins investigated in this work as well as the identifiers of the encoding genes according to the PlasmoDB database are listed in Tab. 2.10.

Tab. 2.10: Gene products investigated in this work and their gene identifiers of the database PlasmoDB (<http://plasmodb.org/plasmo/>).

Name of encoded protein	Gene ID	Previous Gene ID
PfactinI	PF3D7_1246200	PFL2215w
PfactinII	PF3D7_1412500	PF14_0124
PfAMA1	PF3D7_1133400	PF11_0344
PfCCp1	PF3D7_1475500	PF14_0723
PfCCp2	PF3D7_1455800	PF14_0532
PfCCp3	PF3D7_1407000	PF14_0067
PfCCp4	PF3D7_0903800	PFI0185w
PfCCp5	PF3D7_0109100	PFA0445w
PfFNPA	PF3D7_1451600	PF14_0491
PfEXP-1 (CRA)	PF3D7_1121600	PF11_0224
Pfg377	PF3D7_1250100	PFL2405c
PfGAP50	PF3D7_0918000	PFI0880c
PfMR5 (Pfs230p)	PF3D7_0208900	PFB0400w
Pfpeg3 (MDV1)	PF3D7_1216500	PFL0795c
Pfpeg4 (ETRAMP10.3)	PF3D7_1016900	PF10_0164
Pfs16	PF3D7_0406200	PFD0310w
Pfs25	PF3D7_1031000	PF10_0303
Pfs28	PF3D7_1030900	PF10_0302
Pfs230	PF3D7_0209000	PFB0405w
Pfs47	PF3D7_1346800	PF13_0248
Pfs48/45	PF3D7_1346700	PF13_0247
α -tubulin II	PF3D7_0422300	PFD1050w
Pf39 (PfERC)	PF3D7_1108600	PF11_0098
PfWLP1	PF3D7_1443400	PF14_0412
PfSR1	PF3D7_1131100	PF11_0321
G-protein coupled receptor, putative	PF3D7_0525400	PFE1265w

2.1.12 Plasmids

For the generation of gene disruptant mutants of *P. falciparum* the pCAM-BSD vector was employed. In order to obtain parasites expressing a gene of interest fused to the sequence encoding a double hemagglutinin (HA) tag, parasites were transfected with the pCAM-BSD-HA plasmid. These plasmids contain the *BSD* gene of *Aspergillus terreus* that encodes a blasticidin S deaminase conferring resistance to Blasticidine S (Mamoun *et al.*, 1999). Both pCAM-BSD and pCAM-BSD-HA were kindly provided by Prof. Christian Doerig (Melbourne, Australia). For the generation of antisera via immunization of mice with inclusion bodies or recombinant protein, the expression vectors pGEX-4T-1 and pIH902 (the latter kindly provided by Prof. Kim Williamson, Chicago) were used. Before insertion into the final vector, PCR products were subcloned into the pGEM-T-Easy vector. Maps of the vector backbones are listed in appendix, Fig. 8.1–8.4.

2.1.13 DNA- and protein ladders

The protein molecular weight standards Page Ruler™ Prestained Protein Ladder and Page Ruler™ Plus Prestained Protein Ladder (Fig. 2.1) were purchased from Fisher Scientific GmbH (Schwerte, formerly Fermentas GmbH). 5 µl of the respective protein ladder were applied per gel lane. For high molecular weight proteins 10 µl per lane of the Spectra™ Multicolor High Range Protein Ladder served as molecular weight standard (Fisher Scientific GmbH, Schwerte).

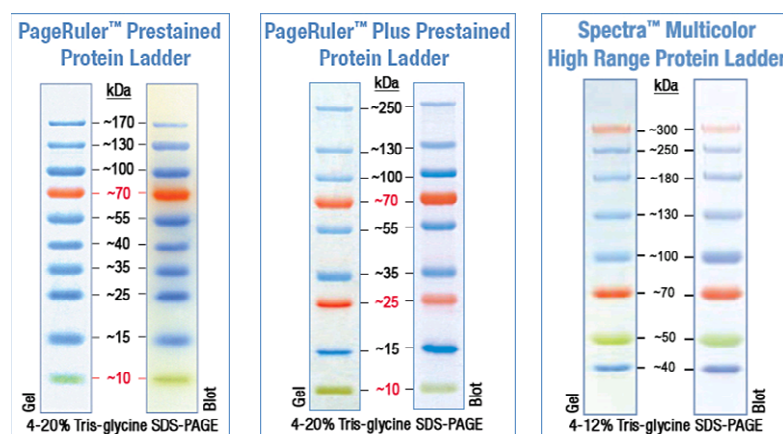


Fig. 2.1: The protein molecular weight standards used for SDS-PAGE. (<http://www.thermoscientificbio.com/nucleic-acid-purification-and-electrophoresis/protein-electrophoresis/protein-ladders>, accessed 11 May 11, 2013).

As DNA marker the 1kb DNA Ladder and 100 bp DNA Ladder by NEB GmbH (Frankfurt/Main) were used (Fig. 2.2). Depending on the size of the gel pockets 4-10 µl of the ladder were applied.

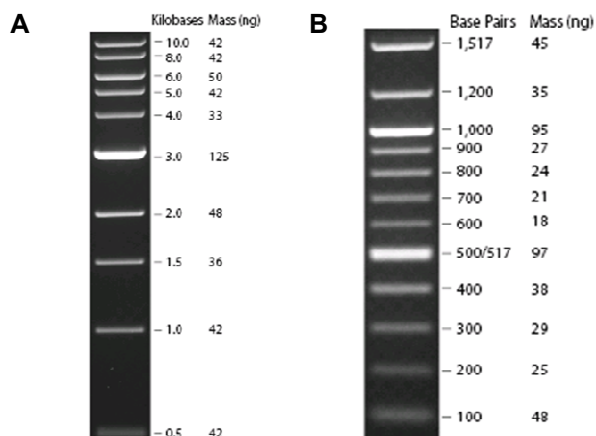


Fig. 2.2: The 1 kb DNA Ladder (A) and 100 bp DNA Ladder (B) by NEB GmbH (Frankfurt/Main) which were used for agarose gel electrophoresis (NEB) (<https://www.neb.com/products/n3232-1-kb-dna-ladder>, <https://www.neb.com/products/N3231-100-bp-DNA-Ladder>, accessed 11 May 11, 2013).

2.1.14 Computer programs and online tools

- CorelDraw® Graphics Suite X4
- BioEdit sequence alignment editor version 7.1.3
- NCBI BLAST (<http://blast.ncbi.nlm.nih.gov/>)
- GraphPad Prism 5
- Zeiss LSM Image Browser Version 4,2,0,121
- ImageJ 1.45 • Vector NTI®
- Melting Temperature (T_m) Calculation (<http://insilico.ehu.es/tm.php>)
- T_m Calculator Phusion polymerase (http://www.finnzymes.fi/tm_determination.html)
- Primer3 version 0.4.0 (<http://frodo.wi.mit.edu/>)
- PlasmDB (<http://plasmodb.org/plasmo/>)
- SMART (<http://smart.embl-heidelberg.de/>)
- Microsoft® Office 2002, Microsoft® Office 2007

2.2 Cell biological methods

2.2.1 Culturing of *Plasmodium falciparum*

Continuous cultures

Culturing of *P. falciparum* blood stages was carried out as described by Ifediba and Vanderberg (1981). Continuous parasite cultures were maintained in small cell culture flasks (25 cm²) in 5 ml pre-warmed culture medium at a hematocrit of 5% at 37°C. Medium was changed daily followed by gassing the culture with 5% CO₂/ 5% O₂ in N₂

(Westfalien AG, Münster) for 10 sec. When a parasitemia of approximately 2% was reached, continuous cultures were diluted in order to avoid density stress that can lead to growth inhibition or formation of sexual parasite stages (Stephens and Christophers, 1908). Dilution was carried out at a ratio of 1:5 to 1:12 by transferring the infected culture to a new cell culture flask filled with fresh medium and human RBCs. At the day after passaging no medium exchange was carried out. Instead flasks were shaken carefully in order to redistribute cells. Wild-type parasites were grown in RPMI medium containing heat-inactivated human serum of the blood type A⁺. Media for culturing KO parasites were supplemented with the respective substance which has been used for selection of transfected parasites.

Gametocyte cultures

Gametocyte cultures were set up by adding 2–4 ml of a continuous culture to a 75 cm² cell culture flask filled with 20 ml of medium and RBCs at a hematocrit of 5%. As for the continuous cultures at the day after passaging, instead of changing medium, flasks were shaken to redistribute cells. Spent medium was aspirated daily and replaced with 15–20 ml fresh medium. To avoid gamete formation upon cooling, gametocyte cultures were kept at 37°C on a slide stretching table and only medium pre-warmed to 37°C was used for these cultures. Induction of gametocyte formation was induced by applying stress to a culture of a parasitemia > 5% containing mainly ring stages. As described by Fivelman *et al.* (2007) spent medium was removed only partially and replaced by an accordant amount of fresh medium. Alternatively, gametocytogenesis was induced by applying stress by low hematocrit as described by Buchholz *et al.*, 2011. In order to obtain gametocyte cultures devoid of asexual blood stages, cultures containing gametocytes of stage II–III were grown in medium containing 50 mM GlcNAc for two to three days. GlcNAc has been reported to kill trophozoites and schizonts (Ponnudurai *et al.*, 1982).

Cryopreservation of cultures

Only cultures of a parasitemia > 2% with > 50% ring stages were frozen for long term storage because other parasite stages would be harmed by the freezing and thawing procedures. A 5 ml culture was transferred to a 15 ml reaction tube and pelleted by centrifugation at 470 x g for 5 min. The cell pellet was resuspended in 1.2 ml glycerolyte solution, shifted to a 2 ml cryotube and incubated for 5 min at RT. The culture then was frozen at –80°C for long-term storage.

Thawing cultures

The frozen parasite culture was rapidly thawed and subsequently transferred to a 15 ml reaction tube. The following solutions were added slowly in order to avoid an osmotic shock of the cells when incubating in decreasing salt concentrations. Centrifugation

steps were carried out at 470 x g for 5 min. Firstly, 200 µl of a 12% NaCl solution were added dropwise followed by incubation for 5 min at RT. The cell suspension was then dropwise supplemented with 10 ml of a 1.6% NaCl solution. After centrifugation the supernatant was removed and the cell pellet was cautiously resuspended in 10 ml of 0.2% Glucose/0.9% NaCl solution. Cells were pelleted by centrifugation and the supernatant was aspirated. Lastly, the cell pellet was resuspended in 5 ml RPMI 1640 complete A⁺ medium, transferred to a 25 cm² cell culture flask and cultivated as above. From day 3 after thawing on, growth of parasites was monitored by preparing blood smears. As soon as the parasitemia was sufficient, 1–2 vials of the culture were frozen to maintain the stock of cryopreserved cultures. KO cultures carrying a blasticidin-resistance gene were immediately taken up in blasticidin medium, whilst other KO parasite lines were kept in A⁺ medium after thawing. Drug pressure was only started when a parasitemia of $\geq 2\%$ was reached.

Synchronization

To obtain synchronized parasite cultures, a culture containing young ring stages at $> 5\%$ was pelleted and subsequently dissolved in 5% sorbitol/ICM. The cell suspension was kept for 10 min at room temperature. After centrifugation (470 x g, 5 min) the cells were washed once with RPMI complete medium. Thereafter, cells were resuspended in complete medium and transferred to a fresh culturing flask. After sorbitol treatment the culture almost exclusively contained ring stages (Lambros and Vanderberg, 1979). If a highly synchronized culture was required as for isolation of schizonts, the procedure was repeated after 4 h.

2.2.2 Monitoring parasite growth via Giemsa-stained blood smears and test for exflagellation

Parasitemia and condition of continuous parasite cultures was controlled thrice per week via thin blood smears. Approximately 100 µl of the culture were pelleted by centrifugation at 3 400 x g. Upon removal of the supernatant the pellet was resuspended in an equal volume of medium as compared to pellet size. A small drop of the cell suspension was transferred onto a glass microscope slide and spread with a second glass slide held in a 45° angle by a single smooth movement. The thin film was allowed to air-dry and fixed with methanol. The slide was air-dried again followed by staining in Giemsa dye bath for 15 min which was prepared by 1:25 dilution of the Giemsa stock solution in Giemsa buffer. By rinsing the slide with dH₂O residual staining solution was removed. Blood smears were viewed at 1 000 x magnification using an oil immersion objective.

The stage of maturation of gametocyte cultures was examined twice a week via Giemsa-stained thin blood smears. The ability of mature gametocyte cultures to undergo gametogenesis was tested via induction of exflagellation of male gametocytes. Depending on

culture density, 100–500 μl of the culture were taken off and xanthurenic acid was added to a final concentration of 20 μM . After incubation at RT for 15 min the sample was placed onto a microscope slide and covered with a cover slip. Exflagellation was monitored light microscopically at 400 x magnification.

2.2.3 Gametocyte purification

Gametocytes were isolated via density gradient centrifugation with Percoll, a sol of silica particles coated with polyvinylpyrrolidone (Pertoft *et al.*, 1978). The gradient was prepared as described by Kariuki *et al.* (1998), with the exception that it only consisted of three layers. A 15 ml reaction tube was filled with 2 ml of 65% and 50% and 4 ml of 35% Percoll dilutions, respectively. All solutions and disposable material used during gametocyte purification were preheated to 37°C. Furthermore, gametocytes were kept at 37°C during purification process in order to avoid early gamete formation. Firstly, gametocyte cultures were pelleted (1 000 x g for 5 min) and washed once in 10 ml ICM. The cell pellet then was resuspended in 1.2 ml ICM and layered on top of the Percoll gradient. Cells were separated via centrifugation at 470 x g for 10 min. Gametocytes were collected from the 35%/50% Percoll interface and transferred to a new test tube. After one more washing step, gametocytes were frozen at –20°C either as cell pellet or in an appropriate buffer. If necessary for downstream applications, the number of isolated gametocytes was determined using a Neubauer chamber and a thin smear was prepared to assess maturation level and composition of isolated parasite material.

2.2.4 Transfection of *Plasmodium falciparum*

P. falciparum parasites were transfected with plasmid constructs based on pCAM-BSD-KO and pCAM-BSD-2 x HA vectors in order to generate either gene-disruptant parasite lines or parasite lines with the gene of interest fused to the DNA sequence encoding a double HA-tag (see 2.1.12, appendix, Fig. 8.4). The KO plasmids constructs were generated by introducing a fragment homologous to the 5' region of the respective gene, omitting the start codon, into the multiple cloning site of the pCAM-BSD-KO vector. Plasmids used for generation of HA-fusion proteins contained a region homologous to the 3' end of the gene of interest omitting the stop codon. Oligonucleotides used for amplification of gene fragments and sizes of PCR products are listed in Tab. 2.7.

The transfection protocol was adapted from Wu, 2008 and Cowman *et al.*, 2008. A synchronized culture was split two days before transfection and freshly isolated human erythrocytes of blood group A⁺ were added. The culture was kept under slow agitation until the day of transfection to avoid double infections of red blood cells. Only cultures at a parasitaemia of $\geq 5\%$ with mainly ring stages were used for transfection. Parasite cultures were supplied with fresh medium and allowed to rest for at least one hour. Then

4–5 ml the culture was pelleted at 4°C and washed once with cold cytomix buffer (Wu *et al.*, 1995). 60 µg of plasmid DNA were resuspended in cold cytomix buffer to a final volume of 400 µl. The plasmid solution was added to the pellet. The resuspended infected RBCs were transferred to a pre-cooled 0.2 cm electroporation cuvette. Cells were electroporated at a voltage of 0.310 kV and a capacity of 950 µF, with a time constant between 10–13 msec. Immediately 500 µl of medium were added and the cuvette was kept on ice for 5 min. Next, the infected RBCs were transferred to a 25 cm³ cell culture flask supplied with 5 ml complete medium and erythrocyte concentrate at a hematocrit of 5% for cultivation. Approximately 4–6 h after transfection drug pressure was initiated by adding blasticidin medium. Thereby only parasites carrying the transfection plasmid containing the blasticidin resistance cassette will survive selection process. As a control parasites were electroporated after addition of cytomix buffer devoid of plasmid DNA. This control culture was split 4–6 h after transfection into two cultures, of which one was exposed to drug pressure, the other one was further cultivated in complete medium lacking blasticidin. From the day after the transfection onwards medium was exchanged daily and 50 µl of RBC concentrate was added once per week. Growth of transfectants was monitored via Giemsa-stained blood smears. Approximately 3 days after transfections no parasites were visible. First parasites resurged after 2–10 weeks. Once a parasitemia of 2% was reached, cultures were split. Aliquots were frozen for cryopreservation regularly. Genomic DNA was isolated on a regular basis in order to examine integration of the plasmid into the gene locus of interest (see 2.3.15). Stably transfected parasites were observed after 5–31 weeks post transfection.

2.2.5 Obtaining clones via limiting dilution and detection of clones by Malstat assay

Cultures of transfectants were split and incubated under agitation two days before dilutional cloning. Total cell number per ml was determined using a Neubauer chamber. After determination of the parasitemia the number of infected RBCs per ml was calculated. The culture was diluted in 25 ml of ICM in three sequential steps to obtain a parasite concentration of 50–200 parasites per ml. A last dilution was carried out to obtain 12 parasites in 38.4 ml complete BSD medium containing 5% RBCs. 200 µl of the suspension were transferred to each well of a 96-well plate, thus distributing 12 parasite-infected RBCs per 96-well plate. For each transfectant 2 96-well plates were set up. Every other day medium was exchanged. Gassing of the incubation chamber with 5% CO₂/5% O₂/ N₂ was carried out daily. Every third time of medium change 1% RBC concentrate was added.

After approximately three weeks the presences of parasite clones was tested by means of Malstat assay. This assay measures the activity of the *Plasmodium* lactate dehydrogenase and can detect parasites at a parasitemia as low as 0.2% (Makler *et al.*, 1998).

20 μ l cell suspension per well were transferred into a new 96-well plate and 100 μ l of the Malstat reagent were added per well. Then, 20 μ l of a mixture of diaphorase and NBT (0.5 mg/ml each) was pipetted into each well. After 30–50 min under agitation medium of wells containing parasites turned purple due to the reduction of NBT. For detection of parasite clones at low parasitemia that did not result of in an obvious color change optical density was determined spectrophotometrically at a wavelength of 630 nm. Cells from wells tested positive were transferred into 25 cm² cell culture flasks and cultivated as described above (see 2.2.1). Once a parasitemia of 2% was reached, cultures were split and aliquots were frozen for cryopreservation. Genomic DNA was isolated in order to confirm absence of parasites with WT genotype (see 2.3.15).

2.2.6 Indirect Immunofluorescence Assay

Methanol fixation

Indirect immunofluorescence assays (IFAs) were carried out to investigate presence and subcellular localization of proteins of interest by means of antisera. Blood stage parasites, gametes and zygotes resuspended in cell culture medium were applied to the wells of teflon coated microscope slides resulting in a single layer of cells. To obtain gametes and zygotes, cultures of mature gametocytes were activated by addition of XA at a final concentration of 20 μ M. Gametes were applied to teflon coated slides 30 min post activation, zygotes after approximately 16 h. For ookinete preparations mosquito midguts were isolated 24 h after a bloodmeal on gametocyte-infected RBCs via membrane feeds (see 2.5.2). Midguts were resuspended in PBS and applied to teflon coated slides. Parasite preparations were air dried followed by fixation in methanol for 10 min at -80°C . Slides were stored at -20°C or processed directly after fixation. Samples were incubated for 30 min in 0.5% BSA/0.01% saponin/PBS followed by a 30 min incubation in 0.5% BSA/0.01% saponin/PBS containing 1% neutral goat serum in order to permeabilize cells and to block unspecific antisera binding sites. Subsequently the primary antiserum in 0.5% BSA/0.01% saponin/PBS was added and incubated for 1.5 h at 37°C . After washing of the slides with 0.5% BSA/0.01% saponin/PBS for 2 x 5 min the samples were incubated with secondary antibodies in 0.5% BSA/0.01% saponin/PBS for 1 h at 37°C . During this step and further steps slides were incubated protected from light due to the light sensitivity of the fluorochrome coupled secondary antibody. After washing in PBS for 2 x 5 min erythrocytes were counterstained with 0.01% Evans Blue in PBS for 1 min except when using Alexa Fluor 594 coupled secondary antibody. After two further washing steps (2 x 10 min in PBS) parasites DNA was stained with Hoechst nuclear stain (1:5000 in PBS) for 1 min. The slides were washed once and anti-fading medium was added to the wells. Preparations were covered with a cover slip, which was sealed with nail polish. Slides were examined with the confocal laser scanning microscope LSM 510 by Zeiss. For storage slides were kept at 4°C .

Paraformaldehyde fixation

Paraformaldehyde (PFA) fixation method was employed to achieve a better preservation of cellular structures, as needed for protein co-localization studies. 1 ml of a gametocyte culture was centrifuged (2 min at 1 600 x g). The cell pellet was resuspended in 4 % PFA/PBS and fixation was carried out overnight at 4°C. Cells were washed twice with sterile-filtered PBS and either processed directly or stored up to several days at 4°C. The following incubation steps were carried out with minor modifications according to Tonkin *et al.*, 2004. Incubation was carried out in 1.5 ml reaction tubes under rotating conditions at room temperature. Cells were centrifuged at 1 500 x g for 1 min between incubation steps. Firstly, cells were permeabilized for 10 min in 0.1 % Triton X-100/PBS. After washing twice, cells were blocked 30 min in 3 % BSA/PBS and further 30 min in 3 % BSA/PBS containing 1 % neutral goat serum. Incubation with primary antibody in 3 % BSA/PBS was carried out for 2 h. After washing (3 x 10 min), iRBCs were incubated for 1 h with the secondary antibody in a 1:1 000 dilution in 3 % BSA/PBS. Subsequently, cells were washed (3 x 10 min) and stained with a 1:2 500 dilution of Hoechst in PBS. After rinsing of cells in PBS for 5 min, cells were pelleted, resuspended in PBS and the suspension was applied to poly-L-lysine coated slides in a single cell layer. Slides were dried at 37°C and subsequently covered with anti-fading mounting medium. A cover slip was placed on the slide and sealed with nail polish. Slides were examined with the confocal laser scanning microscope TCS SP1 by Leica. Slides were kept at 4°C for long term storage.

2.2.7 Transmission electron microscopy

For the investigation of the ultrastructure of gametocytes parasite samples were embedded in epoxy resin (Epon) which allowed the preparation of ultra-thin sections. Pelleted parasites were fixed with 1 % glutaraldehyde/4 % PFA in PBS for 1–16 h at 4 °C. Specimens were washed 2 x 30 min with PBS at room temperature and subsequently post-fixed and contrasted in 1 % OsO₄/1.5 % K₃Fe(CN)₆/PBS for 2 h. After washing twice with MQH₂O cells were incubated in 0.5 % uranyl acetate for 1 h at room temperature. After two further washing steps samples were dehydrated by applying increasing concentrations of ethanol. In detail, 2 x 15 min of incubation were carried out in 70 %, 80 %, 95 % and 100 % of ethanol, respectively. The samples were incubated in propylene oxide for 2 x 30 min. Propylene oxide then was replaced by a 1:1 mixture of propylene oxide and Epon. After 1 h of incubation the mixture was removed after centrifugation and Epon was added. Epon was exchanged after 16 h followed by polymerization for two days at 60°C. Cutting of ultra-thin sections and post-contrastation were carried out by the electron microscopy team of Prof. Georg Krohne at the Biocenter of the University of Würzburg. Specimens were examined and documented by means of a Zeiss

EM10 transmission electron microscope. Scanned images were processed using Corel PHOTO-PAINT X4.

2.2.8 Exflagellation assays

The effects of potential inhibitors or activators of gametogenesis were investigated via exflagellation assays. In these *in vitro* bioassays the formation of male gametes via exflagellation was studied. Depending on the cell density 100–500 μ l of a gametocyte culture were used per sample investigated. In most cases gametocytes were incubated with potentially inhibiting substances prior to induction of gametogenesis for 15 min at 37°C. Inhibitors were added directly into the cell culture medium. Alternatively, the culture aliquot was centrifuged (3 000 x g, 15–30 s) and the substance of interest dissolved in ICM, pH 7.4 was added. After pre-incubation the sample was centrifuged (3 000 x g, 15–30 s) and the cell pellet was resuspended in 10–20 μ l of the substance in PBS or ICM, pH 7.4 and 10 μ M XA followed by incubation at room temperature for 15 min. 10–15 μ l of the sample were transferred to a microscopic slide, covered with a cover slip and evaluated microscopically at 400 x magnification. For each sample the number of exflagellation centers for 30 visual fields was determined. For each test condition three independent samples were investigated, if not otherwise indicated. Samples were taken off individually, gassing the gametocyte culture after each withdrawal of a sample. Alternatively, samples for each test condition were taken off at once and samples were stored at 37°C until used. In this case, a positive control was tested before and after all additional samples to confirm stable condition of the parasites.

Preparation of RBC homogenate

To investigate the uptake of XA by non-infected RBCs the latter were incubated with XA under different conditions. 1.5 ml of RBC concentrate per sample were centrifuged, the supernatant was removed and cells were resuspended in 4 ml PBS containing the substances to be investigated, e. g. XA at different concentrations or XA combined with potential inhibitors. Pre-incubation with inhibitors was carried out at 37°C. After incubation with XA at room temperature the incubation solution was diluted with ice-cold PBS ad 50 ml and centrifuged (1 260 x g, 5 min, at 4°C). The RBC pellet was washed 4 times with PBS to remove residual extracellular XA. The pellet was finally resuspended in 750 μ l PBS. The cell suspension (referred to as XA-RBCH, homogenated of XA-incubated RBCs) was sonicated (2 min 50% intensity; 50% duty cycle) on ice. Cell debris was pelleted by centrifugation (5 min, 15 500 x g) and the cell lysate was further cleared by filtration through a 0.22 μ m syringe (referred to as XA-RBCF). The ability of XA-RBCF to induce gametogenesis was investigated via exflagellation assays. 10–20 μ l of the XA-RBCF were added to the pelleted gametocyte culture and incubated for

15 min at room temperature. Handling of gametocyte culture and microscopically evaluation were carried out as described above.

The composition of stock solutions, working concentrations and literature values for working concentrations of published inhibitors of transport proteins are listed in Tab. 8.1 (Appendix). Data for other substances used in the study of gametocyte activation/ XA uptake by RBCs are listed in Tab. 8.2 (Appendix).

When producing XA-RBCH for ultracentrifugation cells were ruptured via three freezing/thawing cycles and passaging through a 26 g injection needle. Samples were centrifuged to remove debris. Thereafter the lysate was centrifuged 25 min at 50 000 rpm. The pellet fraction was washed two times with PBS (50 000 rpm, 30 min).

2.3 Molecular biological methods

2.3.1 Polymerase chain reaction

The polymerase chain reaction (PCR) was used for to amplify DNA fragments of genes of interest, which subsequently were cloned into an appropriate DNA plasmid for downstream applications such as production of inclusion bodies and recombinant proteins or the generation of transfection plasmids. For these purposes the Phusion High Fidelity DNA Polymerase was chosen due to its high proofreading capacity as well as its high fidelity. Genomic DNA obtained from mixed asexual parasite stages served as template (see 2.3.15).

Tab. 2.11: Composition of PCRs using Phusion polymerase.

Component	Final concentration	Volume
5 x Phusion HF Buffer	1 x	10 μ l
dNTPs (10 mM)	200 μ M	1 μ l
Sense primer (100 μ M)	1 μ M	0.5 μ l
Antisense primer(100 μ M)	1 μ M	0.5 μ l
DNA template (100 ng/ μ l)	2 ng/ μ l	1 μ l
Phusion DNA Polymerase	0.2 U/ μ l	0.5 μ l
Autoclaved MQH ₂ O		36.5 μ l
Total volume		50 μ l

The primer annealing temperature was calculated as suggested by the internet-based tool provided by the manufacturer. The annealing temperature for Phusion PCRs is about 5°C higher than that determined for other polymerases. As recommended by the manufacturer for primers >20 nucleotides an annealing temperature of $T_m + 3^\circ\text{C}$ of the

lower T_m of both primers was used. For primers ≤ 20 nucleotides an annealing temperature equal to the lowest calculated T_m was used. The composition of ingredients of the PCR is listed in Tab. 2.11. The program used for amplification of DNA fragments employing fusion polymerase is depicted in Tab. 2.12.

Tab. 2.12: PCR program for Phusion polymerase.

Reaction step	Temperature	Duration	Number of cycles
Initial denaturation	98°C	30 s	1
Denaturation	98°C	10 s	33
Annealing	as calculated	30 s	
Elongation	72°C	30 s/kb	
Final elongation	72°C	5 min	1
Storage	12°C	∞	–

For diagnostic PCRs aiming at investigation of modified gene loci (see 2.2.4) as well as for colony PCRs (see 2.3.8) the GoTaq polymerase was used. The following reaction composition and PCR program was applied (Tab. 2.13, Tab. 2.14). For difficult PCR primer combinations which did not result in any PCR product a modified version of the L60 PCR program (Kim Williamson, Chicago) was used. In this program a lower temperature for primer extension is used which improves amplification of templates with high A + T content (Tab. 2.15, Su *et al.*, 1996).

Tab. 2.13: Composition of PCRs using GoTaq DNA polymerase.

Component	Final concentration	Volume
5 x GoTaq Flexi Green Buffer	1 x	10 μ l
MgCl ₂ (25 mM)	2 mM	4 μ l
dNTPs (10 mM)	200 μ M	1 μ l
Sense primer (100 μ M)	1 μ M	0.5 μ l
Antisense primer(100 μ M)	1 μ M	0.5 μ l
DNA template (100 ng)	2 ng/ μ l	XY μ l
GoTaq DNA polymerase (5 U/ μ l)	0.025 U/ μ l	0.25 μ l
autoclaved MQH ₂ O	-	ad 50 μ l

The annealing temperature for the primers of the PCR reaction was determined from the melting temperature (T_m) of the respective oligonucleotides which was obtained from the internet-based tool “Melting Temperature (T_m) Calculation”. The annealing temperature was chosen approximately 3°C below the calculated melting temperature in order to ensure efficient hybridization of the primers to the PCR template. Only the part of the

primer sequence which was complementary to the gene of interest was used for the calculations omitting additional nucleotides like restriction sites. Amplification of the desired PCR product was examined via agarose gel electrophoresis (see 2.3.2). Prior to further usage the PCR amplified DNA fragments were purified as described in 2.3.4.

Tab. 2.14: PCR program for GoTaq polymerase.

Reaction step	Temperature	Duration	Number of cycles
Initial denaturation	95°C	2 min	1
Denaturation	95°C	40 s	33
Annealing	as calculated	50 s	
Elongation	72°C	1 min/kb	
Final elongation	72°C	5 min	1
Storage	12°C	∞	–

Tab. 2.15: Modified version of L60 PCR program for GoTaq polymerase.

Reaction step	Temperature	Duration	Number of cycles
Initial denaturation	94°C	5 min	1
Denaturation	94°C	40 s	35
Annealing	40°C	50 s	
Elongation	60°C	3 min	
Storage	12°C	∞	–

2.3.2 Agarose gel electrophoresis

Agarose gel electrophoresis allows the separation of DNA fragments of a size ranging from 0.5–25 kb. Depending on the size of the PCR products that were to be analyzed 0.8–2% agarose in TAE buffer was prepared. The voltage applied was 5–7 V/cm (distance between electrodes). Approximately 10 µl of GoTaq amplified PCR products were loaded directly into the gel slots, since the reaction buffer already contained loading buffer. Phusion polymerase amplified PCR products were diluted in MQH₂O and supplied with 6x loading dye. After separation of DNA fragments agarose gels were stained in ethidium bromide solution (0.5 µg/ml) for 15 min. After rinsing, gels were examined and documented with a UV transilluminator. Alternatively, ethidium bromide stain was added directly to agarose solution (0.3 µg/ml) prior to casting the agarose gel.

2.3.3 Subcloning of PCR products

In most cases PCR products were subcloned into the shuttle vector pGEM-T Easy prior to insertion into the destination vector. Thereby, complete digestion of PCR products restriction endonucleases is ensured. The 3' overhangs of the commercially available pGEM-T Easy vector (Promega) were removed and the vector was ligated to allow replication. The circular plasmid was kindly provided by the laboratory of Prof. Ute Hentschel, Würzburg. The plasmid was linearized by digestion with EcoRV thereby enabling blunt end ligation with PCR products. The vector was dephosphorylated with antarctic phosphatase or calve intestinal phosphatase (CIP, see 2.3.5) to prevent religation of vector backbone not containing an insert. The PCR products were phosphorylated by means of a polynucleotide kinase (PNK). Composition of the reaction mix is depicted in Tab. 2.16. Firstly, a dilution of the purified PCR product in MQH₂O containing the PNK reaction buffer was denaturated by incubation at 70°C for 10 min. After incubation on ice for 2 min, dATP and the PNK were added, followed by incubation at 37°C for 30 min. The enzyme was heat inactivated by incubation at 65°C for 20 min. The phosphorylated PCR product was purified as described in 2.3.4.

Tab. 2.16: Composition of phosphorylation reactions.

Component	Concentration	Amount
Purified PCR product	12.5 ng/μl	500 ng
PNK Buffer 4	10 x	4 μl
ATP	0.2 mM	1 μl
T4 PNK	10 U/ μl	2 μl
MQH ₂ O	–	ad 40 μl

2.3.4 Purification of PCR products and gel purification of vectors

Purification of PCR products was carried out using the NucleoSpin Gel and PCR Clean up kit (Macherey-Nagel). The columns provided with the kit contain a silica membrane. The purification is based on the binding of DNA to the silica membrane in the presence of chaotropic salts. During washing steps PCR components that might interfere with following application (e.g. dNTPs, enzymes) are removed. The same kit was used for the gel elution of DNA bands cut out from agarose gels. Gel purification was used for purification of vectors after digestion with restriction endonucleases or to isolate PCR fragments ligated into pGEM-T easy vector after digestion with restriction enzymes. For purification of both PCR products and vectors 30–50 μl MQH₂O was used for elution of DNA. The eluate was loaded a second time onto the silica membrane and a second elution was performed when high DNA concentrations were required. All other steps were carried out as described in the manufacturer's protocol.

2.3.5 Preparative restriction digest

Destination vectors and PCR products beforehand cloned into pGEM-T-Easy vector were digested with restriction enzymes to provide sticky ends for subsequent ligation. Digest was carried out as a 50 µl reaction containing 3–5 µg of plasmid DNA and 36 U of each restriction enzyme. Double digests and addition of BSA was performed as suggested by the manufacturer. The reaction was performed for at least 3 h at 37°C. One hour before stopping the reaction antarctic phosphatase and the 10x antarctic phosphatase reaction buffer were added when digesting the destination vector. Due to hydrolysis of terminal phosphate residues a religation of cut vector can be avoided. Where applicable the restriction enzymes were heat-inactivated. The restriction digested vectors and PCR products were separated via agarose gel electrophoresis and subsequently purified with the NucleoSpin Gel and PCR Clean up Kit (see 2.3.4). Beside the isolation of restriction fragments of interest this procedure also ensures the removal of not inactivated restriction enzymes which might interfere with further reactions.

2.3.6 Ligation

The ligation of PCR product and vector were mediated by T4 DNA Ligase. For blunt end ligation reactions PCR product and vector were used in a molar ratio of 5:1, for sticky end ligations a molar ratio of 3:1 was used. The following equation was used to determine the amount of PCR product needed for sticky end reactions:

$$\text{Mass}_{\text{Fragment}} [\text{ng}] = 3 \times \text{Mass}_{\text{Vector}} [\text{ng}] \times \text{Length}_{\text{Fragment}} [\text{bp}] / \text{Length}_{\text{Vector}} [\text{bp}]$$

A mass of 50 ng of the respective vector was used. The volumes of the components of the reaction are listed in Tab. 2.17. Blunt end ligations were incubated at 4°C overnight. Sticky end ligations were incubated at least for 1 h at room temperature. For extended ligation reaction longer than 1 h, the reaction tubes were stored at 4°C.

Tab. 2.17: Composition of ligation reactions.

Component	Concentration	Volume
Vector		X µl
PCR product		Y µl
T4 DNA Ligase Buffer	10x	10 µl
T4 DNA Ligase	400 U/µl	1 µl
MQH ₂ O	–	ad 20 µl

2.3.7 Transformation of *E. coli*

Both *E. coli* NovaBlue and BL21 CodonPlus®(DE3)-RIL were transformed via heat shock. 20 µl of competent *E. coli* cells were thawed on ice. Of a ligation reaction a vo-

lume of 2 μl were added to the *E. coli* cells, of a plasmid preparation 1 μl was added followed by incubation on ice for 30 min. Heat shock was applied for 30 s at 42°C. The bacteria were returned to ice immediately for 2 min. After addition of 200 μl SOC medium cells were incubated under rotation for 1 h. For the transformation of *E. coli* NovaBlue cells with a ligated plasmid the entire bacteria suspension was streaked onto LB agar plates with the appropriate antibiotic for selection of successfully transformed bacteria. Only 100 μl of the bacteria suspension were distributed onto LB agar plates containing the respective antibiotic when transforming *E. coli* BL21CodonPlus® (DE3)-RIL cells with a plasmid. Plates were incubated at 37°C overnight.

2.3.8 Analysis of transformants

Bacteria clones obtained after transformation of ligated plasmid constructs were analyzed via colony PCR or via diagnostic restriction digest. For colony PCR clones were picked, streaked on a master LB agar plate and resuspended in 25 μl MQH₂O. 2 μl of this suspension was then used in a diagnostic PCR as described above (see 2.3.1) using primers complementary to the region of the vector flanking the insert. Alternatively, bacteria clones carrying a plasmid with the DNA fragment of interest inserted correctly were identified via restriction digest. Overnight cultures were set up and plasmid DNA was isolated via a column-free method as described (see 2.3.9). A small scale digest reaction was used (Tab. 2.18) and the reaction was incubated for a minimum of one hour at 37°C.

Tab. 2.18: Composition of diagnostic restriction digests.

Component	Concentration	Volume
Plasmid DNA		2 μl
Enzyme 1	20 U/ μl	0.5 μl
Enzyme 2	20 U/ μl	0.5 μl
Buffer 4	10 x	1 μl
BSA (if applicable)	10 x	1 μl
MQH ₂ O	–	ad 10 μl

2.3.9 Isolation of plasmid DNA

Plasmid DNA isolation with commercially available kits

Plasmid DNA for sequencing, for transfection and expression of recombinant proteins was isolated using the NucleoSpin® Plasmid kit (Macherey-Nagel) allowing isolation of up to 40 μg plasmid DNA from a 1–5 ml overnight culture. The kit was used according to the manufacturer's description. Usually 4 ml of a 5 ml overnight culture were used. For elution of the plasmid DNA bound the silica membrane of the columns pro-

vided MQH₂O was used. The eluate was applied to the silica membrane and a second elution was carried out if a high yield of plasmid DNA was required. For isolation of larger amounts of plasmid DNA the NucleoBond® Xtra Midi kit (Macherey-Nagel) was used as indicated by the manufacturer, which allows isolation of up to 250 µg plasmid DNA from a 200 ml overnight culture.

Column-free protocol for plasmid DNA isolation

When plasmid DNA was isolated to screen plasmids for the presence of the PCR product inserted into a vector an alternative column-free protocol based on alkaline lysis of the bacteria was applied (“Dirty mini”). 4 ml of an overnight bacteria culture were centrifuged at 9 500 x g for 1 min. The resulting pellet was resuspended in 100 µl of buffer P1 and incubated on ice for 10 min. Subsequently, 200 µl of the lysis buffer P2 were added. After mixing by inversion of reaction tubes, samples were incubated on ice for further 5 min. After addition of 150 µl cold 3 M potassium acetate (pH 4.8) the suspension was again incubated on ice for 10 min. This step results in precipitation of genomic DNA, proteins and cell debris. 450 µl of 5 M LiCl were added to precipitate RNA. After cautious mixing of the samples contaminants were pelleted by centrifugation at 15 500 x g for 15 min. The supernatant was transferred into a new reaction tube and plasmid DNA was precipitated by addition of 600 µl isopropanol. After mixing the reaction tubes were centrifuged for 10 min at 15 500 x g. The pellet was washed with 70 % ethanol and centrifuged again. Finally, the pellet was air-dried and resuspended in 30 µl MQH₂O.

2.3.10 Determination of DNA concentration

DNA concentration was determined via spectrophotometer or via Nanodrop® spectrophotometer. In both cases optical density of the DNA solution at a wavelength of 260 nm was measured and the concentration was calculated with the following equation:

$$c [\mu\text{g/ml}] = \text{OD}_{260} \times D \times F$$

D represents the dilution factor and F the multiplication factor, 50 for dsDNA and 40 for RNA. The quotient of OD₂₆₀ und OD₂₈₀ allows estimation of purity of the DNA solution. A solution devoid of protein contaminations exhibits a quotient between 1.8 and 2.0. When measuring the DNA concentration with the Nanodrop® spectrophotometer 1 µl of the solution was applied without further dilution. For measurements with the spectrophotometer 2 µl of DNA solution were diluted in 68 µl MQH₂O.

2.3.11 DNA Sequencing

The sequencing method used is based on the principle of the chain-termination method (Sanger *et al.*, 1977). Beside deoxynucleotides fluorescently labeled dideoxynucleotides

are utilized during the sequencing PCR. These do not exhibit a hydroxyl group at their 3' C atom, which results in termination of DNA strand synthesis and PCR products of different lengths are produced. During the separation of these chain-termination products the fluorescent dyes are excited and the resulting fluorescence signal is detected, analyzed and depicted as chromatogram.

Sequencing of plasmid constructs was performed at the Institute for Virology of the University of Würzburg on a fee for service basis. The sequencing PCR was carried out as listed in Tab. 2.19 using the BigDye™ Terminator Cycle Sequencing Kit (Applied Biosystems™). The ready to use sequencing mix contained the AmpliTaq® DNA polymerase, FS, deoxynucleotides, fluorescently labeled dideoxynucleotides und MgCl₂. The primers used for sequencing of the different vectors used are listed in Tab. 2.9. A standard program was used for all plasmids sequenced (Tab. 2.20).

Tab. 2.19: Composition of sequencing PCRs using the Big Dye® Terminator Cycle Sequencing Kit.

Component	Amount
5 x sequencing mix	2 µl
5 x Buffer	2 µl
Template	0.1–0.4 µg
Primer	15–50 pmol
ddH ₂ O	ad 10 µl

Tab. 2.20: PCR program for sequencing PCRs.

Reaction step	Temperature	Duration	Number of cycles
Initial denaturation	95°C	4 min	1
Denaturation	96°C	30 s	30
Annealing	50°C	30 s	
Elongation	62°C	4 min	
Final elongation	72°C	3 min	1
Storage	12°C	∞	-

The PCR products were purified via DNA precipitation. Reagents were added to the PCR product as listed in Tab. 2.21. After mixing of all components the samples were centrifuged for 15 min at 15 500 x g. The resulting pellet was washed with 70 % ethanol. After further centrifugation 15 min at 15 500 x g) the supernatant was removed and the pellet was air-dried. Finally the precipitated plasmid DNA was resolved in 25 µl HiDi formamide.

Tab. 2.21: Components used for purification of sequencing PCR reactions.

Component	Amount
PCR reaction	10 μ l
ddH ₂ O	90 μ l
3 M NaAc pH 4.6	10 μ l
100 % ethanol	250 μ l

2.3.12 RNA isolation

Column-free protocol for RNA purification

RNA isolation was performed using the reagent TRIzol, a monophasic solution of phenol and guanidine isothiocyanate as described (Kyes, 2008). For isolation of gametocyte RNA the gametocytes were isolated via Percoll gradient (see 2.2.3) omitting all washing steps except the washing of parasites after aspirating the gametocyte-containing interphase between 50% and 65% Percoll. When isolating RNA of asexual parasite stages no saponin lysis was performed. Instead, the parasite pellet was resuspended directly in 20 pellet volumes of prewarmed TRIzol followed by incubation at 37°C for 5 min. If not processed immediately suspensions were stored at -80°C. Next, 0.2 TRIzol volumes of chloroform were added and samples were mixed by rotation. Reaction tubes were centrifuged (9 000 x g for 1.5 ml reaction tubes, 1 400 x g for 15 ml reaction tubes) for 30 min at 4°C. The aqueous layer which located to the top layer was transferred to a new collection tube avoiding carrying over of interface containing DNA. Subsequently, 0.5 volumes of isopropanol were added and tubes were inverted several times. Samples were precipitated for a minimum of 2 h at 4°C up to several days. After centrifugation for 3 min at 4°C (15 500 x g) supernatant was removed and the RNA pellet was washed in 750 μ l of 75 % ethanol. Subsequently, the pellet was air-dried at room temperature for 5 min. 50 μ l DEPC-H₂O were added and samples were heated at 60°C for 10 min. Finally the pellet was dissolved by resuspension. RNA concentration was determined and aliquots were prepared for storage at -80°C as repeated freezing-thawing cycles destroys RNA stored in DEPC-H₂O.

DNase treatment

In order to remove potential contaminations of RNA with genomic DNA a DNase treatment was carried out for 10 min at RT as recommended by the manufacturer of the enzyme (QIAGEN, see Tab. 2.22). DNase treated RNA was purified via phenol-chloroform extraction. 250 μ l of DEPC-H₂O, 150 μ l phenol and 150 μ l chloroform were added after DNase treatment and mixed well. After incubation at room temperature for 3 min samples were centrifuged for 10 min at 10 000 x g at 4°C. The aqueous top phase was transferred to a new tube, 300 μ l chloroform were added and samples were mixed

by agitation. After 5 min of incubation at RT samples were centrifuged for 10 min at 10 000 x g at 4°C. The aqueous top phase again was transferred to a new collection tube and RNA was precipitated by adding 0.1 volumes of cold 3 M NaAc (pH 4.8-5.2, DEPC-treated) and 2.5 volumes of cold 100% ethanol. After incubation at 4°C for 30 min to 24 h samples were centrifuged for 30 min at 15 500 x g at 4°C. The pellet was washed with 1 ml of ice-cold RNase-free 75% ethanol. After vortexing the pellet was centrifuged at 4°C (10 min, 15 500 x g). The RNA pellet was air-dried for 5 min at RT. Resolving and storage of RNA was performed as mentioned above for RNA isolation.

Tab. 2.22: Components and respective amounts used for DNase treatment.

Component	Amount
RNA in DEPC-H ₂ O	up to 87.5 µl
Buffer RDD	10 µl
DNase I (2.73 Kunitz U/µl)	2.5 µl
DEPC-H ₂ O	ad 100 µl

RNA isolation with commercially available kits

RNA of wild-type gametocytes was mainly obtained by means of the innuPREP RNA Mini Kit (Analytik Jena AG). This approach was chosen due to the very low yields obtained when RNA of gametocytes was isolated via the Trizol-based method. The kit contains a genomic DNA-binding column, which allows removal of the major part of genomic DNA from the samples. Additionally, an on-column DNase treatment was applied to the RNA bound by the second column. RNA was eluted with RNase-free water and elution was carried out twice in order to increase the yield of isolated RNA. The RNA samples were stored as described above.

2.3.13 cDNA synthesis and RT-PCR

Synthesis of cDNA was performed by means of the Superscript III First Strand Synthesis Kit II for RT-PCR (Invitrogen). The reaction was set up as recommended by the manufacturer (Tab. 2.23).

Tab. 2.23: Components used for preparing RNA for cDNA synthesis.

Component	Amount
RNA	up to 5 µg
Random hexamers (50 ng/µl)	1 µl
dNTP mix (10 mM)	2.5 µl
DEPC-H ₂ O	ad 10 µl

The reaction mix was incubated at 65°C for 5 min and subsequently incubated on ice for at least 1 min. The cDNA synthesis continued by adding the reagents necessary for reverse transcription as listed in Tab. 2.24.

10 µl of the reverse transcription mix (Tab. 2.14) was added to the RNA primer mix. For each RNA preparation one control reaction was carried out where instead of the SuperScript III RT DEPC-H₂O was added (–RT control). This control served as negative control to confirm absence of genomic DNA. After mixing, samples were incubated at room temperature for 10 min followed by incubation at 50°C for 50 min. The reaction was terminated by incubation at 80°C for 5 min and subsequently incubated on ice. Finally, 1 µl of RNase H was added to each reaction and incubated at 37°C for 20 min.

Tab. 2.24: Components and respective amounts used for cDNA synthesis.

Component	Amount
10x RT buffer	2 µl
25 mM MgCl ₂	4 µl
0.1 M DTT	2 µl
RNase OUT	1 µl
SuperScript III RT	1 µl

The final concentration was calculated according to the amount of RNA used for cDNA synthesis. 125 ng of cDNA were used per RT-PCR reaction. The reaction was prepared as described for PCRs employing GoTaq polymerase (see 2.3.1). The PCR program was altered for RT-PCRs as listed in Tab. 2.25.

Tab. 2.25: PCR program for RT-PCR using GoTaq polymerase.

Reaction step	Temperature	Duration	Number of cycles
Initial denaturation	95°C	4 min	1
Denaturation	95°C	30 s	25
Annealing	as calculated	30 s	
Elongation	72°C	1.5 min	
Final elongation	72°C	5 min	1
Storage	12°C	∞	–

2.3.14 Southern Blot

DNA digest, separation, transfer

Southern blot analysis was carried out in order to confirm mutated gene loci of parasites transfected with pCAM-BSD vector or pCAM-BSD-HA vector. Concentration of isolated genomic DNA was determined spectrophotometrically and confirmed by separation of 0.5 µg DNA via agarose gel electrophoresis. 3 µg of DNA were digested with restriction endonucleases. Reactions were prepared in a total volume of 20 µl and incubated for 6–16 h. Restriction digested DNA (3 µg per lane) was separated via a 0.8% agarose gel at low voltage (e.g. 2 V/cm electrode distance for 15 min and 1 V/cm overnight) to ensure high resolution of separation. After electrophoresis the gel was incubated in 0.25 M HCl under agitation for 30 min in order to achieve depurination of fragments >5 kb. After rinsing the gel briefly in MQH₂O the gel was incubated in 0.5 M NaOH/1.5 M NaCl for 30 min to denature DNA. The gel was rinsed in MQH₂O again and neutralized by incubation in 0.5 M Tris-HCl/1.5 M NaCl for 3 x 15 min. The DNA was transferred via capillary transfer onto a nylon membrane. Three layers of whatman paper were soaked with 20 x SSC and placed onto a sponge lying in a tray filled with 20 x SSC. The nylon membrane was firstly soaked in MQH₂O, secondly in 20 x SSC for 5 min and then placed onto the gel. The membrane was covered by three layers of whatman paper soaked in 2 x SSC. Air bubbles between the different layers were removed. Finally a stack of paper towels were placed on top and transfer was carried out for approximately 16 h. The efficiency of transfer was controlled after staining of the agarose gel with ethidium bromide. The damp membrane was UV crosslinked placed on a sheet of whatman paper soaked with 10 x SSC. The membrane was rinsed in MQH₂O briefly. When not proceeding with hybridization immediately the membrane was air-dried and stored at 4°C. Alternatively to the capillary transfer DNA was transferred via electro blot from the gel to the nylon membrane. In this case, the gel and the nylon membrane soaked in MQH₂O and 20 x SSC were placed onto the vacuum blot apparatus. Depurination, denaturation and neutralization were carried out with the solutions mentioned above for 15 min each with the vacuum pump set to 0.05 bar. The transfer was carried out for 90 min with 20 x SSC. The DNA was fixed via UV crosslinking as described above.

Preparation of probe

A DNA fragment of 100–1000 bp (primers see Tab. 2.9) was amplified via PCR by 5 reactions of 50 µl each. The PCR products were pooled and purified via gel purification (see 2.3.4). 1 µg of the probe was diluted in 16 µl MQH₂O and denatured by incubation at 95°C for 3 min and immediate cooling on ice. The labeling of the probe was carried out using the DIG High Prime DNA Labeling and Detection Starter Kit II (Roche) as described in the manual. Subsequently 4 µl of DIG High Prime was added and incubated

for 20 h at 37°C. Thereby a digoxigenin (DIG)-label was transferred to the DNA probe. The labeling reaction was terminated by addition of 2 µl 0.2 M EDTA or heat inactivation for 10 min at 65°C.

Hybridization and detection of DNA probe

Hybridization and detection were carried out as recommended by the kit's manufacturer. The optimal hybridization temperature (T_{opt}) was calculated with the following equation:

$$T_m = 49.82 + 0.41 (\% \text{ G+C}) - (600/\text{length of hybrid in bp})$$

$$T_{opt} = T_m - 20 \text{ to } 25^\circ\text{C}$$

The DIG Easy Hyb granules were dissolved as described and preheated to T_{opt} . 10 ml per 100 cm² membrane (at least 20 ml) were added to the membrane placed into a hybridization tube. The membrane was incubated for 30 min to 1 h under rotation to prepare it for hybridization. The DIG-labeled probe was denatured by heating to 95°C for 5 min followed by rapid cooling. The probe was added to preheated DIG Easy Hyb to achieve a final concentration of 25 ng/ml. 3.5 ml/100 cm² of the probe solution (at least 20 ml) was added to the membrane after removal of prehybridization solution and the hybridization process was carried out overnight at T_{opt} under rotation.

The membrane then was washed twice in 2 x SSC/0.1% SDS for 10 min at room temperature and 2 x 30 min in prewarmed 0.5 x SSC/0.1% SDS at 54°C. The membrane was washed in Southern blot washing buffer for 3 min shaking, then the membrane was incubated for 30 min in 100 ml blocking solution under rotation at room temperature. Anti-DIG alkaline phosphatase-conjugated antibody supplied with the detection kit was centrifuged for 5 min at 10 000 x g and an aliquot was taken from the top of the antibody solution. The membrane was incubated with anti-DIG antibody diluted 1:10 000 in blocking buffer. After washing twice with washing buffer for 15 min each, the membrane was incubated for 2 x 5 min in equilibration buffer. The nitrocellulose membrane was placed into a plastic folder and CSPD solution was added, followed by a 5 min of incubation at room temperature. After further incubation at 37°C for 10 min the luminescence signal was detected either by exposure on an X-ray film or by a luminescence image analyzer. Exposure times ranged from 15–45 min.

If the membrane was to be reused it was not allowed to dry out. After rinsing the membrane thoroughly in MQH₂O it was washed 3 x 15 min at 37°C in 0.2 M NaOH/0.1% SDS. Then it was rinsed thoroughly in 2 x SSC and stored in either 2 x SSC or Maleic acid at 4°C. DIG Easy Hyb containing DIG-labeled probe was stored at -20°C if reused for a second hybridization. Prior to use it was then denatured by incubation at 68°C for 10 min.

2.3.15 Isolation of genomic DNA

Genomic DNA isolation with commercially available kits

The isolation of genomic DNA for investigation of the genotype of mutated parasites via PCR was carried out by means of the NucleoSpin® Blood kit (Macherey-Nagel). 5–10 ml of a parasite culture of a parasitemia of $\leq 5\%$ were supplied with 10% saponin/PBS to a final concentration of 0.2% saponin. After 10 min of incubation at RT the lysed culture was centrifuged (5 min, 3 200 x g). After washing with 10 ml PBS the sample was centrifuged again at 3 200 x g for 5 min. The resulting pellet was stored at -20°C or processed directly as described in the manual of the kit.

For investigation of the genotype of mutated parasites via Southern blot the MasterPure™ DNA Purification Kit (Epicenter®) was employed. At least 20 ml of an asexual culture (parasitemia of $\leq 5\%$) were saponin-treated as described above. The pellets were treated as recommended by the manufacturer.

Column-free protocol for isolation of genomic DNA

Genomic DNA as template for cloning PCRs was obtained via phenol-chloroform extraction. A 20 ml culture of asexual parasites of a parasitemia of $\leq 5\%$ was pelleted and lysed by adding 0.15% saponin in PBS (5 min, RT). Parasites were pelleted and washed twice with PBS. The pellet was taken up in 500 μl TSE buffer, 100 μl 10% SDS and 50 μl of 6 M NaClO_4 . The suspension was incubated overnight under agitation at room temperature. Then, an equal volume of phenol was added and the samples were incubated for 5 min under agitation. After centrifugation (15 500 x g, 5 min) the colorless aqueous top phase was transferred to a clean tube. 0.5 volumes each of phenol and chloroform were added followed by 5 min of incubation and centrifugation (15 500 x g, 5 min). Again the top phase was transferred to a new reaction tube and 1 volume of chloroform was added, incubated under agitation and centrifuged. Subsequently, 2 volumes of ethanol were added and the samples were incubated under gentle agitation for 5 min. After centrifugation the pellet was washed with ice-cold 70% ethanol and air-dried. Finally, the pellet was dissolved in 40 μl of MQH_2O by incubation at $55\text{--}60^{\circ}\text{C}$.

2.3.16 Cultivation and storage of bacteria

E. coli bacteria cells were cultivated in LB medium containing the antibiotic required for selection of bacteria cells of interest. Overnight cultures were incubated 14–18 h at 37°C in Kapsenberg tubes at 225 rpm. Larger volumes cultivated in Erlenmeyer flask were incubated at 150 rpm. Bacteria suspensions streaked onto LB agar plates were incubated at 37°C for 14–18 h. For long-term conservation of bacteria 1 ml of a 3–5 ml overnight culture was resuspended with 1 ml bacteria freezing solution containing glycerol, transferred to cryotubes and stored at -80°C .

2.4 Protein biochemical Methods

2.4.1 Expression of recombinant proteins

For expression of recombinant proteins the *E. coli* expression strain BL21 Codon-Plus®(DE3)-RIL (Agilent Technologies) was used. It possesses the following genotype: *E. coli* B F⁻ *ompT hsdS* (r_B⁻ m_B⁻) *dcm*⁺ Tet^r *gal λ*(DE3) *endA* Hte [*argU ileY leuW* Cam^r]. These cells contain additional copies of tRNA genes that are common in organisms with AT-rich genomes. They are encoded by a plasmid conferring chloramphenicol resistance. The expression vectors used possess the *tac* promoter, which is a strong promoter that can be repressed by the LacI protein, repressor of the *lac* operon.

Small scale protein expression

Expression in a small scale culturing volume was carried out as a first test to investigate whether the synthesized recombinant protein possesses the correct size and is expressed in sufficient amounts. After transformation of BL21-CodonPlus®-(DE3)-RIL cells with the respective plasmid as described (see 2.3.7) 5 ml overnight cultures were prepared. LB medium contained the antibiotic required for selection of bacteria possessing the expression plasmid as well as chloramphenicol which prevents loss of the plasmid encoding additional tRNAs. After the overnight incubation, two tubes with 1:5 dilutions of the original cultures were set up and incubated at 37°C until an OD of 0.5 was reached. Then protein expression was induced in one of the samples by addition of 0.75 mM IPTG (Isopropyl-β-D-thiogalactopyranosid) whilst the other culture served as non-induced control. Both cultures were incubated under shaking conditions at 30°C for 2-3 h. 30 μl of each culture were mixed with SDS sample buffer and subjected to SDS-PAGE (2.4.3).

Large scale protein expression and purification of GST-fusion proteins

A 20 ml starter culture of BL21-CodonPlus®-(DE3)-RIL cells transformed with the respective expression plasmid was set up in LB medium containing ampicillin and chloramphenicol. After overnight incubation the culture volume was increased to 1 l and was incubated for 1.5 h at 37°C. The temperature was then decreased to room temperature. Protein expression was induced by adding IPTG to a final concentration of 0.75 mM. After 4-5 h of incubation cells were pelleted by centrifugation for 10 min at 5 000 x g. All following steps were carried out on ice. Firstly, the pellet was resuspended in 20 ml 50 mM Tris, pH 8.0 and 10% glycerol. Then lysis buffer components were added to result in final concentrations of 350 mM NaCl, 10 mM Imidazol, 20% IGEPAL and 1 mM β-Mercaptoethanol. The mixture was incubated rotating for 1 h at 4°C. Further cell lysis was achieved by pressure cell disruption on ice (3 x 1000 psi) and sonication (2 min 50% intensity, 50% duty cycle). The samples were centrifuged for 1 h at 30 000 x g at 4°C. The supernatant was filtered through a 0.2 μm syringe filter. Subse-

quently 500 μ l of glutathione sepharose (washed 3 x with PBS) were added and the mixture was incubated overnight rotating at 4°C. The samples were applied to chromatography columns and glutathione sepharose was washed 5 x with PBS. Bound recombinant protein was eluted with 4 ml elution buffer. 8 fractions were collected which subsequently were analyzed via sodiumdodecylsulfat polyacrylamid gel electrophoresis (SDS-PAGE) and staining of the gel. To concentrate protein and for replacing the elution buffer with 5 % glycerol/PBS centrifugal filter units with an appropriate molecular weight cut-off were used.

Large scale protein expression and purification of MBP-fusion proteins

BL21-CodonPlus®-(DE3)-RIL cells were transformed with the respective plasmid based on the vector pIH902. A 5ml starter culture in 0.1 % glucose/LB medium was set up. Cultivation in large volume, induction of protein expression and harvesting of cells was carried out as described for GST-tag fusion proteins. Per gram pellet 3 ml MBP lysis buffer, 80 μ l lysozyme and 30 μ l PMSF were used to resuspend the pellet. After 20 min of incubation on ice the cells were disrupted via pressure cell disruption (3 x 1000 psi) and sonication (2 min 50 % intensity, 50 % duty cycle). Per ml of suspension 6 μ l 1 M MgCl₂ and 0.08 g NaCl were added and incubated under rotation for 1 h at 4°C. After centrifugation for 20 min at 20 000–30 000 x g the supernatant was filtrated if necessary. 1 ml amylose resin was washed with MBP column buffer and resuspended in 2.5 ml TE buffer (pH 7.5). The supernatant containing the recombinant protein was incubated with the amylose resin under rotation at 4°C overnight. Subsequently, the suspension was transferred to a chromatography column. After several washing steps the MBP-tagged protein was eluted via addition of MBP column buffer containing maltose.

2.4.2 Isolation of inclusion bodies

When then the purification of recombinant proteins only resulted in a low yield of protein, inclusion bodies formed within the bacteria cytosol were isolated. These then were used for the immunization of mice to obtain antisera reactive against the recombinant protein enclosed in inclusion bodies (see 2.4.6). A 100 ml starter culture of BL21-CodonPlus®-(DE3)-RIL cells transformed with the respective expression plasmid was set up in LB medium containing ampicillin and chloramphenicol. After overnight incubation the starter culture was added to 1.5 l LB medium containing ampicillin and chloramphenicol followed by incubation for 1 h at 37°C. The bacteria culture was then cooled down to 30°C and induced with 0.75 mM IPTG when an optical density of 0.5–0.8 was reached. After 5 h of incubation the cells were pelleted (3 000 x g for 5 min) and resuspended in 100 ml ice-cold lysis buffer. After addition of lysozyme (2 mg/ml final concentration) the suspension was incubated on ice for 10 min. Further cell disruption was achieved by sonication on ice for 10 min (50 % intensity, 50 % duty cycle). Subse-

quently, 200 ml of detergent buffer was added and the mixture was centrifuged (6 000 x g for 10 min). The supernatant was removed carefully and the pellet was resuspended in 250 ml washing buffer. Several washing steps were carried out until a tight pellet was obtained. Then the pellet was washed with 250 ml 75 % ethanol by thoroughly resuspending it. After centrifugation (6 000 x g for 10 min) the pellet was air-dried on ice to avoid carry-over of ethanol. Finally the pellet was taken up in 2–5 ml sterile PBS and was sonicated shortly to obtain a homogenous suspension. The concentration of the protein of interest was estimated by subjecting serial dilutions to SDS-PAGE.

2.4.3 SDS-PAGE

The SDS-PAGE enables the analysis of proteins by separation of the proteins of a protein mixture according to their mass. The discontinuous PAGE is comprised of a resolving gel and a 5 % stacking gel. Depending on the mass of proteins of interest an acrylamid concentration of 8–15 % was chosen for the resolving gel. Protein solutions or parasite lysates were resuspended in 2 x SDS sample buffer containing 2.5 mM DTT and denatured by heating for 8 min for 95 min. After loading the samples onto the gel a voltage of 80 V was applied for 20–30 min until the samples had entered the resolving gel. Subsequently, voltage was increased to 120 V for up to 2 h. After protein separation gels were either used for Western blot (see 2.4.5) or gels were stained to visualize proteins.

Staining of gels

Gels were washed in dH₂O for 3 x 10 min under agitation. DH₂O was replaced by Gel Blue Stain Solution and gels were stained for 1 h under agitation. Subsequently gels were incubated in dH₂O to remove residual staining solution.

2.4.4 Co-immunoprecipitation

Co-immunoprecipitation (CoIP) assays were carried out to investigate protein-protein interactions. In this assay a protein mixture is incubated with antibodies directed against the protein of interest. The antibodies are covalently bound to agarose beads. The resulting complex comprising agarose beads, antibody and the protein of interest bound to its interaction partners can thus be isolated.

The AminoLink Coupling Resin (Pierce/ThermoScientific) was washed in PBS and subsequently incubated with the respective antiserum and cyanoborohydride at a final concentration of 50 mM at 4°C overnight. The activated agarose support contains aldehyde functional groups that react with primary amines of the antibodies under formation of a Schiff base bond. Upon incubation with cyanoborohydride these bonds are reduced resulting in a stable secondary amine bond. The agarose beads were washed 3 x with PBS to remove unbound antiserum. After two washing steps with 1 M Tris/HCl pH7.4 beads were incubated under rotation for 30 min at room temperature with 1 M Tris/HCl

pH7.4 containing cyanoborohydrid at a final concentration of 50 mM. Thereby, remaining active sites were blocked.

The entire preparation of samples was carried out on ice or at 4°C. Pellets of enriched gametocytes were combined and resuspended in Co-IP lysis buffer. Further disruption of cells was achieved by means of ultrasound homogenization for 1 min at 50% intensity/50 cycles. The homogenate was centrifuged at 14 200 x g for 1 min and the resulting pellet containing cell debris was discarded. The supernatant was incubated with 8 µl of normal mouse serum per 2 gametocyte cultures being processed. After 30 min of incubation under rotation approximately 20 µl of protein G agarose beads were added and incubated for further 30 min. The protein G agarose was centrifuged (225 x g, 5 min) and the resulting pellet was discarded, thereby avoiding unspecific interactions of mouse sera with the proteins of interest. The supernatant was transferred to a new reaction tube and the antiserum bound to AminoLink Coupling Resin was added. Incubation was carried out overnight under rotation. After centrifugation (225 x g, 5 min) the agarose bead pellet was washed twice with Co-IP lysis buffer and two further times with PBS containing 1 % PIC and 0.5 mM EDTA (centrifugation at 225 x g, 5 min). The pellet was resuspended in PBS and 2 x SDS-PAGE sample buffer containing 25 mM DTT. The samples then were denatured by incubation at 95°C for 8 min. The samples were centrifuged once more, to remove the antisera bound to agarose beads prior to loading the samples to a protein gel. SDS-PAGE was carried out as described in 2.4.3 and detection of interaction partners of the protein of interest was proven by detection of the suspected proteins via Western blot (see 2.4.5).

2.4.5 Western Blot analysis

In order to detect a specific protein of interest within mixture of proteins that was separated via SDS-PAGE proteins were transferred to a nitrocellulose membrane via electroblotting. Binding of proteins to the membrane is based on hydrophobic interactions. The SDS polyacrylamid gels were placed onto two layers of whatman paper soaked in transfer buffer lying on a foam pad, likewise soaked with transfer buffer. The membrane was also wetted with transfer buffer, put on top of the gel and covered by additional two sheets of pre-soaked whatman paper. The stack was covered by a second foam pad. Air bubbles residing between the single layers were excluded and the stack was enclosed by a cassette of the blotting device. The cassette was placed into the blotting chamber with the membrane facing to the anode resulting in the negatively charged proteins to be transferred from gel to membrane. Transfer was usually carried out overnight at a voltage of 15 V or, alternatively at 25 V for 2 h.

After the transfer the membrane was briefly rinsed in TBS buffer followed by blocking of free binding sites by incubation with 5 % TBSM/ 1 % BSA for 1 h at room tempera-

ture or 4°C overnight. After rinsing the membrane for 2 x 5 min in TBS the primary antibody diluted in 3% TBSM was added (for dilution see Tab. 2.6) and incubated for 2 h at room temperature. After incubation of the membrane with primary antibody the membrane was washed four times. Firstly, the membrane was rinsed in 3% TBSM, followed by two washing steps for 10 min each in 0.1% Tween/3% TBSM. After washing once more with 3% TBSM, the secondary alkaline phosphatase-conjugated antibody was added in a concentration of 1:6 000 in 3% TBSM. Incubation of secondary antibody was for 2 h at room temperature. After four washing steps (TBS, 2 x 0.1% Tween/TBS, TBS) of 10 min each the membrane was incubated in equilibration buffer for 3 min. Finally, the NBT/BCIP substrate tablet dissolved in dH₂O was added which is converted into a violet precipitate by the alkaline phosphatase. Once a sufficient grade of coloration of protein bands was reached the reaction was stopped by addition of stopping buffer. After 30 min of incubation the membrane was air-dried.

2.4.6 Generation of antisera via immunization of mice

Antisera were generated via immunization of six week old female NMRI mice. 100 µg of solutions containing recombinant proteins or emulsions containing or inclusion bodies were diluted in 200 µl sterile PBS. 200 µl Freund's incomplete adjuvant were added and the mixture was injected subcutaneously. After four week a second dose of either 50 µg inclusion bodies or 100 µg recombinant protein was administered. After 10 days mice were anesthetized by intraperitoneal injection of ketamine and xylazine according to protocol of the manufacturer (Sigma-Aldrich). Whole blood of mice was obtained via heart puncture. Sera from naïve mice served as negative controls.

2.5 Entomological methods

2.5.1 Rearing of *Anopheles stephensi*

Anopheles stephensi mosquitoes were reared in an insectary at 26±0.5°C with a humidity of 80±2% and a light/dark cycle of 12 h each. Alimentation of mosquitoes that were used for colony maintenance was by means of sterile 5% saccharose/0.1% sea salt solution containing 0.05% para-aminobenzoic acid. Once per week egg production was induced by alimentation with mouse blood. After four days eggs were collected in a small glass beaker containing a solution of 0.1% sea salt. With maturation of larvae, density of larvae per tray was reduced resulting in a density of approximately 300 larvae per 3 l of 0.1% sea salt solution. Larvae were fed with fodder pellets. Pupae were transferred into a small glass beaker residing within a new mosquito cage.

2.5.2 Infection of *Anopheles stephensi*

Mosquitoes which were reared for infection by *P. falciparum* were fed with 5% saccharose/0.1% sea salt solution containing 0.05% para-aminobenzoic acid and 40 µg/ml gentamicin (Beier *et al.*, 1994). One day prior to infection female mosquitoes were starved. Percoll-purified gametocytes were mixed with an equal volume of freshly drawn human erythrocytes. The combined pellet was mixed with an equal volume of prewarmed heat-inactivated human serum. The mixture was transferred to a glass feeder that was kept at 37°C. The mosquitoes were allowed to feed for 20 min in the dark. Only mosquitoes with fully engorged midguts were kept. After 24 h mosquito midguts were isolated and prepared for indirect IFA as described above (see 2.2.6).

2.6 Mass spectrometry

Sample preparation

2 ml of RBC concentrate per sample were centrifuged, the supernatant was removed and cells were resuspended in 8 ml PBS containing the substances to be investigated, i.e. XA at different concentrations or XA combined with potential inhibitors. After incubation at room temperature the incubation solution was diluted with ice-cold PBS to 50 ml and centrifuged (1260 x g, 5 min, at 4°C). The RBC pellet was washed 4x with PBS to remove residual extracellular XA. The cell suspension was sonicated (2 min 50% intensity; 50% duty cycle) on ice. Cell debris was pelleted by centrifugation (5 min, 15 500 x g) and the cell lysate was further cleared by filtration through a 0.22 µm syringe filter and a centrifuge filter unit with 5 kDa cut-off.

LC/ESI/MS/MS analysis

LC/ESI/MS/MS (Liquid chromatography/ electrospray injection/ tandem mass spectrometry) analyses to quantify XA in the RBC samples were kindly carried out by Michael Völker of the laboratory of PD Dr. Matthias Unger at the Institute for Pharmacy and Food Chemistry, University of Würzburg. Briefly, samples were injected into a HPLC (high performance liquid chromatography) system (Agilent 1200, Agilent Technologies) and separated via a reverse phase HPLC column (Synergi MAX-RP 50 x 2.0 mm 4 µm, Phenomenex®). Subsequently the eluate was ionized via electrospray ionization (ESI) and ions were transferred to the triple quadrupole mass analyzer which was operated in the multi-reaction monitoring mode (MRM). The system was calibrated by analyzing solutions containing different concentrations of the analyte (1 - 250 ng/ml XA). Parameters for HPLC and MS are listed in Tab. 8.3 -8.4 (Appendix).

3 Results

3.1 Reverse genetics studies on PfCCp5 and PfFNPA

The gene loci encoding two PfCCp family proteins, PfCCp5 and PfFNPA, were disrupted in order to gain information on the potential roles of the proteins by studying the phenotype of the KO parasites. Two parasite lines possessing disrupted *pfccp5* loci and one parasite line with disrupted *pfhnpa* gene locus were constructed by Dr. Marie-Adrienne Dude (Dude, 2009). Additionally, she generated two parasite lines in which the *pfccp5* loci were modified by adding the sequence encoding a double HA-tag to the 3' end of the gene upstream of the stop codon.

3.1.1 Verification of modified gene loci

Diagnostic PCR

As Dr. Dude did not observe growth of parasites after transfection with the PfCCp5-KO plasmid, two new vials of parasites were thawed that had been cryopreserved directly after transfection. In contrary to the observations of Dr. Dude the transfected parasites started to grow within few weeks. Thus, it was possible to isolate genomic DNA of the above mentioned five parasite lines.

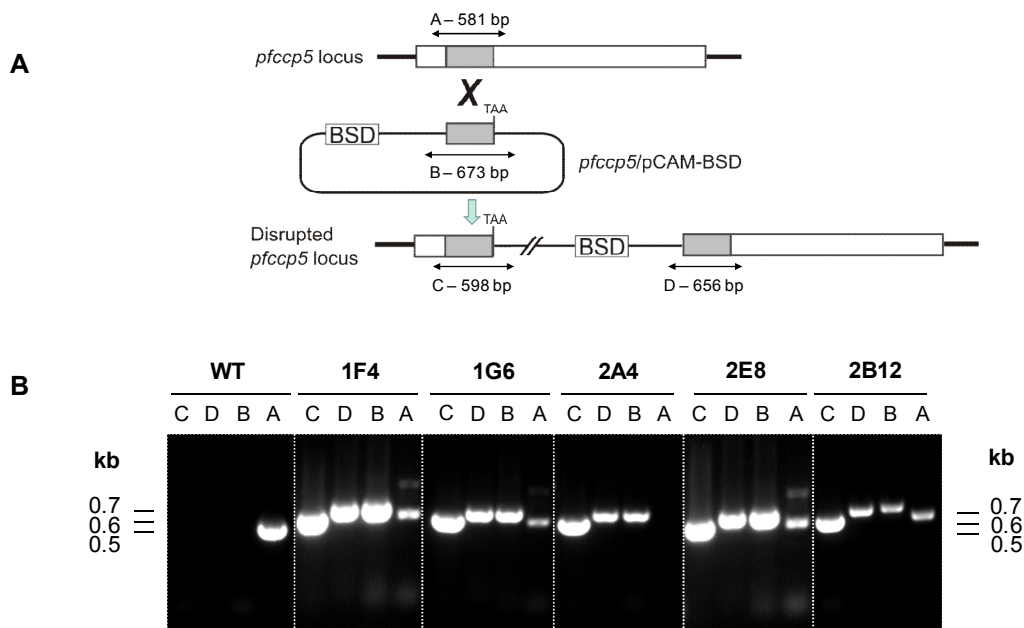


Fig. 3.1: **A.** Schematic depicting the *pfccp5* gene locus and the modified KO locus resulting from homologous recombination. Regions used for discrimination between wild-type (WT) and KO locus by means of diagnostic PCR are marked with A–D. **B.** Diagnostic PCR on genomic DNA of WT parasites and five PfCCp5-KO clones. Clone 2A4 clearly shows absence of the WT locus. Gel lanes are labeled according to panel A.

The site-specific integration of the respective transfection plasmid was then confirmed by diagnostic PCR. Limiting dilution was carried out to obtain clonal lines devoid of parasites carrying a wild-type locus of the respective gene of interest. Only for one of the two independently transfected PfCCp5-KO parasite lines clones were detectable. The obtained clones were isolated and the genotypes of five of the clones were investigated via diagnostic PCR. For the clone PfCCp5-KO-2A4 absence of the wild-type *pfccp5* locus was clearly confirmed. The other four clones, however, showed a band corresponding to the wild-type *pfccp5* locus and were thus excluded from further studies (Fig. 3.1).

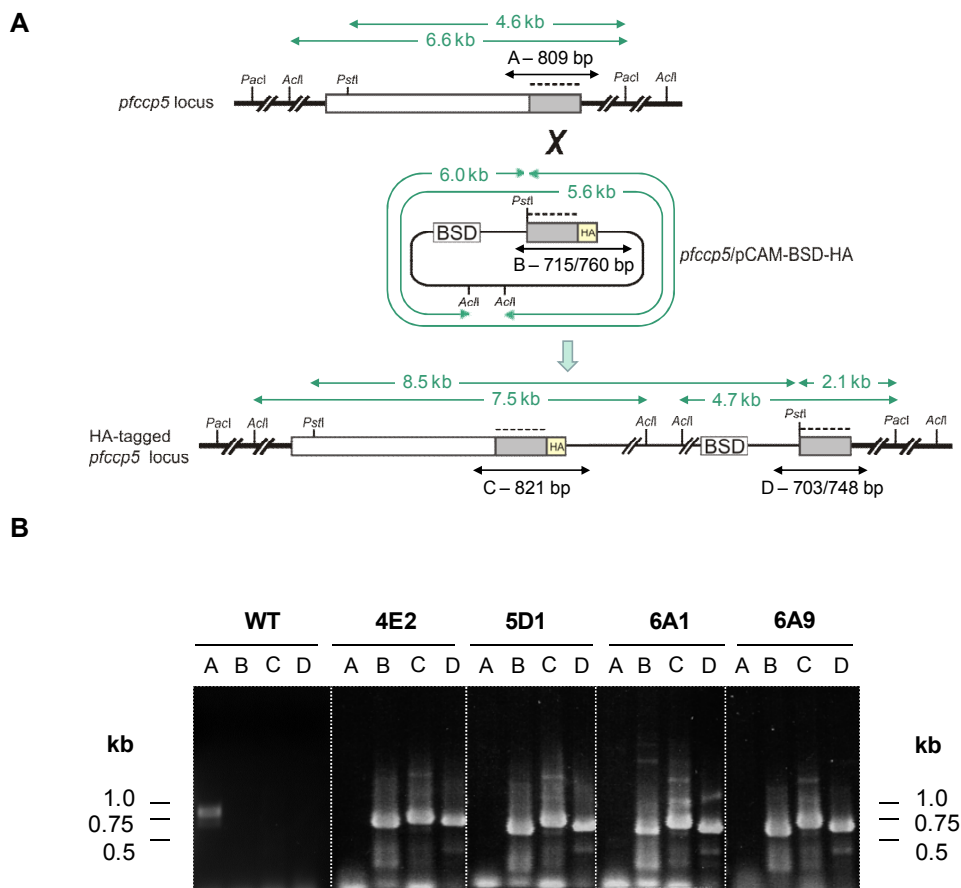


Fig. 3.2: **A.** Schematic depicting the *pfccp5* gene locus and the modified HA locus resulting from homologous recombination. Regions used for discrimination between wild-type (WT) and HA locus via diagnostic PCR are marked with A–D. Restriction enzyme recognition sites used for examination of the genotype via Southern blot are shown and resulting fragments are marked in green. Binding site of the Southern blot probe is indicated with a dashed line. **B.** Diagnostic PCR on genomic DNA of WT parasites and four PfCCp5-HA clones. All clones showed bands representing the modified *pfccp5* locus after vector integration. Gel lanes are labeled according to panel A.

After limiting dilution of the two individually transfected PfCCp5-HA parasite lines seven clones were isolated in total. For the four clones further investigated, PfCCp5-HA1-4E2, PfCCp5-HA2-5D1, PfCCp5-HA2-6A1 and PfCCp5-HA2-6A9 absence of parasites possessing wild-type *pfccp5* locus was confirmed by means of diagnostic PCR

(Fig. 3.2). Of the PfFNPA-KO line eight clones were obtained after dilutional cloning. The genotype of six clones was investigated via diagnostic PCR and clearly showed absence of wild-type *pfhnpa* locus for the clones PfFNPA-KO-1H4, PfFNPA-KO-2D2 and PfFNPA-KO-2F1 (Fig. 3.3).

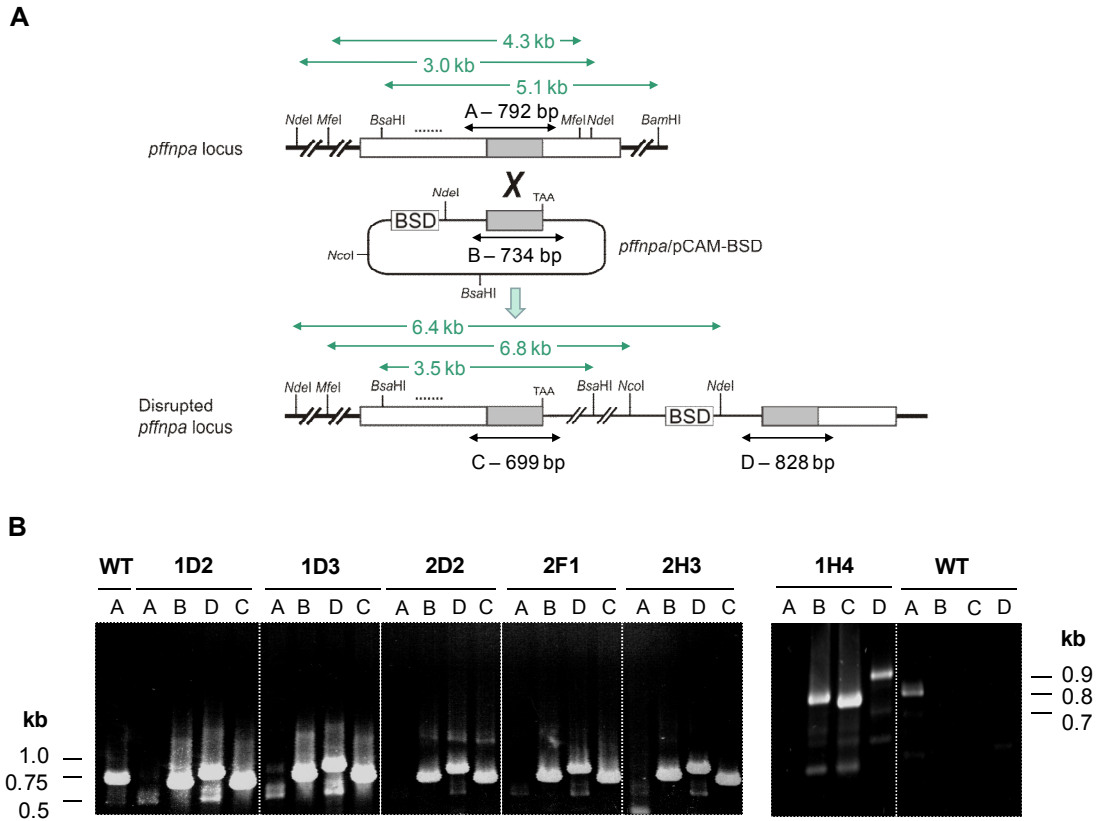


Fig. 3.3: **A.** Schematic depicting the *pffnpa* gene locus and the modified KO locus resulting from homologous recombination. Regions used for discrimination between wild-type (WT) and KO locus by means of diagnostic PCR are marked with A–D. Restriction enzyme recognition sites used for examination of the genotype via Southern blot are shown and resulting fragments are marked in green. Binding site of the Southern blot probe is indicated with a dashed line. **B.** Diagnostic PCR on genomic DNA of WT parasites and six PfFNPA-KO clones. All clones showed bands representing the *pffnpa* locus after vector integration. Gel lanes are labeled according to panel A.

Southern Blot

The modification of the *pfccp5* locus in the clones PfCCp5-HA-5D1 and PfCCp5-HA-6A1 was investigated via Southern blot by Dipl.-Biol. Maik Gieseke. Genomic DNA of the two genetically modified parasite lines and of wild-type parasites was digested with either PacI and AclI or PacI and PstI. Analysis of the products of the restriction digest by means of Southern blot showed that both clones were devoid of the wild-type *pfccp5* locus (Gieseke, 2010). Clone PfCCp5-HA-5D1 showed bands corresponding to restriction digested episomal *pfccp5*/pCAM-HA plasmid in addition to bands characteristic for the disrupted *pfccp5* locus (Fig. 3.4 A).

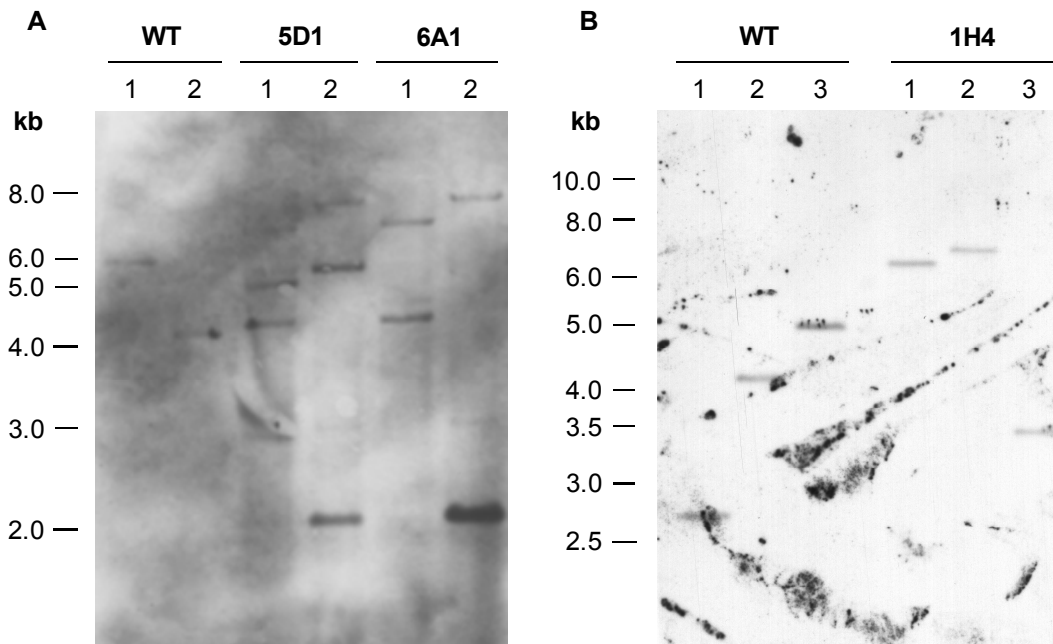


Fig. 3.4: Southern blot confirming the modification of gene loci and absence of (wild-type) WT locus of the respective gene of interest. **A.** Genomic DNA of WT and PfCCp5-HA clones 5D1 and 6A1 was restriction digested with PaclI and AclI (1) or PaclI and PstI (2). Location and lengths of the resulting restriction fragments are marked in Fig. 3.2 A. In contrast to clone 6A1, clone 5D1 shows bands corresponding to the episomal transfection plasmid (Figure from Gieseke, 2010). **B.** Genomic DNA of (wild-type) WT and PffNPA-KO clones 1H4 was restriction digested with NdeI (1), MfeI and NcoI (2) or BsaHI and BamHI (3). Location and lengths of the resulting restriction fragments are marked in Fig. 3.3 A.

Integration of the transfected plasmid into the *pffnpa* locus was also investigated via Southern blot analysis. Genomic DNA of clone 1H4 of the FNPA-KO parasite line and of wild-type parasites was either restriction digested with NdeI only, with MfeI and NcoI or with BsaHI and BamHI. A DIG-labeled probe complementary to a region upstream of the integration site of the transfection plasmid was used to detect the DNA fragments obtained after the restriction digest (Fig. 3.3 A). For either combination of restriction enzymes used the disruption of the *pffnpa* gene was verified and absence of parasites carrying the wild-type *pffnpa* locus was proven Fig. 3.4 B). For the most recently isolated clone PfCCp5-KO-2A4 Southern blot analysis still is to be carried out.

3.1.2 Phenotype analyses of genetically modified parasites

Indirect IFAs and Western Blots

After the modifications of the gene loci of interest had been confirmed, the absence of the respective gene product was examined at the protein level. The absence of PfCCp5 was confirmed in the PfCCp5-KO-2A4 parasite line via Western blot and indirect IFA using anti-PfCCp5 antisera (Fig. 3.5). Likewise, no PffNPA protein was detected in PffNPA-KO-1H4 parasites in Western Blot and indirect IFA (Fig. 3.6). The expression of the PfCCp5-HA fusion protein by the parasite line PfCCp5-HA-6A1 was confirmed

via Western blot probed with anti-HA antibody (Fig. 3.7). The protein band obtained with the anti-HA antibody was of approximately the same molecular weight as the protein band obtained using anti- PfCCp5 antisera. It was not possible to detect the fusion protein in indirect IFAs (data not shown).

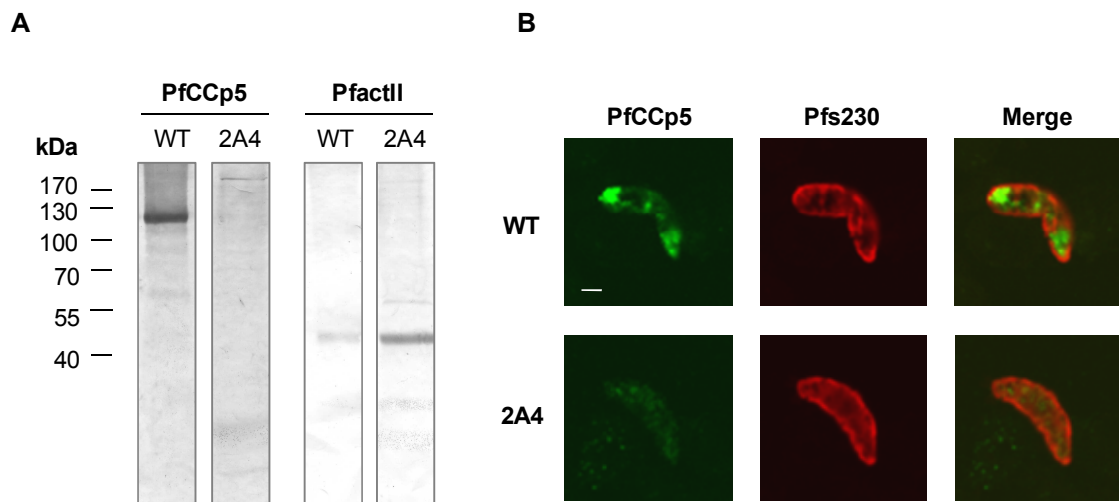


Fig. 3.5: **A.** Western blot analysis of gametocyte lysate of PfCCp5-KO clone 2A4 showed absence of PfCCp5 (118.6 kDa). PfactII (42.6 kDa) served as loading control. **B.** Indirect IFA confirmed absence of PfCCp5 in PfCCp5-KO-2A4 gametocytes. Scale bar - 2 μ m.

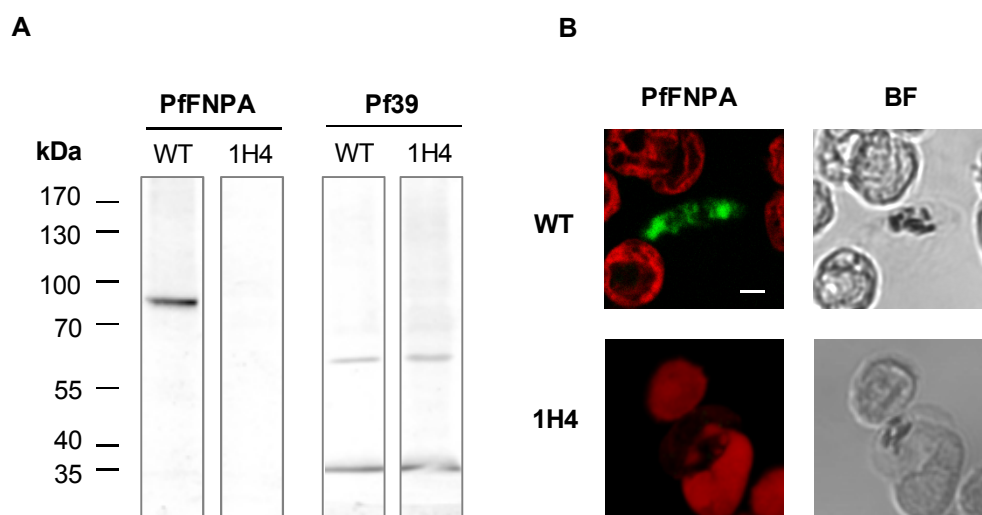


Fig. 3.6: **A.** Western blot analysis of gametocyte lysate of PfnNPA-KO clone 1H4 showed absence of PfnNPA (100.1 kDa). Pf39 (39.4 kDa) served as loading control. **B.** Indirect IFA confirmed absence of PfnNPA (green) in PfnNPA-KO-1H4 gametocytes. Erythrocytes were counterstained with Evans Blue, scale bar - 2 μ m, WT - wild-type.

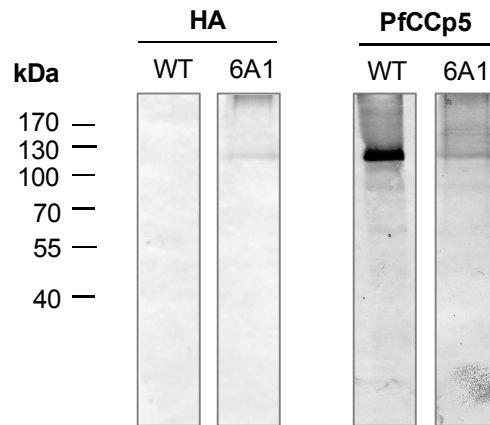


Fig. 3.7: Western blot analysis of gametocyte lysate of PfCCp5-HA clone 6A1 showed a band at approximately 120 kDa when probed with anti-HA antibody (HA), whilst no band was observed in wild-type (WT) gametocyte lysate. For both lysates a band at approximately 120 kDa was observed when probing with anti-PfCCp5 antiserum. Probing with anti-CCp5 antiserum served as loading control and demonstrated that in the parasite lysate of the mutant less PfCCp5 protein was present as compared to WT parasite lysate.

Gametocyte formation, gametogenesis and fertilization

Both asexual parasite replication and gametocytes development of PfCCp5-KO and PffNPA-KO mutants did not show obvious alterations as compared to wild-type parasites. The formation of gametes and zygotes of the gene-disruptant mutants was induced *in vitro* by triggering gametogenesis with XA and incubation of the parasite cultures at RT. For the investigation of ookinete development PffNPA-KO gametocytes were fed to female *An. stephensi* mosquitos. After 24 h the mosquito midguts were isolated and investigated for the present of retort stages, an intermediate stage between zygote and ookinete, and the presence of ookinetes. The different development stages were detected via indirect IFA using antisera directed against stage-specific proteins (Fig. 3.8).

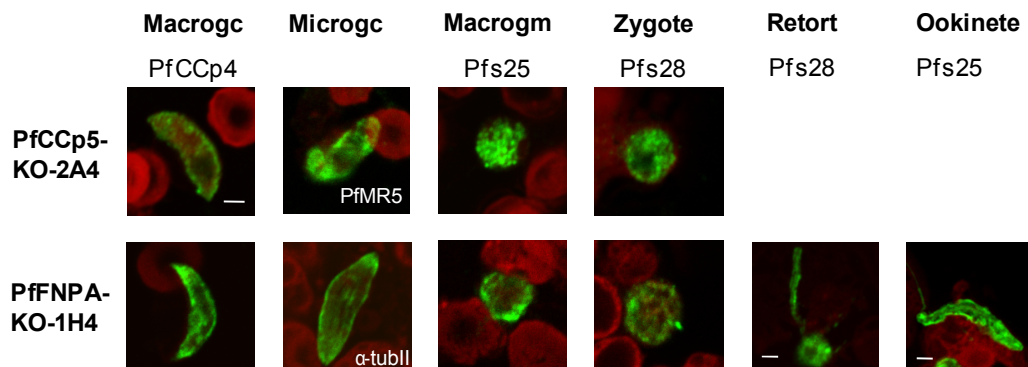


Fig. 3.8: Indirect IFA showed that development of PfCCp5-KO-2A4 and PffNPA-KO-1H4 parasites throughout the sexual phase is not affected by absence of the respective protein. Proteins expressed in the respective life cycle stage are shown in green. Erythrocytes were counterstained with Evans Blue. Macrogc - macrogametocyte, Microgc - microgametocyte, Macrogm - macrogamete, scale bar - 2 μ m.

The formation of microgametocytes was investigated light-microscopically after inducing gametogenesis with XA. Neither PfCCp5-KO nor PffNPA-KO parasites showed alterations in gamete formation or zygote formation. The development of PffNPA-KO parasites into ookinetes was not affected by absence of PffNPA. Investigation of ookinete development of PfCCp5-KO parasites was not achieved due to time limitations. For the PfCCp5-HA parasite lines a reduced gametocyte formation was observed as it is often the case for parasites undergoing periods of extended cultivation. Further studies on the generated KO parasite lines are described below (3.2.1).

3.2 Co-dependent expression of sexual stage-specific proteins

Amongst the members of the PfCCp protein family the phenomenon of co-dependent expression has been observed. It manifests in the absence or reduced abundance of all proteins if only one of the six PfCCp proteins is not expressed due to disruption of its gene locus (Pradel *et al.*, 2006; Simon *et al.*, 2009). In the present work ten mutants, lacking one sexual stage-specific protein each, were screened for the expression of 20 proteins expressed in sexual stage parasites. The study aimed at discovering further interdependencies of protein expression and protein localization.

3.2.1 Analysis of co-dependent expression via indirect IFA

In accordance with previous studies the results of indirect IFAs showed co-dependent expression amongst PfCCp proteins. Thus, all PfCCp proteins were absent or present in only reduced amount in PfCCp1-KO, PfCCp4-KO, PfCCp5-KO and PffNPA-KO. The decrease in protein abundance was less prominent for PfCCp4 as compared to the other five PfCCp proteins. In PfCCp5-KO and PffNPA-KO parasites the reduced expression of some PfCCp proteins was less prominent than in the PfCCp1-KO. Expression of all other proteins investigated was not altered in the absence of PfCCp1, PfCCp4, PfCCp5 or PffNPA (see Tab. 3.1, Appendix Fig. 8.5). As PfCCp5 is expressed already in the schizont stage, its expression was additionally investigated in this parasite stage via indirect IFA. Whilst in PfCCp1-KO gametocytes only very low amounts of PfCCp5 were detectable, the expression of PfCCp5 was not altered in schizonts of the PfCCp1-KO parasite line (Fig. 3.9). Amongst the 200 combinations of mutants and proteins screened for interdependencies of protein expression via indirect IFA, one pair of proteins showed to be expressed co-dependently, beside the co-dependently expressed PfCCp proteins. In both mutants expressing only truncated versions of Pfs230, Pfs230-KOd1 and Pfs230-KOd2, PfactinII did not localize homogeneously to the periphery of gametocytes as in wild-type parasites. Instead, in Pfs230-KOd1 parasites, expressing only a fragment of Pfs230

Tab. 3.1: Summary of results of indirect IFAs investigating the expression of sexual stage proteins in eight KO parasite lines. Localization of all proteins was investigated in gametocytes except that of Pfs25 (macrogametes) and Pfs28 (zygotes). For IFA images see Appendix Fig. 8.5.

	CCp1-KO	CCp4-KO	CCp5-KO	FNPA-KO	Pfs230-KOd1	Pfs230-KOd2	Pfs48/45-KO	Pfg377-KO
PfCCp1	+	+/-	+	+	++	++	++	++
PfCCp2	+/-	+	+	+	++	+	++	++
PfCCp3	+/-	+	+	+	++	+	++	++
PfCCp4	+	+/-	++	++	++	++	++	++
PfCCp5	+/- ^{a)}	+/+++	+/-	++	++	++	++	++
PfFNPA	+/-	+/+++	+/-	-	++	++	++	++
Pfpeg3	++	++	++	++	++	++	++	++
Pfs16	++	+	++	++	++	++	++	++
PfGAP50	++	++	++	++	++	++	++	++
PfWLP1	++	++	++	++	++	++	++	+
MYO1C / PfmyoA	++ ^{b)}	++ ^{c)}	++ ^{b)}	+ ^{c)}	+ ^{c)}	++ ^{c)}	++ ^{c)}	++ ^{c)}
Pfs230	++	++	++	++	- ^{d)}	+/-, # ^{e)}	++ ^{f)}	++
PfMR5	++	++	++	++	+, # ^{g)}	+, # ^{g)}	++	++
Pfs47	+	++	++	++	++	++	++	++
Pfs25	++	++	++	++	+	++	++	++
Pfs28	+	++	++	++	++	++	++	++
PfactinI	++	++	++	++	++	++	++	++
PfactinII	++	++	++	++	-	+/-, #	+	++
alpha-tubII	++	++	nd	++	+	++	++	++
Tubulin	++	++	++	++	++	++	++	++

Expression on protein level:

++ = as wild-type

+ = reduced

+/- = low expression

- = absent

= altered localization

nd = not determined

a) expression in schizonts as in wild-type

b) PfMyoA

c) MYO1C

d) small fragment still detectable with certain antibody, altered localization

e) fragment only

f) expression altered in macrogametes: reduced and altered localization

g) in KO rather punctuate expression, in wild-type homogenous

(452 aa instead of full length protein of 3135 aa), PfactinII was not detectable in indirect IFAs. In Pfs230-KOd2 parasites, expressing a longer fragment of Pf230 than Pfs230-KOd1 mutants (950 aa), labeling with antiserum directed against PfactinII showed distribution of PfactinII in a spotted pattern in contrast to the homogenous expression in wild-type parasites. Further experiments investigating the co-dependent expression of the two proteins are described in section 3.4.2. All other combinations of mutants and sexual stage proteins investigated did not show an expression differing from that in wild-type parasites in a pronounced way (Tab. 3.1, Appendix Fig. 8.5).

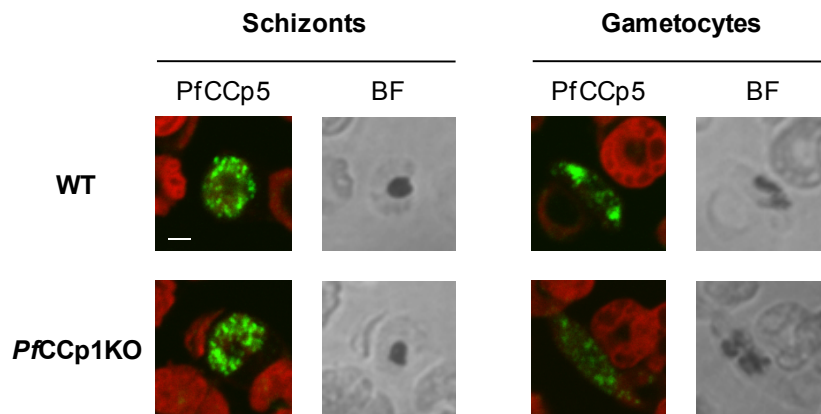


Fig. 3.9: Indirect IFA showed that expression of PfCCp5 is not altered in PfCCp1-KO schizonts. In contrast, in PfCCp1-KO gametocytes only very low amounts of PfCCp5 (green) were detectable. Erythrocytes were counterstained with Evans Blue. BF - bright field, WT - wild-type, scale bar - 2 μ m.

3.2.2 Analysis of co-dependent expression via RT-PCR

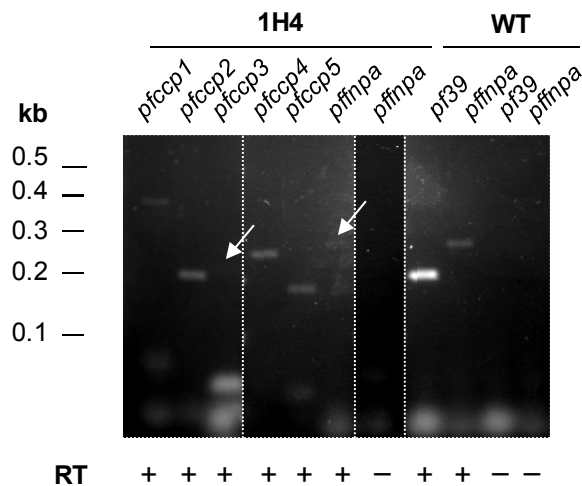


Fig. 3.10: RT-PCR on cDNA of PfFNP A-KO, clone 1H4 and wild-type (WT), showed presence of transcripts of the pfccp genes. Primers detecting Pf39 were used as control. RT-PCR carried out without adding reverse transcriptase (RT-) served as control for presence of genomic DNA.

Co-dependent expression was investigated at transcript level for clone 1H4 of the FNPA-KO parasite line. In accordance with previous reports on PfCCp gene-disruptant parasite lines, transcripts of all *pfccp* genes were detected employing RT-PCR (Fig. 3.10). In the current analysis of clone 1H4 of the PfFNPA-KO, however, the band for *pfccp3* was very faint. For *pffnpa* also a faint band was observed. Similar results had been obtained for the other PfCCp gene-disruptant parasite lines so far investigated, as well. In each case, low level residual expression of the disrupted gene was observed (Simon *et al.*, 2009).

3.3 Studies on the IMC of *P. falciparum* gametocytes

Although well studied in asexual malaria parasites, the presence and composition of the IMC of *P. falciparum* had not been studied in gametocytes. Hence, we investigated the expression of select genes encoding IMC components on transcript and protein level. Furthermore, EM studies were carried out to gain information on the composition of the membranes surrounding the gametocyte.

3.3.1 Transcript analysis of genes encoding components of the IMC

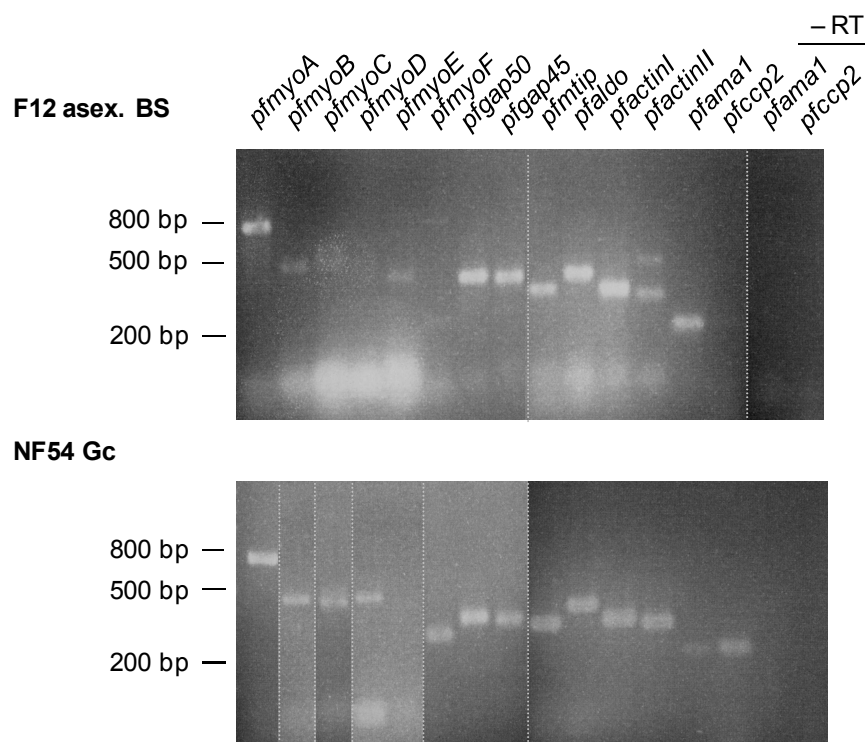


Fig. 3.11: RT-PCR on cDNA obtained from asexual parasites of F12 strain as well as of wild-type NF54 parasite culture containing mainly gametocytes showed expression of six myosin genes as well as of several genes encoding IMC components. *Pfama1* and *pfccp2* served as stage-specific controls. The negative control to which no reverse transcriptase (RT) was added, confirmed absence of genomic DNA (Tews, 2011; Simon *et al.*, 2012).

Beside the components of the IMC, the six myosin isoforms encoded in the genome of *P. falciparum* had not been described in gametocytes until now, either. We therefore included the six myosins expressed in *Plasmodium* spp. in the transcript analyses. To ensure functionality of the oligonucleotides used in RT-PCRs, the transcript of the genes was firstly detected in asexual parasites of the gametocyte-less subclone F12, where expression of all 14 genes investigated was observed, with the exception of *pfmyoD*, *pfmyoF* and *pfccp2*. The latter served as control for the presence of gametocytes. In gametocytes, transcripts of all 14 genes were detected, except that of *pfmyoE*. A faint band for *pfama1* which served as control for the presence of cDNA of asexual parasites was detected. The RT-PCRs were carried out in great part by undergraduate student Sabrina Tews, BSc in the course of her bachelor thesis (Tews, 2011). Taken together the results of this study showed that the components of the IMC known from invasive stages of the malaria parasite are expressed in gametocytes. The six myosins on the other hand seem to be expressed differentially in asexual blood stages and in gametocytes (Fig. 3.11).

3.3.2 Ultrastructural study on IMC composition

In addition to studying the expression of IMC components via RT-PCR, the IMC was investigated at ultrastructural level. Both in wild-type gametocytes as well as gametocytes of three KO mutants were prepared for transmission electron microscopical analysis. Gametocytes of the mutants Pfs230-KOd2 and Pfs48/45-KO exhibited the typical trilamellar membrane structure comprised of cisternae of the IMC, parasite plasma membrane and PVM. However, in Pfs230-KOd1 gametocytes only two membranes

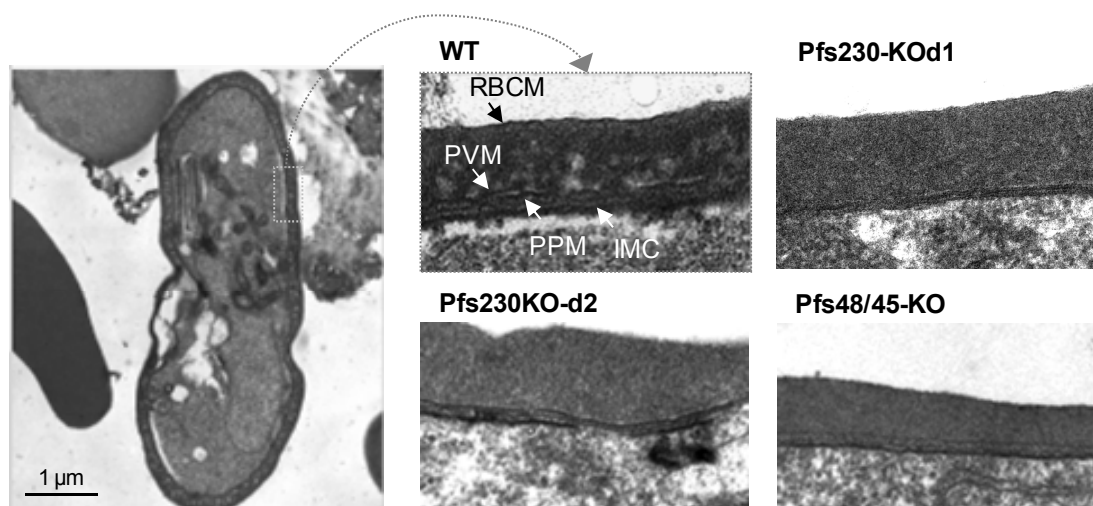


Fig. 3.12: Electron micrographs showing the membrane structure of gametocytes of WT parasites and of KO strains Pfs230-KOd1, Pfs230-KOd2 and Pfs48/45-KO. In gametocytes of strain Pfs230-KOd1 only two membranes were visible at the periphery of gametocytes, in contrast to gametocytes of the other strains exhibiting three membranes as observed in WT gametocytes. IMC - inner membrane complex, PPM - parasite plasma membrane, RBCM - RBC membrane.

were visible (Fig. 3.12). The number of membranes surrounding the gametocytes was quantified in 15 gametocytes of each parasite strain. According to the quantification, both mutants expressing truncated versions of Pfs230 showed altered membrane composition in comparison to wild-type gametocytes. As listed in Tab. 3.2 in Pfs230-KOd1 gametocytes only one of the 15 gametocytes investigated showed the typical membrane composition, whilst in the Pfs230-KOd2 parasite line only four gametocytes of 15 showed the trilamellar membrane composition as observed in wild-type parasites.

Tab. 3.2: Investigation of the membrane structure of WT gametocytes and the three KO parasite lines Pfs230-KOd1, Pfs230-KOd2 and Pfs48/45-KO was investigated at the ultrastructural level. Quantification of presence of the three membranes surrounding the gametocytes showed obvious differences in KO parasite lines Pfs230-KOd1 and Pfs230-KOd2 (n=15).

No. of membranes	WT	Pfs230d1	Pfs230d2	Pfs48/45-KO
3	15	1	4	12
2	0	10	6	2
partially 2	0	4	5	1

3.3.3 Generation of anti-PfmyoA antiserum

To investigate the expression of the IMC protein PfmyoA in gametocytes, an antiserum directed against a fragment of the protein was generated. A 750 bp region of the protein (corresponding to amino acids 227 – 476) was chosen for amplification as previously published by Pinder *et al.* (1998). The PCR product was cloned into the expression vector pGEX-4T-1. The recombinant protein was expressed in *E. coli* BL21 CodonPlus® (DE3)-RIL cells fused to an N-terminal GST tag (26.1 kDa).

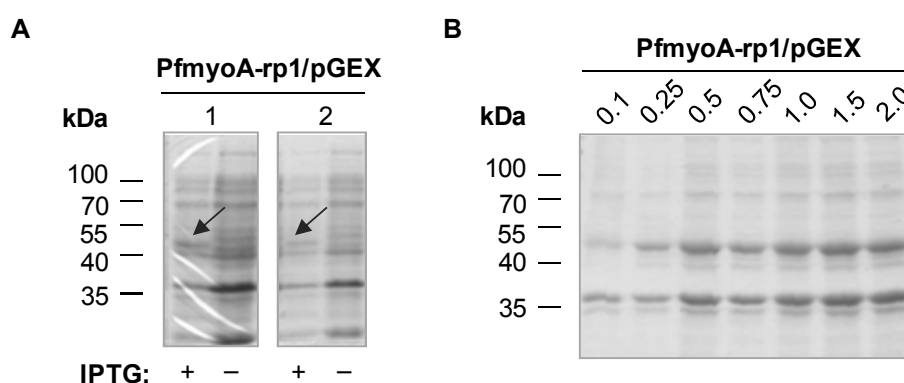


Fig. 3.13: **A.** SDS-PAGE after expression of recombinant protein of PfmyoA (28.2 kDa) by *E. coli* BL21 CodonPlus® (DE3)-RIL. After induction of transcription (+ IPTG) a band of 54.3 kDa was observed for the recombinant protein PfmyoArp1 fused to GST tag (arrow). Two clones (1, 2) are depicted. For comparison, the lysate of control bacteria (–, no IPTG added) is shown. **B.** Different volumes (µl) of recombinant protein PfmyoA-rp1 were applied to SDS-PAGE after isolation via inclusion bodies for estimation of protein concentration.

The expected molecular weight including the GST tag was approximately 54.3 kDa. The IPTG-induced expression was first carried out in small scale and the obtained recombinant protein was analyzed via SDS-PAGE. An aliquot of the bacteria culture was isolated before induction of protein expression to discriminate endogenous bacterial proteins from the recombinant protein of PfmYoA. The two bacteria clones investigated showed a band at the expected molecular weight of 54.3 kDa, whilst the control bacteria did not show a band of the same size (Fig. 3.13). The recombinant protein was isolated within inclusion bodies of the bacteria. The inclusion bodies were used for immunization of mice in order to obtain a polyclonal antiserum directed against PfmYoA.

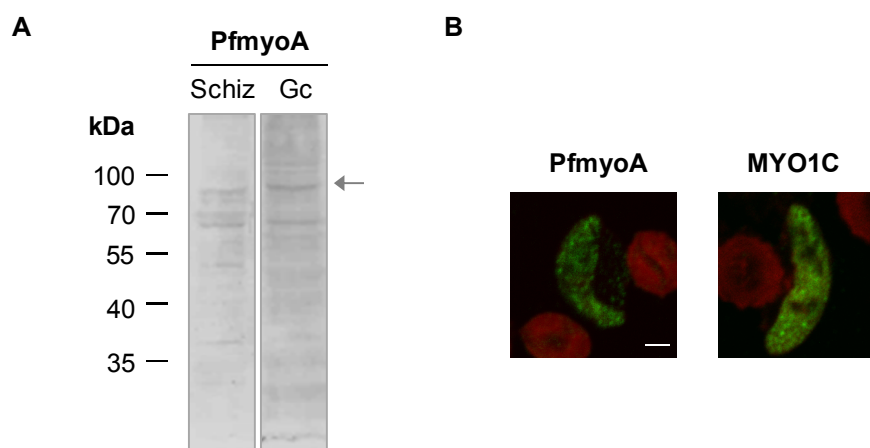


Fig. 3.14: **A.** Western Blot using anti-PfmYoA antiserum showed a band of the expected size (92.3 kDa, arrow) in both schizont and gametocyte lysate. **B.** Indirect IFAs detecting PfmYoA (Alexa-488, green) in a stage V gametocyte. The rabbit antiserum directed against human MYO1C showed a similar fluorescence pattern. Erythrocytes were counterstained with Evans Blue. Scale bar - 2 μ m.

The PfmYoA antiserum was tested in Western Blot and indirect IFA (Fig. 3.14). In both schizont lysate and gametocyte lysate a band of the expected molecular weight of 92.3 kDa was detected with anti-PfmYoA antiserum. In indirect IFA on gametocytes the antiserum show a similar fluorescence pattern as anti-MYO1C antiserum. This antiserum is directed against the human myosin isoform MYO1C. The sequence of the corresponding immunogen exhibits 62% identity and 75% similarity to PfmYoC and 58% identity and 80% similarity to PfmYoA.

3.3.4 Indirect IFAs investigating presence of PV and IMC

After observing alterations of the trilaminar pellicule in gametocyte of the mutants Pfs230-KOd1 and Pfs230-KOd2, the presence of both PVM and IMC was investigated in these parasites via indirect IFAs. The antisera applied were directed against proteins associated with one of the two membranes. Both Pfs16 and PfEXP-1, proteins of the PVM, were expressed in gametocytes of the Pfs230-deficient mutants similar as in wild-type gametocytes. Expression of PfSERP, a soluble protein of the PV, was also not al-

tered in the absence of full-length Pfs230. The IMC proteins PfGAP50 and PfmyoA (detected by means of anti-MYO1C antiserum) were expressed in the mutants comparably to wild-type parasites (Fig. 3.15). Since the PPM is essential for gametocyte survival, the presence of this membrane was not investigated in detail, however in earlier experiments expression of several proteins associated with the PPM had been shown (e.g. PfCCp1, see Tab. 3.1). Thus, it was concluded that although only two membranes surrounding the parasite were observed via electron microscopy, all three membranes were present in the mutant parasite lines. Most likely the space between two of the membranes was reduced dramatically and therefore was beneath solution limit.

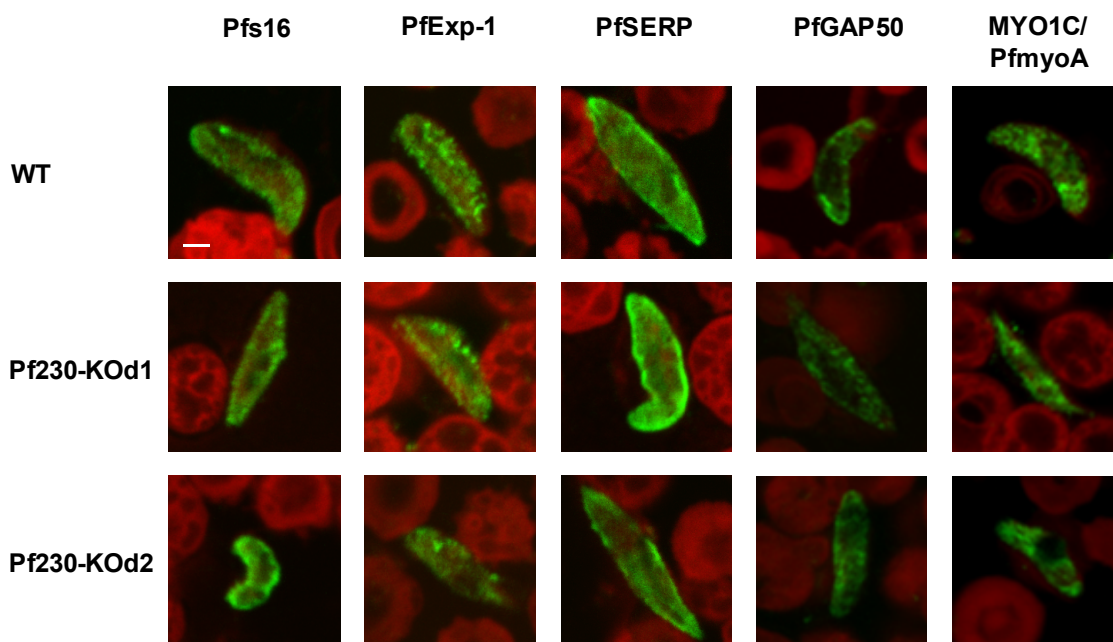


Fig. 3.15: Indirect IFAs investigating the expression of proteins of the PV or PVM Pfs16, PfEXP-1 and PfSERP as well as IMC-associated proteins PfGAP50 and PfmyoA in gametocytes. All five proteins (Alexa Fluor-488 labeled, shown in green) were expressed in the two mutant parasite strains similarly as in wild-type (WT) gametocytes. Anti-MYO1C antiserum was used to detect PfmyoA. Erythrocytes were counterstained with Evans Blue. Scale bar- 2 μ m.

3.4 Characterization of PfactinII

Plasmodium spp. represent the only genus of the Apicomplexan clade that expresses two isoforms of actin. Although PfactinII had already been described to be specifically expressed in sexual parasite stages (Wesseling *et al.*, 1989), its role remained unknown. In order to gain more information on PfactinII, its expression as well as interactions with other proteins were investigated.

3.4.1 Expression of PfactinII throughout the life cycle of *P. falciparum*

A recombinant protein corresponding to amino acids 169–345 of PfactinII had been generated in our laboratory (see Fig. 3.24). *E. coli* inclusion bodies containing the recombinant protein were injected in mice and antiserum directed against PfactinII was obtained. Specificity of the antiserum was confirmed in WB analyses. The antiserum was employed in indirect IFAs to examine the expression of PfactinII in different life-cycle stages. For comparison the expression pattern of PfactinI was also investigated.

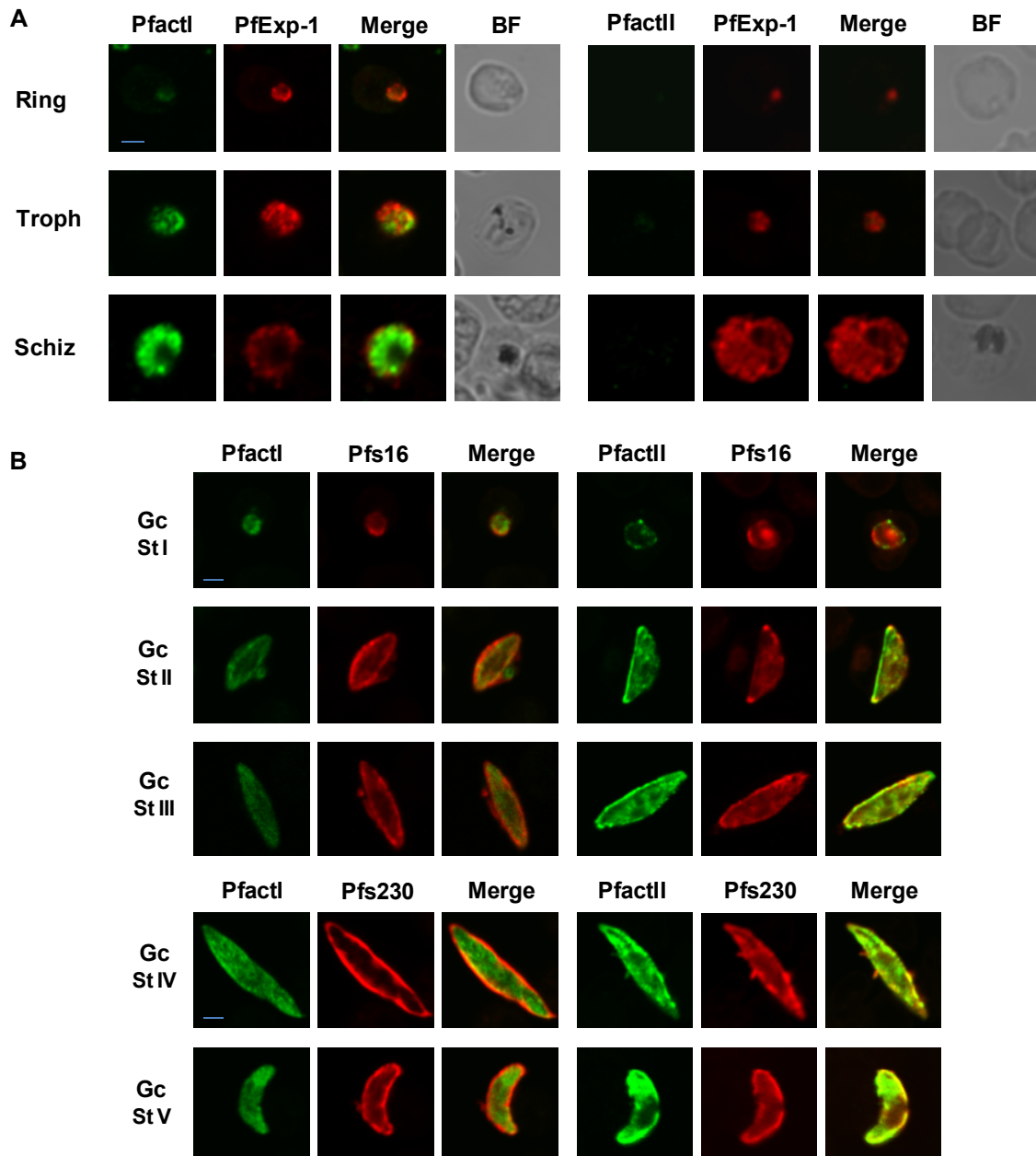


Fig. 3.16: Indirect IFAs investigating the expression of PfactinII in different parasite stages. **A.** PfactinII is not expressed in asexual blood stages, whilst PfactinI was detected in ring, trophozoite and schizont stage. **B.** PfactinI and PfactinII are expressed in Stage I–V gametocytes. PfactinI and PfactinII are labeled with Alexa Fluor-488 (green), other proteins are labeled with Alexa Fluor-594 (red). BF - bright field, scale bar - 2 μ m.

PfactinII was not detected in asexual blood stages, whilst PfactinI was present in ring stage parasites, in trophozoites and in schizonts (Fig. 3.16 A). The labeling of PfactinI was located within that of PfExp-1, a protein localizing to the PVM. Both PfactinII and PfactinI were detected in gametocytes stage I–V. The signal for PfactinII increased with gametocyte maturation (Fig. 3.16 B). In macrogametes the protein was still expressed intensely, whilst in zygotes the signal ceased. In retort stages only very weak expression was seen in the residual body. PfactinII was detected neither in the developing microgametes nor in the residual body of the microgametocyte. In all stages in which PfactinII was detectable, the protein localized predominantly to the cell periphery. In contrast, PfactinI showed a rather diffuse distribution within the parasite cell.

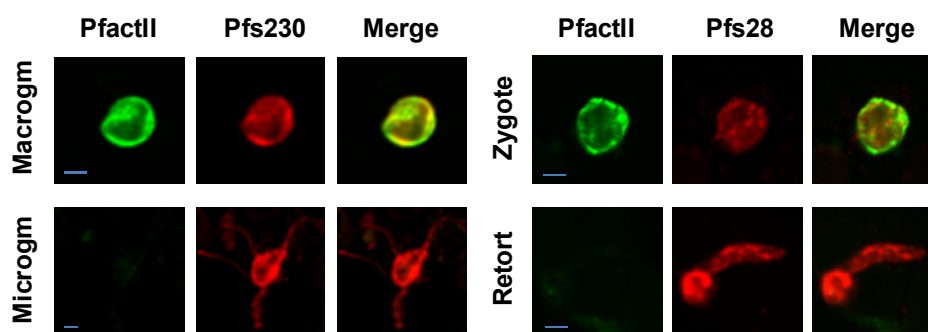


Fig. 3.17: Indirect IFAs investigating the expression of PfactinII in different parasite stages. PfactinII is expressed in macrogametes and zygotes. PfactinII was labeled with Alexa Fluor-488 (green), other proteins were labeled with Alexa Fluor-594 (red). Scale bar - 2 μ m.

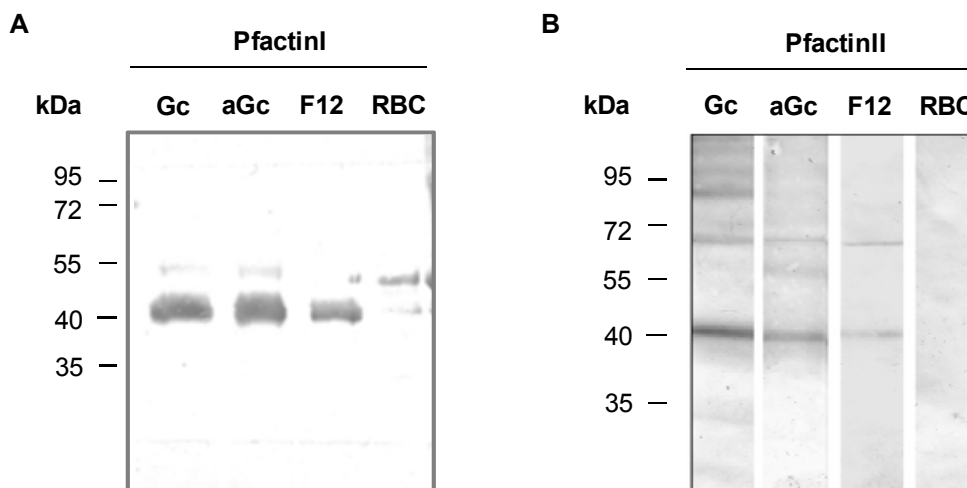


Fig. 3.18: **A.** Western blot analysis using anti-PfactinI antiserum showed expression of PfactinI (41.9kDa) in gametocytes (Gc), activated gametocytes (aGc) and mixed blood stages of the gametocyte-less strain F12. A faint band detected in RBC lysate at 42kDa resulted from a neighboring band (Western blot kindly provided by L. Sologub). **B.** Western blot analysis using anti-PfactinII antiserum showed expression of PfactinII (42.6kDa) in Gc and aGc. A faint protein band was observed for the gametocyte-less strain F12. No protein band was observed in uninfected RBCs (Rupp *et al.*, 2010).

PfactinII expression was also investigated via Western blot using the same anti-PfactinII antiserum. A protein band at the expected molecular weight of 42.6 kDa was observed in both gametocytes and gametocytes activated to undergo gamete formation (Fig. 3.18). A faint protein band was observed in the gametocyte-less strain F12. An additional band was observed at approximately 70 kDa and in non-activated gametocytes a third band at 90 kDa. The observation of a weak expression in the gametocyte-less strain F12 is in concordance with the faint band observed in F12 cDNA when carrying out RT-PCR (Fig. 3.11). PfactinI was detected in lysates of both gametocytes and activated gametocytes as well as in lysate of mixed asexual blood stages of the F12 strain. The Western blot results thus confirmed the results of indirect IFA that were obtained on expression of the two actin isoforms.

3.4.2 Co-dependent expression of PfactinII and Pfs230

As PfactinII was not detectable via indirect IFAs in mutants lacking full-length Pfs230 (Tab. 3.1, Appendix Fig. 8.5) this co-dependent expression was further investigated. RT-PCR was carried out to see whether transcription or transcript stability was effected. For both mutants, Pfs230-KOd1 and Pfs230-KOd2, and for wild-type parasites RNA was obtained from cultures containing both asexual blood stages and gametocytes. In the subsequent RT-PCR using cDNA derived from both mutants as well as from wild-type a PCR product corresponding to *pfactinII* transcript was detected (Fig. 3.19).

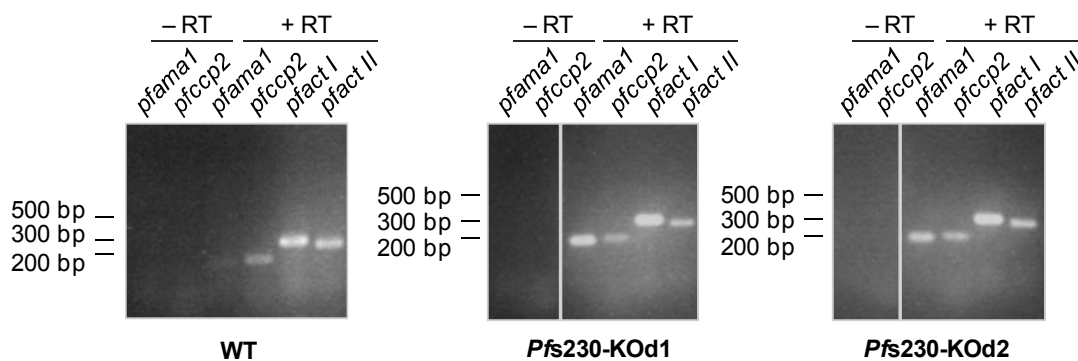


Fig. 3.19: RT-PCR on cDNA of wild-type (WT), Pfs230-KOd1 and Pfs230-KOd2 parasite lines showed presence of *pfactinII* transcript in both mutants. Amplification of *pfama1* served as control for presence of cDNA of asexual blood stages, *pfccp2* as stage-specific control for gametocytes. RT-PCR carried out without adding reverse transcriptase (-RT) served as control for presence of genomic DNA.

Similarly, a DNA fragment was amplified from *pfactinI* transcript when using the three cDNA samples as template. Oligonucleotides targeting *pfama1* and *pfccp2* were used to test for presence of asexual blood stage parasites and gametocytes, respectively. For the two mutants the signal of *pfactinI* was considerably stronger than that of *pfactinII*. This can be explained by the greater amount of asexual parasites in the samples as concluded

from the strong *pfama1* signal. The intensity of the *pfactinII* signal was in concordance with that of the signal observed for *pfccp2*. For all cDNA samples a RT-PCR reaction was carried out without adding reverse transcriptase to confirm absence of genomic DNA.

Next, the presence of PfactinII in the two mutants lacking wild-type Pfs230 was investigated via Western blot. In both mutants a band corresponding to PfactinII was detected at the expected molecular weight of approximately 43 kDa as in WT gametocytes (Fig. 3.20). As observed before (Fig. 3.18), additional bands were visible at around 70 kDa in wild-type and KO parasite lines and for wild-type and Pfs230-KOd2 also at approximately 90 kDa. As a gametocyte loading control PfCCp2 was detected in the parasite lysates. The band running at the expected molecular weight of 185 kDa was comparable in the two mutants, the band observed in wild-type lysate was less intense. In contrast, the bands for PfactinII were of the same intensity in all of the three lysates. Thus, it seems that the amount of PfactinII is reduced in the two mutants (Fig. 3.20). In contrary to the observations of indirect IFAs these results suggest, that PfactinII is still present in Pfs230-KOd1 parasites. It is possible that it is mislocated or misfolded and thus not detectable in indirect IFA.

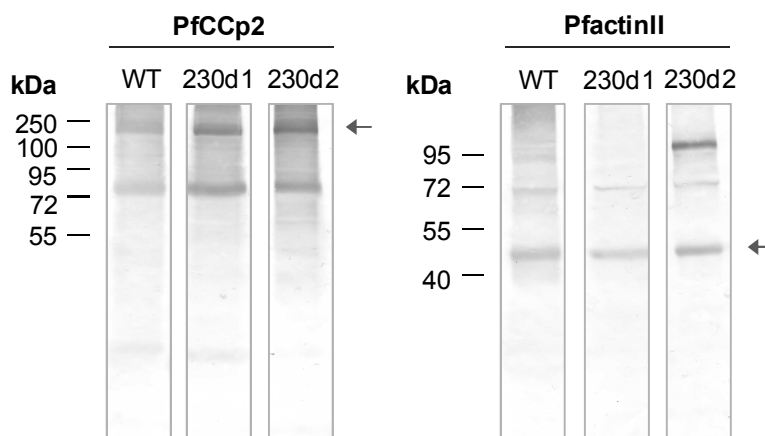


Fig. 3.20: Western Blot analysis investigating the presence of PfactinII in gametocyte lysates of wild-type (WT), and the two mutant strains Pfs230-KOd1 (230d1) and Pfs230-KOd2 (230d2). PfactinII was detected in all of the three lysates. Detection of PfCCp2 served as gametocyte loading control. Arrows highlight bands of the expected molecular weight.

Observing a co-dependent expression of PfactinII and Pfs230 via indirect IFAs was suggestive of a protein-protein interaction, as observed for the proteins of the PfCCp protein family. Hence, co-immunoprecipitation assays were carried out to investigate this possibility. When investigating the presence of Pfs230 via Western blot after precipitating PfactinI or PfactinII from gametocyte lysate, a band for Pfs230 was observed that pointed at an interaction between Pfs230 and PfactinII. A protein band correspond-

ing to an interaction between PfactinI and Pfs230 was not visible. The precipitation of PfactinI and Pfs230 from gametocyte lysate followed by detection of PfactinII in Western blot showed an interaction between PfactinII and Pfs230 but not between PfactinII and PfactinI. After precipitation of PfactinII and Pfs230 followed by probing with anti-PfactinI antiserum in Western blot, bands suggestive of protein-protein interactions were observed both between PfactinII and PfactinI as well as between Pfs230 and PfactinI (Fig. 3.21). In regard of these observations a protein-protein interaction between PfactinII and Pfs230 seems to be likely. However, further investigations are needed to clarify the partially contradictory results on interaction of PfactinI with PfactinII and Pfs230.

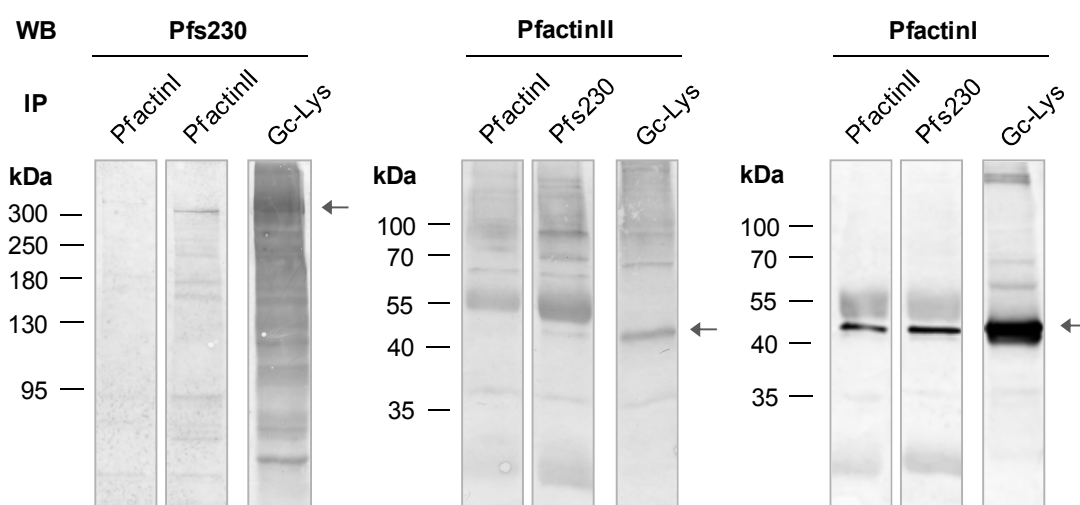


Fig. 3.21: Co-immunoprecipitations investigating the potential interaction of PfactinII and Pfs230. When probing with anti-Pfs230 antiserum after immunoprecipitation, interaction was observed between PfactinII but not with PfactinI. When precipitating PfactinI and Pfs230 from gametocyte lysate, interaction of PfactinII with Pfs230 was observed but not with PfactinI. When precipitating PfactinII or Pfs230 followed by Western blot detecting PfactinI, interactions between both PfactinII and Pfs230 with PfactinI were observed. Gametocyte lysate (Gc-Lys) was subjected to Western blot analysis to illustrate the protein bands detected by the respective antiserum.

After a protein-protein interaction between PfactinII and Pfs230 had been observed in gametocyte lysates, the localization of both proteins was investigated in gametocytes in order to see whether the subcellular localization of the proteins would enable them to interact. Gametocytes of both wild-type and Pfs230-KOd2 strain were fixed with PFA to preserve the structure of the cells. Antiserum directed against Pfs230 derived from rabbit and antisera directed against PfactinI and PfactinII, derived from mice, respectively were employed in the co-localization study. PfactinI was located intracellularly in homogenous distribution. It was surrounded by the signal for Pfs230 which was located at the cell periphery of gametocytes. No difference of PfactinI expression was observed between KO and wild-type gametocytes (Fig. 3.22). In Pfs230-KOd2 mutants Pfs230

was only visible in small patches (also see Appendix Fig. 8.5). PfactinII showed a co-localization with Pfs230 at the periphery of gametocytes in wild-type gametocytes. In Pfs230-KOd2 gametocytes the two proteins also co-localized. PfactinII was distributed in exactly the same patchy pattern as Pfs230 in this mutant parasite line (Fig. 3.22).

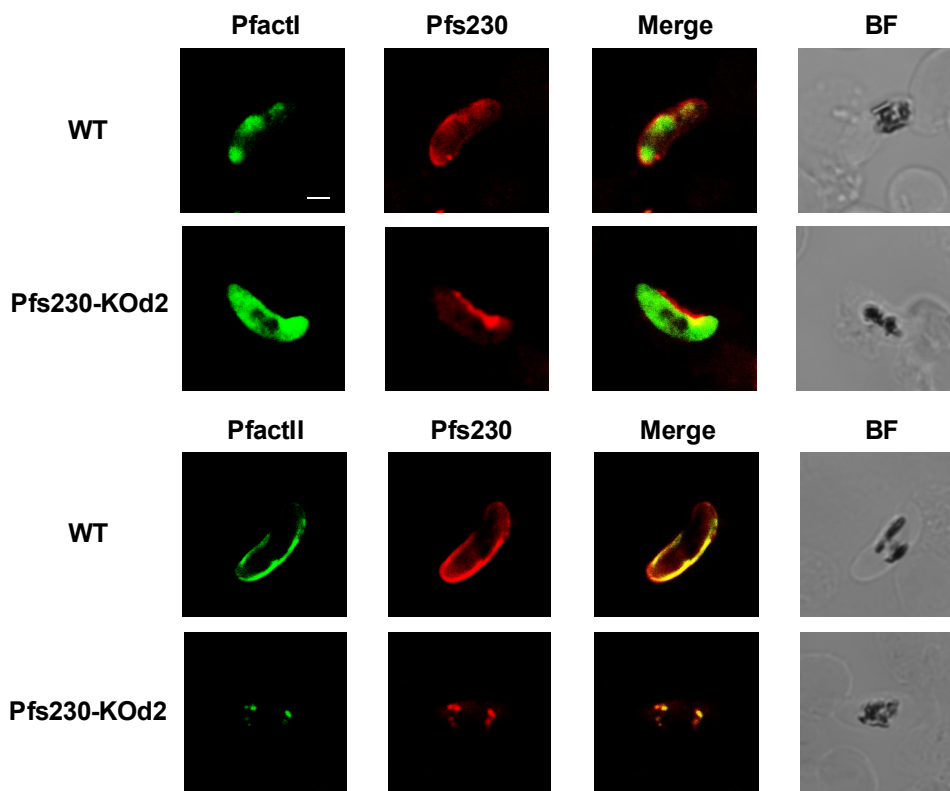


Fig. 3.22: Indirect IFA of PFA-fixed gametocytes showed co-localization of PfactinII (Alexa-488 labeled, green) and Pfs230 (Alexa-594, red) both in gametocytes of wild-type (WT) and of Pfs230-KOd2 parasites expressing a truncated version of Pfs230. For comparison PfactinI was detected which clearly was located within Pfs230-labeling. Scale bar - 2 μ m.

As gametes of Pfs48/45-KO parasites show dramatically reduced expression of Pfs230 (Eksi *et al.*, 2006), we wanted to see, whether the expression of PfactinII would also be affected in gametes of this parasite line. However, in contrast to Pfs230, the expression of PfactinII was only slightly reduced (Fig. 3.23 A). Instead of the homogenous expression of PfactinII in wild-type macrogametes, in the Pfs48/45-KO parasites PfactinII showed a punctuate expression. Quantification of the fluorescent signal of 30 wild-type and 30 Pfs48/45-KO macrogametes showed expectedly a highly significant reduction of Pfs230 expression in the mutant (Fig. 3.23 B). The fluorescence signal of PfactinII was also significantly reduced, when comparing wild-type and mutant macrogametes. However, the reduction was less strong. These results show that correct localization of PfactinII in gametes does not completely depend on presence of Pfs230 as observed in gametocytes.

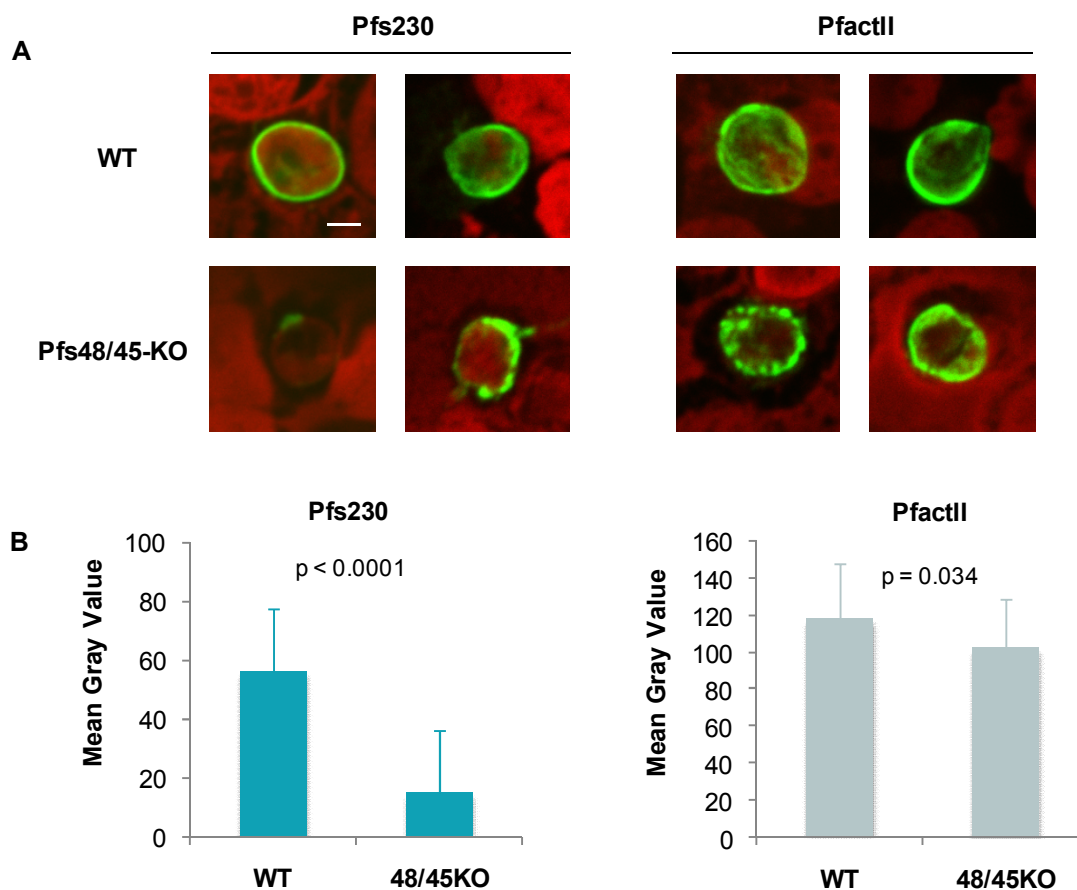


Fig. 3.23: **A.** Indirect IFAs showed that expression of Pfs230 was dramatically reduced and restricted to focal areas in Pfs48/45-KO macrogametes. Expression of PfactinII on the contrary did not show an obviously altered expression compared to wild-type (WT) gametes. Erythrocytes were counterstained with Evans Blue. Scale bar—2 μ m. **B.** Quantification of fluorescence intensity of Pfs230 or PfactinII labeling in WT and Pfs48/45-KO (48/45KO) macrogametes. 30 gametocytes of WT and KO were investigated, respectively. Mean values and SD are depicted. Unpaired t test analysis showed significant differences between WT and Pfs48/45-KO both for expression of Pfs230 and PfactinII.

3.4.3 Modifications of the *pfactinII* locus via single crossing-over homologous recombination

The gene locus encoding PfactinII was disrupted via plasmid integration in order to gain information on the potential role of the protein by studying the phenotype of the resulting KO parasites. In addition, a parasite line was generated in which the sequence encoding a double HA-tag was introduced at the 3' end of the gene upstream of the stop codon.

Diagnostic PCR

After integration of the plasmid into the genome of the transfected parasites limiting dilution was carried out to obtain clonal lines devoid of parasites carrying a wild-type locus of the gene of interest. Several clones of the PfactinII-KO parasite line were isolated. Absence of the wild-type allele was only shown for the clone PfactinII-KO-1A11

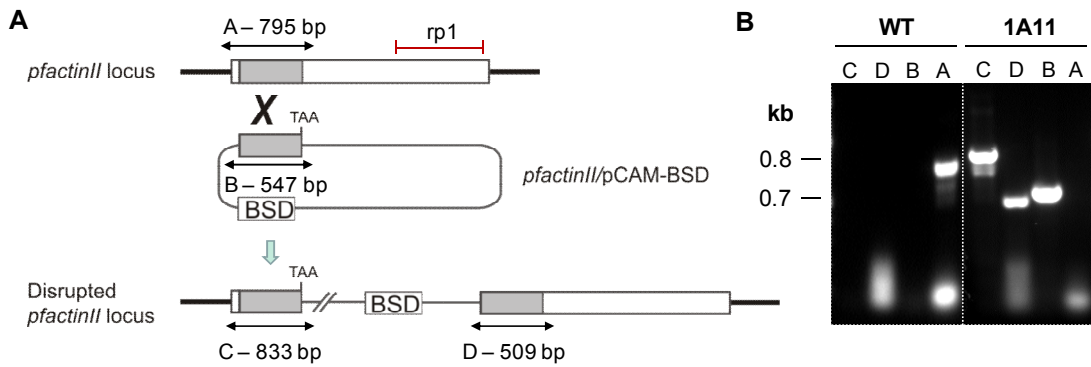


Fig. 3.24: **A.** Schematic depicting the *pfactinII* wild-type (WT) gene locus and the modified KO locus resulting from homologous recombination. Regions used for discrimination between WT and KO locus are marked with A–D. Location of the recombinant protein rp1 used for generation of antiserum is marked with a red line. **B.** Diagnostic PCR on genomic DNA of WT parasites and the PfactinII-KO clone 1A11 which showed absence of the WT locus. Gel lanes are labeled according to panel A.

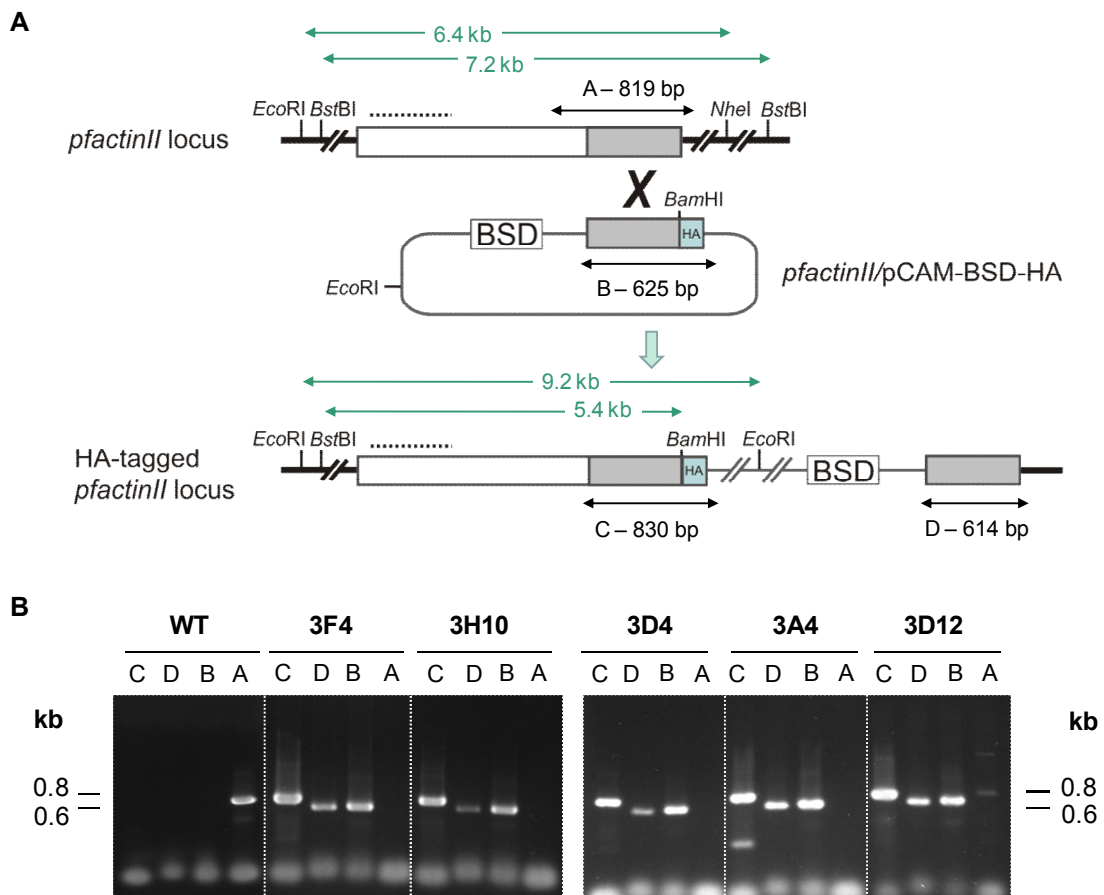


Fig. 3.25: **A.** Schematic depicting the *pfactinII* wild-type (WT) gene locus and the modified HA locus resulting from homologous recombination. Regions used for discrimination between WT and HA locus are marked with A–D. Restriction enzyme recognition sites are shown and resulting fragments are marked in green. Binding site of probe is indicated with a dashed line. **B.** Diagnostic PCR on genomic DNA of WT parasites and five PfactinII-HA clones. All clones showed bands reflecting vector integration. All clones except PfactinII-HA-3D12 were devoid of WT *pfactinII* allele. Gel lanes are labeled according to panel A.

when carrying out diagnostic PCR (Fig. 3.24 B). After limiting dilution of the PfactinII-HA parasite line several clones were isolated. For four of the five clones further investigated absence of parasites possessing wild-type *pfactinII* locus was confirmed by diagnostic PCR (Fig. 3.25).

Southern Blot

The modification of the *pfactinII* locus in the clones PfactinII-HA-3A4 and PfactinII-HA-3D4 was additionally investigated via Southern blot. Genomic DNA of both genetically modified parasite lines and of wild-type parasites was digested with either EcoRI and NheI or BamHI and BstBI. Analysis of the products of the restriction digest showed that both clones are devoid of the wild-type *pfactinII* locus (Fig. 3.26).

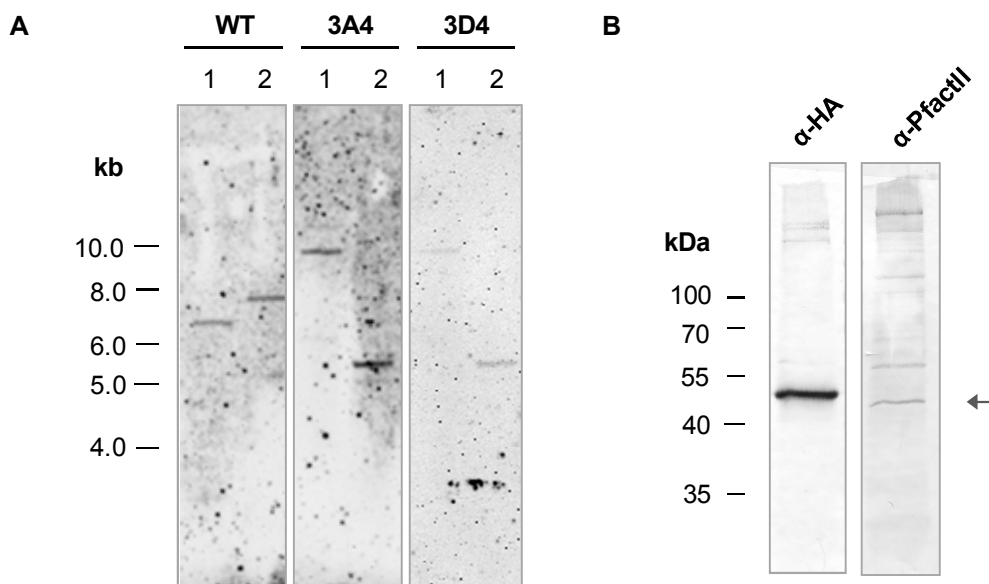


Fig. 3.26: Southern blot confirming the modification of gene loci and absence of wild-type (WT) locus of *pfactinII*. **A.** Genomic DNA of WT and PfactinII-HA clones 3A4 and 3D4 was restriction digested with EcoRI and NheI (1) or BamHI and BstBI (2). Location and lengths of the resulting restriction fragments are marked in Fig. 3.25 A. **B.** Western blot investigating the expression of HA-tagged PfactinII in gametocytes of the uncloned PfactinII-HA parasite line. Both anti-HA antibody and anti-PfactinII antiserum detected the approximately 43 kDa protein as well as several additional bands.

Indirect IFAs and Western Blots

The expression of PfactinII-HA fusion protein was investigated via Western blot analysis in gametocytes of the PfactinII-HA parasite line prior to obtaining clones via limiting dilution. The fusion protein was detected with anti-HA antibody at the expected height. The band detected with anti-PfactinII antiserum from the same lysate runs at a slightly lower molecular weight and was weaker than the band detected by anti-HA antibody (Fig. 3.26 B). The detection of the PfactinII-HA fusion protein via indirect IFA was not achieved.

The presence of PfactinII in the PfactinII-KO clone 1A11 was investigated via indirect IFA. The signal detected in the KO mutant was weaker than in wild-type parasites, however there was still quite pronounced expression of the protein observed (Fig. 3.27).

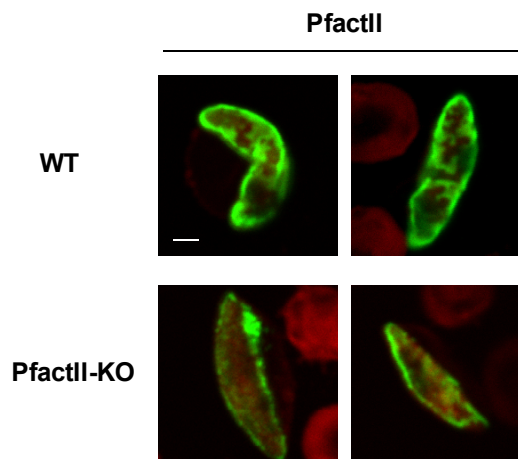


Fig. 3.27: Indirect IFA showed residual expression of PfactinII (Alexa-488, green) in PfactinII-KO clone 1A11. Erythrocytes were counterstained with Evans Blue. WT – wild-type, scale bar – 2 μ m.

3.5 Characterization of the WD domain containing protein PFWLP1

The WD40-domain containing protein PFWLP1 had been discovered due to its interaction with PfCCp1 (see 1.5.2). It had so far been undescribed in the literature. Hence, the expression throughout the life cycle was investigated and genetically modified parasite lines were generated in order to gain more information about this protein.

3.5.1 Generation of anti-PFWLP1 antiserum

To investigate the expression of PFWLP1 throughout the parasite life cycle antiserum directed against a fragment of the protein was generated. An 822 bp region (corresponding to amino acids 226–499) comprising three of the five WD40 domains was cloned into the expression vectors pGEX-4T-1 and pIH902 (see Fig. 3.28 and Fig. 3.35 A). The recombinant proteins that were expressed in *E. coli* BL21 CodonPlus® (DE3)-RIL cells had a molecular weight of 31.7 kDa and were fused to an N-terminal GST tag (26.2 kDa) or MBP tag (42.8 kDa), respectively. The expression of PFWLP1rp2 upon addition of IPTG was tested in small scale followed by analysis via SDS-PAGE. PFWLP1rp2 fused to a GST tag was visible as a band at a molecular weight of approximately 58 kDa. The MBP fusion protein ran at a molecular weight of approximately 72 kDa (Fig. 3.29 A). Before inducing the transcription of the gene of interest an aliquot of the bacteria culture was isolated. It served as control to discriminate endogenous bac-

terial proteins from the introduced recombinant protein. In all clones investigated for the two constructs, the control bacteria did not show a protein band of comparable intensity at the respective molecular weight of the recombinant proteins. The GST-tagged recombinant protein was obtained from inclusion bodies, whilst the MBP-tagged version was isolated via protein purification employing amylose resin. The isolation of the MBP-tagged PfwLp1 was kindly carried out by Dr. Nina Simon. Both inclusion bodies and purified protein were used to immunize mice in order to obtain polyclonal antisera directed against PfwLp1 (Fig. 3.29 B). For indirect IFAs antiserum derived from immunization with purified protein was used. For Western Blot analyses antiserum obtained after immunization with inclusion bodies was employed. Two further recombinant proteins used for generation of antisera in mice were generated by Vanesa N. Ngongang, MSc (Ngongang, 2012).

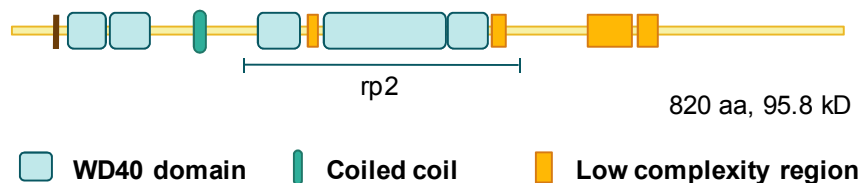


Fig. 3.28: Domain structure of the uncharacterized WD40 repeat-containing protein PfwLp1. The WD40 domains were depicted according to the SMART protein domain database (<http://smart.embl-heidelberg.de/>). The immunogenic region used for production of antiserum is labeled with blue line (rp2).

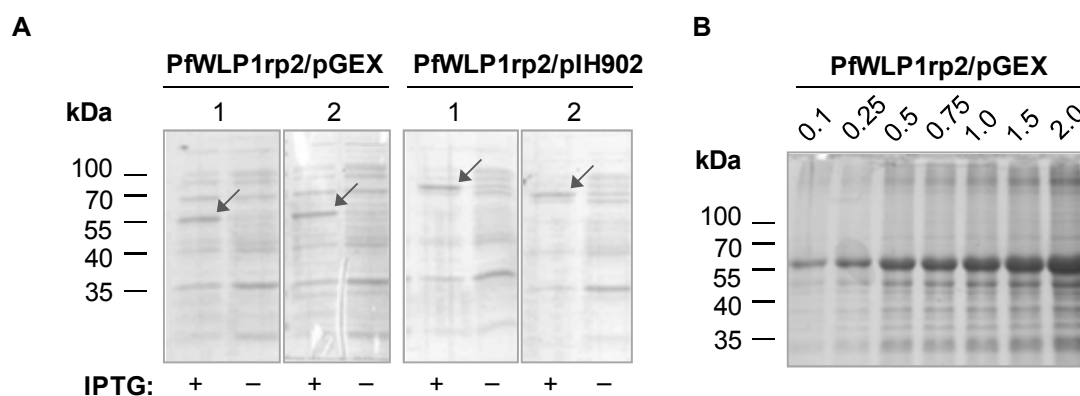


Fig. 3.29: **A.** SDS-PAGE after expression of recombinant protein of PfwLp1 (~32 kDa) by *E. coli* BL21 CodonPlus® (DE3)-RIL. After induction of transcription (+ IPTG) a band of ~58 kDa was observed for the recombinant protein PfwLp1rp2 fused to GST tag (pGEX, left panel). A protein of ~72 kDa was produced when PfwLp1rp2 was fused to MBP tag (pIH902, left panel). For both plasmid constructs two clones (1, 2) are depicted. For comparison, the lysate of control bacteria (-, no IPTG added) is shown. **B.** Different volumes (μ l) of recombinant protein PfwLp1rp2 were applied to SDS-PAGE after isolation via inclusion bodies for estimation of protein concentration.

3.5.2 Expression of PfWLP1 throughout the life cycle of *P. falciparum*

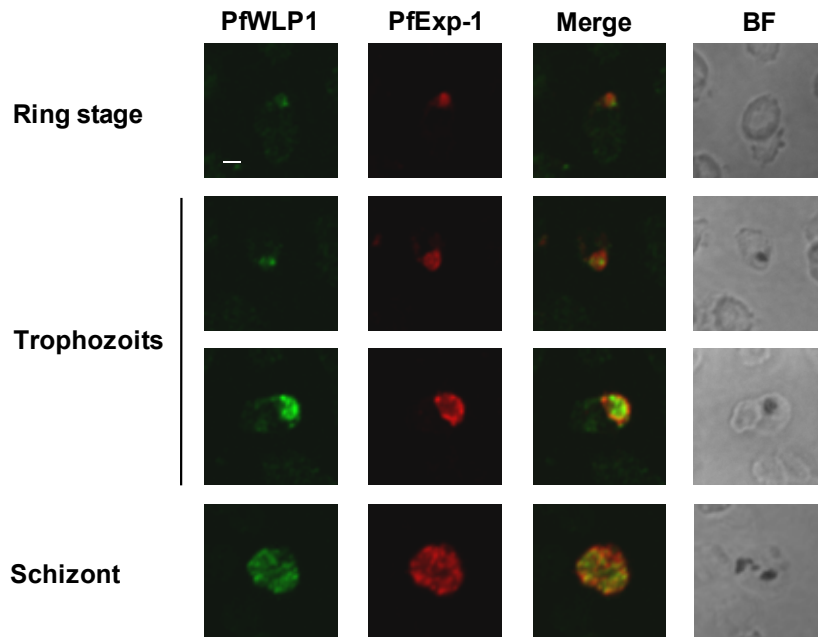


Fig. 3.30: Indirect IFAs showed that PfWLP1 (Alexa-488, green) is expressed in asexual blood stages and that expression increases with maturation of parasites. Antiserum directed against PfExp-1 (Alexa-594, red) which locates to the PVM was used for visualization of the different parasite stages. BF - bright field, scale bar - 2 μ m.

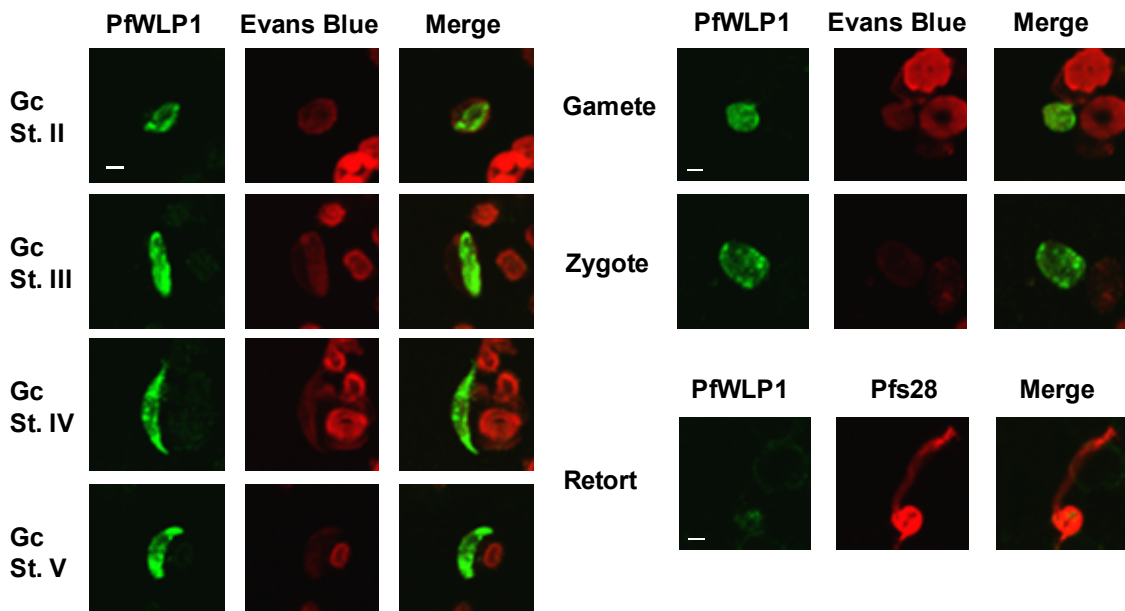


Fig. 3.31: Indirect IFAs showed that PfWLP1 (Alexa-488, green) is expressed in gametocyte stages II–V as well as in gametes and zygotes. Erythrocytes were counterstained with Evans Blue. In retort stages only a faint signal for PfWLP1 was detected in the residual body of the retort stage. Antiserum directed against Pfs28 (Alexa-594, red) were used for visualization of retort stages. Scale bar - 2 μ m.

The investigation of the expression of PfWLP1 using the generated antiserum showed that PfWLP1 is expressed throughout the development of asexual blood stages. Intensity of the fluorescent signal increased with the maturation of parasites (Fig. 3.30). PfWLP1 was detected in gametocytes stage II–V. In the course of gametocyte development intensity of PfWLP1 expression increased. The fluorescent signal of gametocytes was stronger as compared to asexual blood stage parasites. The distribution was mainly homogenous with a partially spotted expression pattern. Stage I gametocytes were not investigated due to the difficulty to identify this first stage of gametocytogenesis without using a stage-specific marker. In macrogametes the protein was also detected in a rather homogenous distribution. In zygotes the fluorescent signal had decreased as compared to gametes. In retort stages only very faint expression was observed in the residual body (Fig. 3.31). Indirect IFAs were also carried out using neutral mouse serum, in order to rule out unspecific reaction of the immune sera with *P. falciparum* antigens (Fig. 3.32).



Fig. 3.32: Indirect IFAs were carried out with serum from naive mice. The serum (Alexa-488, green) did not show specific labeling of *P. falciparum* parasites. Stage specific proteins were labeled with Alexa-594 (red). Scale bar - 5 μ m. Kindly provided by Dr. Nina Simon.

The expression of PfWLP1 in different parasite stages was further investigated via Western blot analyses by MSc. Vanesa N. Ngongang, MSc (Ngongang, 2012). In ring stage lysates and schizont lysates of the gametocyte-less strain F12 and of wild-type NF54 parasites a band of approximately 70 kDa was observed when probing with anti-PfWLP1 antiserum (Fig. 3.33 A). In wild-type gametocytes and gametocytes activated to undergo gametogenesis a band of the same molecular weight was detected, respectively. As the molecular weight of PfWLP1 is 95.8 kDa it is probable that the protein had been processed. In a second set of Western blot analysis using the same antiserum, a band of approximately 90 kDa was detected in ring stages, schizonts and gametocytes (Fig. 3.33 B). In gametocyte lysate, additionally a band of 70 kDa was observed. In activated gametocytes, on the contrary, only the 70 kDa protein band was visible. The Western blot results are in accordance with the expression of PfWLP1 observed in indirect IFAs. The different species of bands observed suggest that PfWLP1 is subject to proteolytic processing. Whilst in asexual blood stages and in gametocytes both the full length and the processed band occurred, it seems as if in activated gametocyte the processed form dominates.

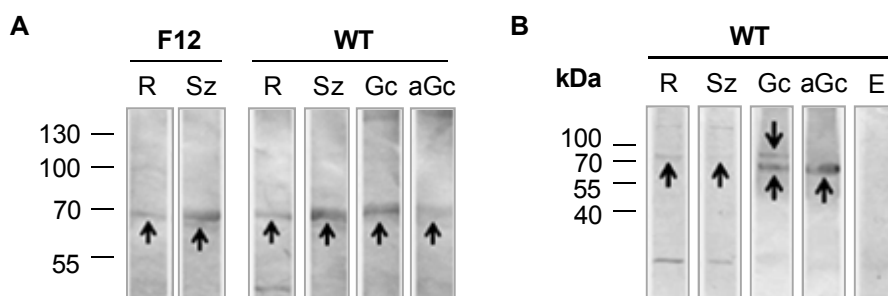


Fig. 3.33: **A.** Western blot analysis using anti-PfWLP1 antiserum detected a band of approximately 70 kDa in ring stage parasites (R) and schizonts (Sz) in lysates of both the gametocyteless strain F12 and WT NF54 parasites. The band was also observed for lysates of gametocytes (Gc) and gametocytes activated to undergo gametogenesis (aGc). **B.** In a second set of Western blot analysis a band of approximately 90 kDa was observed in ring stages, schizonts and gametocytes, while the previously detected band of 70 kDa was detected in lysates of gametocytes and activated gametocytes (Data from Ngongang, 2012).

3.5.3 Modifications of the *pfwlp1* locus via single crossing-over homologous recombination

In order to gain information on the function of PfWLP1 the corresponding gene was disrupted via single crossing-over homologous recombination strategy. Using the same technique the sequence encoding a double HA-tag was introduced at the 3' end of the gene. The thereupon expressed PfWLP1-HA fusion protein would allow further characterization of the protein. Integration of the transfected plasmids into the *pfwlp1* gene was investigated via diagnostic PCR. For the PfWLP1-HA mutant plasmid integration was observed 48 days after transfection of parasites and bands for both the 5' and 3' end of the integrated plasmid were detected (Fig. 3.34 B).

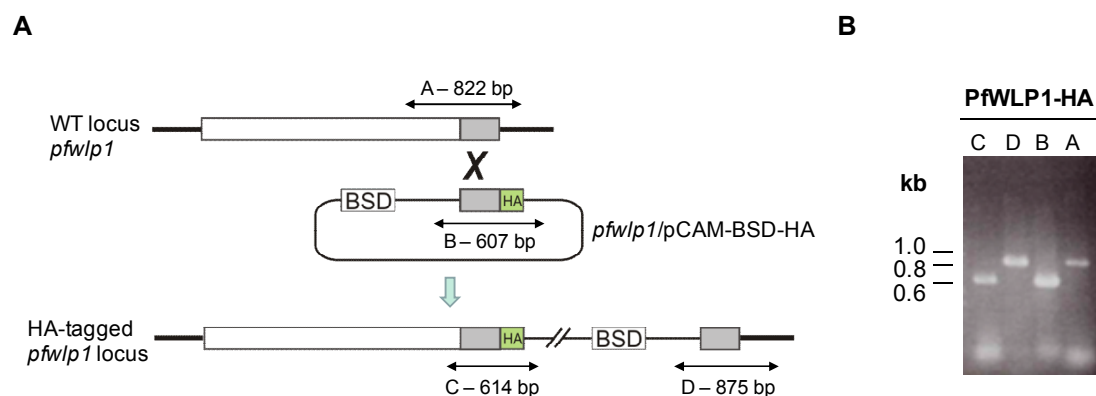


Fig. 3.34: **A.** Schematic depicting the *pfwlp1* wild-type (WT) gene locus and the modified HA locus resulting from vector integration via homologous recombination. Regions used for discrimination between WT and KO locus are marked with A–D. **B.** Diagnostic PCR on genomic DNA of PfWLP1-HA parasites showed bands corresponding to integration of the plasmid detected at the 5' region and at the 3' region of the gene. Gel lanes labeled according to panel A.

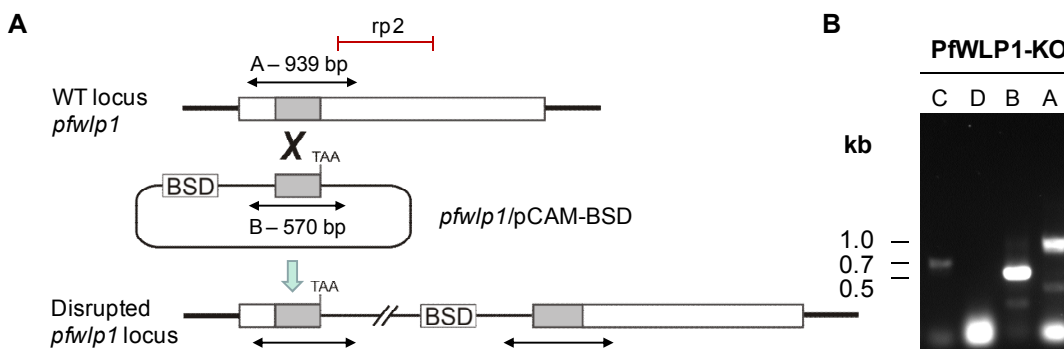


Fig. 3.35: **A.** Schematic depicting the *pfwlp1* wild-type (WT) gene locus and the modified KO locus resulting from vector integration via homologous recombination. Regions used for discrimination between WT and KO locus are marked with A–D. Location of the recombinant protein rp2 used for generation of antisera is marked with a red line. **B.** Diagnostic PCR on genomic DNA of PfwLp1-KO parasites showing a band corresponding to integration of the plasmid detected at the 5' region of the gene. Gel lanes are labeled according to panel A.

On the contrary, integration of the PfwLp1-KO plasmid was only detectable after approximately seven months. A PCR product corresponding to plasmid integration was observed for the 5' region of the disrupted gene only (Fig. 3.35 B). Dilutional cloning and further investigations of the two mutant parasite lines were carried out by Vanesa N. Ngongang, MSc (Ngongang, 2012). For the PfwLp1-HA mutant genomic DNA of five clones obtained from limiting dilution was isolated for diagnostic PCR. All of the five clones showed integration of the plasmid and no bands corresponding to the wild-type *pfwlp1* locus were observed. Western blot assays were carried out in order to verify expression of the HA fusion protein. In both investigated clones, PfwLp1-HA-1A7 and PfwLp1-HA-2F12 a band of approximately 110 kDa was observed in schizont lysates but not in gametocyte lysates when using anti-HA antibodies (Fig. 3.36 A). In WT lysates no bands were observed. The detection of PfwLp1 with anti-PfwLp1 antiserum showed a band in gametocyte and schizont lysates of both clones, respectively (Fig. 3.36 B). In indirect IFAs labeling with anti-HA antibodies did not result in a strong signal in asexual parasites, in gametocytes a slightly stronger signal was observed (Ngongang, 2012). Thus, as observed for PfactinII-HA parasites detection of the HA-tagged protein of interest with anti-HA antibody was more successful in Western blot analyses as compared to indirect IFA.

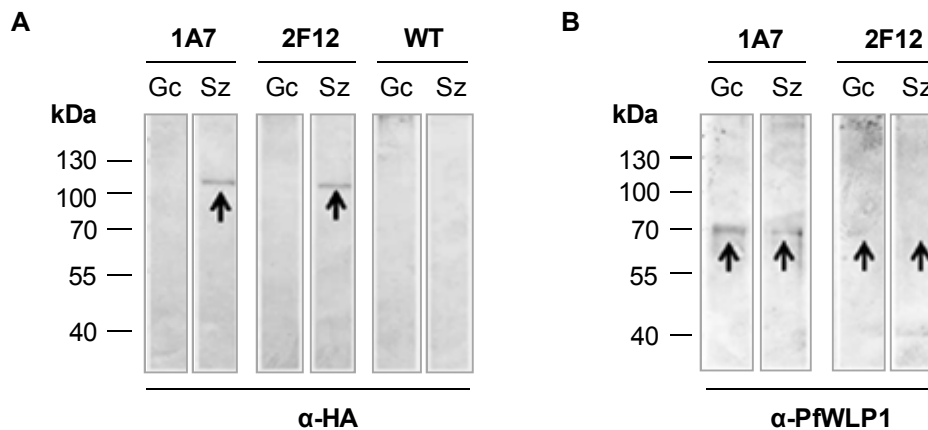


Fig. 3.36: Western blot analysis investigating the expression of the PfWLP1-HA fusion proteins in two of the obtained clones, PfWLP1-HA-1A7 and PfWLP1-HA-2F12. **A.** When probing with anti-HA antibody, in schizont lysates of both mutants a band of approximately 110 kDa was observed. **B.** Probing lysates of the two mutants with anti-PfWLP1 antiserum resulted in a band at approximately 70 kDa in both gametocyte and schizont lysate (Ngongang, 2012).

For the PfWLP1-KO parasite line 21 clones were obtained after dilutional cloning. The genomic DNA of 12 of the clones was isolated and diagnostic PCR was carried out in order to verify integration of the plasmid into the *pfwlp1* gene. Only three of the clones showed bands corresponding to integration of the plasmid, the other clones were carrying episomal plasmid only. The three clones showing plasmid integration, however also showed a band corresponding to the wild-type genotype (Ngongang, 2012). Thus, until now no PfWLP1-KO clone was isolated that was devoid of a wild-type parasite population. Considering the band pattern of the diagnostic PCR before dilutional cloning, that showed a very strong band for wild-type locus, it becomes clear that the wild-typic genotype dominated in the clones investigated (Fig. 3.35 B).

3.6 Induction of gametogenesis

The gamete formation of *P. falciparum* was studied on the molecular level in order to gain information on how the stimuli triggering this process are perceived by the parasite. Additionally, investigations on the ultrastructural level were carried out to decipher the sequential processes occurring during gametogenesis.

3.6.1 Interaction of XA with non-infected RBCs

In previous studies I observed that XA apparently interacts with niRBCs (Kuehn, 2007). In detail, niRBCs were incubated with XA followed by extensive washing of the cells. The subsequently produced homogenate of niRBCs (in the following referred to as XA-RBCH) induced exflagellation when added to mature male gametocytes. The XA concentration remaining in the supernatant after the washing steps on the contrary did not

lead to exflagellation. RBC homogenate incubated with PBS instead of XA likewise did not induce exflagellation (Fig. 3.37).

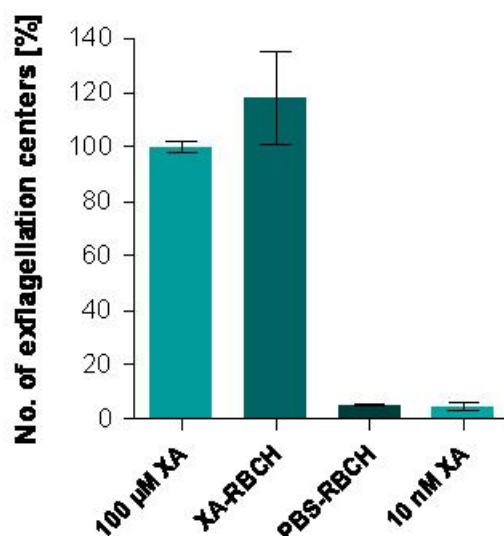


Fig. 3.37: Exflagellation assay applying the homogenate of niRBCs after incubation with XA (XA-RBCH) exhibited an exflagellation rate comparable to that of a 100 µM XA solution in PBS whilst RBC homogenate after incubation in PBS (PBS-RBCH) did not induce exflagellation. 10 nM XA in PBS, the concentration of XA expected after washing of the cell several times, did not lead to exflagellation, either.

Upon these observations we supposed that XA might be taken up by the niRBC or interact with the RBCM. The following experiments aimed at investigating whether XA is taken up into the RBC cytosol and to characterize this potentially occurring transport.

3.6.2 Uptake of XA by non-infected RBCs

In order to see whether XA was taken up into the RBC cytosol XA-RBCH was subjected to ultracentrifugation to separate membrane and cytosol fraction. The resulting pellet and supernatant fractions were analyzed via Western blot. Probing with antibodies directed against the transmembrane protein glycoprotein A (GpA) confirmed almost complete absence of RBC membranes from the supernatant fraction. In the pellet fraction prominent bands corresponding to the GpA homodimer, GpA/GpB heterodimer and GpA monomer (Auffray *et al.* 2001) were detected (Fig. 3.38 A). The fractions obtained by ultracentrifugation were tested for their gametogenesis-inducing activity. Therefore the fractions were added to a culture of mature gametocytes and exflagellation centers were counted. The cytosol fraction (supernatant) induced exflagellation comparably to the positive control (10 µM XA) ($p = 0.0745$, unpaired t-test). The membrane pellet, in contrary, was not capable to induce exflagellation in male gametocytes (Fig. 3.38 B). The values obtained for the membrane pellet were comparable to the negative control ($p = 0.3252$, unpaired t-test). Upon these findings in the subsequent experiments only

the cytosolic fraction of XA-RBCH, in the following referred to as XA-RBCF, was used. XA-RBCF was obtained via ultrafiltration through a 0.22 μm syringe filter.

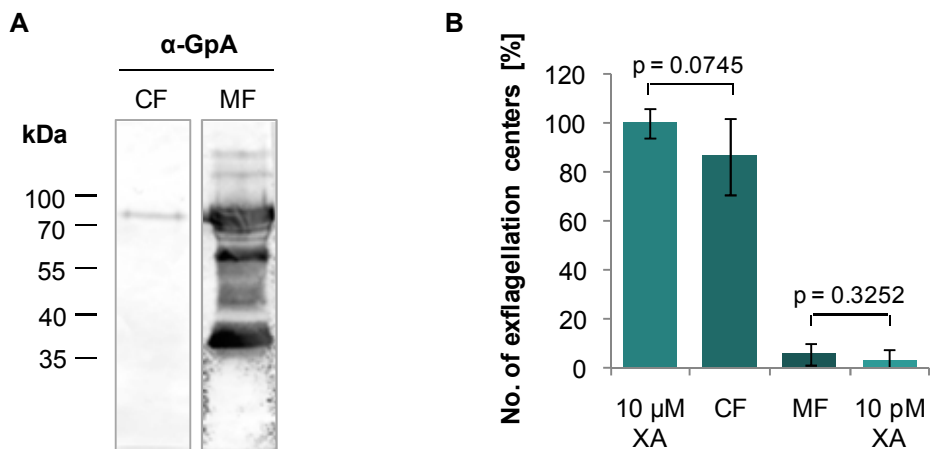


Fig. 3.38: **A.** Western blot analysis detected Glycophorin A (GpA) in the membrane fraction (MF) of homogenate of XA-RBCH after ultracentrifugation. The cytosol fraction (CF) showed almost complete absence of GpA. **B.** When applied to a mature gametocyte culture, the CF obtained after ultracentrifugation of XA-RBCH induced exflagellation comparable to the positive control (10 μM XA), whilst the MF resulted in exflagellation events comparable to the negative control (10 pM XA). Combined results (Mean and SD) of two independent experiments, comprising six counts per sample in total, are shown in percent of positive control. P-values were determined by unpaired t test.

Qualitative analysis of XA uptake

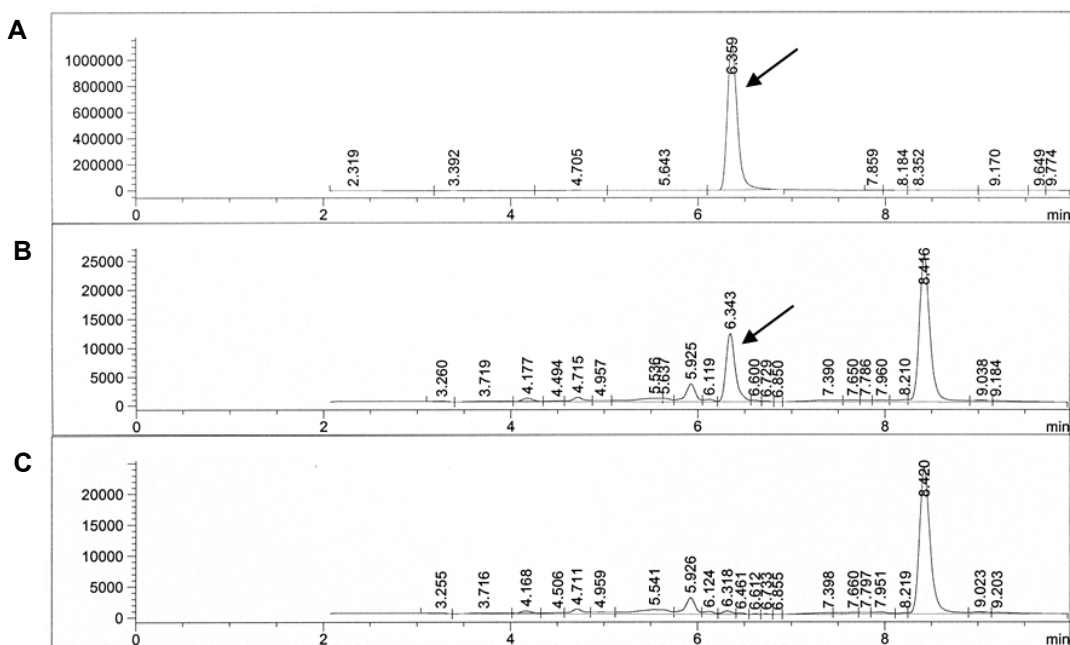


Fig. 3.39: Mass spectrogram after separation of samples via HPLC. An extracted ion chromatogram from 205.7 - 206.7 was measured (the molecular mass of the protonated XA is 206.17). **A** Standard of 10 mg/ml XA. **B.** Ultrafiltrate of homogenized RBCs after incubation with 10 μM XA followed by four washing steps. **C.** Ultrafiltrate of homogenized RBCs after incubation with PBS followed by four washing steps. Arrows highlight peaks of XA.

To confirm the uptake of XA by niRBCs HPLC followed by mass spectrometry analyses were carried out. All experiments employing HPLC and mass spectrometry were accomplished in the laboratory of Dr. Matthias Unger (Institute of Pharmacy and Food Chemistry, University of Würzburg). Firstly, we compared the mass spectrograms of XA-RBCF and of the homogenate of PBS-incubated RBC with that of the 10 mg/ml XA which served as standard. XA-RBCF showed the same characteristic peak representing the XA molecule as the XA standard. The mass spectrogram of the homogenate of PBS-incubated RBC on the contrary did not show this peak (Fig. 3.39).

Quantitative analysis of XA uptake

The uptake of XA by RBCs was further investigated quantitatively by detecting XA within the filtrate of XA-incubated RBCs via LC/ESI/MS/MS. RBCs were incubated with different XA concentrations at RT for 30 min. The concentration of XA detected in the XA-RBCF samples increased with the concentration applied during incubation and accounted for 11–14% of the original concentration (Tab. 3.3, Fig. 3.40 A)

Tab. 3.3: RBCs were incubated with different concentrations of XA for 30 min at RT. The XA concentrations present in the resulting XA-RBCFs were investigated via LC/ESI/MS/MS analyses. Detected XA concentration increased linearly with the XA concentration used for incubation.

Incubation XA [μ M]	XA detected [nM]	Uptake [%]
PBS control (0.00)	0.2	–
0.01	1.4	14.0
0.10	11.8	11.8
1.00	111.4	11.1
10.00	1100.2	11.0

Tab. 3.4: RBCs were incubated in 10 μ M XA/ PBS and incubated for different durations. The XA concentrations present in the resulting XA-RBCFs were investigated via LC/ESI/MS/MS. Uptake of XA increased linearly with incubation time.

Incubation time [min]	XA detected [nM]	Uptake [%]
1	55.2	0.6
5	220.6	2.2
10	478.4	4.8
15	668.8	6.7
20	853.8	8.5
25	897.2	9.0
30	1185.0	11.9

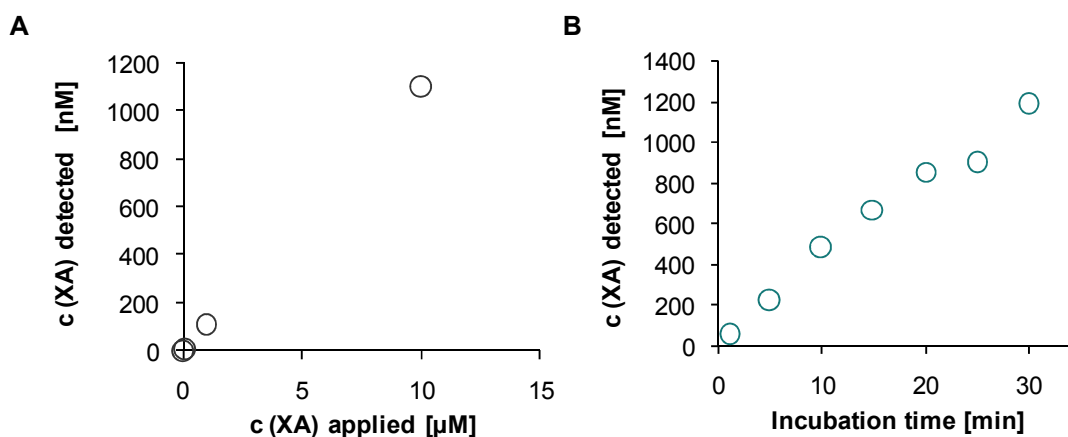


Fig. 3.40: **A.** Concentration of XA detected via LC/ESI/MS/MS of XA-RBCF increased linearly with XA concentration applied during incubation of RBCs (see Tab. 3.3). **B.** Concentration of XA detected via LC/ESI/MS/MS analysis of XA-RBCF increased linearly with duration of incubation of RBCs with 10 μM XA (see Tab. 3.4).

Furthermore, the influence of incubation time with XA was investigated. The XA concentration detected in the XA-RBCF increased linearly with incubation time. The durations of incubation tested ranged between 1 min and 30 min (Tab. 3.4, Fig. 3.40 B).

Next we tested whether the XA uptake would be saturable with increasing concentrations of XA. When applying different concentrations of XA ranging from 0.025 to 7.5 mM XA a saturation of XA uptake was observed (Fig. 3.41). Thus, we were able to determine the Michaelis Menten value (K_m) for XA uptake. The K_m value showed to be 1.74 ± 0.12 mM, whilst V_{max} was 178.2 ± 4.69 μM.

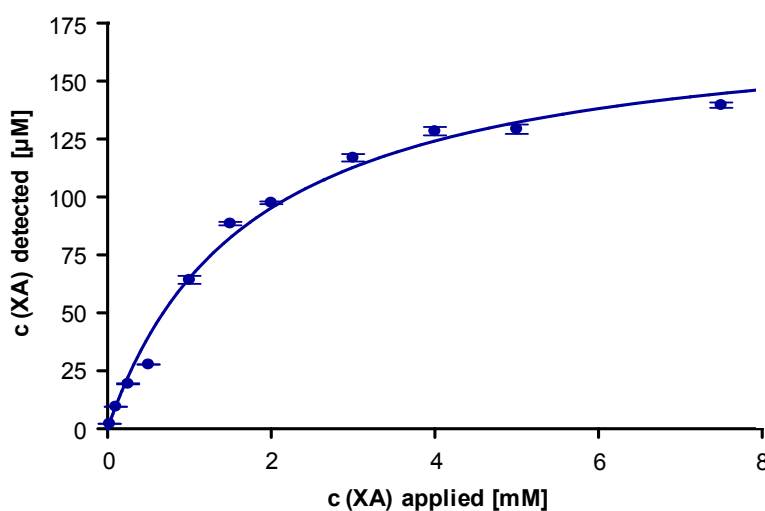


Fig. 3.41: With increasing XA concentration a saturation of XA uptake occurs (incubation for 30 min). A K_m value of 1.74 ± 0.12 mM for XA uptake was determined. V_{max} was calculated as 178.2 ± 4.69 μM.

3.6.3 Inhibitors of RBC transport pathways

After demonstrating that XA is taken up by niRBCs we wanted to identify the transport mechanism of the RBC membrane that might be responsible for XA uptake. Therefore, inhibitor studies using previously described inhibitors of transport proteins were carried out. The inhibitors included in the following studies were targeting nucleobase and nucleoside transporters, amino acid transporters, a glucose transporter as well as organic anion transporters (OATPs). The mentioned transport proteins were considered as potential candidates for XA uptake due to the heterocyclic structure of their substrates.

As inhibitors for the nucleobase transporter hFNT1 adenine and hypoxanthine were chosen that had previously been as competitive inhibitors of hFNT1 (Domin *et al.*, 1988; Wallace *et al.*, 2002). NBTI (NBMPR) had been reported to inhibit the nucleoside transporter hENT1 (Plagemann and Woffendin, 1988; Mahony *et al.*, 2004). The three substances were tested in two different types of exflagellation assays. Firstly, the inhibitors were added directly to a mature gametocyte culture prior to and/or during incubation with XA at RT. All inhibitors tested, the concentrations used and references for published inhibitor studies are summarized in Tab. 8.1 (Appendix).

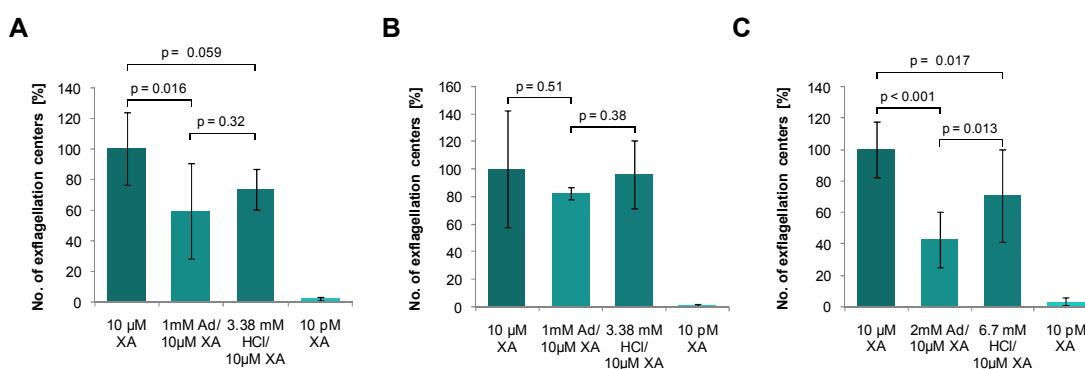


Fig. 3.42: **A.** The addition of 1 mM adenine to a mature gametocyte culture resulted in significant reduction of the number of exflagellation centers. However, there was no significant reduction when comparing with the control containing the solvent of adenine, HCl. Combined results (Mean and SD) of three independent experiments, comprising eight counts per sample in total, are shown. **B.** When 1 mM adenine was added 15 min prior to activation of mature gametocytes and during the 15 min of incubation with XA no significant inhibition was observed. Mean and SD of one experiment are shown. **C.** The increased concentration of 2 mM adenine was tested in exflagellation assays without incubation of adenine prior to activation of gametocytes. The addition of 2 mM adenine inhibited exflagellation of male gametocytes significantly compared to the solvent control. Combined results (Mean and SD) of three independent experiments, comprising eleven counts per sample in total, are shown in percent of positive control (10 μ M XA). P-values were determined by unpaired t test.

The addition of 1 mM adenine to the gametocyte culture concurrently with XA resulted in a significant reduction of exflagellation centers compared to the sample containing 10 μ M XA only ($p=0.016$, unpaired t-test). However, the results of 1 mM adenine did not differ significantly from that of the control containing the solvent of adenine ($p=0.32$). The solvent control also inhibited exflagellation, although less pronounced as

1 mM adenine ($p=0.059$, Fig. 3.42 A). When adding 1 mM adenine prior to and during incubation with XA exflagellation of male gametocytes exflagellation was not reduced significantly compared to the control containing the solvent of adenine ($p=0.38$, Fig. 3.42 B). The effect of adenine was additionally tested for a concentration of 2 mM, added to a gametocyte culture concurrently with XA at RT. The combined results of three independent experiments showed a significant decrease in the number of exflagellation centers as compared the positive control, 10 μM XA ($p<0.001$). The solvent of adenine, HCl at a final concentration of 6.7 mM, also had an inhibitory effect and a decreased number of exflagellation centers was observed ($p=0.017$). However, when comparing results obtained after addition of 2 mM adenine with those of the solvent control the number of exflagellation centers was still significantly lower ($p=0.013$, Fig. 3.42 C).

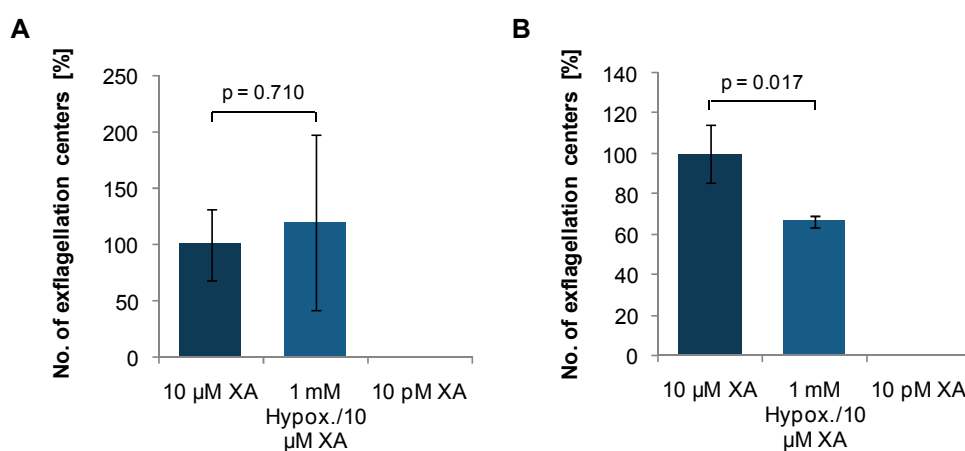


Fig. 3.43: **A.** The addition of 1 mM hypoxanthine to a mature gametocyte culture did not result in a significant reduction of number of exflagellation centers. **B.** When 1 mM hypoxanthine was added 15 min prior to activation of mature gametocytes and during the 15 min of incubation with XA the observed number of exflagellation centers was strongly decreased. Mean and SD of one experiment are shown, respectively, in percent of positive control (10 μM XA). P values were determined by unpaired t test (**A**, **B**). No solvent control has been included as hypoxanthine was dissolved in PBS.

As a second inhibitor of the nucleobase transporter hFNT1, hypoxanthine was tested (see Appendix Tab. 8.1, Mahony *et al.* 2004). When 1 mM hypoxanthine was added simultaneously with XA to a mature gametocyte culture, no reduction of exflagellation of male gametocytes was observed in comparison to the positive control (10 μM XA) (Fig. 3.43 A). Additionally, gametocytes were incubated for 15 min at 37°C with hypoxanthine, and subsequently with hypoxanthine and XA to activate gamete formation. Under these conditions gametocytes treated with hypoxanthine showed a significantly decreased number of exflagellation centers ($p=0.017$, unpaired t-test) (Fig. 3.43 B).

To investigate if the nucleoside transporter hENT1 is involved in XA uptake, the previously described inhibitor NBTI (Mahony *et al.*, 2004) was tested in exflagellation assays. When 5 μM NBTI were added to mature gametocytes, a slight reduction of exflagellation was observed, compared to the positive control, 10 μM XA. However, the

results obtained for the solvent control (0.05% DMSO) were similar (Fig. 3.44 A). When gametocytes were pre-incubated with NBTI prior to activation with XA and upon addition of XA, a significant reduction of exflagellation was observed. Incubation with 0.05% DMSO resulted in an even more pronounced inhibition (Fig. 3.44 B).

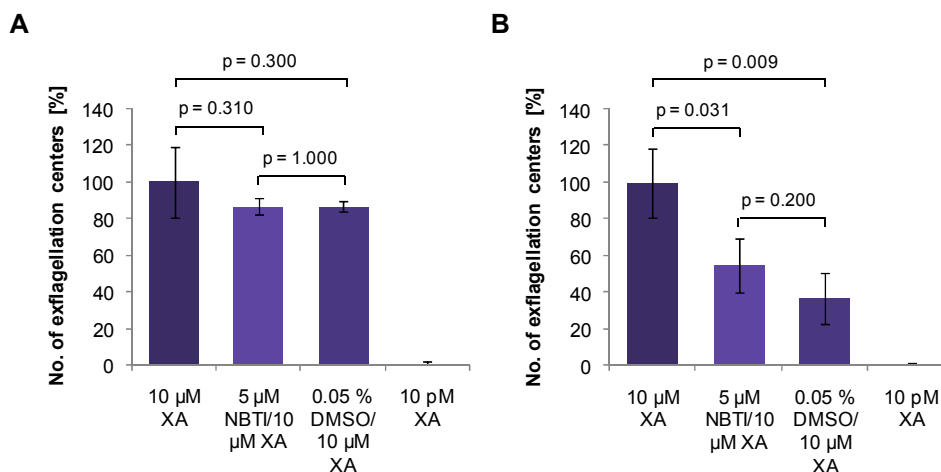


Fig. 3.44: **A.** The addition of 5 µM NBTI to a mature gametocyte culture did not result in a significant reduction of number of exflagellation centers. **B.** When 5 µM NBTI were added 15 min prior to activation of mature gametocytes and during the 15 min of incubation with XA the observed number of exflagellation centers was considerably decreased. Exflagellation was also inhibited upon addition of the solvent of NBTI, DMSO. Mean and SD of one experiment, respectively, are shown in percent of positive control (10 µM XA). P values were determined by unpaired t test. (**A**, **B**).

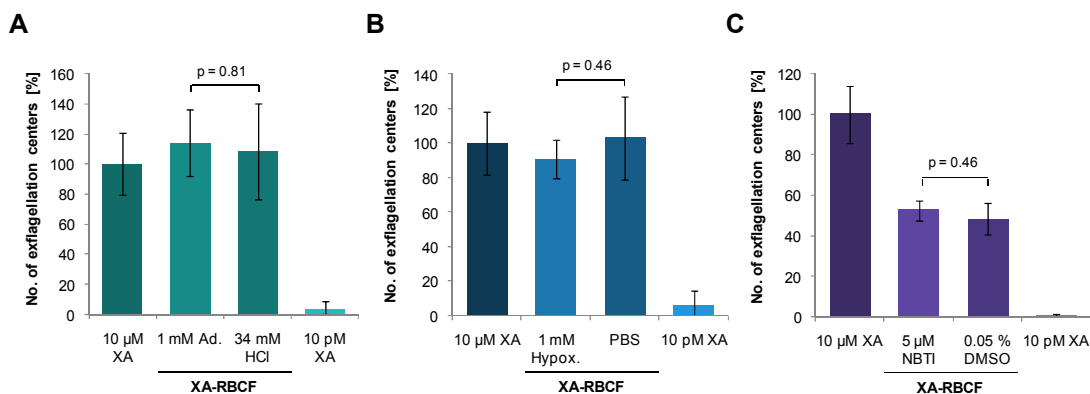


Fig. 3.45: Influence of inhibitors of nucleobase/nucleoside transport on XA uptake by RBCs. RBCs were incubated for 30 min with the respective inhibitor followed by 30 min of incubation with XA and inhibitor. The subsequently obtained XA-RBCF was applied in exflagellation assays. Neither for adenine (**A**), hypoxanthine (**B**) nor for NBTI (**C**) a significant reduction of exflagellation was observed compared to the respective control. As control XA-RBCF of RBCs incubated with solvent instead of inhibitor were used. Mean and SD of one experiment, respectively, are shown in percent of positive control (10 µM XA). P values were determined by unpaired t test.

The influence of inhibitors of nucleoside and nucleobase transport on XA uptake by RBCs was tested in a second type of exflagellation assay. Non-infected RBCs were incubated with adenine, hypoxanthine or NBTI at RT for 30 min. Thereafter, an additional 30 min of incubation with inhibitor and XA followed. As a control, RBCs were incu-

bated with the solvent of the respective inhibitor. After incubation, RBCs were washed and XA-RBCFs were obtained as described above (2.2.8, 3.6.2). When XA-RBCFs were tested in exflagellation assays, for neither inhibitor a significant reduction of microgamete formation was observed (Fig. 3.45). The combined results on exflagellation assays employing inhibitors of RBC nucleobase and nucleoside transporters showed significant reduction of exflagellation when applying inhibitors of the nucleobase transporter, but not of the nucleoside transporter. However, experiments with niRBCs revealed that the inhibitors did affect XA uptake by RBCs. Thus, the impact of the inhibitors on exflagellation was caused by distinct unknown mechanism.

As a second group of potential inhibitors of XA transport the inhibitors of transporters of aromatic amino acids, system T and system L, were considered. While system T is responsible for transport of the amino acids tryptophan (Trp), tyrosine and phenylalanine, system L mediates uptake of tyrosine, phenylalanine (Phe), leucine (Leu) and isoleucine. L-Phe, L-Leu and L-Trp had been described to competitively inhibit the respective transport system (Lopez-Burillo *et al.*, 1985; Tate *et al.* 1992, see Appendix, Tab. 8.1). The three amino acids were thus tested in exflagellation assays to investigate their potential to inhibit XA uptake. When applied to a mature gametocyte culture, none of the three inhibitors led to a reduction of exflagellation in male gametocytes (Fig. 3.46).

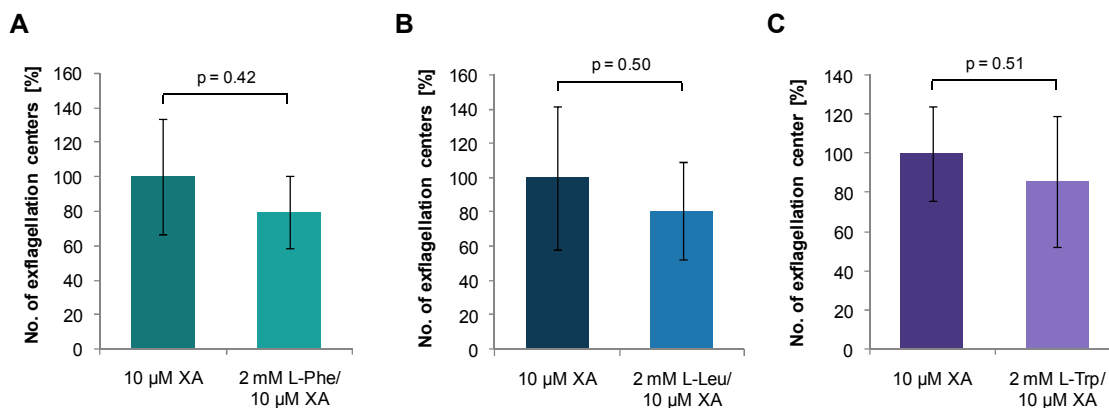


Fig. 3.46: Influence of inhibitors of system T and system L on induction of gametogenesis in male gametocytes. All inhibitors were incubated with culture of mature gametocytes for 15 min prior to activation of gametocytes. Mean and SD are shown in percent of positive control (10 µM XA). P values are determined by unpaired t test. **A.** 2 mM of L-phenylalanine did not reduce exflagellation (1 experiment, 3 counts per sample). **B.** Addition of 2 mM of L-leucine did not affect exflagellation (1 experiment, 4 counts per sample). **C.** Incubation with 2 mM of L-tryptophan did not influence exflagellation (combined data of two experiments, total of 5 counts per sample).

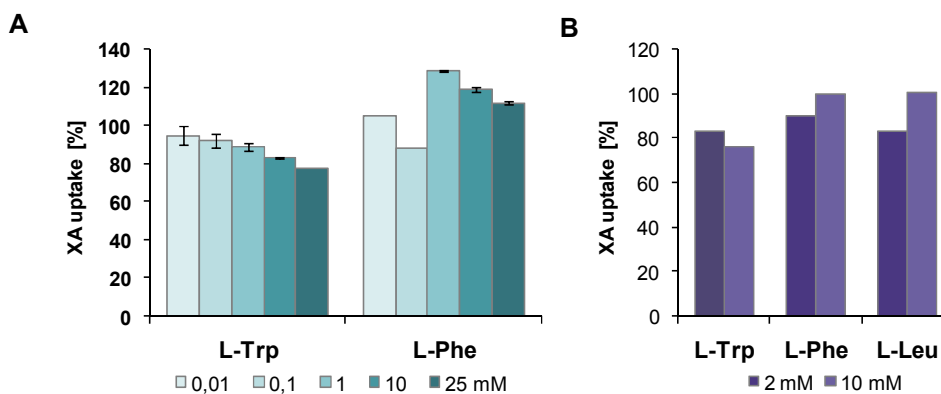


Fig. 3.47: The uptake of XA in the presence of inhibitors of aromatic amino acid transporters was measured via LC/ESI/MS/MS. **A.** Non-infected RBCs were incubated with 1 μ M XA in the presence of either L-Trp or L-Phe of varying concentrations for 30 min at 37°C. Mean and SD of one experiment measured in triplicates is shown in percent of PBS control. **B.** RBCs were pre-incubated with L-Trp, L-Phe or L-Leu for 15 min at 37°C and further 30 min in the presence of inhibitors and 1 μ M XA at RT. Values of one experiment shown in percent of PBS control.

Secondly, competitive inhibitors of aromatic amino acid transport were tested in studies measuring the uptake of XA by RBCs via LC/ESI/MS/MS. RBCs were incubated with L-Trp or L-Phe in the presence of 1 μ M XA for 30 min at 37°C. For L-Trp a slight reduction of XA uptake was observed which increased with L-Trp concentration. (Fig. 3.47 A). For L-Phe no linearity between inhibitor concentration and inhibition of uptake was observed. The lowest XA concentration taken up was measured after incubation with 0.1 mM L-Phe. For other concentrations of L-Phe applied to the RBCs did not result in reduction of XA uptake (Fig. 3.47 A). The three inhibitors L-Trp, L-Phe and L-Leu were also tested with pre-incubation of RBCs for 15 min before XA was added. Here, for RBCs incubated with 10 mM L-Trp 76% of the XA concentration of the inhibitor-free control was measured. L-Phe and L-Leu showed approximately 90% and 83% of the XA uptake of the positive control (Fig. 3.48 B).

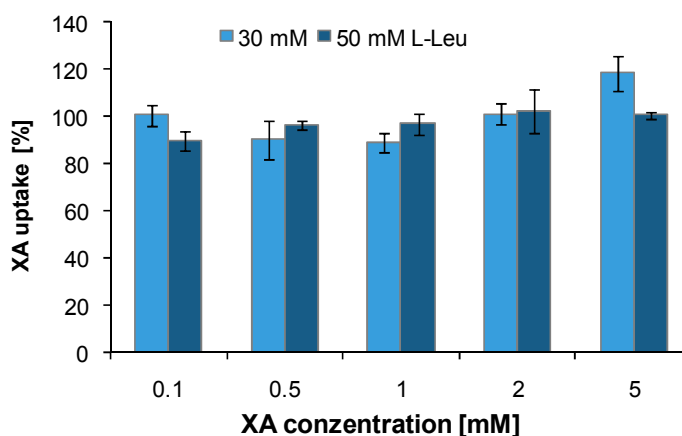


Fig. 3.48: The uptake of XA in the presence of the inhibitor of aromatic amino acid transport L-Leu was measured via LC/ESI/MS/MS. Non-infected RBCs were incubated with varying concentrations of XA in the presence of either 30 mM or 50 mM L-Leu for 30 min at 37°C. Mean and SD of one experiment measured in triplicates as percentage of control are presented.

The uptake of XA in the presence of the inhibitor of the system L, L-Leu was investigated for varying XA concentrations applied with two high L-Leu concentrations which were described to inhibit the non-saturable component of the system L (Lopez-Burillo *et al.*, 1985). The lowest uptake was observed when incubating 30 mM L-Leu with 1 mM XA. In that case XA uptake accounted for approximately 90% of that of the inhibitor-free control (Fig. 3.48). Thus, the combined results on inhibitors of aromatic amino acid transporters did not reveal involvement of these transporters on XA uptake by RBCs.

As a third candidate for XA transports across the RBC plasma membrane the glucose transport protein 1 (GLUT1) was included into the uptake studies. GLUT1-mediated hexose transport had been reported to be inhibited by cytochalasin B (Concha *et al.*, 1997, see Appendix Tab. 8.1). RBCs were incubated with different concentrations of the inhibitor cytochalasin B for 15 min at RT, followed by further 30 min of incubation in the presence of inhibitor and XA. The measurement of XA via LC/ESI/MS/MS did not reveal a prominent reduction of XA uptake. After incubation of RBCs with 1 mM cytochalasin B, XA uptake accounted for 83% of the solvent control, containing ethanol in the same concentration as in the sample. For the other concentrations of cytochalasin B tested, no effect on XA uptake was detected (Fig. 3.49).

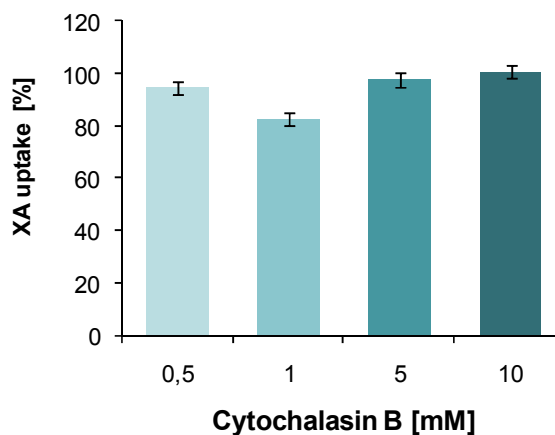


Fig. 3.49: The uptake of XA in the presence of the inhibitor of the glucose transporter GLUT1, cytochalasin B, was measured via LC/MS/MS. The inhibitor caused slightly reduced uptake of XA as compared to the corresponding control. XA uptake is depicted in percent of the respective control containing equal amounts of the solvent ethanol as the sample. Mean and SD of one experiment measured in triplicates are presented.

Finally, inhibitors of the OATP transporter family were tested for their potential impact on XA uptake by RBCs (Vavricka *et al.*, 2002; Seithel *et al.*, 2006, see Appendix Tab. 8.1). The addition of rifampicin to a mature gametocyte culture 15 min prior to and during incubation with XA resulted in reduction of exflagellation. At 300 μ M and at higher concentrations presence of rifampicin decreased the number of exflagellation centers significantly as compared to the positive control containing 10 μ M XA and the solvent of rifampicin, DMSO (Fig. 3.50). Similar results were obtained for the second

OATP inhibitor tested, erythromycin. The addition of 200 μM erythromycin 15 min prior to and during incubation with 10 μM XA resulted in a significant reduction of exflagellation of male gametocytes. At an erythromycin concentration of 500 μM this effect was even more pronounced (Fig. 3.50 B).

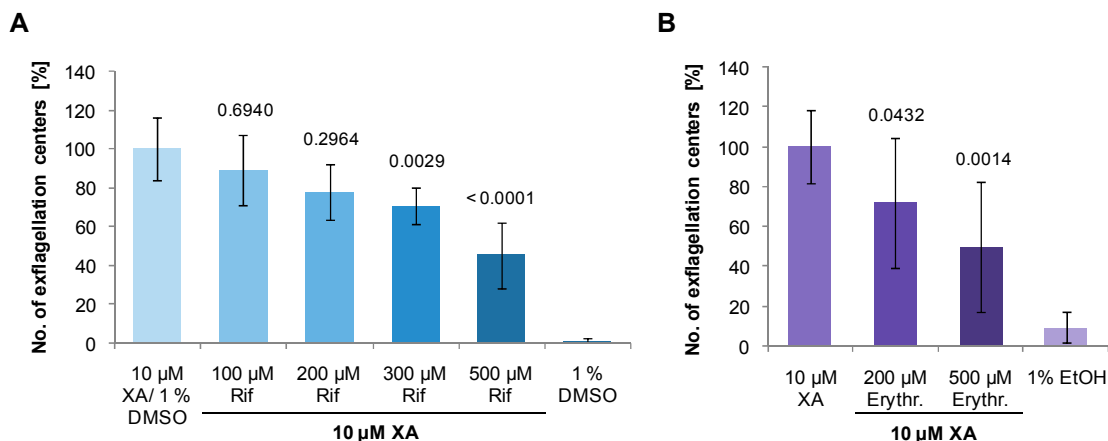


Fig. 3.50: A. The OATP inhibitor rifampicin caused a significant reduction of exflagellation of male gametocytes when applied at a concentration of 300 μM or higher with 15 min incubation prior to addition of XA. P values comparing samples with positive control (10 μM XA/ 1% DMSO) were determined by unpaired t test. Data of independent experiments were combined (total of at least four counts per sample). **B.** The OATP inhibitor erythromycin caused a significant reduction of exflagellation of male gametocytes when applied at a concentration of 200 μM or higher. Data of two independent experiments were combined (total of at least six counts per sample). Mean and SD are shown. P values comparing samples with positive control (10 μM XA) were determined by unpaired t test (**A**, **B**).

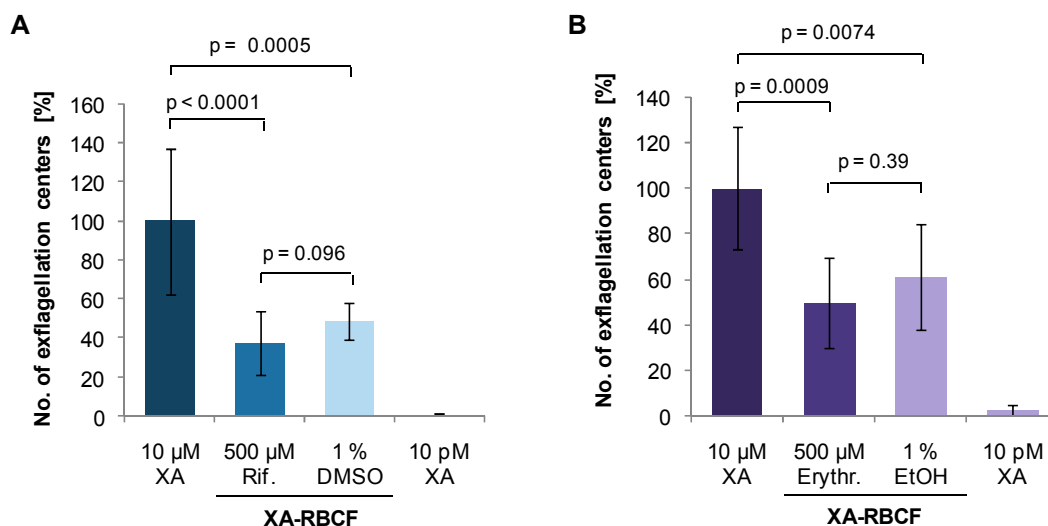


Fig. 3.51: A. XA-RBCF obtained after incubation of RBCs with 500 μM rifampicin did not show a significantly reduced exflagellation as compared to XA-RBCF of RBCs incubated with DMSO. Combined data of three independent experiments comprising at least nine counts per sample is depicted. **B.** XA-RBCF obtained after incubation of RBCs with 500 μM erythromycin did not show a significantly reduced exflagellation as compared to XA-RBCF of RBCs incubated with ethanol. Combined data of two independent experiments comprising in total at least 6 counts per sample is presented. P values were determined by unpaired t test. Mean and SD are shown. Data depicted in percent of positive control (10 μM XA) (**A**, **B**).

The influence of OATP inhibitors on XA uptake by RBCs was also tested with non-infected RBCs. After incubation with the inhibitor for 15 min at 37°C XA was added at a final concentration of 10 μ M and RBCs were incubated for further 15 min at RT. As a control, RBCs were incubated with the solvent of the respective inhibitor. After incubation, RBCs were washed and XA-RBCFs were obtained as described above (2.2.8). When XA-RBCFs were tested in exflagellation assays, for neither inhibitor a significantly reduced microgamete formation was observed (Fig. 3.51).

3.6.4 Effect of alterations of RBC membrane composition on XA uptake and gametogenesis

Various RBC surface proteins are sensitive to protease treatment. This fact has been exploited to identify receptor proteins of the RBCM and to gain information on the structure of RBC surface proteins including transport proteins (Thompson, J.K. *et al.*, 2001; Poole *et al.*, 1996). In order to investigate the structural properties of the putative transport protein responsible for XA uptake, influence of different proteases on XA uptake was investigated (see Appendix Tab. 8.2 for overview on conditions). RBCs were subjected to protease treatment, washed several times and subsequently incubated with XA as described above (2.2.8 and 3.6.2). Firstly, niRBCs were treated with proteinase K. When employing the obtained XA-RBCF in exflagellation assays we found that proteinase K treatment did not alter the ability of RBCs to take up XA. Both XA-RBCF of protease K treated RBCs and of RBCs treated with 1mM CaCl₂ (solvent of protease K) induced exflagellation similarly to XA directly applied to the gametocyte culture in a final concentration of 10 μ M (Fig. 3.52).

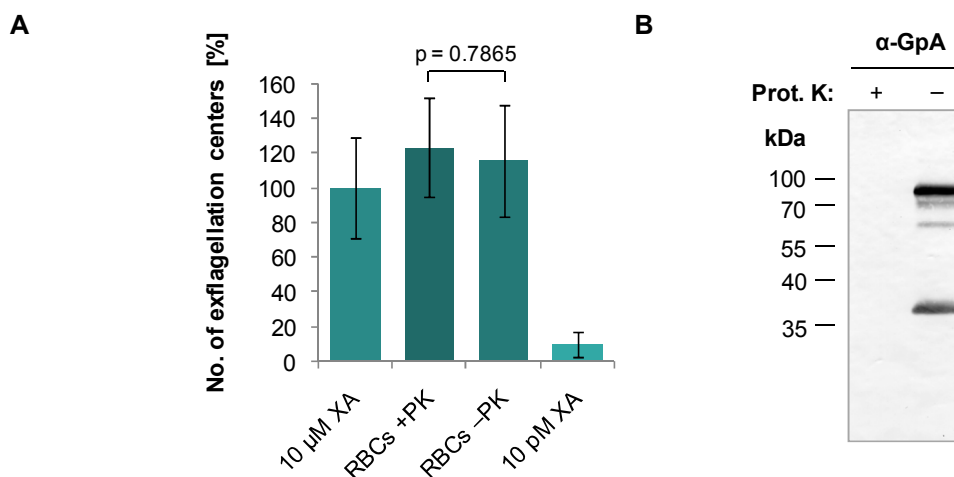


Fig. 3.52: **A.** XA-RBCF pre-treated with proteinase K (RBCs +PK) or CaCl₂ (RBCs -PK) were tested in exflagellation assays. No significant difference was observed between the two differently treated XA-RBCFs (p-value determined with unpaired t-test). Mean values and SD are shown. **B.** The efficiency of treatment with 0.5 mg/ml proteinase K was tested via WB analysis detecting glycophorin A. No glycophorin A was detected after protease treatment (+ Prot. K).

Furthermore, RBCs were treated with chymotrypsin or as a control with the solvent of the protease, CaCl₂, prior to incubation with XA. No significant difference was observed between the two XA-RBCF samples when tested in exflagellation assays ($p=0.7302$, unpaired t-test). Compared to the positive control, XA added to a final concentration of 10 μM , both XA-RBCF samples were less efficient in the induction of exflagellation (Fig. 3.53).

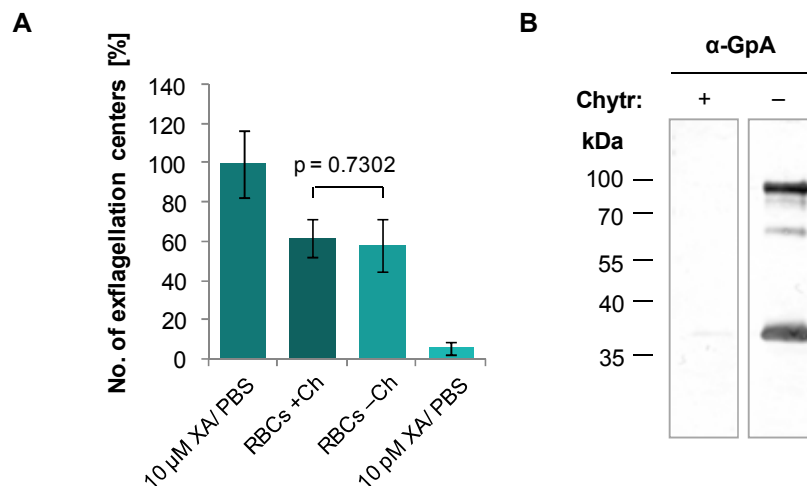


Fig. 3.53: **A.** XA-RBCF of RBCs pre-treated with chymotrypsin (RBCs +Ch) or CaCl₂ (RBCs -Ch) were tested in exflagellation assays. No significant difference was observed between RBCs incubated with chymotrypsin and RBCs incubated with the solvent CaCl₂ ($p=0.7302$, unpaired t-test). **B.** WB detecting glycophorin A (GpA) confirmed efficiency of protease treatment of RBCs.

The effect of the protease chymotrypsin was also tested on parasitized RBCs since it had been shown to alter the permeability of the ‘new permeability pathways’ that are responsible for the uptake of several molecule classes (Baumeister *et al.*, 2006).

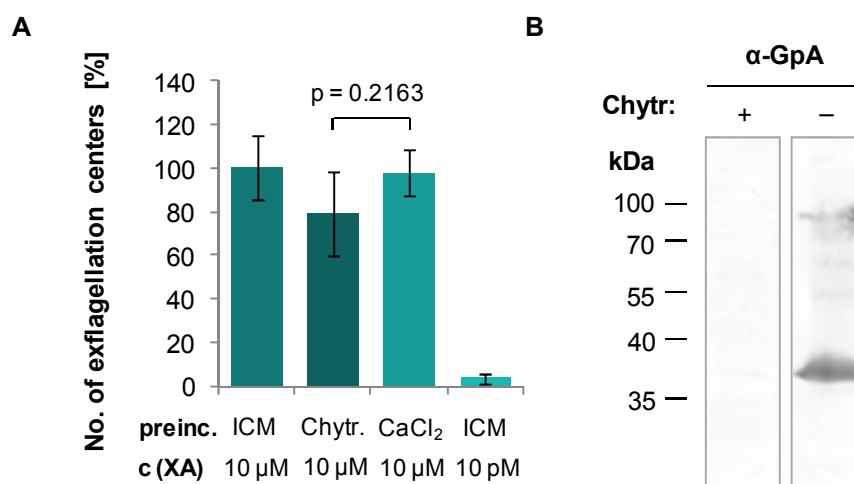


Fig. 3.54: **A.** A culture of mature gametocytes was pre-incubated with ICM, chymotrypsin or CaCl₂ (solvent control) at 37°C. Subsequently, exflagellation was induced via addition of XA. No significant difference was observed between the different treatment groups (mean and SD shown). 10 pM XA/ICM served as negative control. **B.** WB detecting glycophorin A (GpA) confirmed efficiency of protease treatment of iRBCs.

Aliquots of a culture of mature gametocytes were pre-incubated at 37°C with ICM, chymotrypsin or CaCl₂ (solvent of chymotrypsin) prior to activation of gametogenesis via addition of XA. The number of exflagellation centers between chymotrypsin- and CaCl₂-treated gametocytes did not differ significantly (Fig. 3.54, p-value: 0.2163, unpaired t-test).

In a second experiment manipulating the membranes surrounding the gametocytes, 0.07% saponin was added to a culture of mature gametocytes in order to permeabilize RBCM and PVM. Gametocytes treated with saponin were able to undergo exflagellation when 10 μM XA was added. The observed reduction of the number of exflagellation centers did not differ significantly from control gametocytes incubated with ICM instead of saponin (p=0.0912, unpaired t-test, Fig. 3.55 A). As an additional control, gametocytes were treated with saponin, but instead of XA, ICM was added. Under these conditions, a small proportion of gametocytes was activated to undergo gametogenesis. Nevertheless, compared to gametocytes activated by addition of XA, the number of exflagellation centers was significantly reduced (p=0.0076, unpaired t-test).

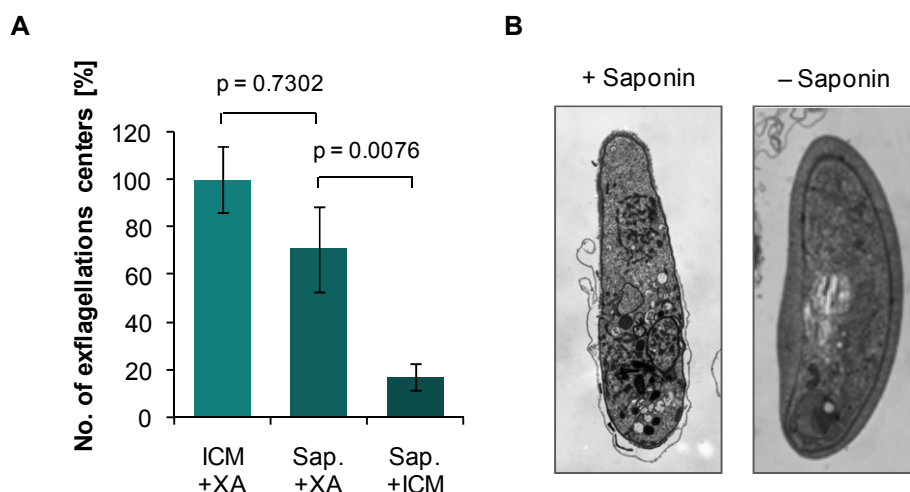


Fig. 3.55: **A.** A culture of mature gametocytes was treated with saponin in order to permeabilize RBCM and PVM. Subsequently, cells were activated with 10 μM XA and the number of exflagellation centers was determined (shown as mean and SD). No significant difference was observed between the positive control (incubated with ICM instead of saponin) and the saponin treated culture (unpaired t-test). Saponin treatment without addition of XA resulted only in low numbers of exflagellation centers. **B.** Absence of RBCM and PVM was confirmed via electron microscopy.

The efficiency of permeabilization was confirmed via transmission electron microscopy (TEM, Fig. 3.55 B). Of each sample tested in the exflagellation assay, an aliquot was fixed immediately with PFA and glutaraldehyde and was processed for TEM. Per sample 20 gametocytes were examined electron microscopically. For the control sample treated with ICM instead of saponin, all gametocytes investigated showed a normal ap-

pearance. Both PVM and RBCM were intact. In the samples activated with XA upon saponin treatment 34 of the 60 gametocytes investigated in total were devoid of RBCM and PVM (Fig. 3.56). The remaining 26 gametocytes were surrounded by a single membrane only, either PVM or RBCM. Samples that were treated with saponin and subsequently incubated with ICM showed absence of PVM and RBCM in 25 gametocytes of 60 gametocytes investigated. 31 gametocytes were surrounded by RBCM only and 3 gametocytes by both PVM and RBCM. In all cases where gametocytes were surrounded by RBCM after saponin treatment, the cytosol of the RBC was disintegrated, pointing at a permeabilization of the membrane in a way not detectable via the magnification used.

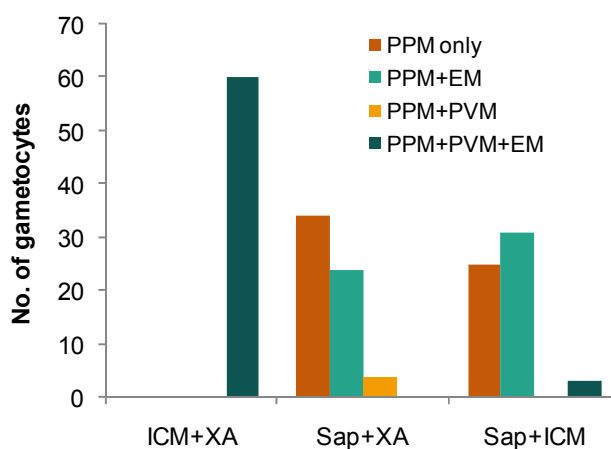


Fig. 3.56: The efficiency of saponin treatment of gametocytes was quantified via electron microscopy by investigating the presence of the membranes surrounding the gametocytes. In three independently treated samples for each condition 20 gametocytes were examined. The combined data for each condition (60 gametocytes) is shown.

3.6.5 Influence of ionophores on induction of gamete formation

In the Apicomplexan parasite *T. gondii* a decrease of the K^+ concentration within the host cell renders the intracellular parasites motile and triggers egress from the host cell (Fruth and Arrizabalaga, 2007). Hence, we tested if membrane potential or ion gradients also play a role during gametocyte activation and egress of *P. falciparum*. The K^+/H^+ ionophore nigericin and the K^+ ionophore valinomycin were tested in exflagellation assays. Nigericin was capable of inducing exflagellation of male gametocytes. The concentration most effective was $5 \mu\text{M}$ nigericin when incubated for 30 min at RT (Fig. 3.57). The number of exflagellation centers observed under these conditions accounted for $48.7 \pm 10.1\%$ of the value obtained for $10 \mu\text{M}$ XA incubated for 30 min at RT ($p=0.0013$, unpaired t-test). With increasing concentration of nigericin the number of exflagellation centers decreased when nigericin was incubated for 30 min.

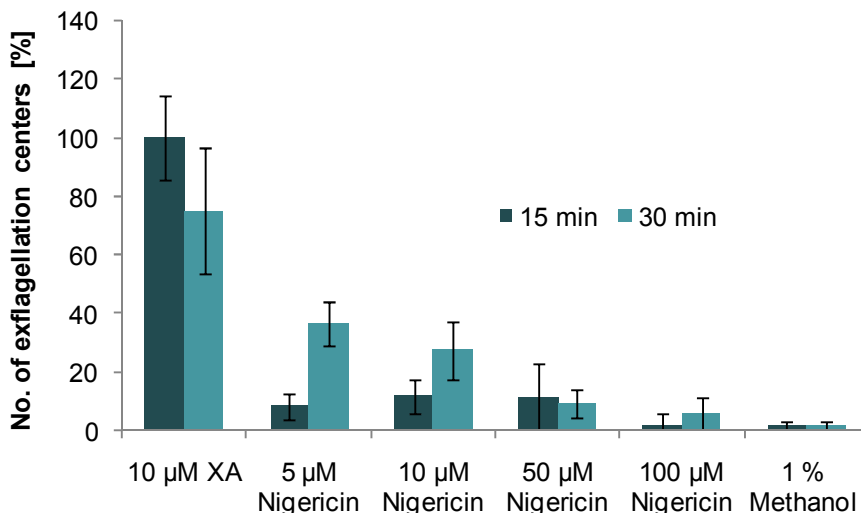


Fig. 3.57: Exflagellation of male gametocytes was induced by the addition of the K^+/H^+ ionophore nigericin with the lowest concentration tested being most effective. In contrast to XA, nigericin showed stronger activity when incubated with the gametocyte culture for 30 min. Combined data (mean and SD) of two independent experiments per incubation time comprising at least 6 counts per sample is presented. Values are depicted in percent of 10 µM XA incubated for 15 min.

Very low numbers of exflagellation centers were observed when gametocytes were incubated with nigericin only for 15 min. The nigericin concentrations of 50 µM and 100 µM did not differ significantly from the negative control containing 1% methanol (solvent of nigericin) (p values: 0.072 and 0.93). In contrast to nigericin, the number of exflagellation centers observed after 30 min of incubation with XA was significantly lower than after 15 min of incubation ($p=0.0053$) indicating a faster action of XA (Fig. 3.57).

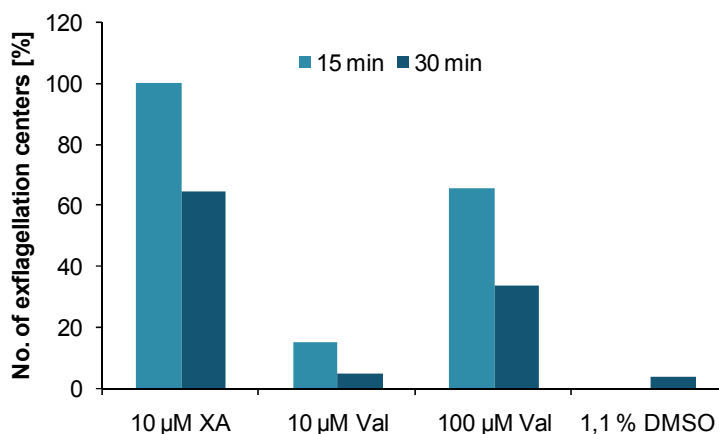


Fig. 3.58: Exflagellation of male gametocytes was induced when adding 100 µM of the K^+ ionophore valinomycin. The lower concentration of 10 µM was not able to induce exflagellation and showed similar results as the negative control. Values are depicted in percent of 10 µM XA incubated for 15 min (one count per sample).

The K⁺ ionophore valinomycin also seemed to induce exflagellation in male gametocytes. However, in contrast to nigericin valinomycin showed to be able to induce exflagellation at an incubation time of 15 min already. The concentration of 100 μM was more effective than 10 μM of valinomycin (Fig. 3.58).

3.6.6 Reverse genetics study on XA receptor candidate genes

Our observations of the uptake of XA by niRBCs as well as the observation of activation of gametocytes devoid of both RBCM and PVM by addition of XA led us speculate that the perception of XA might occur at the PPM. We therefore carried out a database search in order to identify candidate genes of a potential XA receptor. The XA-induced signal transduction pathway includes a PLC (Martin *et al.*, 1994; see Fig. 1.5) which has been described to be induced by G-protein coupled receptors in other organisms (reviewed in Dorsam and Gutkind, 2007). Hence, we searched for G-protein coupled receptors/ serpentine receptors in the PlasmoDB database. The search revealed five genes. Four of them, PfSR1, PfSR10, PfSR12 and PfSR25 had been identified as serpentine receptor-like proteins before (Madeira *et al.*, 2008). The respective genes were described to be expressed in asexual blood stages (Madeira *et al.*, 2008). The fifth putative serpentine receptor of our database search had not been described before in the literature. Its PlasmoDB identifier is PF3D7_0525400 (previously PFE1265w) and it has been classified as putative G-protein coupled receptor.

For two of the putative receptor proteins gene-disruptant mutants were generated in order to gain information of the function of the respective protein. The above described strategy of gene disruption via plasmid integration after single crossing over homologous recombination was chosen. For PFE1265w integration of the PFE1265w-KO/pCAM plasmid was observed 72 days after transfection. Limiting dilution was carried out in order to obtain clonal parasite lines of the gene-disruptant mutant. Three clones were isolated and diagnostic PCR on genomic DNA was carried out to investigate the respective genotype. Clone PFE1265w-KO 1H9 showed bands corresponding to the episomal plasmid and the wild-type locus, thus plasmid integration had not occurred in this clone (Fig. 3.59 B). Clone PFE1265w-KO 1D12 showed bands corresponding to episome and plasmid integration detected at the 5' end of the PFE1265w locus. No PCR band for the wild-type locus was detected. The third clone, PFE1265w-KO 2E6 was also devoid of the wild-type gene locus. Diagnostic PCR showed bands for plasmid integration both at 5' and 3' region of the gene. No episomal plasmid was detected for this clone (Fig. 3.59 B).

Further characterization of the two clones devoid of wild-type locus was carried out by Andreas von Bohl, MSc. Development of asexual blood stages in these gene-disruptant parasites was comparable to wild-type parasites. Gametocyte formation and maturation was not affected, neither, by disruption of the gene with the identifier PFE1265w. Stu-

dies on further stages of parasite development are currently underway, however did not reveal any certain phenotyp of the mutants, yet.

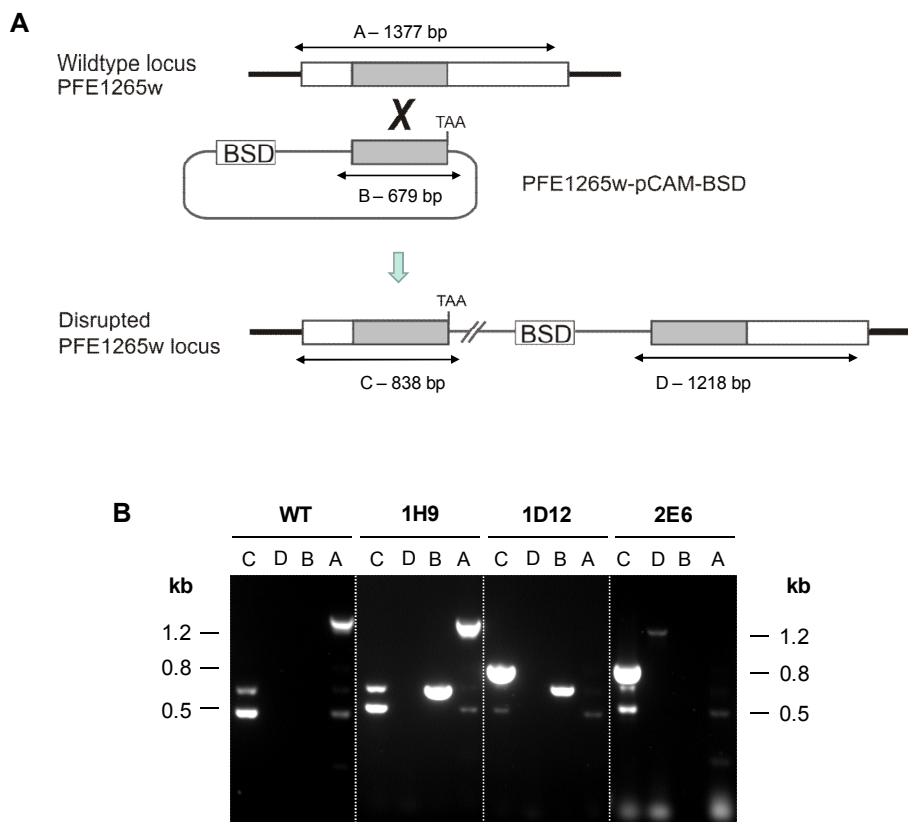


Fig. 3.59: **A.** Schematic depicting the PFE1265w wild-type (WT) gene locus and the modified KO locus resulting from vector integration via homologous recombination. Regions used for discrimination between wild-type and KO locus are marked with A–D. **B.** Diagnostic PCR on genomic DNA of three clones of PFE1265w-KO showed absence of wild-type locus for clones 1D12 and 2E6. Clone 1H9 still possessed the wild-type locus and did not show bands corresponding to plasmid integration. Gel lanes are labeled according to panel A.

Transfection of wild-type NF54 parasites with the PfSR1/pCAM construct was carried out in two independent experiments. Parasites started to appear in the blood smear approximately four weeks after transfection. The parasite lines were kept in culture for 22 weeks and 51 weeks respectively. However, no integration of the plasmid into the *pfsr1* gene locus was observed (Fig. 3.60).

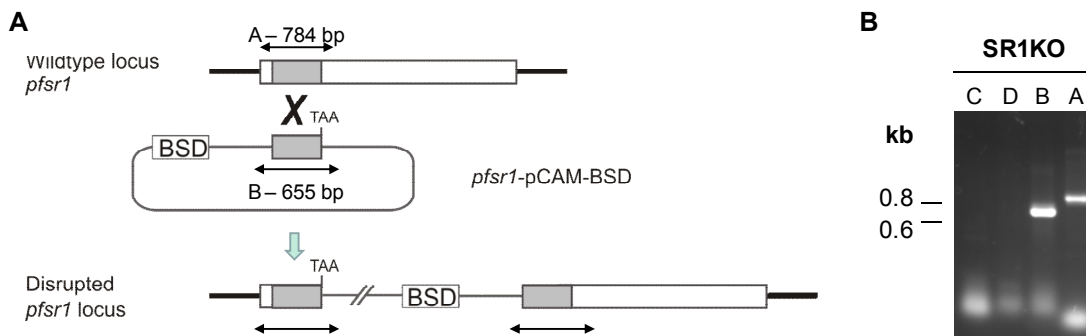


Fig. 3.60: **A.** Schematic depicting the *pfsr1* wild-type (WT) gene locus and the modified KO locus resulting from vector integration via homologous recombination. Regions used for discrimination between WT and KO locus are marked with A–D. **B.** Diagnostic PCR on genomic DNA of parasites transfected with the PfSR1-KO/pCAM plasmid detected bands corresponding to episome and wild-type gene locus. No bands were detected for integration of the plasmid into the *pfsr1* locus. A representative picture of two independent transfections is shown. Gel lanes are labeled according to panel A.

3.6.7 Ultrastructural investigations of gametocyte activation

In order to better understand the sequence of processes occurring at the cellular level during activation of gametocytes electron microscopical experiments were carried out. Mature gametocytes were activated to undergo gamete formation. At different time points post activation (p.act.) gametocytes were fixed and subsequently prepared for TEM. The observations were quantified and are summarized in Tab. 3.5. At time point 0, i.e. in the moment of adding XA, the gametocytes showed the typical foot print form of mature, non-activated gametocytes (Fig. 3.61). The gametocytes were surrounded by the PVM, which separated gametocytes from the rather thin layer of the RBC cytosol. Beneath the PPM the IMC was visible. In close association with the IMC osmiophilic bodies were detected. At 2 min p.act. the RBC cytoplasm started to disintegrate and 90% of investigated gametocyte sections showed rupture of PVM (Fig. 3.61, Tab. 3.5). In most cases, multiple rupture sites of the PVM were observed. In female gametocytes most of the osmiophilic bodies visible were associated with the rupture site, suggesting a role of these organelles in PVM lysis. At 6 min p.act. 80% of the host cells of activated gametocytes were devoid of cytoplasm (Tab. 3.5). The PVM was absent in all activated gametocytes investigated and the parasites were only surrounded by the RBCM at that time point. In 35% of the gametocytes investigated the IMC started to disintegrate. Both remnants of the PVM as well as parasite-derived membranes were observed as vesicular structures within the RBCM (Fig. 3.61 and Fig. 3.64). At 12 min p.act. all RBCs carrying activated gametocytes were devoid of RBC cytosol. The RBCM was ruptured in 60% of the gametocytes investigated and similarly the IMC was disintegrated in the majority of all activated gametocytes (Tab. 3.5). At the next time point, 15 min p.act. only 20% of gametocytes were still surrounded by an intact RBCM,

whilst 80% had completed their egress from the host cell. (Fig. 3.61, Tab. 3.5). The parasites now exhibited the round, spherical shape typical for *P. falciparum* gametes. In contrast to the multiple rupture sites of the PVM (see Fig. 3.61, 2 min p.act.) RBCM rupture only occurred in a single rupture site (50 gametocytes investigated, Fig. 3.61, 15 min). The data on the sequential processes occurring during gametocyte activation investigated at the ultrastructural level were kindly provided by L. Sologub and G. Pradel.

Tab. 3.5: Observations on presence of RBC cytosol (RBCC) or membrane structures in the course of gametocyte activation. For each time point 20 sections were investigated. Quantification was carried out by G. Pradel.

Time p.act.	RBCC		RBCM		PVM		IMC	
	Present	Absent	Intact	Ruptured	Intact	Ruptured	Intact	Disintegr.
0 min	100 %	0	100 %	0	100 %	0	100 %	0
2 min	100 %	0	100 %	0	10 %	90 %	100 %	0
6 min	20 %	80 %	75 %	25 %	0	100 %	65 %	35 %
12 min	0	100 %	40 %	60 %	0	100 %	20 %	80 %
15 min	0	100 %	20 %	80 %	0	100 %	25 %	75 %
30 min	0	100 %	0	100 %	0	100 %	0	100 %

In order to resolve the very early proceedings of gametocyte activation, gametocytes were fixed for TEM at 0 sec, 30 sec, 60 sec and 90 sec p.act. As described above at 0 sec p.act. the gametocyte periphery exhibited the typical three-lamellar membrane structure comprising PVM, PPM and IMC. At 30 sec p.act. the three membranes were still present in 15 of 20 gametocytes investigated, however, the PVM appeared now in an undulated shape (Fig. 3.62). Subpellicular microtubules were detected similarly to non-activated gametocytes. At 60 sec. p.act. the first rupture sites were detected in the PVM of 70% of gametocytes investigated. No longitudinal microtubules were observed after 60 sec p.act. Data were kindly provided by L. Sologub and G. Pradel.

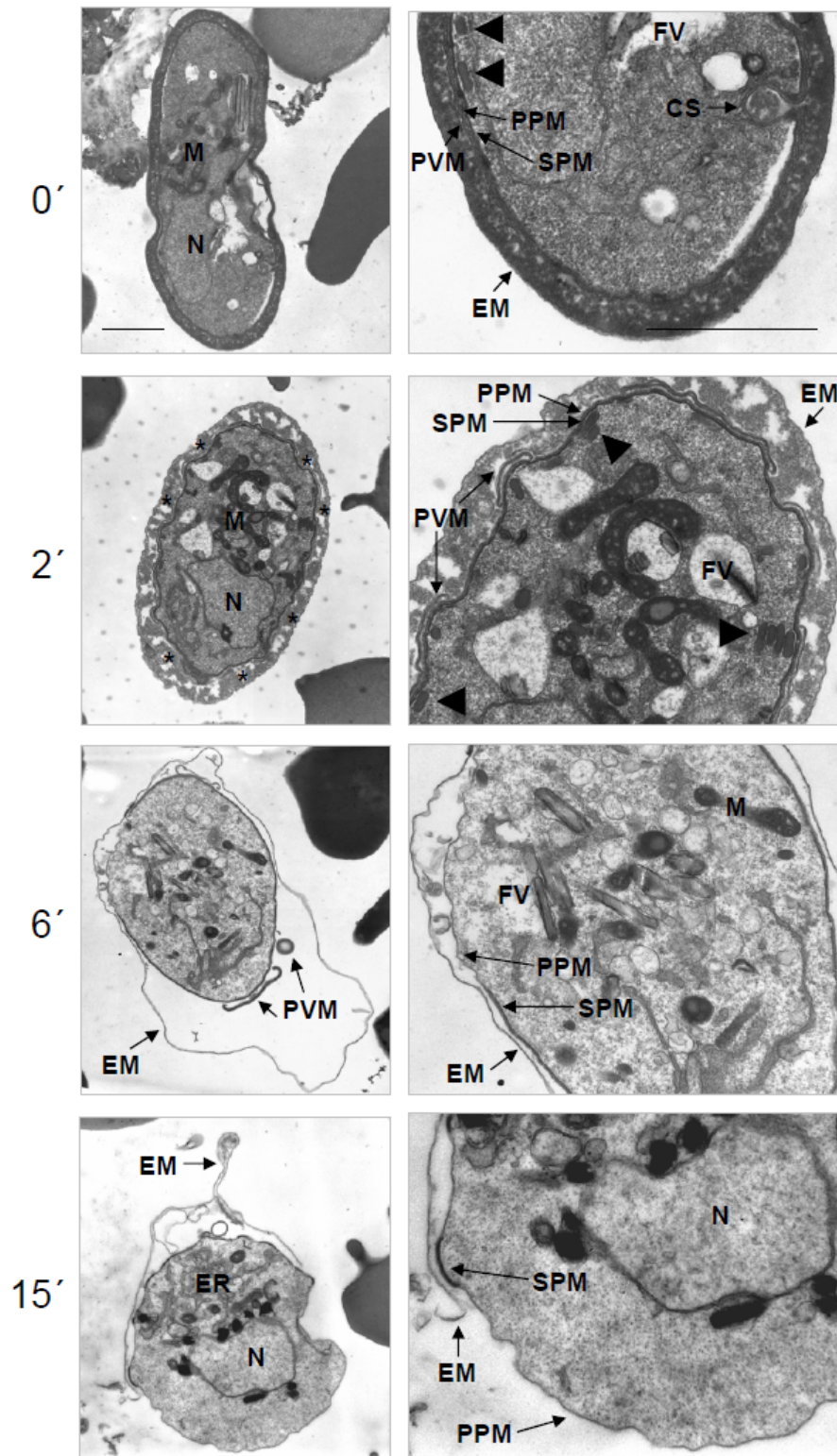


Fig. 3.61: A timeline of gametocytes egress was investigated via electron microscopy. Gamete formation was induced by addition of XA to a final concentration of 100 μM and gametocytes were fixed at different time points after activation. The right panel shows a detailed view of the left panel. Arrow heads point at osmiophilic bodies and asterisks mark sights of PVM rupture. CS—cystostome, EM—erythrocyte membrane, ER—endoplasmic reticulum, FV—food vacuole, M—mitochondrion, N—nucleus, SPM—subpellicular membrane=IMC. Scale bar—1 μm . Electron micrographs were kindly provided by L. Sologub and G. Pradel (Image from Sologub *et al.*, 2011).

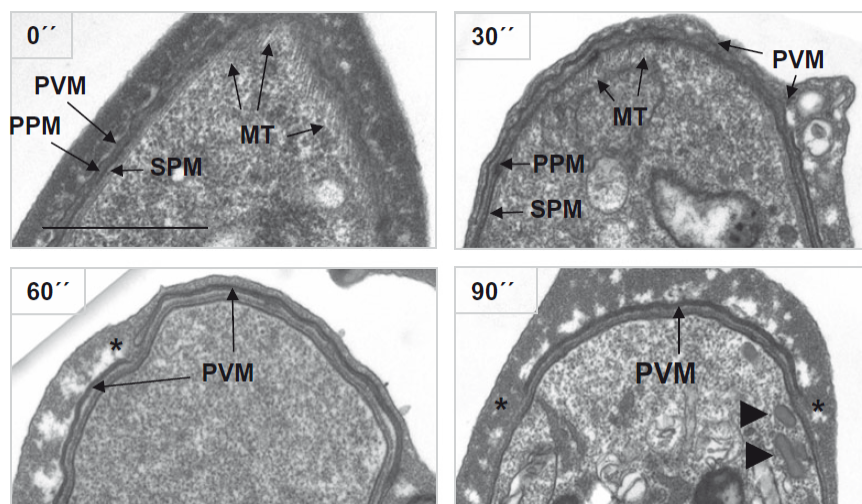


Fig. 3.62: PVM rupture was investigated in the first 90 seconds p.act. At 0 sec the PVM was intact and longitudinal microtubules (MT) were observed. At 30 sec p.act. the PVM appeared undulated. At 60 sec p.act. first rupture sites of PVM were visible (labeled with asterisk). At 90 sec p.act. several ruptures sites were present and disintegration of RBC cytosol was observed. Osmiophilic bodies are labeled with arrow head. SPM—subpellicular membrane=IMC. Scale bar - 1 μ m. Electron micrographs were kindly provided by L. Sologub and G. Pradel (Image from Sologub *et al.*, 2011).

Since several stimuli had been described to induce gametogenesis in mature gametocytes we wanted to investigate the impact of the described stimuli on PVM rupture. Gametocytes were incubated under various conditions. Specimens for TEM were prepared and evaluated quantitatively. Gametocytes incubated for 30 min in ICM (serum-free RPMI medium) at 37°C (negative control) and at RT did not show rupture of PVM (Fig. 3.63). After incubation at 37°C in the presence of XA only a very small proportion of gametocytes showed absence of PVM. ICM medium of an increased pH value (8.0 instead of 7.4) had been reported to induce gametocyte activation in concert with a drop of temperature from 37°C to ambient temperature (Nijhout and Carter, 1978). If pH was increased but temperature was kept constantly at 37°C PVM was shown to be intact in almost all gametocytes investigated. As expected, the drop in temperature combined with the presence of XA resulted in gametocyte activation reflected by PVM rupture. In the presence of human serum the proportion of activated gametocytes showing absence of PVM was even increased. In contrast, upon 30 min incubation with XA at RT in ICM of a lower pH value of 6.6 PVM rupture was almost completely inhibited. Upon treatment with 5 μ M of the K^+/H^+ ionophore nigericin for 30 min at RT a large proportion of gametocytes was devoid of the PVM similarly to the positive control incubated with XA. These observations show, that nigericin not only induces gamete formation in male gametocytes as seen in exflagellation assays (see 3.6.5), but it also stimulates female gametocytes to undergo gametogenesis.

The divalent cation Ca^{2+} has been described as an important messenger during gametogenesis. The addition of the calcium chelator BAPTA-AM to mature gametocytes re-

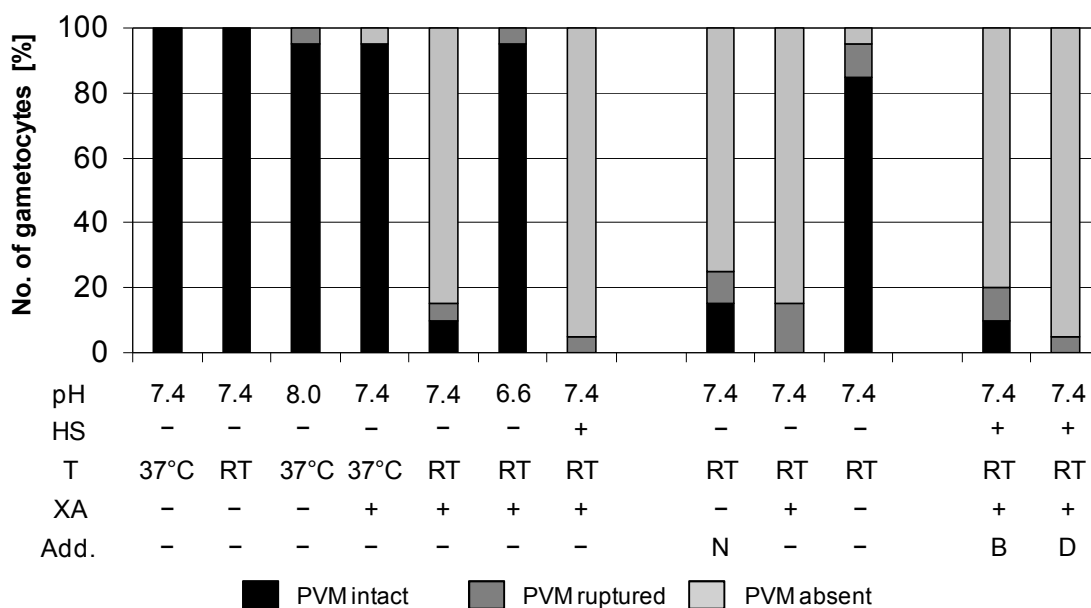


Fig. 3.63: Different stimuli were investigated for their effect on PVM rupture via electron microscopy. Only gametocytes treated with XA or nigericin showed rupture of PVM in the majority of gametocytes investigated (20 gametocytes per sample). Add. - additives, B-BAPTA-AM, D-DMSO, HS-human serum, N-nigericin. Preparation of specimens for electron microscopy was carried out in collaboration with L. Sologub. Quantification data was supplied by G. Pradel (Image from Sologub *et al.*, 2011).

sulted in an inhibition of exflagellation and of gametocyte egress from their host cells (Billker *et al.*, 2004; McRoberts *et al.*, 2008). We hence wanted to test whether BAPTA-AM would also prevent PVM rupture. A concentration of 25 μM BAPTA-AM that had previously shown to completely inhibit exflagellation of male gametocytes was added prior to activation of mature gametocytes as well as during activation. The presence of BAPTA-AM did not inhibit PVM rupture and only very few gametocytes showed an intact PVM. The number of gametocytes whose PVM was still present but ruptured was comparable to that of control gametocytes incubated with the solvent of BAPTA-AM, DMSO (Fig. 3.63). However, gametocytes activated in the presence of BAPTA-AM often showed an irregular shape (Fig. 3.64). In contrast to untreated activated gametocytes, gametocytes activated in the presence of BAPTA-AM in many cases still exhibited subpellicular microtubules and the IMC. Thus, the treatment with BAPTA-AM clearly resulted in a disturbed gametogenesis even if not affecting PVM rupture.

In conclusion the study of gametocyte egress on the ultrastructural level revealed that *P. falciparum* gametocytes egress from the host cell by lysing firstly the PVM. Only thereafter the RBCM ruptures. Gametocyte egress including PVM rupture can be induced by the K^+/H^+ ionophore nigericin, suggesting that that beside Ca^{2+} signal further changes in ion gradients are involved. Depletion of Ca^{2+} signaling does not inhibit PVM rupture, thus PVM rupture seems to be induced by an alternative signal.

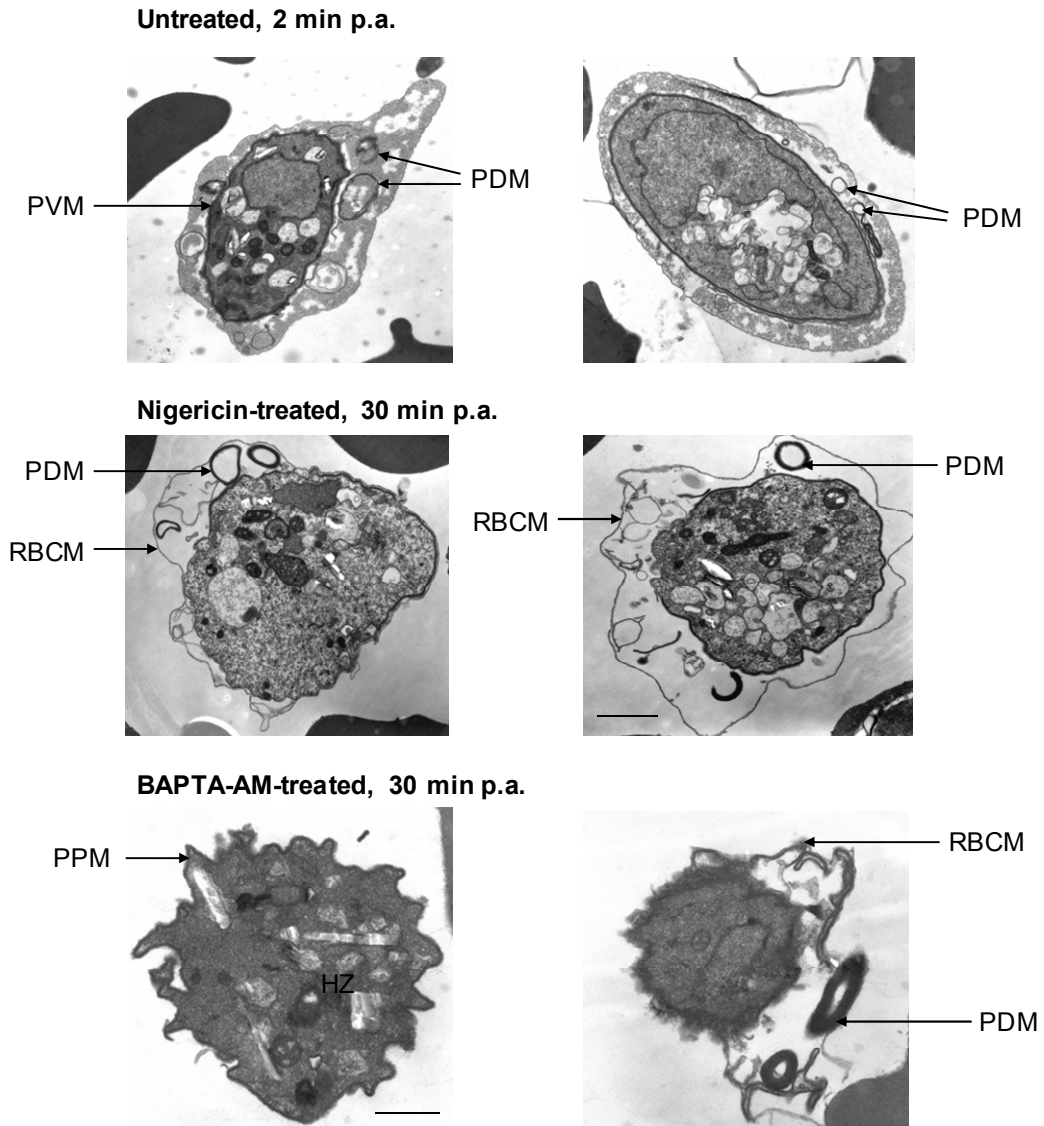


Fig. 3.64: After activation both treated and untreated gametocytes show an accumulation of parasite derived membranes (PDM). After 30 min of incubation with 5 μ M nigericin at RT gametocytes were fixed and embedded for electron microscopy. PVM was absent, and IMC was partially disintegrated. If RBCM was not ruptured, RBC cytosol was absent, indicating disintegration of RBCM. Treatment with BAPTA-AM does not affect PVM rupture, however morphogenesis of the developing gamete is disturbed. Scale bar - 1 μ m. Electron microscopy by carried out by G. Pradel (Image from Sologub *et al.*, 2011).

4 Discussion

4.1 Surface proteins of sexual stages of *Plasmodium falciparum*

4.1.1 Expression of PfCCp proteins

The sexual phase of the malaria parasite *P. falciparum* starts with the differentiation of a proportion of blood-stage parasites into gametocytes. The gametocyte represents the parasite stage responsible for transmission of the disease from human to the insect vector and thus is crucial for completion of the life cycle. A great number of proteins encoded in the genome of *P. falciparum* is exclusively expressed in the sexual phase of the life cycle (Khan et al., 2005). Amongst these are many adhesion proteins locating to the parasite surface, such as the six members of the PfCCp protein family (reviewed in Pradel, 2007). The PfCCp protein family had been discovered due to the proteins' architecture comprising multiple adhesion domains (Pradel et al., 2004; Scholz et al., 2008). Most of these domains have been described in other organisms like animals and bacteria and presumably have been acquired via lateral transfer (Templeton et al., 2004; Pradel et al., 2004). In view of the diversity of adhesion domains found in these proteins a role in lipid, carbohydrate or protein binding has been suggested for the six proteins (Claudianos et al., 2002; Pradel et al., 2004). The PfCCp proteins are widely conserved in Apicomplexan parasites (Pradel et al., 2004; Templeton et al., 2010; reviewed in Kuehn et al., 2010).

Within the gene sequence of each PfCCp protein a signal peptide is encoded, thus it is anticipated that the proteins are secreted. However no sequence for a GPI anchor or transmembrane domains had been identified (Pradel et al., 2004). PfCCp1 to PfCCp3 have been found to associate with the parasite plasma membrane within the PV (Pradel et al. 2004). Whilst expression of *pfccp1* to *pfccp4* and *pfnpa* starts in the gametocyte stage, PfCCp5 was detected in schizonts already (Scholz et al., 2008; Gieseke, 2010) Recently, minor expression of *pfccp5* has also been detected in trophozoites (G. Pradel, unpublished results).

While PfCCp1 to PfCCp3 are expressed in a spotted distribution, PfCCp5 and PFFNPA localize to the cell poles of gametocytes as had been shown by indirect IFAs (Pradel et al., 2004; Scholz et al., 2008). Immuno EM studies using alkaline phosphate secondary antibody showed that PfCCp5 and PFFNPA localize to both the cell surface and the cytosol of gametocytes (Dude, 2009) as it had been shown before for PfCCp1 to PfCCp3 (Pradel et al., 2004).

After gametocyte activation PfCCp proteins are present in macrogametes, but not in microgametes (Scholz et al., 2008). Approximately six hours after gametogenesis expression of the proteins ceases (Ngongang, 2010). In retort stages the proteins concentrate in a single spot in the residual body of the zygote. For PfCCp2 additionally a second focal expression site was observed in the apical end of the developing ookinete (Ngongang, 2010). PfCCp4 was found to be newly expressed in the ookinete stage homogeneously in an intensity comparable to that in the gametocyte stage (Scholz, 2007; Ngongang, 2010). In the rodent malaria parasite *Plasmodium berghei* expression of the orthologous proteins of the six PfCCp proteins (termed PbLAP1 to PbLAP6) had been described to concentrate in one to two focal spots in ookinetes (Carter et al., 2008; Saeed et al., 2010; Saeed et al., 2013). These focal expression sites had been identified as crystalloid, a cluster of vesicles expressed exclusively in ookinetes and young oocysts. The crystalloids have been suggested to serve as reservoir of proteins needed at later development stages, i.e. in the oocyst (Garnham, 1969; reviewed in Dessens et al., 2011). In gametocytes of *P. berghei* the orthologs of PfCCp2, PfCCp4 and PffNPA reveal a distribution comparable to that observed in *P. falciparum* gametocytes (Carter et al., 2008; Saeed et al., 2010). The other three orthologous genes have been reported to be translationally repressed. They are transcribed in gametocytes, but protein synthesis only starts upon gametocyte activation (Saeed et al., 2013).

In this thesis the so far uncharacterized PfCCp5-KO and PffNPA-KO parasite lines were focus of investigations in order to gain knowledge about a potential function of these proteins. Clonal parasite lines were obtained via limiting dilution and absence of wild-type allele of the respective gene of interest was verified. The development of asexual blood stages and gametocyte formation was for both PfCCp5-KO and PffNPA-KO clones comparable to that of wild-type parasites. Furthermore, the formation of male and female gametes as well as zygote formation after fertilization was not affected by the absence of functional PfCCp5 or PffNPA protein. The same observations had been made for the gene-disruptant mutants for PfCCp1 to PfCCp4 (Pradel et al., 2004; Scholz et al., 2008; Simon et al., 2009). Thus, it can be concluded, that none of the PfCCp proteins is essential for the development of blood stage parasite and for the sexual development until the zygote stage *in vitro*. Development in the mosquito was investigated for PffNPA-KO parasites which was comparable to development of wild-type parasites until the ookinete stage. However a role of the PfCCp proteins during gametogenesis and fertilization had been anticipated as formation of microgametes was significantly reduced *in vitro* in the presence of anti-PfCCp antisera and active complement (Scholz et al., 2008). Anti-PfCCp5 antisera did not show significant reduction at that time, however, an effect with more specific antiserum is probable. Transmission blocking assays using anti-PfCCp antisera showed an only moderate reduction of oocyst formation by approximately 30% (M. Scheuermayer, V. Ngongang, G. Pradel, unpub-

lished results). Studies of gene-disruptant parasite lines however suggested an essential role of PfCCp2 and PfCCp3 during transition of the parasites from oocysts to the salivary glands of the mosquito vector (Pradel et al., 2004).

Expression of PfCCp5 during the life cycle had been investigated via Western blot. Here, the protein was detected in gametocyte lysate in its full length of 120 kDa and additional bands of 50, 60, 70 and 80 kDa were observed. In schizonts on the contrary, the main band was observed at 65 kDa, suggesting processing of the protein in this parasite stage (Gieseke, 2010; G. Pradel unpublished results). In this thesis clonal parasite lines expressing PfCCp5 fused to a C-terminal HA tag were obtained. In Western blot analyses the full length fusion protein was detected both with anti-HA antibodies and with anti-PfCCp5 antiserum. However, until now, it was not possible to detect the PfCCp5-HA fusion protein in schizont lysate via Western blot. Thus it might be that the shorter version of PfCCp5 in schizonts comprises the N terminal part of the protein after proteolytical processing. However, further investigations are needed and it would be worth including an additional mutant expressing a protein tag fused to the N-terminal of PfCCp5.

4.1.2 Co-dependent expression of PfCCp proteins and other sexual stage-specific proteins

Proteins of the PfCCp protein family have been reported to be expressed in co-dependent manner. When one of the genes encoding for a PfCCp protein had been disrupted all PfCCp proteins were either absent or present in reduced abundance (Pradel et al., 2006; Simon et al., 2009). This phenomenon of co-dependent expression has now been studied via IFAs for the PfCCp5 and PffNPA gene-disruptant mutants, as well. It turned out, that the correct localization of the PfCCp proteins does depend on presence of PfCCp5 and PffNPA. However, in these two mutants the reduction of PfCCp proteins was – similar to that of PfCCp4 gene-disruptant parasites – less prominent as compared to the observations made for PfCCp1 to PfCCp3 (Simon et al., 2009). The disruption of *pfccp5* and *pffnpa* gene loci did not impact on expression of PfCCp4. In PffNPA-KO parasite co-dependent expression was also investigated via Western blot analyses, which detected reduced amounts of PfCCp proteins. Thus, as reported for the other PfCCp-proteins, not only correct localization of the PfCCp proteins does depend on presence of all other members of the protein family, but also the protein stability seems to be affected. As observed in IFAs the reduction of protein in Western blot was less prominent in PffNPA-KO parasites as compared to PfCCp1- to PfCCp3-deficient parasite lines. In accordance with studies on PfCCp1- to PfCCp4-gene-disruptant parasite lines (Simon et al., 2009), co-dependent expression was detected only on protein level, whilst transcript levels remained comparable to that in wild-type parasites. For the only recently obtained clones of the PfCCp5-KO parasite line it can be assumed that

here, too, co-dependent expression will only be observable at the protein level. As PfCCp5 is expressed in asexual parasites already, its expression was not only investigated in gametocytes, but also in schizonts of PfCCp1-KO parasites. Here, PfCCp5 was expressed as in wild-type parasites. This observation, together with the observed presumably processed form of the proteins in schizonts suggest a different function of PfCCp5 in schizonts than in gametocytes, which is independent of the presence of other PfCCp proteins.

For the orthologous proteins of the PfCCp proteins in *P. berghei* similar observations regarding the co-dependent expression of the members of the protein family have been described (Saeed et al., 2012). However, co-dependent expression was not observable in gametocytes, but only later during expression of the protein family, in the ookinete stage. Here, expression of PbLAP3 (ortholog of PfCCp5) was dramatically reduced in the absence of PbLAP1 (ortholog of PfCCp3). The authors suggested, that PbLAP3 was in a misfolded state in the absence of PbLAP1 and thus degraded. A possible explanation of the later occurring lack of PbLAP3 was the shorter duration of gametocyte formation as compared to *P. falciparum* (Saeed, et al., 2012). Investigation of interdependency between other members of the PbLAP protein family is needed as for other proteins (e.g. orthologs of PfCCp1 to PfCCp3) the effect might be even more pronounced.

Beside co-dependent expression within the PfCCp protein family co-dependent expression was also investigated with other proteins expressed in the sexual stages. However, no prominent differences were observed in the eight gene-disruptant parasite lines investigated. The only dramatically modified protein localization was observed for PfactinII in the two parasite lines expressing truncated versions of Pfs230 (discussed below). Co-dependent expression manifesting at the protein level has been described in other Apicomplexan parasites, as well. For instance, the microneme protein TgMIC6 of *Toxoplasma gondii* serves as an escorter for the soluble proteins TgMIC1 and TgMIC4 that in the absence of TgMIC6 do not localize to the micronemes as observed in wild-type parasites (Reiss et al., 2001).

4.1.3 Interactions of sexual-stage adhesion proteins

The members of the PfCCp protein family undergo multiple protein-protein interactions (reviewed in Kuehn et al., 2010). By means of co-immunoprecipitation it was shown that protein-protein interactions occur between all PfCCp proteins with exception of PfCCp4 and PfCCp5 (Simon et al., 2009). Thus the formation of multimeric protein complexes has been proposed (Simon et al., 2009; Kuehn et al., 2010). In view of the above described co-dependent expression of PfCCp proteins it is anticipated, that lack of one PfCCp protein leads to complex instability and disassembly of the protein complex. A similar effect had been observed for the two TBV candidate proteins Pfs48/45 and Pfs230. In gametes of a Pfs48/45-deficient parasite line, Pfs230 does not localize

homogenously to the cell surface as observed in wild-type parasites (Eksi et al., 2006). In addition it had been reported that Pfs230 and Pfs48/45 interact with each other thus it was suggested that the secreted Pfs230 is retained to the cell surface via binding to the GPI-anchored Pfs48/45 (Kumar et al., 1987; Kumar and Wizek, 1992; Eksi et al., 2006). It had been shown that the multimeric protein complex of PfCCp proteins might include further sexual stage-specific proteins such as Pfs230 and Pfs48/45 in gametocytes and Pfs25 after gametocyte activation (Kuehn, 2007; N. Simon, S.M. Scholz, and G. Pradel, unpublished observations). Such interaction with further sexual stage-specific proteins would explain, how PfCCp proteins that lack both GPI-anchor sequence and transmembrane domain are retained to the parasite plasma membrane after secretion.

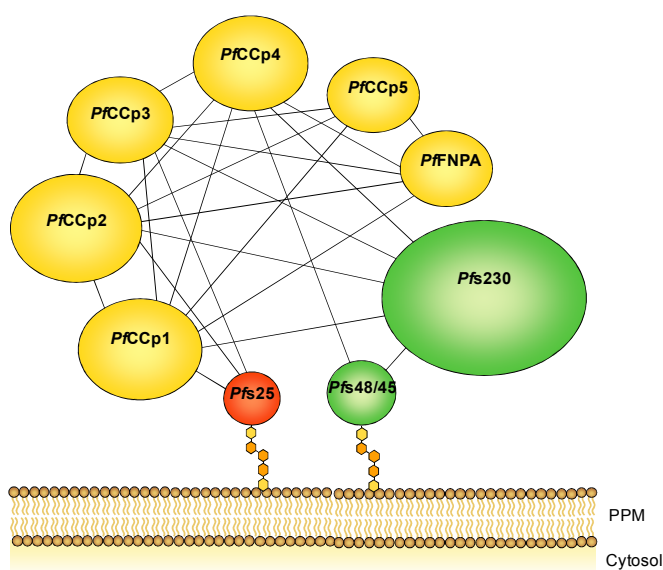


Fig. 4.1: Schematic depicting the manifold interactions between PfCCp proteins and further sexual stage proteins. It is anticipated the multimeric protein complex is retained to the gametocyte surface via the GPI-anchored Pfs48/45. After gametocyte activation Pfs25 provides an additional anchor site. (Kuehn et al., 2010).

Retention of secreting proteins via interaction with a GPI-anchored protein has been observed for another pair of cysteine-rich domain proteins. Pf41 has been reported to form a stable complex with the GPI-anchored Pf12 on the surface of merozoites (Taechalerpaisarn et al., 2012). As Pf41 is still detectable at the merozoite surface in Pf12-KO parasites it has been suggested that the protein interacts with further merozoite surface proteins (Taechalerpaisarn et al., 2012). Indeed, another multimeric protein complex has been discovered on the merozoite surface, namely the protein complex around PfMSP-1. As Pfs25 PfMSP-1 possess EGF-like domains that can mediate contact to parasite or host proteins, and it is retained to the parasite surface via a GPI anchor (Blackman et al., 1991). PfMSP-1 has been reported form a complex with PfMSP-3 and PfMSP-6/PfMSP-7. The three proteins possess neither GPI anchor nor transmembrane domain and are retained to the merozoite surface via interaction with PfMSP-1. (Ranjan

et al., 2012). Recently, it was shown that PfMSP-1 might interact with seven additional merozoite proteins, including PfRhopH3, part of the RhopH complex (Ranjan et al., 2011). Thus, it seems as the merozoite surface has an intensive network of interacting proteins.

Very recently a new component of the PfCCp-based multimeric protein complex was identified. Via co-immunoprecipitation a so far uncharacterized protein was identified as interaction partner of PfCCp1 (Simon, 2012). Analysis of the protein sequence revealed possession of several WD40 domains, thus the protein was named PfWLP1 (Ngongang, 2012). The protein was observed to be expressed in asexual blood stages and gametocytes. Expression increased with gametocyte maturation, persisted in macrogametes and ceased after fertilization with only low abundance of the protein in the residual body of the ookinete. In Western blot analyses protein bands of different molecular weight were observed in different life cycle stages. Whilst in gametocytes both a band of 70 kDa and 95 kDa were observed, after gametocytes activation only the 70 kDa band was detected. It can thus be assumed that processing of the proteins takes place upon induction of gamete formation. This had been described for the TBV candidate protein Pfs230 which is postulated to be part of the multimeric protein complex of gametocytes (Williamson et al., 1996; Brooks and Williamson, 2000). Both intensity of expression in the different life cycle stages and spotted to homogenous distribution of the proteins resemble expression of PfCCp proteins. These observations and the fact that WD40 proteins generally serve as scaffolds for protein complexes (reviewed in Stirnimann et al., 2010) suggests that the novel WD40 protein PfWLP1 is part of the PfCCp-containing multimeric protein complexes on the cell surface of *P. falciparum* gametocytes. Apart from the results of the original co-immunoprecipitation assays this hypothesis is supported by the observation that PfWLP1 co-localizes with Pfs230, interaction partner of several PfCCp proteins (Ngongang, 2012). The investigation of co-dependent expression via IFAs showed, that correct localization of PfWLP1 seemingly does not depend on presence of the PfCCp proteins. However, it will of special interest if absence of PfWLP1 will affect the correct assembly of the PfCCp containing protein complexes. As described above (3.5.3) the study of PfWLP1-disruptant parasite line is underway. As for PfCCp5 it would also be possible for PfWLP1 that it fulfills distinct rolls in asexual parasite stages, where other PfCCp proteins are absent, and in gametocytes in conjunction with PfCCp proteins.

4.1.4 Potential role of PfCCp-based multimeric protein complexes

The numerous PfCCp and PbCCp gene-disruptant parasite lines studied did not show a phenotyp differing from that of WT parasites during gametocyte development or gametogenesis (Pradel et al. 2004; Scholz et al., 2008; Simon et al., 2009; Claudianos et al., 2002; Raine et al. 2007). Instead, the phenotype of the mutants was observed at a later

time point of the life cycle – the sporogonic phase. Whilst in PfCCp mutants the transition of sporozoites from midgut oocyst to the salivary glands was disturbed, in PbCCp mutants sporulation within the oocyst was impaired. This leads to speculate whether PfCCp proteins have two different functions in the life cycle of *Plasmodium* spp.: One redundant function in gametocytes, where loss of PCCp proteins can be compensated by other proteins, and a second role for sporozoite development. Alternatively, absence of the proteins in gametocytes might have a quantitative rather than a qualitative effect (Saeed et al., 2010). Development from gametocyte to oocyst represents one of the major population bottlenecks in the parasite's life cycle. The reduced number of successfully formed zygotes might thus lead to fewer healthy oocysts that can give rise to infective sporozoites.

In gametocytes PfCCp proteins might be responsible for ensuring contact between gametes followed by fertilization. A protein termed HAP2 has been reported to be responsible for membrane fusion in the course of fertilization of macrogamete by microgamete (Liu et al., 2008). However it remains elusive, how the initial contact of the gametes within the midgut is achieved. The predominantly in female gametes expressed PfCCp proteins with their numerous adhesion domains thus represent promising candidates for binding to a surface protein of microgametes such as Pfs230 or Pfs48/45.

Another role of PfCCp proteins in gametocytes might also be the protection of the emerging gametes after gametocyte activation. The mosquito midgut contains a variety of harmful components such as digestion enzymes, midgut bacteria and also factors of the mosquito immune system might be present. In addition to vector-specific factors, the blood meal also bears antagonistic components such as antibodies of the human host and the human complement system. As it had been reported, the PfCCp proteins and other proteins like Pfs230 become processed upon gametocyte activation and egress and might thus function as a shield captivating hostile factors of the mosquito midgut.

4.2 The inner membrane complex of gametocytes and cytoskeleton proteins

4.2.1 Molecular composition of the inner membrane complex of gametocytes

The motile stages of Apicomplexan parasites possess a trilaminar pellicle comprising the plasma membrane and flat membrane cisternae which in their entity are also referred to as IMC. This IMC is scaffold for the molecular motor, a complex structure comprising several proteins which in concert enable the movement of parasites during gliding motility on surfaces and during invasion. Gametocytes of *Plasmodium* spp. exhibit a similar membrane structure, referred to as subpellicular membrane. Until recently nei-

ther the exact composition nor the function of this subpellicular membrane was known. In this thesis expression of six genes encoding components of the IMC of asexual parasites, *pfmyoA*, *pfgap45*, *pfgap50*, *pfmtip*, *pfaldo* and *pfactinI*, was confirmed in gametocytes via RT-PCR. The presence of two of the respective proteins, PfGAP50 and PfmyoA was further investigated via IFA. Whilst PfmyoA showed distribution in a rather punctuate pattern in the entire gametocyte, PfGAP50 located to a great part to the cell periphery (see Fig. 3.15 and Fig. 8.5). PfactinI which in the motor complex interacts with PfmyoA showed a distribution similar to that of PfGAP50 (see Fig. 3.22 and Fig. 8.5). Thus it can be concluded that the components of the molecular motor are expressed in gametocytes. Staining of PfactinI was similar to that observed in *P. berghei* ookinetes, except of a local concentration of the protein at the apical pole of ookinetes (Sidén-Kiamos et al., 2006). PfmyoA staining on the other hand was rather diffuse in gametocytes, whilst in *P. berghei* ookinetes it was restricted to the cell periphery (Sidén-Kiamos et al., 2006).

A number of publications addressed the composition of the subpellicular membrane of gametocytes recently (Dearnley et al., 2012; Kono et al., 2012; reviewed in Dixon et al., 2012). Results were in good concordance with the here described observations. IFAs on *P. falciparum* stage II–IV gametocytes detected PfGAP50, PfGAP45, PfMTIP and PfMyoA, in a similar pattern as in the present work (Dearnley et al., 2012) Kono et al., (2012) reported the presence of five further IMC proteins in gametocytes. Thus, the combined results show that the molecular composition of the IMC of the motile parasite stages is analogous to the subpellicular membrane complex of gametocytes. As gametocytes are amotile a structural role of the IMC is plausible. More than 30 years ago, a structural role of the microtubules that run beneath the IMC in determining the crescent shape of *P. falciparum* gametocytes had been suggested already (Sinden, 1982; Sinden, 1983). Several recent publications confirmed this hypothesis. It was reported that deformability of gametocytes decreases with establishing the IMC and the microtubules during gametocyte maturation (Aingaran et al., 2012; Dearnley et al., 2012; Tibúrcio et al., 2012). With further maturation and reaching stage V gametocytes become less rigid coincident with disassembly of the longitudinal microtubules. Up to date no adhesins responsible for sequestration of immature gametocytes have been identified (Saeed et al., 2008). It has therefore been suggested that increased rigidity of stage II–IV gametocytes and maybe of their host cell, too, is mediating mechanical sequestration. Reaching stage V, the gametocytes become more flexible. They enter the circulation by an unknown mechanism and thereafter are available to be taken up by Anopheline mosquitoes during their blood meal.

4.2.2 Expression of myosin isoforms in *P. falciparum* gametocytes

Six myosin genes have been described to be encoded in the *P. falciparum* genome (Chaparro-Olaya et al., 2003; reviewed in Vale, 2003). Expression of the myosins has been investigated in asexual blood stages via RT-PCR and in part via IFA. Until now, nothing was known about expression of myosins in sexual stage parasites of *P. falciparum*. In the course of this PhD thesis and a recently submitted Bachelor thesis (Tews, 2011) the expression of the six myosin was investigated via RT-PCR. We were able to detect transcripts of all myosin genes with the exception of *pfmyoE* in cDNA obtained from total RNA gametocytes of the NF54 strain. Our data was in partial agreement with the observations of Chaparro-Olaya et al. (2005). We were able to detect transcripts of *pfmyoA*, *pfmyoB*, *pfmyoC* and *pfmyoE* in mixed asexual blood stages of the gametocyte-less strain F12 (Tews, 2011; Simon et al., 2012). The differences might result from different experimental procedures of RNA isolation. The isolation of mRNA via a commercial kit as obtained by Chaparro-Olaya et al. (2005) might have been more efficient as isolation of total RNA with TRIzol. Until today only for PfMyoA a role has been assigned. As described above PfMyoA is part of the molecular motor mediating invasion and gliding on surfaces (reviewed in Baum et al., 2008). According to its expression profile with a peak in mature schizonts and merozoites for PfmyoB a role during invasion has been proposed as well (Chaparro-Olaya et al., 2003). For PfmyoD a role in formation of merozoites has been implicated according to its cellular location in maturing schizonts (Chaparro-Olaya et al., 2005). As the six *P. falciparum* myosins cluster with other Apicomplexan myosin in an own class within the myosin superfamily it is difficult to draw any conclusions about their function according to the protein structure (Chaparro-Olaya et al., 2005; reviewed in Heintzelman and Schwartzman, 2001). Myosin functions are as diverse as the filament sliding as observed for conventional class II myosins, vesicle transport, trafficking of cell surface receptors, transport of protein complexes, cell migration and adhesion (reviewed in Krendel and Mooseker, 2005; Hartman and Spudich, 2012).

In order to gain knowledge on function of myosins in gametocytes more detailed studies focusing on proteins localization as well as reverse genetic approaches might be useful. In a recent work PbMyoA which is essential for asexual blood stage development was expressed under the promoter of PfAMA1 (Sidén-Kiamos et al., 2011). Thereby expression of *pbmyoA* in asexual blood stages was as in wild-type parasite, however from gametocyte stage onwards, expression was abolished. No altered phenotype was observed in gametocytes and gametes. Viable ookinetes were formed. However, ookinetes were amotile and thus not able to cross the midgut epithelium (Sidén-Kiamos et al., 2011). In the background of the novel findings on the IMC in gametocytes of *P. falciparum* it would be of special interest to see whether PfMyoA is likewise dispensable during gametocytes development. In contrast to the spherical *P. berghei* gametocytes, PfMyoA

might be important for stability of the IMC of gametocytes and thus, the formation of the crescent shape of *P. falciparum* gametocytes.

4.3 Characterization of PfactinII

4.3.1 Expression of PfactinII

The genome of *P. falciparum* encodes two distinct actin genes sharing 75% of identity at the transcript level and 79% at the protein level (PlasmoDB). Early studies reported that *pfactinI* is expressed in all blood stages whilst transcript *pfactinII* was only detected in sexual parasite stages (Wesseling et al., 1989). However, no details on the location of PfactinII or on the function of the protein were known. As observed during IFAs in this thesis, PfactinII is indeed specific to sexual parasite stages. In contrast to PfactinI which showed even distribution both in cytosol and gametocyte periphery, PfactinII was found predominantly at the periphery of the gametocytes and was further expressed in macrogametes and zygotes at the periphery. Western blot analyses confirmed these observations showing ubiquitous expression of PfactinI in all blood stages, whilst PfactinII was detected almost exclusively in gametocytes and activated gametocytes (Fig. 3.18, Rupp et al., 2011). A faint band was detected in lysate of asexual blood stage parasite of the gametocyte-less F12 strain. A similar observation had been made in RT-PCR on cDNA of a culture of mixed blood stages of the gametocyte-less F12 strain (Fig. 3.11). However it is not known, at what exact stage of gametocytogenesis the F12 strain is defective (Alano et al., 1995). Thus, it is possible that the faint signal observed for PfactinII in this strain resulted from sexually determined parasites. As IFAs double-labeled with the early gametocyte marker Pfs16 showed, expression of PfactinII, indeed starts very early.

In a recent report the orthologous protein, PbactinII was characterized in *P. berghei*. In this study expression of *pbactinII* started as early as 15 h post invasion of the RBC by the determined merozoite. No transcript was detected in asexual parasites (Deligianni et al., 2011). As observed in this thesis, the distributions of PactinI and PactinII were clearly distinct from one another in IFAs in *P. berghei*. It can thus be assumed that both in *P. falciparum* and in *P. berghei* the proteins carry out different functions in the sexual stages. However there were also differences observed in the expression of PactinII in *P. berghei* and *P. falciparum*. In the present study absence of PfactinII from the nucleus seemed to be likely in some gametocytes. However no detailed analysis on nuclear expression was carried out due to technical restrictions. Another discrepancy was observed regarding the expression in microgametes. In the present study PfactinII was not detected on microgametes. However in an earlier study employing antisera targeting the same region of the protein, *P. falciparum* microgametes were clearly positive for PfactinII

(Rupp et al., 2011). It thus is possible that PfactinII is present in microgametes. In contrast to the weak expression of PfactinII in *P. berghei*, both in Rupp et al. (2011) and in the present thesis PfactinII showed high abundance in macrogametes. In *P. falciparum* the *pfactinII* thus does not seem to be gender-specifically expressed (Rupp et al., 2011).

4.3.2 Interaction of Pfs230 and PfactinII

Indirect IFA studies on the two mutants expressing truncated version of the *pfs230* gene revealed that PfactinII and Pfs230 are co-dependently expressed. In the mutant expressing the first 950 amino acids, Pfs230-KOd2, a patchy distribution of PfactinII was observed. Thus protein abundance as detected by IFA was dramatically reduced comparing in contrast to wild-type parasite. In the second mutant synthesizing the first 542 amino acids (Pfs230-KOd1) no PfactinII was detectable via IFA. Co-localization experiments showed that PfactinII and Pfs230 were co-localizing. This was also true for the Pfs230-KOd2 mutant in which Pfs230 and PfactinII showed exactly the same patchy distribution. RT-PCR showed expression of *pfactinII* at a level comparable to wild-type parasites in the two mutants, thus demonstrating that the co-dependent expression is occurring exclusively at the protein level as observed for PfCCp proteins. However, in contrast to co-dependent expression amongst PfCCp proteins, stability of PfactinII did not depend on presence of Pfs230. In Western blot analyses PfactinII was detected in gametocyte lysates of both Pfs230-KOd1 and Pfs230-KOd2. In view of these results it might be possible that in absence of full length Pfs230 PfactinII reveals a slightly different conformation that is not recognized by the antibody used in this study. Such “conformational interdependence” had been reported for the PfCCp orthologs in *P. berghei*. In that study PbCCp5 (termed PbLAP3) had been detected by Western blot but not by IFA when expression of *pbcpp3* (*pblap1*) was abolished by gene KO (Saeed et al., 2012). Co-immunoprecipitation assays were carried out in order to see if the co-dependent expression is a result of a protein-protein interaction between PfactinII and Pfs230. Indeed, an interaction between the two proteins was observed. However the results were not clear, as PfactinI and Pfs230 also seemed to interact, even if not in such pronounced way as observed for PfactinII and Pfs230. The results of co-immunoprecipitation assays not necessarily reflect interactions actually occurring *in vivo*. It is thus possible that Pfs230 interacts (directly or indirectly) with PfactinII in the gametocyte, but *in vitro* it also interacts with PfactinI due to structural similarity with PfactinII. Functions of actins and actin-related proteins in general are manifold and therefore many actin-binding protein exist. Other controls used (e.g. the ER protein Pf39 and the proteasom β -subunit) showed similarly contradictory results (data not shown). It is therefore necessary to chose additional approaches such as protein cross-linking for investigating the interaction of PfactinII and Pfs230 within the gametocyte. What also remains unclear is the exact localization of PfactinII. If it was for instance in

association with the IMC interaction with Pfs230 would be possible via a transmembrane adaptor protein. Pfs230 itself has been reported to possess a potential transmembrane domain (reviewed in Williamson, 2003).

It might also be possible that the co-dependent expression of PfactinII and Pfs230 is an indirect effect. As studies on the ultrastructure of mutants with truncated Pfs230 showed, the typical trilaminar membrane structure of those gametocytes was disturbed. Pfs230 is a very large protein of 363 kDa which is quite abundant in gametocytes. Alteration of the membrane structure might interfere with correct localization of PfactinII which like Pfs230 is expressed in the gametocyte periphery. However, until now, no further gametocyte proteins revealed an alteration in expression site upon disruption of Pfs230.

4.3.3 Possible functions of PfactinII

In order to gain information on possible functions of PfactinII a KO mutant was generated via single crossing-over homologous recombination. However in this PfactinII-KO mutant PfactinII was still detectable in a quite high abundance, even if reduced in comparison to wild-type parasites. The protein was also detected via Western blot in gametocyte lysate of the PfactinII-KO (A. von Bohl, MSc, personal communication). A possible explanation for these observations is the reversion to wild-typic allele due to expulsion of the plasmid via single crossing-over recombination. Resistances against Blastidicin S had been reported (Hill et al., 2007; Lisk et al., 2010) and the mechanism resistance is based on was discovered recently (Mira-Martínez et al., 2013). Thus it is imaginable that a small subpopulation of resistant parasites expressing PfactinII had developed. Another reason for detection of PfactinII is that expression of the residual gene is driven by the plasmid-internal calmodulin promoter (Crabb and Cowman, 1996; Crabb et al., 1997; Sanders et al., 2006). As the location for plasmid integration was in proximity to the 5' end of the gene, downstream of the integrated linearized plasmid a large fragment of the gene would still be intact which might be transcribed via the promoter activity of the plasmid and an alternative start codon. To circumvent these difficulties observed in some cases of single crossing-over homologous recombination, a new mutant is currently created (A. von Bohl, MSc, personal communication). This approach is based on double crossing homologous recombination, by which the major part of the gene will be removed from the respective chromosome.

In view of the here observed increase of expression of PfactinII in the course of gametocyte maturation it seems likely that PfactinII fulfills a function during gamete formation or fertilization. This assumption is corroborated by the observed decrease of expression in zygotes and retort stages. In a previous study of our laboratory PfactinII had been detected in filamentous cell protrusions formed by macro- and microgametes (Rupp et al., 2011). These filaments resemble a type of cell-cell connections termed

nanotubes. Nanotubes have been described in a variety of mammalian cells like HEK (human embryonic kidney) cells, neuronal cells (Rustom *et al.*, 2004) and immune cells (B cells, T cells natural killer cells and macrophages) (Stinchcombe *et al.*, 2001; Önfelt *et al.*, 2004). Nanotubes contain filamentous actin (F-actin) and up to 11 filaments had been observed to protrude from activated gametocytes and gametes of *P. falciparum*. It has been suggested that the filaments formed by gametes are facilitating the contact between gametes in the mosquito midgut, thus promoting fertilization (Rupp *et al.*, 2011). In *P. berghei* a role of PbactinII motility of microgametes was suggested (Deligianni *et al.*, 2011). PbactinII-deficient microgametocytes formed structurally normal microgametes. However, those were amotile and unable to egress from their host cell (Deligianni *et al.*, 2011). As egress of microgametes seems to be promoted by flagellar movement it is not surprisingly that the amotile microgametes remain trapped within the RBC. Taken together PactinII seems to be of great importance for sexual development and therefore further studies are promising for identifying valuable targets for intervention strategies.

4.4 Gametocyte activation and egress

4.4.1 Induction of gametogenesis by xanthurenic acid

The signaling pathway resulting in gametocyte activation and gamete formation are quite well studied already. However, until today it remains elusive, how the triggering factors, a drop in temperature by at least 5 degrees and XA, a molecule present in the mosquito midgut, are perceived by mature gametocytes. In the present study we addressed the question how XA is perceived by the parasite. We observed that XA is taken up by niRBCs and characterized the transport of XA via LC/MS/MS. XA uptake increased linearly with increasing incubation time or concentration applied. Uptake was saturable when increasing XA concentrations were applied. The properties observed are thus suggestive for facilitated diffusion being the mechanism for XA uptake (reviewed Carruthers, 1990).

Several inhibitors were used in uptake studies with niRBC as well as in exflagellation assays with mature gametocyte cultures. Adenine was used as competitive inhibitor of the nucleobase transporter hFNT1. Inhibitor studies with human RBCs had shown that a concentration of 1 mM adenine inhibited the uptake of 7 μ M of the carbocyclic nucleoside analogues carbovir and abacavir by 94% and 25%, respectively (Mahony *et al.*, 2004). Application of 3 mM adenine resulted in a similar inhibition of uptake of the nucleoside analogues by RBCs. In the exflagellation assay an inhibition of approximately 40% of the solvent control had been achieved. Thus, the observed reduction is not as pronounced as for uptake of the nucleoside analogue carbovir. The low reduction of

abacavir had been interpreted as unspecific and uptake of abacavir by RBCs was reported to be mediated via non-facilitated diffusion (Mahony et al., 2004). Another study also showed a very efficient inhibition of hFNT1. Here, 1 mM adenine resulted in 92% inhibition of permeant uptake (Wallace *et al.*, 2002).

The second inhibitor of the nucleobase transporter, hypoxanthine resulted in a similar inhibition of exflagellation of approximately 33%. Reduction of exflagellation by the nucleoside transporter inhibitor NBTI (5 μ M) was not significant as compared to the solvent control. In contrast, Plagemann and Woffendin (1988) reported an IC₅₀ value of 10 nM for the uptake of uridine. When using the same inhibitors for investigating the uptake of XA by niRBCs no differences were observed when applying inhibitor or solvent control. Thus it can be concluded, that neither the nucleobase transporter hFNT1 nor nucleoside transporter hENT1 are involved in uptake of XA by niRBC.

Further inhibitors tested were the amino acids L-Trp, L-Phe and L-Leu, that had been described as competitive inhibitors of transporters of aromatic amino acids (Lopez-Burillo et al., 1985; Tate et al., 1992). Furthermore the influence of cytochalasin B, inhibitor of the glucose transporter GLUT1 (Basketter and Widdas, 1978; Concha et al., 1997; Lu et al., 1997; Kasahara et al., 2009) was tested during XA uptake. And finally the OAPT inhibitors rifampicin and erythromycin (Vavricka et al., 2002; Seithel et al., 2006) were tested. None of these inhibitors showed an influence on XA uptake by niRBCs. Thus a potential transporter for XA remains elusive.

Beside transport proteins of the RBC parasitized erythrocytes possess a number of parasite-derived proteins that have been transported to the RBC cytosol or the RBC membrane (Ginsburg *et al.*, 1983; Elford *et al.*, 1985). Furthermore, the modification of transport properties of RBC-owned proteins by the parasite have been proposed (reviewed in Staines et al., 2004). Thus, it is possible that in the gametocyte-infected RBC XA uptake is even more efficient due to alteration of RBC transport proteins or insertion of parasite derived proteins into the RBCM.

We therefore tested the influence of the protease chymotrypsin on XA-mediated egress of male gametocytes from their host cells. Chymotrypsin had been described to inhibit uptake of NPP mediated transport (Baumeister et al., 2006). However there was only a weak, non-significant reduction of exflagellation centers when mature gametocytes were incubated with chymotrypsin prior to activation with XA. Similarly the uptake of XA by niRBCs was not affected by incubation with chymotrypsin prior to incubation with XA. Proteinase K has been used to study the conformation of transmembrane proteins (Poole *et al.*, 1996). For instance, treatment of RBCs with proteinase K had been described to digest GpA. However treatment of niRBC likewise did not influence the uptake of XA.

However, a very intriguing observation was made when mature gametocytes were incubated with saponin before activation. Microgametocytes were activated and underwent exflagellation when RBCM and PVM were removed prior to addition of XA. This observation supported our hypothesis that XA is detected beyond the RBCM. Thus the putative receptor for XA most probably is located at the PPM.

The combined results on exflagellation assays employing inhibitors of RBC nucleobase and nucleoside transporters showed significant reduction of exflagellation when applying inhibitors of the nucleobase transporter, but not of the nucleoside transporter. However, experiments with niRBCs revealed that the inhibitors did not have an effect on XA uptake by RBCs. Thus, the impact of nucleobase/nucleoside transporter inhibitors on exflagellation was caused by another unknown mechanism.

4.4.2 Reverse genetics study on XA receptor candidate genes

In order to identify a potential receptor protein for XA we searched the PlasmoDB database for G-protein coupled receptors/ serpentine receptors, as these are known to induce PLC (reviewed in Dorsam and Gutkind, 2007), which is a component of the XA-induced signal cascade (Martin et al., 1994). For two of the five identified genes, gene-disruptant mutant were generated. Generating a KO mutant for the *pfsr1* gene was attempted in two independent transfections. In both attempts integration of the PfsR1/pCAM-KO plasmid was not achieved, even after prolonged cultivation of transfectants. As the *pfsr1* gene is expressed in asexual blood stages, with a peak in the schizont stage, an essential role, for instance in egress of parasites from the iRBC is possible (Madeira et al., 2008). In contrast, it was possible to disrupt the gene with the gene identifier PFE1265w (new PlasmoDB identifier PF3D7_0525400). Preliminary results show that PFE1265w is predominantly expressed in gametocytes, however the PFE1265w-disruptant parasite line is able to form macro- and microgametes (A. von Bohl, MSc, personal communication). Thus, the protein is not involved in perception of XA. A role for development in the mosquito vector is anticipated as preliminary results showed a reduced number of oocysts and sporozoites during infection of *An. stephensi* (A. v. Bohl, M. Scheuermayer, G. Pradel, unpublished results).

In view of these results it will be necessary to generate and screen further gene-disruptant parasite lines in order to identify the receptor of XA. An alternative approach would be the labeling of XA in order to be able to identify the putative receptor via pull-down followed by mass-spectrometry. The generation of a biotinylated XA was attempted, but seems to be technically challenging. Thus, labeling of XA with tritium seems to be more promising in the search for a potential XA receptor.

Recently, a GPCR has been described to be involved in signaling processes preceding egress of asexual blood stages from the iRBC. The GPCR has been reported to be of

erythrocytic origin and induction by a parasite-derived ligand has been supposed (Millholland et al., 2013). However, the signal proteins downstream of the GPCR have been suggested to be entirely of host cell origin (Millholland et al., 2013), being in contrast to studies on *P. berghei* gametocytes where involvement of a parasite-derived PLC has been suggested (Raabe et al., 2011).

4.4.3 Influence of ionophores on gametocyte activation

Previously it had been shown for the Apicomplexan parasite *T. gondii* (Fruth and Arrizabalaga, 2007), that egress from the host cell was inducible by the K^+/H^+ ionophore nigericin. In the present study similar observations were made in *P. falciparum* gametocytes. The effect of nigericin was visible both for male gametocytes in exflagellation assays and for gametocytes of both genders in EM studies. As observed by Fruth and Arrizabalaga (2007) incubation with the ionophore for 30 min was more efficient than incubation for 15 min. It is thus possible that whilst XA signal reaches various downstream signal molecules (see Fig. 1.5), nigericin only activates one of these pathways. In contrast to *T. gondii* egress of male *P. falciparum* gametocytes was less efficient with only approximately 40% of male gametocytes exflagellating (as compared to nearly 100% of parasites egressed in *T. gondii*) (Fruth and Arrizabalaga, 2007). When investigating nigericin-induced egress on the ultrastructural level 85% of the investigated gametocytes showed lyses of the PVM. One explanation for this observation would be that nigericin activates female gametocytes more efficiently. Until today only few data have been gathered on activation of female gametocytes, thus, differences between the two genders are possible.

The antibiotic nigericin has been described to have a variety of effects. It acts as ionophore for K^+ , H^+ and Pb^{2+} (Shavit et al., 1968). Valinomycin on the other hand has been described as ionophore for K^+ ions (Heinen et al., 2007). Preliminary results indicated that valinomycin was able to induce exflagellation of male gametocytes as described for nigericin. However, EM studies investigating PVM rupture upon valinomycin treatment did not show activation of the gametocytes investigated.

Due to the conflicting results obtained for valinomycin it is not clear, whether the change of permeability of H^+ or K^+ ions is responsible for gametocyte activation. To test whether nigericin was changing permeability of K^+ ions, we activated exflagellation by nigericin in the presence of high extracellular K^+ concentrations (100-150 mM, data not shown). Under these conditions gametocyte activation was completely abolished. For *T. gondii* similar results were observed, however no complete inhibition by high K^+ concentrations was reported (Fruth and Arrizabalaga, 2007). It thus remains to be tested whether parasite viability was affected by these high K^+ concentrations or whether the nigericin-mediated ion efflux was abolished. Further experiments are necessary to investigate this. A possibility would be to employ zaprinast, inhibitor of phosphodiesterase-

rase (McRobert et al., 2008) that supposedly acts downstream of the nigericin-induced alteration of K^+ permeability. If parasites were still viable and able to undergo gametogenesis in the presence of high K^+ concentrations zaprinast would induce exflagellation even under these conditions. In *T. gondii* egress from the host cell is also inducible via host cell lysis which results in decrease of intracellular K^+ concentration of the host cell (Moudy et al., 2001). Upon host cell lysis with saponin there was also activation of a small proportion of gametocytes observed (see Fig. 3.55 vs. Fig. 3.54), however this effect was much smaller as in *T. gondii* where egress was induced in more than 70% of parasites upon host cell lysis.

The combined results of the ionophore experiments point at an influence of changes in host cell K^+ concentrations, however this is much less pronounced as observed in *T. gondii* (Moudy et al., 2001; Fruth and Arrizabalaga, 2007). It is probable that K^+ concentrations play only a minor role and that nigericin-induced exflagellation is partially due to changes in H^+ permeability. This would make sense considering the influence of changes of pH that have been reported to influence gametogenesis (Sinden, 1983, Nijhout and Carter, 1978).

4.4.4 Ultrastructural investigations of gametocyte activation

The study of gametocyte egress on the ultrastructural level showed the sequence of steps finally resulting in gamete formation and parasite egress from the host cell. Rupture of the PVM was observed as early as one minute upon induction of gametogenesis. Subsequently the RBC cytoplasm started to disintegrate and from 12 min p. act. onwards rupture of the RBCM was observed. Thus, the inside-out model, describing rupture of PVM prior to RBCM in asexual parasites (Wickham et al., 2003; Aikawa, 1971) is also true for gametocytes. These observations are also in agreement with an early study reporting PVM rupture prior to rupture of RBCM (Quakyi et al., 1989). The inside-out model also applies for liver schizonts. After rupture of the PVM merozoites are released into the blood stream within the so-called merozoite, which is derived from the hepatocyte plasma membrane (Sturm et al., 2006; Sturm and Heussler, 2007, reviewed in Wirth and Pradel, 2012).

We further studied PVM rupture as sign for occurring gamete formation under several conditions. We wanted to see if one of the signals perceived by the parasite within the mosquito midgut, drop in temperature by at least $5^{\circ}C$ or XA, is sufficient for induction of gamete formation. However, neither of the signals applied by itself was capable to induce PVM rupture. Thus, it seems as if at the very beginning gametocyte activation both signals are integrated and transduced in a common signal cascade. We further observed that incubation of mature gametocytes in a very low pH of 6.6 had an inhibitory effect on induction of gamete formation. Considering reports of the capability of extracellular pH to induce gamete formation (Sinden, 1983, Nijhout and Carter, 1978) our

result affirms the assumption of an increase of intracellular H^+ concentration playing an important signal during gamete formation. In an environment of very low pH such high intracellular pH most likely was not achievable. A high extracellular pH had been described to be able to replace the decrease of intracellular H^+ concentration as response of extracellular signals in mammalian cells (Kawamoto et al., 1991). In the budding yeast *Saccharomyces cerevisiae* H^+ ions have been described as secondary messengers. A rise of cytosolic pH here leads to activation of a cAMP-dependent proteinase kinase A (Dechant et al., 2010). The observations on nigericin being able to induce gamete formation would hence point at action as H^+/K^+ exchanger (Shavit et al., 1968) transporting K^+ ions from the RBC cytosol to the extracellular and simultaneously transporting H^+ into the RBC cytosol thus increasing the pH surrounding the gametocyte.

The signal cascade induced by XA and the drop in temperature (Fig. 1.5) finally leads to activation of several effector proteins mediating the egress of gametocytes from the host cell. Several types of proteases seem to participate in host cell lyses (Sologub et al., 2011). Those might include as recently reported for asexual blood stage parasites host cell proteases that mediate disintegration of the RBC cytoskeleton (Millholland et al., 2013). An additional class of proteins involved in RBC rupture are the perforins. A recent study reported that the perforin-like protein PPLP2 plays an important role for RBCM lysis (Deligianni et al., 2013).

4.4.5 Conclusions

In the present thesis several adhesion proteins of *P. falciparum* gametocytes were studied. Two newly obtained gene-disruptant parasite lines, PfCCp5-KO and PFFNPA-KO, completed the set of KO parasite lines of the PfCCp protein family. In contrast, for *P. berghei* only five of the six genes encoding the orthologous PbLAP proteins have been disrupted until today. The characterization of PfCCp5-KO and PFFNPA-KO parasites was in concordance with previous reports on the other PfCCp proteins. Although expressed in gametocytes, the PfCCp proteins are not essential for gametocyte development and gamete formation. The phenomenon of co-dependent expression amongst PfCCp proteins was confirmed for the two new gene-disruptant parasite lines as well. In the absence of PfCCp5 or PFFNPA most PfCCp proteins were present in reduced abundance whilst transcript levels were unchanged. PfCCp5 was shown to differ in certain extent from the other members of the protein family. It was detected already in trophozoites and expression of different isoforms upon proteolytical processing seems likely.

Expression of two so far barely characterized proteins, PfactinII and the recently discovered PfwLp1, was investigated, thus providing new promising targets for intervention strategies against *P. falciparum* transmission stages. The interaction and co-localization of PfactinII with Pfs230, a protein most important during fertilization, emphasizes the potential importance of PfactinII.

After being neglected for decades, after its first mention in the literature, the IMC of gametocyte was now studied on the molecular level. Considering findings from other groups the IMC seems to be a structural feature crucial for gametocyte development within the human host organism. Hence, the IMC also warrants further research in order to identify targets for interventions strategies.

The results on gametocyte egress shed light on the sequential processes occurring during this crucial part of the *P. falciparum* life cycle. In analogy to asexual blood stage parasites gametocytes egress via an inside-out mechanism, first lysing the PVM and thereafter the RBCM. The ability of the K^+/H^+ ionophore nigericin pointed at the possible involvement of K^+ ion concentration to play a role during gametocyte activation. The observation of gametocytes devoid of PVM and RBCM being able to percept XA provides information about the site of XA perception, possibly at the gametocyte PPM.

5 Summary

Transmission of the malaria parasite from man to the mosquito requires the formation of sexual parasite stages, the gametocytes. The gametocytes are the only parasite stage that is able to survive in the mosquito midgut and to undergo further development – gamete formation and fertilization. Numerous sexual stage-specific proteins have been discovered, some of which play crucial roles for parasite transmission. However, the functions of many sexual stage proteins remain elusive. Amongst the sexual stage-specific proteins are the proteins of the PfCCp proteins family, which exhibit numerous adhesion domains in their protein structures. For four members of the protein family, PfCCp1 to PfCCp4 gene-disruptant parasite lines had been already studied. Amongst these, PfCCp2 and PfCCp3 showed an important role for development of the parasites in the mosquito. In the present work the study of gene-disrupted parasites of the PfCCp protein family was completed. PfCCp5-KO and PffNPA-KO parasite lines were characterized to a great extent and many properties were similar to those of other PfCCp proteins. The co-dependent expression previously reported to be a phenomenon of PfCCp proteins was also observed in these two mutants, although to lesser extent. When either PfCCp5 or PffNPA were absent, all other proteins were detected in reduced abundance only. Co-dependent expression manifests exclusively on the protein level. Transcript levels were not altered as RT-PCR showed. Amongst PfCCp proteins numerous protein-protein interactions are taking place. The previously described multimeric protein complexes also include further sexual stage-specific proteins like Pfs230, Pfs48/45 and Pfs25. Recently, a new component of PfCCp-based multimeric protein complexes had been identified. The protein was named PfWLP1 (WD repeat protein-like protein 1) due to its possession of several WD40 repeats. In the present study expression of this uncharacterized protein was investigated via indirect IFA. It was expressed in asexual blood stages and gametocytes. Upon gamete formation and fertilization its expression ceased. Another sexual stage protein studied in this work was PfactinII. It was shown to be exclusively expressed in sexual stages. In gametocytes it co-localizes with Pfs230 and correct localization of PfactinII depends on presence of Pfs230.

Transcript analysis by means of RT-PCR revealed the expression of several components of the IMC in gametocytes. Furthermore, five or six myosin genes encoded in the *P. falciparum* genome were detected in gametocytes. Gametocyte egress was studied on the ultrastructural level via transmission electron microscopy and an inside-out type of egress was observed. Firstly, the membrane of the parasitophorous vacuole (PVM) was lysed and only thereafter the membrane of the red blood cell (RBCM) ruptured. Furthermore, a new inductor of gametogenesis was identified: The K^+/H^+ ionophore nigericin induced gametocytes activation in the absence of xanthurenic acid (XA), which is

responsible for gametocyte activation in the mosquito midgut. Selective permeabilization of RBCM and PVM by the mild detergent saponin, showed that in the absence of these membranes male gametocytes were still able to perceive both XA and the drop in temperature. Thus, the receptors for both factors signaling the parasite transmission to the mosquito, seem to be of parasitic origin. LC/MS/MS analysis confirmed the ability of RBCs to take up XA..

With malaria eradication on the agenda of malaria research targeting the sexual stages becomes a crucial part of intervention strategies. The sexual stages are especially attractive target as they represent a population bottleneck. The here reported findings on *P. falciparum* gametocytes provide several potential candidate proteins for developing tools to interrupt transmission from man to mosquito. Such tools might include transmission blocking vaccines and drugs.

6 Zusammenfassung

Die Übertragung der Malaria vom menschlichen Wirt auf die Überträgermücke erfordert die Bildung von Sexualstadien, der Gametozyten. Dieses Parasitenstadium ist in der Lage im Mitteldarm der Mücke zu überleben und sich zu Gameten zu entwickeln, gefolgt von Befruchtung und Zygotenbildung. Eine Vielzahl von in den Sexualstadien exprimierter Proteine wurde bereits entdeckt. Einige von diesen haben essentielle Funktionen für die Transmission der Parasiten auf die Mücke. Die Rolle der meisten dieser spezifisch exprimierter Protein ist jedoch ungeklärt. Zu den sexualstadienspezifischen Proteinen gehören die Proteine der PfCCp-Proteinfamilie. Für vier Proteine diese Proteinfamilie wurden bereits KO-Mutanten untersucht. Zwei Mutanten, PfCCp2-KO und PfCCp3-KO besitzen eine wichtige Funktion während der Entwicklung der Parasiten in der Mücke. In der vorliegenden Arbeit wurde die Studie der PfCCp-Proteine komplettiert. PfCCp5- und PffNPA-defiziente Parasitenlinien wurden zu einem Großteil charakterisiert. Viele Eigenschaften dieser beiden Parasitenlinien wiesen Ähnlichkeiten zu den bisher untersuchten PfCCp-KO-Mutanten auf. Die ko-abhängige Expression welche in der PfCCp-Proteinfamilie vorkommt, wurde auch in diesen beiden Mutanten beobachtet, wenngleich in geringerem Ausmaß. In den Mutanten, in welchem entweder PfCCp5 oder PffNPA fehlten, waren alle übrigen PfCCp-Proteine nur in reduzierter Menge nachzuweisen. Diese ko-abhängige Expression ist ausschließlich auf dem Proteinlevel zu beobachten. Die Transkription der jeweiligen Gene hingegen ist unbeeinflusst. Zahlreiche Protein-Protein-Interaktionen finden zwischen den Proteinen der Proteinfamilie statt. The zuvor beschriebenen multimeren Proteinkomplexe schließen auch weitere sexualstadienspezifische Proteine ein, wie Pfs230, Pfs48/45 und Pfs25. Kürzlich wurde eine neue Komponente der PfCCp-basierten Multiproteinkomplexe identifiziert. Dieses Protein wurde PfWLP1 (*WD repeat protein-like protein 1*) genannt, da es mehrere *WD40 repeat* Domänen besitzt. In der vorliegenden Arbeit wurde das bisher unbeschriebene Protein mittels indirekter Immunfluoreszenzstudien charakterisiert. PfWLP1 ist sowohl in asexuellen Blutstadien als auch in Gametozyten exprimiert. Nach der Gametenbildung und Fertilisation nimmt die Expression des Proteins ab. Ein weiteres Protein der Sexualstadien, welches in dieser Arbeit untersucht wurde, ist PfactinII. Es wurde gezeigt, dass dieses Protein ausschließlich in den Sexualstadien vorliegt. In Gametozyten ko-lokalisiert es mit Pfs230 und die korrekte Lokalisierung ist abhängig von der Anwesenheit von Pfs230.

Mittels RT-PCR wurden mehrere Komponenten des inneren Membrankomplexes in Gametozyten nachgewiesen. Weiterhin wurden Transkripte für fünf der sechs Myosin-Gene, welche im Genom von *P. falciparum* exprimiert sind, nachgewiesen. Der Austritt der Gametozyten aus der Wirtszelle wurde auf ultrastruktureller Ebene mittels Trans-

missionselektronenmikroskopie untersucht. Hierbei wurde gezeigt, dass die Lyse der den Parasiten umgebenden Membranen von innen nach außen geschieht. Das heißt, dass zunächst die Membran der parasitophoren Vakuole (PVM) lysiert wird, und erst anschließend die Erythrozyten-Plasmamembran (RBCM). Als neuer Induktor der Gametozytenaktivierung wurde Nigericin identifiziert. Nigericin ist ein K^+/H^+ -Ionophor, welcher in Abwesenheit von XA in der Lage ist, die Gametenbildung zu identifizieren. Die selektive Permeabilisierung der beiden den Gametozyten umgebenden Membranen, PVM und RBCM, zeigte, dass männliche Gametozyten nach Entfernung der beiden Membranen, in der Lage sind, den Temperaturabfall und XA zu perzipieren. Somit kann geschlussfolgert werden, dass die Rezeptoren beider Stimuli parasitischen Ursprungs sind. LC/MS/MS-Analysen bestätigten, dass Erythrozyten in der Lage sind, XA aufzunehmen.

Die Sexualstadien des Malariaparasiten nehmen mehr und mehr an Bedeutung zu, da langfristig nicht nur eine Eindämmung der Malaria in endemischen Gebieten sondern die Auslöschung der Malaria angestrebt wird. Die Sexualstadien sind ein attraktiver Angriffspunkt aufgrund ihrer Bedeutung für die Transmission der Krankheit. Zum anderen ist die auf den Vektor übertragene Parasitenanzahl vergleichsweise gering. Die Ergebnisse der vorliegenden Arbeit zeigen mehrere potentielle Kandidatenproteine auf, welche für die Entwicklung von Interventionsstrategien von Bedeutung sein könnten. Als Interventionsstrategien wären sowohl transmissionsblockierenden Vakzine als auch transmissionsblockierende Wirkstoffe denkbar.

7 References

- Agre, P. (2006) The aquaporin water channels. *Proc. Am. Thorac. Soc.* 3: 5–13.
- Aikawa, M. (1971) Parasitological review. *Plasmodium*: the fine structure of malarial parasites. *Exp. Parasitol.* 30: 284–320.
- Aikawa, M., Carter, R., Ito, Y., Nijhout, M.M. (1984) New observations on gametogenesis, fertilization, and zygote transformation in *Plasmodium gallinaceum*. *J. Protozool.* 31: 403-413.
- Alano, P., Premawansa, S., Bruce, M.C., Carter, R. (1991) A stage specific gene expressed at the onset of gametocytogenesis in *Plasmodium falciparum*. *Mol. Biochem. Parasitol.* 46: 81-88.
- Alano, P., Roca, L., Smith, D., Read, D., Carter, R., Day, K. (1995) *Plasmodium falciparum*: parasites defective in early stages of gametocytogenesis. *Exp. Parasitol.* 81: 227-235.
- Alano, P., Read, D., Bruce, M., Aikawa, M., Kaido, T., Tegoshi, T., Bhatti, S., Smith, D.K., Luo, C., Hansra, S., Carter, R., Elliott, J.F. (1995) COS cell expression cloning of *Pfg377*, a *Plasmodium falciparum* gametocyte antigen associated with osmiophilic bodies. *Mol. Biochem. Parasitol.* 74: 143-156.
- Alonso, P.L., Brown, G., Arevalo-Herrera, M., Binka, F., Chitnis, C., Collins, F., Doumbo, O.K., Greenwood, B., Hall, B.F., Levine, M.M., Mendis, K., Newman, R.D., Plowe, C.V., Rodriguez, M.H., Sinden, R., Slutsker, L., Tanner, M. (2011) A research agenda to underpin malaria eradication. *PLoS Med.* 8: e1000406.
- Alonso, P.L., Tanner, M. (2013) Public health challenges and prospects for malaria control and elimination. *Nat. Med.* 19: 150-155.
- Amino, R., Giovannini, D., Thiberge, S., Gueirard, P., Boisson, B., Dubremetz, J.F., Prévost, M.C., Ishino, T., Yuda, M., Ménard, R. (2008) Host cell traversal is important for progression of the malaria parasite through the dermis to the liver. *Cell Host Microbe.* 3: 88-96.
- Aingaran, M., Zhang, R., Law, S.K., Peng, Z., Undisz, A., Meyer, E., Diez-Silva, M., Burke, T.A., Spielmann, T., Lim, C.T., Suresh, S., Dao, M., Marti, M. (2012) Host cell deformability is linked to transmission in the human malaria parasite *Plasmodium falciparum*. *Cell. Microbiol.* 14: 983-993.

- Appella, E., Weber, I.T., Blasi, F. (1988) Structure and function of epidermal growth factor-like regions in proteins. *FEBS Lett.* 231: 1-4.
- Arrighi, R. B., Hurd, H. (2002) The role of *Plasmodium berghei* ookinete proteins in binding to basal lamina components and transformation into oocysts. *Int. J. Parasitol.* 32: 91–98.
- Atkinson, C.T., Aikawa, M. (1990) Ultrastructure of malaria-infected erythrocytes. *Blood Cells* 16: 351–368.
- Auffray, I., Marfatia, S., de Jong, K., Lee, G., Huang, C.H., Paszty, C., Tanner, M.J., Mohandas, N., Chasis, J.A. (2001) Glycophorin A dimerization and band 3 interaction during erythroid membrane biogenesis: in vivo studies in human glycophorin A transgenic mice. *Blood.* 97: 2872-2878.
- Ayala, F.J., Escalante, A.A., Rich, S.M. (1999) Evolution of *Plasmodium* and the recent origin of the world populations of *Plasmodium falciparum*. *Parassitologia.* 41: 55–68.
- Baer, K., Roosevelt, M., Clarkson, A.B., Jr., van Rooijen, N., Schnieder, T., and Frevert, U. (2007). Kupffer cells are obligatory for *Plasmodium yoelii* sporozoite infection of the liver. *Cell. Microbiol.* 9: 397–412.
- Baker, D.A. (2010) Malaria gametocytogenesis. *Mol. Biochem. Parasitol.* 172: 57-65.
- Baker, D.A., Daramola, O., McCrossan, M.V., Harmer, J., Targett, G.A. (1994) Subcellular localization of Pfs16, a *Plasmodium falciparum* gametocyte antigen. *Parasitology* 108: 129-137.
- Basketter, D.A., Widdas, W.F. (1978) Asymmetry of the hexose transfer system in human erythrocytes. Comparison of the effects of cytochalasin B, phloretin and maltose as competitive inhibitors. *J. Physiol.* 278: 389-401.
- Baton, L.A., Ranford-Cartwright, L.C. (2005) Do malaria ookinete surface proteins P25 and P28 mediate parasite entry into mosquito midgut epithelial cells? *Malar. J.* ;4: 15.
- Baum, J., Richard, D., Healer, J., Rug, M., Krnajski, Z., Gilberger, T.W., Green, J.L., Holder, A.A., Cowman, A.F. (2006) A conserved molecular motor drives cell invasion and gliding motility across malaria life cycle stages and other apicomplexan parasites. *J. Biol. Chem.* 281: 5197-5208.
- Baum, J., Gilberger, T.W., Frischknecht, F., Meissner, M. (2008) Host-cell invasion by malaria parasites: insights from *Plasmodium* and *Toxoplasma*. *Trends. Parasitol.* 24: 557-563.
- Baumeister, S., Winterberg, M., Duranton, C., Huber, S.M., Lang, F., Kirk, K., Lingelbach, K. (2006) Evidence for the involvement of *Plasmodium falciparum* proteins

- in the formation of new permeability pathways in the erythrocyte membrane. *Mol. Microbiol.* 60: 493-504.
- Beard, C.B., Benedict, M.Q., Primus, J.P., Finnerty, V., Collins, F.H. (1995) Eye pigments in wild-type and eye-color mutant strains of the African malaria vector *Anopheles gambiae*. *J. Hered.* 86: 375-380.
- Behari, R., Haldar, K. (1994) *Plasmodium falciparum*: protein localization along a novel, lipid-rich tubovesicular membrane network in infected erythrocytes. *Exp. Parasitol.* 79: 250-259.
- Beier, M.S., Pumpuni, C.B., Beier, J.C., Davis, J.R. (1994) Effects of para-aminobenzoic acid, insulin, and gentamicin on *Plasmodium falciparum* development in anopheline mosquitoes (Diptera: Culicidae). *J. Med. Entomol.* 31: 561-565.
- Bergman, L.W., Kaiser, K., Fujioka, H., Coppens, I., Daly, T.M., Fox, S., Matuschewski, K., Nussenzweig, V., Kappe, S.H. (2003) Myosin A tail domain interacting protein (MTIP) localizes to the inner membrane complex of *Plasmodium* sporozoites. *J. Cell. Sci.* 116: 39-49.
- Billker, O., Shaw, M.K., Margos, G., Sinden, R.E. (1997) The roles of temperature, pH and mosquito factors as triggers of male and female gametogenesis of *Plasmodium berghei* *in vitro*. *Parasitology* 115: 1-7.
- Billker, O., Lindo, V., Panico, M., Etienne, A.E., Paxton, T., Dell, A., Rogers, M., Sinden, R.E., Morris, H.R. (1998) Identification of xanthurenic acid as the putative inducer of malaria development in the mosquito. *Nature* 392: 289-292.
- Billker, O., Dechamps, S., Tewari, R., Wenig, G., Franke-Fayard, B., Brinkmann, V. (2004) Calcium and a calcium-dependent protein kinase regulate gamete formation and mosquito transmission in a malaria parasite. *Cell* 117: 503-514.
- Black, R.E., Cousens, S., Johnson, H.L., Lawn, J.E., Rudan, I., Bassani, D.G., Jha, P., Campbell, H., Walker, C.F., Cibulskis, R., Eisele, T., Liu, L., Mathers, C. (2010) Child Health Epidemiology Reference Group of WHO and UNICEF. Global, regional, and national causes of child mortality in 2008: a systematic analysis. *Lancet* 375: 1969-1987.
- Blackman, M.J., Ling, I.T., Nicholls, S.C., Holder, A.A. (1991) Proteolytic processing of the *Plasmodium falciparum* merozoite surface protein-1 produces a membrane-bound fragment containing two epidermal growth factor-like domains. *Mol. Biochem. Parasitol.* 49: 29-33.

- Blanchard, J., Hicks, J.S. (1999) The non-photosynthetic plastid in malarial parasites and other apicomplexans is derived from outside the green plastid lineage. *J. Euk. Microbiol.* 46: 367-375.
- Bosch, J., Buscaglia, C.A., Krumm, B., Ingason, B.P., Lucas, R., Roach, C., Cardozo, T., Nussenzweig, V., Hol, W.G. (2007) Aldolase provides an unusual binding site for thrombospondin-related anonymous protein in the invasion machinery of the malaria parasite. *Proc. Natl. Acad. Sci. USA* 104: 7015-7020.
- Bousema, T., Drakeley, C. (2011) Epidemiology and infectivity of *Plasmodium falciparum* and *Plasmodium vivax* gametocytes in relation to malaria control and elimination. *Clin. Microbiol. Rev.* 24: 377-410.
- Bray, R.S. (1963) The malaria parasites of anthropoids apes. *J. Parasitol.* 49: 888-891.
- Brooks, S.R., Williamson, K.C. (2000) Proteolysis of *Plasmodium falciparum* surface antigen, Pfs230, during gametogenesis. *Mol. Biochem. Parasitol.* 106: 77-82.
- Bruce, M.C., Alano, P., Duthie, S., and Carter, R. (1990) Commitment of the malaria parasite *Plasmodium falciparum* to sexual and asexual development. *Parasitology* 100: 191-200.
- Bruce, M.C, Carter, R.N., Nakamura, K., Aikawa, M., Carter, R. (1994) Cellular location and temporal expression of the *Plasmodium falciparum* sexual stage antigen Pfs16. *Mol. Biochem. Parasitol.* 65: 11-22.
- Buchholz, K., Burke, T.A., Williamson, K.C., Wiegand, R.C., Wirth, D.F., Marti, M. (2011) A high-throughput screen targeting malaria transmission stages opens new avenues for drug development. *J. Infect. Dis.* 203: 1445-1453.
- Bullen, H.E., Tonkin, C.J., O'Donnell, R.A., Tham, W.H., Papenfuss, A.T., Gould, S., Cowman, A.F., Crabb, B.S., Gilson, P.R. (2009) A novel family of Apicomplexan glideosome-associated proteins with an inner membrane-anchoring role. *J. Biol. Chem.* 284: 25353-25363.
- Cabantchik, Z.I. (1990) Properties of permeation pathways induced in the human red cell membrane by malaria parasites. *Blood Cells* 16: 421-432.
- Carrier, M.F. (1990) Actin polymerization and ATP hydrolysis. *Adv. Biophys.* 26: 51-73.
- Carruthers, A. (1990) Facilitated diffusion of glucose. *Physiol Rev.* 70: 1135-1176.
- Carter, R. (2001) Transmission blocking malaria vaccines. *Vaccine.* 19: 2309-2314.
- Carter, R., Chen, D.H. (1976) Malaria transmission blocked by immunisation with gametes of the malaria parasite. *Nature* 263: 57-60.

- Carter, R., Graves, P.M. (1988) in: *Malaria – Principles and Practise of Malariology* (Eds. Wernsdorfer, W.H., McGregeor, I.) *Churchill Livingstone* 1: 273-305.
- Carter, R., Gwadz, R.W., McAuliffe, F.M. (1979) *Plasmodium gallinaceum*: transmission-blocking immunity in chickens. I. Comparative immunogenicity of gametocyte- and gamete-containing preparations. *Exp. Parasitol.* 47: 185-193.
- Carter, R., Graves, P.M., Creasey, A., Byrne, K., Read, D., Alano, P., Fenton, B. (1989) *Plasmodium falciparum*: an abundant stage-specific protein expressed during early gametocyte development. *Exp. Parasitol.* 69: 140-149.
- Carter, R., Mendis, K.N., Miller, L.H., Molineaux, L., Saul, A. (2000) Malaria transmission-blocking vaccines – how can their development be supported? *Nat. Med.* 6: 241-244.
- Carter, V., Shimizu, S., Arai, M., Dessens, J.T. (2008) PbSR is synthesized in macrogametocytes and involved in formation of the malaria crystalloids. *Mol. Microbiol.* 68: 1560-1569.
- Chaparro-Olaya, J., Dluzewski, A.R., Margos, G., Wasserman, M.M., Mitchell, G.H., Bannister, L.H., Pinder, J.C. (2003) The multiple myosins of malaria: The smallest malaria myosin, *Plasmodium falciparum* myosin-B (Pfmyo-B) is expressed in mature schizonts and merozoites. *Europ. J. Protistol.* 39: 423-427.
- Chaparro-Olaya, J., Margos, G., Coles, D.J., Dluzewski, A.R., Mitchell, G.H., Wasserman, M.M., Pinder, J.C. (2005) *Plasmodium falciparum* myosins: transcription and translation during asexual parasite development. *Cell Motil. Cytoskeleton.* 60: 200-213.
- Chowdhury, D.R., Angov, E., Kariuki, T., Kumar, N. (2009) A potent malaria transmission blocking vaccine based on codon harmonized full length Pfs48/45 expressed in *Escherichia coli*. *PLoS One.* 4: e6352.
- Claudianos, C., Dessens, J.T., Trueman, H.E., Arai, M., Mendoza, J., Butcher, G.A., Crompton, T., Sinden, R.E. (2002) A malaria scavenger receptor-like protein essential for parasite development. *Mol. Microbiol.* 45: 1473-1484.
- Combe, A., Moreira, C., Ackerman, S., Thiberge, S., Templeton, T.J., Menard R (2009) TREP, a novel protein necessary for gliding motility of the malaria sporozoite. *Int. J. Parasitol.* 39: 489-496.
- Concha, I.I., Velásquez, F.V., Martínez, J.M., Angulo, C., Droppelmann, A., Reyes, A.M., Slebe, J.C., Vera, J.C., Golde, D.W. (1997) Human erythrocytes express GLUT5 and transport fructose. *Blood.* 89: 4190-4195.
- Cooke, B.M., Lingelbach, K., Bannister, L.H., Tilley, L. (2004) Protein trafficking in *Plasmodium falciparum*-infected red blood cells. *Trends Parasitol.* 20: 581-589.

- Cooper JA, Sept D. (2008) New insights into mechanism and regulation of actin capping protein. *Int. Rev. Cell. Mol. Biol.* 267: 183-206.
- Cowman, A.F., Crabb, B.S. (2006) Invasion of Red Blood Cells by Malaria Parasites. *Cell* 124: 755-766.
- Cowman, A., Crabb, B., Maier, A., Tonkin, C., Healer, J., Gibson, P. and de Koning-Ward, T. (2008) Transfection of *Plasmodium falciparum*. In: Moll, K., Ljungström, I., Perlmann, H., Scherf, A., Wahlgren, M. (Eds.) *Methods in Malaria Research*. MR4 / ATCC Manassas, Virginia, pp. 281-284.
- Cox-Singh J. (2012) Zoonotic malaria: *Plasmodium knowlesi*, an emerging pathogen. *Curr. Opin. Infect. Dis.* 25: 530-536.
- Crabb, B.S., Cowman, A.F. (1996) Characterization of promoters and stable transfection by homologous and nonhomologous recombination in *Plasmodium falciparum*. *Proc. Natl. Acad. Sci. USA* 93: 7289–7294.
- Crabb, B.S., Triglia, T., Waterkeyn, J.G., Cowman, A.F. 1997. Stable transgene expression in *Plasmodium falciparum*. *Mol. Biochem. Parasitol.* 90: 131–144.
- Culvenor, J.G., Day, K.P., Anders, R.F. (1991) *Plasmodium falciparum* ring-infected erythrocyte surface antigen is released from merozoite dense granules after erythrocyte invasion. *Infect. Immun.* 59: 1183-1187.
- Daneshvar, C., Davis, T.M., Cox-Singh, J., Rafa'ee, M.Z., Zakaria, S.K., Divis, P.C., Singh, B. (2009) Clinical and laboratory features of human *Plasmodium knowlesi* infection. *Clin. Infect. Dis.* 49: 852–860.
- Dearnley, M.K., Yeoman, J.A., Hanssen, E., Kenny, S., Turnbull, L., Whitchurch, C.B., Tilley, L., Dixon, M.W. (2012) Origin, composition, organization and function of the inner membrane complex of *Plasmodium falciparum* gametocytes. *J. Cell Sci.* 125: 2053-2063.
- Dechant, R., Binda, M., Lee, S.S., Pelet, S., Winderickx, J., Peter, M. (2010) Cytosolic pH is a second messenger for glucose and regulates the PKA pathway through V-ATPase. *EMBO J.* 29: 2515–2526.
- Deligianni, E., Morgan, R.N., Bertuccini, L., Kooij, T.W., Laforge, A., Nahar, C., Poulakakis, N., Schüler, H., Louis, C., Matuschewski, K., Siden-Kiamos, I. (2011) Critical role for a stage-specific actin in male exflagellation of the malaria parasite. *Cell Microbiol.* 13: 1714-1730.
- Deligianni, E., Morgan, R.N., Bertuccini, L., Wirth, C.C., de Monerri, N.C., Spanos, L., Blackman, M.J., Louis, C., Pradel, G., Siden-Kiamos, I. (2013) A perforin-like protein mediates disruption of the erythrocyte membrane during egress of *Plasmodium berghei* male gametocytes. *Cell Microbiol.* 15: 1438-1455.

- Dessens, J.T., Saeed, S., Tremp, A.Z., Carter, V. (2011) Malaria crystalloids: specialized structures for parasite transmission? *Trends Parasitol.* 27: 106-110.
- Dessens, J.T., Beetsma, A.L., Dimopoulos, G., Wengelnik, K., Crisanti, A., Kafatos, F.C., Sinden, R.E. (1999) CTRP is essential for mosquito infection by malaria ookinetes. *EMBO J.* 18: 6221-6227.
- Dessens, J.T., Sidén-Kiamos, I., Mendoza, J., Mahairaki, V., Khater, E., Vlachou, D., Xu, X.J., Kafatos, F.C., Louis, C., Dimopoulos, G., Sinden, R.E. (2003) SOAP, a novel malaria ookinete protein involved in mosquito midgut invasion and oocyst development. *Mol. Microbiol.* 49: 319-329.
- van Dijk, M.R., Janse, C.J., Thompson, J., Waters, A.P., Braks, J.A., Dodemont, H.J., Stunnenberg, H.G., van Gemert, G.J., Sauerwein, R.W., Eling, W. (2001) A central role for P48/45 in malaria parasite male gamete fertility. *Cell* 104: 153-164.
- van Dijk, M.R., van Schaijk, B.C., Khan, S.M., van Dooren, M.W., Ramesar, J., Kaczanowski, S., van Gemert, G.J., Kroeze, H., Stunnenberg, H.G., Eling, W.M., Sauerwein, R.W., Waters, A.P., Janse, C.J. (2010) Three members of the 6-cys protein family of Plasmodium play a role in gamete fertility. *PLoS Pathog.* 6: e1000853.
- Dinglasan, R.R., Jacobs-Lorena, M. (2008) Flipping the paradigm on malaria transmission-blocking vaccines. *Trends Parasitol.* 24: 364-370.
- Dixon, M.W., Thompson, J., Gardiner, D.L., Trenholme, K.R. (2008) Sex in Plasmodium: a sign of commitment. *Trends Parasitol.* 24: 168-175.
- Dixon, M.W., Dearnley, M.K., Hanssen, E., Gilberger, T., Tilley, L. (2012) Shapeshifting gametocytes: how and why does *P. falciparum* go banana-shaped? *Trends Parasitol.* 28: 471-478.
- Domin, B.A., Mahony, W.B., Zimmerman, T.P. (1988) Purine nucleobase transport in human erythrocytes. Reinvestigation with a novel "inhibitor-stop" assay. *J. Biol. Chem.* 263: 9276-9284.
- Dorsam, R.T., Gutkind, J.S. (2007) G-protein-coupled receptors and cancer. *Nat. Rev. Cancer* 7: 79-94.
- Dude, M.-A. (2009) Die Expression der Multiadhäsionsdomänenproteine PfCCp5 und PfFNPA in *Plasmodium falciparum* und Cysteinprotease-Inhibitoren als potentielle Wirkstoffe gegen Malaria. PhD thesis, University of Würzburg, Würzburg.
- Duffy, P.E., Kaslow, D.C. (1997) A novel malaria protein, *Pfs28*, and *Pfs25* are genetically linked and synergistic as falciparum malaria transmission-blocking vaccines. *Infect. Immun.* 65: 1109-1113.

- Eichner, M., Diebner, H.H., Molineaux, L., Collins, W.E., Jeffery, G.M., Dietz, K. (2001) Genesis, sequestration and survival of *Plasmodium falciparum* gametocytes: parameter estimates from fitting a model to malaria therapy data. *Trans. R. Soc. Trop. Med. Hyg.* 95: 497-501.
- Eksi, S., Williamson, K.C. (2002) Male-specific expression of the paralog of malaria transmission-blocking target antigen Pfs230, PfB0400w. *Mol. Biochem. Parasitol.* 122: 127-130.
- Eksi, S., Czesny, B., van Gemert, G.J., Sauerwein, R.W., Eling, W., Williamson, K.C. (2006) Malaria transmission-blocking antigen, Pfs230, mediates human red blood cell binding to exflagellating male parasites and oocyst production. *Mol. Microbiol.* 61: 991-998.
- Eksi, S., Morahan, B.J., Haile, Y., Furuya, T., Jiang, H., Ali, O., Xu, H., Kiattibutr, K., Suri, A., Czesny, B., Adeyemo, A., Myers, T.G., Sattabongkot, J., Su, X.Z., Williamson, K.C. *Plasmodium falciparum* gametocyte development 1 (Pfgdv1) and gametocytogenesis early gene identification and commitment to sexual development. *PLoS Pathog.* 8: e1002964.
- Elabbadi, N., Ancelin, M.L., Vial, H.J. (1994) Characterization of phosphatidylinositol synthase and evidence of a polyphosphoinositide cycle in *Plasmodium*-infected erythrocytes. *Mol. Biochem. Parasitol.* 63: 179-192.
- Engel, J., Fasold, H., Hulla, F.W., Waechter, F., Wegner, A., (1977) The polymerization reaction of muscle actin. *Mol. Cell. Biochem.* 18: 3-13.
- Elford, B.C., Haynes, J.D., Chulay, J.D., Wilson, R.J., (1985). Selective stage-specific changes in the permeability to small hydrophilic solutes of human erythrocytes infected with *Plasmodium falciparum*. *Mol. Biochem. Parasitol.* 16: 43-60.
- Epp, C., Deitsch, K. (2006) Deciphering the export pathway of malaria surface proteins. *Trends Parasitol.* 22: 401-404.
- Farfour, E., Charlotte, F., Settegrana, C., Miyara, M., Buffet, P. (2012) The extravascular compartment of the bone marrow: a niche for *Plasmodium falciparum* gametocyte maturation? *Malar. J.* 11: 285.
- Farrance, C.E., Rhee, A., Jones, R.M., Musiychuk, K., Shamloul, M., Sharma, S., Mett, V., Chichester, J.A., Streatfield, S.J., Roeffen, W., van de Vegte-Bolmer, M., Sauerwein, R.W., Tsuboi, T., Muratova, O.V., Wu, Y., Yusibov, V. (2011) A plant-produced Pfs230 vaccine candidate blocks transmission of *Plasmodium falciparum*. *Clin. Vaccine Immunol.* 18: 1351-1357.

- Fast, N.M., Kissinger, J.C., Roos, D.S., Keeling, P.J. (2001) Nuclear-encoded, plastid-targeted genes suggest a single common origin for apicomplexan and dinoflagellate plastids. *Mol. Biol. Evol.* 18: 418-426.
- Feachem, R.G., Phillips, A.A., Hwang, J., Cotter, C., Wielgosz, B., Greenwood, B.M., Sabot, O., Rodriguez, M.H., Abeyasinghe, R.R., Ghebreyesus, T.A., Snow, R.W. (2010) Shrinking the malaria map: progress and prospects. *Lancet.* 376:1566-1578.
- Fernandez, V., Hommel, M., Chen, Q., Hagblom, P., Wahlgren, M. (1999) Small, clonally variant antigens expressed on the surface of the *Plasmodium falciparum*-infected erythrocyte are encoded by the *rif* gene family and are the target of human immune responses. *J. Exp. Med.* 190: 1393-1404.
- Field, J.; Shute, P. (1956) In: The microscopic diagnosis of human malaria. II. A morphological study of the erythrocytic parasites. Institute for Medical Research, Kuala Lumpur, Malaysia.
- Fivelman, Q.L., McRobert, L., Sharp, S., Taylor, C.J., Saeed, M., Swales, C.A., Sutherland, C.J., Baker, D.A. (2007) Improved synchronous production of *Plasmodium falciparum* gametocytes *in vitro*. *Mol Biochem Parasitol.* 154: 119-123.
- Florens, L., Washburn, M.P., Raine, J.D, Anthony, R.M, Grainger, M., Haynes, J.D., Moch, J.K., Muster, N., Sacci, J.B., Tabb, D.L., Witney, A.A., Wolters, D., Wu, Y., Gardner, M.J., Holder, A.A., Sinden, R.E., Yates, J.R., Carucci, D.J. (2002) A proteomic view of the *Plasmodium falciparum* life cycle. *Nature.* 419: 520-526.
- Fong, H.K., Hurley, J.B., Hopkins, R.S., Miake-Lye, R., Johnson, M.S., Doolittle, R.F., Simon, M.I. (1986) Repetitive segmental structure of the transducin beta subunit: homology with the CDC4 gene and identification of related mRNAs. *Proc. Natl. Acad. Sci. U.S.A.* 83: 2162-2166.
- Frevert, U., Engelmann, S., Zougbede, S., Stange, J., Ng, B., Matuschewski, K., Liebes, L., and Yee, H. (2005). Intravital observation of *Plasmodium berghei* sporozoite infection of the liver. *PLoS Biol.* 3: e192.
- Fruth, I.A., Arrizabalaga, G. (2007) *Toxoplasma gondii*: induction of egress by the potassium ionophore nigericin. *Int. J. Parasitol.* 37: 1559-1567.
- Fujinaga, J., Tang, X.B., Casey, J.R. (1999) Topology of the membrane domain of human erythrocyte anion exchange protein, AE1. *J. Biol. Chem.* 274: 6626–6633.
- Funes, S., Davidson, E., Reyes-Prieto, A., Magallón, S., Herion, P., King, M.P., González-Halphen, D. (2002) A green algal apicoplast ancestor. *Science* 298: 2155.

- Furuya, T., Mu, J., Hayton, K., Liu, A., Duan, J., Nkrumah, L., Joy, D.A., Fidock, D.A., Fujioka, H., Vaidya, A.B., Wellems, T.E., Su, X.Z. (2005) Disruption of a *Plasmodium falciparum* gene linked to male sexual development causes early arrest in gametocytogenesis. *Proc. Natl. Acad. Sci. U.S.A.* 102: 16813-16818.
- Gabay, T., Ginsburg H. (1993) Hemoglobin denaturation and iron release in acidified red blood cell lysate--a possible source of iron for intraerythrocytic malaria parasites. *Exp. Parasitol.* 77: 261-72.
- Gandhi, M., Goode, B.L. (2008) Coronin: the double-edged sword of actin dynamics. *Subcell. Biochem.* 48: 72-87.
- Garcia, G.E., Wirtz, R.A., Barr, J.R., Woolfitt, A., Rosenberg, R. (1998) Xanthurenic acid induces gametogenesis in *Plasmodium*, the malaria parasite. *J. Biol. Chem.* 273: 12003-12005.
- Gardner, M.J., Hall, N., Fung, E., White, O., Berriman, M., Hyman, R.W., Carlton, J.M., Pain, A., Nelson, K.E., Bowman, S., Paulsen, I.T., James, K., Eisen, J.A., Rutherford, K., Salzberg, S.L., Craig, A., Kyes, S., Chan, M.S., Nene, V., Shalloom, S.J., Suh, B., Peterson, J., Angiuoli, S., Pertea, M., Allen, J., Selengut, J., Haft, D., Mather, M.W., Vaidya, A.B., Martin, D.M., Fairlamb, A.H., Fraunholz, M.J., Roos, D.S., Ralph, S.A., McFadden, G.I., Cummings, L.M., Subramanian, G.M., Mungall, C., Venter, J.C., Carucci, D.J., Hoffman, S.L., Newbold, C., Davis, R.W., Fraser, C.M., Barrell, B. (2002) Genome sequence of the human malaria parasite *Plasmodium falciparum*. *Nature.* 419: 498-511.
- Garnham, P.C. (1964) The subgenera of *Plasmodium* in mammals. *Ann. Soc. Belges. Med. Trop. Parasitol. Mycol.* 44: 267-271.
- Garnham, P.C. Electron microscope studies on motile stages of malaria parasites. VI. The ookinete of *Plasmodium berghei yoelii* and its transformation into the early oocyst. (1969) *Trans. R. Soc. Trop. Med. Hyg.* 63: 187-194.
- Gefflaut, T., Blonski, C., Perie, J., Willson, M. (1995) Class I aldolases: substrate specificity, mechanism, inhibitors and structural aspects. *Prog. Biophys. Mol. Biol.* 63: 301-340.
- Géminard, C., de Gassart, A., Vidal, M. (2002) Reticulocyte maturation: mitoptosis and exosome release. *Biocell.* 26: 205-215.
- Gerloff, D.L., Creasey, A., Maslau, S., Carter, R. (2005) Structural models for the protein family characterized by gamete surface protein *Pfs230* of *Plasmodium falciparum*. *Proc. Natl. Acad. Sci. U.S.A.* 102: 13598-13603.

- Gieseke, M. (2010) Funktionale Charakterisierung des Multiadhäsionsproteins PfCCp5 im Malariaerreger *Plasmodium falciparum*. Diploma thesis, University of Würzburg, Würzburg.
- Ginsburg, H., Stein, W.D. (2004) The new permeability pathways induced by the malaria parasite in the membrane of the infected erythrocyte: comparison of results using different experimental techniques. *J. Membr. Biol.* 197: 113-134.
- Ginsburg, H., Krugliak, M., Eidelman, O., Cabantchik, Z.I. (1983) New permeability pathways induced in membranes of *Plasmodium falciparum* infected erythrocytes. *Mol. Biochem. Parasitol.* 8: 177-190.
- Goodman, S.R., Kurdia, A., Ammann, L., Kakhniashvili, D., Daescu, O. (2007) The human red blood cell proteome and interactome. *Exp. Biol. Med.* 232: 1391-1408.
- Gordon, J.L., Sibley, L.D. (2005) Comparative genome analysis reveals a conserved family of actin-like proteins in apicomplexan parasites. *BMC. Genomics.* 6: 179.
- Gould, S.B., Tham, W.H., Cowman, A.F., McFadden, G.I., Waller, R.F. (2008) Alveolins, a new family of cortical proteins that define the protist infrakingdom Alveolata. *Mol. Biol. Evol.* 25:1219-1230.
- Graves, P.M., Carter, R., Burkot, T.R., Quakyi, I.A., Kumar, N. (1988) Antibodies to *Plasmodium falciparum* gamete surface antigens in Papua New Guinea sera. *Parasite Immunol.* 10: 209-218.
- Green, J.L., Martin, S.R., Fielden, J., Ksagoni, A., Grainger, M., Yim Lim, B.Y., Molloy, J.E., Holder, A.A. (2006) The MTIP-myosin A complex in blood stage malaria parasites. *J. Mol. Biol.* 355: 933-941.
- Green, J.L., Rees-Channer, R.R., Howell, S.A., Martin, S.R., Knuepfer, E., Taylor, H.M., Grainger, M., Holder, A.A. (2008) The Motor Complex of *Plasmodium falciparum*: phosphorylation by a calcium dependent protein kinase. *J. Biol. Chem.* 283: 30980-30989.
- Greenwalt, T.J. (1993) The Ernest Witebsky memorial lecture. Red but not dead: not a hapless sac of hemoglobin. *Immunol. Invest.* 24: 3-21.
- Griffith, D.A., Jarvis, S.M. (1996) Nucleoside and nucleobase transport systems of mammalian cells. *Biochim. Biophys. Acta.* 1286: 153-181.
- Gronowicz, G., Swift, H., Steck, T.L. (1984) Maturation of the reticulocyte in vitro. *J. Cell.Sci.* 71: 177-197.
- Gunn, R.B., Froelich, O., King, P.A., Shoemaker, D.G. (1989) Anion Transport. In: Agre, P., Parker, J.C. (Eds.). Red blood cell membranes: Structure, Function, Clinical implications. Dekker, New York, pp. 563-591.

- Guttery, D.S., Holder, A.A., Tewari, R. (2012) Sexual development in *Plasmodium*: lessons from functional analyses. *PLoS Pathog.* 8: e1002404.
- Gwadz, R.W. (1976) Successful immunization against the sexual stages of *Plasmodium gallinaceum*. *Science* 193: 1150-1151.
- Haeggström, M., Kironde, F., Berzins, K., Chen, Q., Wahlgren, M., Fernandez, V. (2004) Common trafficking pathway for variant antigens destined for the surface of the *Plasmodium falciparum*-infected erythrocyte. *Mol. Biochem. Parasitol.* 133: 1-14.
- Harris, P.K., Yeoh, S., Dluzewski, A.R., O'Donnell, R.A., Withers-Martinez, C., Hackett, F., Bannister, L.H., Mitchell, G.H., Blackman, M.J. (2005) Molecular identification of a malaria merozoite surface sheddase. *PLoS Pathog.* 1: 241-251.
- Hartman, M.A., Spudich, J.A. (2012) The myosin superfamily at a glance. *J. Cell Sci.* 125: 1627-1632.
- Hawking, F., Wilson, M.E., Gammage, K. (1971) Evidence for cyclic shortlived maturity in the gametocytes of *Plasmodium falciparum*. *Trans. R. Soc. Trop. Med. Hyg.* 65: 549-559.
- Healer, J., McGuinness, D., Hopcroft, P., Haley, S., Carter, R., Riley, E. (1997) Complement-mediated lysis of *Plasmodium falciparum* gametes by malaria-immune human sera is associated with antibodies to the gamete surface antigen Pfs230. *Infect. Immun.* 65: 3017-3023.
- Healer, J., Crawford, S., Ralph, S., McFadden, G., Cowman, A.F. (2002) Independent translocation of two micronemal proteins in developing *Plasmodium falciparum* merozoites. *Infect. Immun.* 70: 5751-5758.
- Heinen, A., Camara, A.K., Aldakkak, M., Rhodes, S.S., Riess, M.L., Stowe, D.F. (2007) Mitochondrial Ca^{2+} -induced K^{+} influx increases respiration and enhances ROS production while maintaining membrane potential. *Am. J. Physiol. Cell Physiol.* 292: C148-C156.
- Heintzelman, M.B., Schwartzman, J.D. (1997) A novel class of unconventional myosins from *Toxoplasma gondii*. *J. Mol. Biol.* 271: 139-146.
- Heiss, K., Nie, H., Kumar, S., Daly, T.M., Bergman, L.W., Matuschewski, K. (2008) Functional characterization of a redundant *Plasmodium* TRAP family invasin, TRAP-like protein, by aldolase binding and a genetic complementation test. *Eukaryot. Cell.* 7:1062-1070.
- Hepler, P., Huff, C., Sprinz, H. (1966) The fine structure of the exoerythrocytic stages of *Plasmodium fallax*. *J. Cell Biol.* 30: 333-359.

- Hess, R.J., Bayer, G.M. (2007) Red Blood Cell Metabolism during Storage, In: Hillier, C.D., Silberstein, L.E., Ness, P.M., Anderson, K.C., Roback, J.D. (Eds.) Blood Banking And Transfusion Medicine: Basic Principles And Practice (2nd edition) Churchill Livingstone, Philadelphia. pp. 205-211.
- Hill, D.A., Pillai, A.D., Nawaz, F., Hayton, K., Doan, L., Lisk, G., and Desai, S.A. (2007) A blasticidin S-resistant *Plasmodium falciparum* mutant with a defective plasmodial surface anion channel. *Proc. Natl. Acad. Sci. USA* 104: 1063–1068.
- Hisaeda, H., A. W. Stowers, T. Tsuboi, W. E. Collins, J. S. Sattabongkot, N. Suwanabun, M. Torii, and D. C. Kaslow. (2000) Antibodies to malaria vaccine candidates Pvs25 and Pvs28 completely block the ability of *Plasmodium vivax* to infect mosquitoes. *Infect. Immun.* 68: 6618-6623.
- Hodge, T., Cope, M.J. (2000) A myosin family tree. *J. Cell. Sci.* 113: 3353-3354.
- Huberts, D.H., van der Klei, I.J. (2010) Moonlighting proteins: an intriguing mode of multitasking. *Biochim. Biophys. Acta.* 1803: 520-525.
- Ifediba, T., Vanderberg, J.P. (1981) Complete *in vitro* maturation of *Plasmodium falciparum* gametocytes. *Nature.* 294: 364-366.
- Inoue, H., Nojima, H., Okayama, H. (1990) High efficiency transformation of *Escherichia coli* with plasmids. *Gene.* 96: 23-28.
- Ishino, T., Chinzei, Y., Yuda, M. (2005) Two proteins with 6-cys motifs are required for malarial parasites to commit to infection of the hepatocyte. *Mol. Microbiol.* 58: 1264-1275.
- Janse, C.J., van der Klooster, P.F., van der Ploeg, M., Overdulve, J.P. (1986) Rapid repeated DNA replication during microgametogenesis and DNA synthesis in young zygotes of *Plasmodium berghei*. *Trans. R. Soc. Trop. Med. Hyg.* 801: 154-157.
- Janse, C.J., Ponnudurai, T., Lensen, A.H., Meuwissen, J.H., Ramesar, J., van der Ploeg, M., Overdulve, J.P. (1988) DNA synthesis in gametocytes of *Plasmodium falciparum*. *Parasitology.* 96: 1-7.
- Jeffery, C.J. (1999) Moonlighting proteins. *Trends Biochem. Sci.* 24: 8-11.
- Jewett, T. J., and Sibley, L. D. (2003) *Mol. Cell* 11, 885-894.
- Jones, C.S., Luong, T., Hannon, M., Tran, M., Gregory, J.A., Shen, Z., Briggs, S.P., Mayfield, S.P. (2013) Heterologous expression of the C-terminal antigenic domain of the malaria vaccine candidate Pfs48/45 in the green algae *Chlamydomonas reinhardtii*. *Appl. Microbiol. Biotechnol.* 97: 1987-1995.

- Kadota, K., Ishino, T., Matsuyama, T., Chinzei, Y., Yuda, M. (2004) Essential role of membrane-attack protein in malarial transmission to mosquito host. *Proc. Natl. Acad. Sci. U.S.A.* 101: 16310-16315.
- Kakhniashvili, D.G., Bulla, Jr. L.A., Goodman, S.R. (2004) The human erythrocyte proteome: analysis by ion trap mass spectrometry. *Mol. Cell Proteomics* 3: 501–509.
- Kaplan, J.H. (1989) Active transport of sodium and potassium. In: Agre, P., Parker, J.C. (Eds.). *Red blood cell membranes: Structure, Function, Clinical implications*. Dekker, New York, pp. 455–480.
- Kariuki, M.M., Kiara, J.K., Mulaa, F.K., Mwangi, J.K., Wasunna, M.K., Martin, S.K. (1998) *Plasmodium falciparum*: purification of the various gametocyte developmental stages from in vitro-cultivated parasites. *Am. J. Trop. Med. Hyg.* 59: 505-508.
- Karunaweera, N.D., Carter, R., Grau, G.E., Mendis, K.N. (1998) Demonstration of anti-disease immunity to *Plasmodium vivax* malaria in Sri Lanka using a quantitative method to assess clinical disease. *Am. J. Trop. Med. Hyg.* 58: 204-210.
- Kaplan, J.H. (1989) Active transport of sodium and potassium. In: Agre, P., Parker, J.C. (Eds.). *Red blood cell membranes: Structure, Function, Clinical implications*. Dekker, New York, pp. 455–480.
- Kasahara, T., Maeda, M., Boles, E., Kasahara, M. (2009) Identification of a key residue determining substrate affinity in the human glucose transporter GLUT1. *Biochim Biophys. Acta.* 1788: 1051-1055.
- Kaslow, D.C. (2002) Transmission-blocking vaccines. *Chem. Immunol.* 80: 287-307.
- Kaslow, D.C., Quakyi, I.A., Syin, C., Raum, M.G., Keister, D.B., Coligan, J.E., McCutchan, T.F., Miller, L.H. (1988) A vaccine candidate from the sexual stage of human malaria that contains EGF-like domains. *Nature.* 333: 74-76.
- Kawamoto, F., Alejo-Blanco, R., Fleck, S.L., Kawamoto, Y., Sinden, R.E. (1990) Possible roles of Ca and cGMP as mediators of the exflagellation of *Plasmodium berghei* and *Plasmodium falciparum*. *Mol. Biochem. Parasitol.* 42: 101-108.
- Kawamoto, F., Alejo-Blanco, R., Fleck, S.L., and Sinden, R.E. (1991) *Plasmodium berghei*: ionic regulation and the induction of gametogenesis. *Exp. Parasitol.* 72: 33–42.
- Kawamoto, F., Fujioka, H., Murakami, R., Syafruddin, Hagiwara M., Ishikawa, T., Hidak, H. (1993) The roles of Ca²⁺/calmodulin- and cGMP-dependent pathways in gametogenesis of a rodent malaria parasite, *Plasmodium berghei*. *Eur. J. Cell Biol.* 60: 101-107.

- Khan, S.M., Franke-Fayard, B., Mair, G.R., Lasonder, E., Janse, C.J., Mann, M., Waters, A.P. (2005) Proteome analysis of separated male and female gametocytes reveals novel sex-specific *Plasmodium* biology. *Cell* 121: 675-687.
- Khattab, A., Klinkert, M.Q. (2006) Maurer's clefts-restricted localization, orientation and export of a *Plasmodium falciparum* RIFIN. *Traffic* 712: 1654-1665.
- King, A.E., Ackley, M.A., Cass, C.E., Young, J.D., Baldwin, S.A. (2006) Nucleoside transporters: from scavengers to novel therapeutic targets. *Trends Pharmacol. Sci.* 27: 416-425.
- Kirk, K., Saliba, K.J. (2007), Targeting nutrient uptake mechanisms in *Plasmodium*. *Curr. Drug Targets* 8: 75-88.
- Kirk, K., Horner, H.A., Kirk, J., (1996) Glucose uptake in *Plasmodium falciparum*-infected erythrocytes is an equilibrative not an active process. *Mol. Biochem. Parasitol.* 82: 195-205.
- Kiszewski, A., Mellinger, A., Spielman, A., Malaney, P., Sachs, S.E., Sachs, J. (2004) A global index representing the stability of malaria transmission. *Am. J. Trop. Med. Hyg.* 70: 486-498.
- Kocken, C.H., Jansen, J., Kaan, A.M., Beckers, P.J., Ponnudurai, T., Kaslow, D.C., Konings, R.N., Schoenmakers, J.G. (1993) Cloning and expression of the gene coding for the transmission blocking target antigen Pfs48/45 of *Plasmodium falciparum*. *Mol. Biochem. Parasitol.* 61: 59-68.
- Köhler, S., Delwiche, C.F., Denny, P.W., Tilney, L.G., Webster, P., Wilson, R.J., Palmer, J.D., Roos, D.S. (1997) A plastid of probable green algal origin in apicomplexan parasites. *Science* 275: 1485-1488.
- Kokwaro G. (2009) Ongoing challenges in the management of malaria. *Malar. J.* 8 Suppl 1: S2.
- de Koning-Ward, T.F., Olivieri, A., Bertuccini, L., Hood, A., Silvestrini, F., Charvalias, K., Berzosa Díaz, P., Camarda, G., McElwain, T.F., Papenfuss, T., Healer, J., Baldassarri, L., Crabb, B.S., Alano, P., Ranford-Cartwright, L.C. (2008) The role of osmiophilic bodies and Pfg377 expression in female gametocyte emergence and mosquito infectivity in the human malaria parasite *Plasmodium falciparum*. *Mol. Microbiol.* 67: 278-290.
- Kono, M., Herrmann, S., Loughran, N.B., Cabrera, A., Engelberg, K., Lehmann, C., Sinha, D., Prinz, B., Ruch, U., Heussler, V., Spielmann, T., Parkinson, J., Gilberger, T.W. (2012) Evolution and architecture of the inner membrane complex in asexual and sexual stages of the malaria parasite. *Mol. Biol. Evol.* 29: 2113-2132.

- Krendel, M., Mooseker, M.S. (2005) Myosins: tails (and heads) of functional diversity. *Physiology* (Bethesda). 20: 239-251.
- Kriek, N., Tilley, L., Horrocks, P., Pinches, R., Elford, B.C., Ferguson, D.J., Lingelbach, K., Newbold, C.I. (2003) Characterization of the pathway for transport of the cytoadherence-mediating protein, PfEMP1, to the host cell surface in malaria parasite-infected erythrocytes. *Mol. Microbiol.* 50: 1215-1227.
- Kuehn, A. (2007) Molekulare Wechselwirkungen von sexualstadienspezifischen Proteinen im Malariaerreger *Plasmodium falciparum* und die Wirkung des Signalmoleküls Xanthurensäure während Befruchtungsvorgängen. Diploma thesis, University of Würzburg, Würzburg.
- Kuehn A, Pradel G. (2010) The coming-out of malaria gametocytes. *J. Biomed. Biotechnol.* 2010: 976827.
- Kuehn A, Simon N, Pradel G. (2010) Family members stick together: multi-protein complexes of malaria parasites. *Med. Microbiol. Immunol.* 199: 209-226.
- Kumar, N. (1985) Phase separation in Triton X-114 of antigens of transmission blocking immunity in *Plasmodium gallinaceum*. *Mol. Biochem. Parasitol.* 17: 343-358.
- Kumar, N. (1987) Target antigens of malaria transmission blocking immunity exist as a stable membrane bound complex. *Parasite Immunol.* 9: 321-335.
- Kumar, N., Wizel, B. (1992) Further characterization of interactions between gamete surface antigens of *Plasmodium falciparum*. *Mol. Biochem. Parasitol.* 53: 113-120.
- Kyes, Sue (2008) Reliable RNA preparation for *Plasmodium falciparum*. In: Moll, K., Ljungström, I., Perlmann, H., Scherf, A., Wahlgren, M. (Eds.) *Methods in Malaria Research*. MR4 / ATCC Manassas, Virginia, pp. 207-210.
- Lacerda, M.V., Fragoso, S.C., Alecrim, M.G., Alexandre, M.A., Magalhães, B.M., Siqueira, A.M., Ferreira, L.C., Araújo, J.R., Mourão, M.P., Ferrer, M., Castillo, P., Martin-Jaular, L., Fernandez-Becerra, C., del Portillo, H., Ordi, J., Alonso, P.L., Bassat, Q. (2012) Postmortem characterization of patients with clinical diagnosis of *Plasmodium vivax* malaria: to what extent does this parasite kill? *Clin. Infect. Dis.* 55: e67-74.
- Lal, K., Delves, M.J., Bromley, E., Wastling, J.M., Tomley, F.M., Sinden, R.E. (2009) *Plasmodium male* development gene-1 (mdv-1) is important for female sexual development and identifies a polarised plasma membrane during zygote development. *Int. J. Parasitol.* 39: 755-761.
- Lambros, C., Vanderberg, J.P. (1979) Synchronization of *Plasmodium falciparum* erythrocytic stages in culture. *J. Parasitol.* 65: 418-420.

- Lanfrancotti, A., Bertuccini, L., Silvestrini, F., Alano, P. (2007) *Plasmodium falciparum*: mRNA co-expression and protein co-localisation of two gene products up-regulated in early gametocytes. *Exp. Parasitol.* 116: 497-503.
- Langer, R.C., Li, F., Popov, V., Kurosky, A., Vinetz, J.M. (2002) Monoclonal antibody against the *Plasmodium falciparum* chitinase, PfCMT1, recognizes a malaria transmission-blocking epitope in *Plasmodium gallinaceum* ookinetes unrelated to the chitinase PgCMT1. *Infect. Immun.* 70: 1581-1590.
- Lang-Unnasch, N., Murphy, A.D. (1998) Metabolic changes of the malaria parasite during the transition from the human to the mosquito host. *Annu. Rev. Microbiol.* 52: 561-590 .
- Lanzer, M., Wickert, H., Krohne, G., Vincensini, L., Braun Breton C. (2006) Maurer's clefts: a novel multi-functional organelle in the cytoplasm of *Plasmodium falciparum*-infected erythrocytes. *Int. J. Parasitol.* 36: 23-36.
- Lasonder, E., Ishihama, Y., Andersen, J.S., Vermunt, A.M., Pain, A., Sauerwein, R.W., Eling, W.M., Hall, N., Waters, A.P., Stunnenberg, H.G., Mann, M. Analysis of the *Plasmodium falciparum* proteome by high-accuracy mass spectrometry. *Nature* 419: 537-542.
- Laveran, A. (1880) A new parasite found in the blood of malarial patients. Parasitic origin of malarial attacks. *Bull. Mem. Soc. Med. Hosp. Paris* 17: 158-164
- Lemgruber, L., Kudryashev, M., Dekiwadia, C., Riglar, D.T., Baum, J., Stahlberg, H., Ralph, S.A., Frischknecht, F. (2013) Cryo-electron tomography reveals four-membrane architecture of the *Plasmodium* apicoplast. *Malar. J.* 12: 25.
- Li, F., Patra, K.P., Vinetz, J.M. (2005) An anti-Chitinase malaria transmission-blocking single-chain antibody as an effector molecule for creating a *Plasmodium falciparum*-refractory mosquito. *J. Infect. Dis.* 192: 878–887.
- Li, D., Roberts, R. (2001) WD-repeat proteins: structure characteristics, biological function, and their involvement in human diseases. *Cell. Mol. Life Sci.* 58: 2085-2097.
- Li, S., Whorton, A.R. (2007) Functional characterization of two S-nitroso-L-cysteine transporters, which mediate movement of NO equivalents into vascular cells. *Am. J. Physiol. Cell Physiol.* 292: C1263–1271.
- Lisk, G., Pain, M., Sellers, M., Gurnev, P.A., Pillai, A.D., Bezrukov, S.M., Desai, S.A. (2010) Altered plasmodial surface anion channel activity and in vitro resistance to permeating antimalarial compounds. *Biochim. Biophys. Acta* 1798: 1679–1688.
- Liu, L., Johnson, H.L., Cousens, S., Perin, J., Scott, S., Lawn, J.E., Rudan, I., Campbell, H., Cibulskis, R., Li, M., Mathers, C., Black, R.E. (2012) Global, regional, and national causes of child mortality: an updated systematic analysis for 2010 with

- time trends since 2000. Child Health Epidemiology Reference Group of WHO and UNICEF. *Lancet*. 379: 2151-2161.
- Liu, Y., Tewari, R., Ning, J., Blagborough, A.M., Garbom, S., Pei, J., Grishin, N.V., Steele, R.E., Sinden, R.E., Snell, W.J., Billker, O. (2008) The conserved plant sterility gene HAP2 functions after attachment of fusogenic membranes in *Chlamydomonas* and *Plasmodium* gametes. *Genes Dev*. 22: 1051-1068.
- Liu, Z., Miao, J., Cui, L. (2011) Gametocytogenesis in malaria parasite: commitment, development and regulation. *Future Microbiol*. 6: 1351-1369.
- López-Burillo, S., García-Sancho, J., Herreros, B. (1985) Tryptophan transport through transport system T in the human erythrocyte, the Ehrlich cell and the rat intestine. *Biochim. Biophys. Acta*. 820: 85-94.
- Low, T.Y., Seow, T.K., Chung, M.C. (2002) Separation of human erythrocyte membrane associated proteins with one-dimensional and two-dimensional gel electrophoresis followed by identification with matrix-assisted laser desorption/ionization-time of flight mass spectrometry. *Proteomics* 2: 1229-1239.
- Lu, L., Lundqvist, A., Zeng, C.M., Lagerquist, C., Lundahl, P. (1997) D-Glucose, forskolin and cytochalasin B affinities for the glucose transporter Glut1. Study of pH and reconstitution effects by biomembrane affinity chromatography. *J. Chromatogr. A*. 776: 81-86.
- Madeira, L., Galante, P.A., Budu, A., Azevedo, M.F., Malnic, B., Garcia, C.R. (2008) Genome-wide detection of serpentine receptor-like proteins in malaria parasites. *PLoS One*. 3: e1889.
- Mahony, W.B., Domin, B.A., Daluge, S.M., Zimmerman, T.P. (2004) Membrane permeation characteristics of abacavir in human erythrocytes and human T-lymphoblastoid CD4+ CEM cells: comparison with (-)-carbovir. *Biochem. Pharmacol*. 68: 1797-1805.
- Mair, G.R., Braks, J.A., Garver, L.S., Wiegant, J.C., Hall, N., Dirks, R.W., Khan, S.M., Dimopoulos, G., Janse, C.J., Waters, A.P. (2006) Regulation of sexual development of *Plasmodium* by translational repression. *Science* 313: 667-669.
- Mair, G.R., Lasonder, E., Garver, L.S., Franke-Fayard, B.M., Carret, C.K., Wiegant, J.C., Dirks, R.W., Dimopoulos, G., Janse, C.J., Waters, A.P. (2010) Universal features of post-transcriptional gene regulation are critical for *Plasmodium* zygote development. *PLoS Pathog*. 6: e1000767.
- Makler, M.T., Piper, R.C., Milhous, W.K. (1998) Lactate Dehydrogenase and the Diagnosis of Malaria. *Parasitol. Today*. 149: 376-377.

- Malkin, E.M., Durbin, A.P., Diemert, D.J., Sattabongkot, J., Wu, Y., Miura, K., Long, C.A., Lambert, L., Miles, A.P., Wang, J., Stowers, A., Miller, L.H., Saul, A. (2005) Phase 1 vaccine trial of Pvs25H: a transmission blocking vaccine for *Plasmodium vivax* malaria. *Vaccine*. 23: 3131-3138.
- Mamoun, C.B., Gluzman, I.Y., Goyard, S., Beverley, S.M., Goldberg, D.E. (1999) A set of independent selectable markers for transfection of the human malaria parasite *Plasmodium falciparum*. *Proc. Natl. Acad. Sci. U.S.A.* 96: 8716-8720.
- Martin, S.K., Jett, M., Schneider, I. (1994) Correlation of phosphoinositide hydrolysis with exflagellation in the malaria microgametocyte. *J. Parasitol.* 80: 371-378.
- Matsuoka, H., Yoshida, S., Hirai, M., and Ishii, A. (2002). A rodent malaria, *Plasmodium berghei*, is experimentally transmitted to mice by merely probing of infective mosquito, *Anopheles stephensi*. *Parasitol. Int.* 51: 17-23.
- McFadden, G.I. (2011) The apicoplast. *Protoplasma* 248: 641-650.
- McFadden, G.I., Waller, R.F. (1997) Plastids in parasites of humans. *BioEssays* 19: 1033-1040.
- McRobert, L., Taylor, C.J., Deng, W., Fivelman, Q.L., Cummings, R.M., Polley, S.D., Billker, O., Baker, D.A. (2008) Gametogenesis in malaria parasites is mediated by the cGMP-dependent protein kinase. *PLoS Biol.* 6: e139.
- Ménard, R. (2005) Medicine: knockout malaria vaccine? *Nature*. 433: 113-114.
- Mercer, R.T., Schneider, J.W., Benz, E.J. Jr. (1989) Na,K-ATPase Structure. In: Agre, P., Parker, J.C. (Eds.). Red blood cell membranes: Structure, Function, Clinical implications. Dekker, New York, pp. 135-157.
- Meis, J.F., Verhave, J.P. (1988) Exoerythrocytic development of malarial parasites. *Adv. Parasitol.* 27: 1-61.
- Miller, L.H., Baruch, D.I., Marsh, K., Doumbo, O.K. (2002) The pathogenic basis of malaria. *Nature* 415: 673-679.
- Miller, L.H., Ackerman, H.C., Su, X.Z., Wellems, T.E. (2013) Malaria biology and disease pathogenesis: insights for new treatments. *Nat. Med.* 19: 156-167.
- Millholland, M.G., Mishra, S., Dupont, C.D., Love, M.S., Patel, B., Shilling, D., Kazanietz, M.G., Foskett, J.K., Hunter, C.A., Sinnis, P., Greenbaum, D.C. (2013) A host GPCR signaling network required for the cytolysis of infected cells facilitates release of apicomplexan parasites. *Cell Host Microbe*. 13: 15-28.
- Mira-Martínez, S., Rovira-Graells, N., Crowley, V.M., Altenhofen, L.M., Llinás, M., Cortés, A. (2013) Epigenetic switches in clag3 genes mediate blasticidin S resistance in malaria parasites. *Cell Microbiol.* doi: 10.1111/cmi.12162.

- Moonen, B., Cohen, J.M., Snow, R.W., Slutsker, L., Drakeley, C., Smith, D.L., Abeyesinghe, R.R., Rodriguez, M.H., Maharaj, R., Tanner, M., Targett, G., (2010) Operational strategies to achieve and maintain malaria elimination. *Lancet* 376: 1592-1603.
- Moreira, C.K., Templeton, T.J., Lavazec, C., Hayward, R.E., Hobbs, C.V., Kroeze, H., Janse, C.J., Waters, A.P., Sinnis, P., Coppi, A. (2008) The *Plasmodium* TRAP/MIC2 family member, TRAP-Like Protein (TLP), is involved in tissue traversal by sporozoites. *Cell. Microbiol.* 10: 1505–1516.
- Morrisette NS, Sibley LD. (2002) Cytoskeleton of apicomplexan parasites. *Microbiol. Mol. Biol. Rev.* 66: 21-38.
- Mota, M.M., Pradel, G., Vanderberg, J.P., Hafalla, J.C., Frevert, U., Nussenzweig, R.S., Nussenzweig, V., and Rodriguez, A. (2001) Migration of *Plasmodium* sporozoites through cells before infection. *Science* 291: 141-144.
- Moudy, R., Manning, T.J., Beckers, C.J. (2001) The loss of cytoplasmic potassium upon host cell breakdown triggers egress of *Toxoplasma gondii*. *J. Biol. Chem.* 276: 41492-41501.
- Mueckler, M., Caruso, C., Baldwin, S.A., Panico, M., Blemch, I., Morris, H.R., Allard, W.J., Lienhard, G.E., Lodish, H.F. (1985) Sequence and structure of a human glucose transporter. *Science* 229: 941-945.
- Muhia, D.K., Swales, C.A., Deng, W., Kelly, J.M., Baker, D.A. (2001) The gametocyte-activating factor xanthurenic acid stimulates an increase in membrane-associated guanylyl cyclase activity in the human malaria parasite *Plasmodium falciparum*. *Mol. Microbiol.* 42: 553-560.
- Mulder B, Tchuinkam T, Verhave JP, Robert V. (1993) Malaria transmission-blocking activity in the plasma of *Plasmodium falciparum* gametocyte carriers in Cameroon. *Parassitologia* 35: Suppl: 65-67.
- Mulder, B., Tchuinkam, T., Dechering, K., Verhave, J.P., Carnevale, P., Meuwissen, J.H., Robert, V. (1994) Malaria transmission-blocking activity in experimental infections of *Anopheles gambiae* from naturally infected *Plasmodium falciparum* gametocyte carriers. *Trans. R. Soc. Trop. Med. Hyg.* 88: 121-125.
- Müller, I.B., Knöckel, J., Eschbach, M.L., Bergmann, B., Walter, R.D., Wrenger, C. (2010) Secretion of an acid phosphatase provides a possible mechanism to acquire host nutrients by *Plasmodium falciparum*. *Cell. Microbiol.* 12: 677-691.
- Mullins, R.D., Heuser, J.A., Pollard, T.D. (1998) The interaction of Arp2/3 complex with actin: Nucleation, high affinity pointed end capping, and formation of branching networks of filaments. *Proc. Natl. Acad. Sci. U.S.A.* 95: 6181–6186.

- Neer, E.J., Schmidt, C.J., Nambudripad, R., Smith, T.F. (1994) The ancient regulator protein family of WD-repeat proteins. *Nature* 371: 297–300.
- Ngongang, V.N. (2010) Untersuchungen zur Verteilung von sexualspezifischen Adhäsionsproteinen des Malariaerregers *Plasmodium falciparum* in Mückendarmstadien und ihrer Eignung als transmissionsblockierende Vakzine. Bachelor thesis, University of Würzburg, Würzburg.
- Ngongang, V.N. (2012) Die Rolle des WD40-Motivproteins PfWLP1 für die Ausbildung multimerer Proteinkomplexen in *Plasmodium falciparum*. Master thesis, University of Würzburg, Würzburg.
- Nijhout, M.M., Carter, R. (1978) Gamete development in malaria parasites: Bicarbonate-dependent stimulation by pH in vitro. *Parasitology* 76: 39-53.
- Ouédraogo, A.L., Roeffen, W., Luty, A.J., de Vlas, S.J., Nebie, I., Ilboudo-Sanogo, E., Cuzin-Ouattara, N., Teleen, K., Tiono, A.B., Sirima, S.B., Verhave, J.P., Bousema, T., Sauerwein, R. (2011) Naturally acquired immune responses to *Plasmodium falciparum* sexual stage antigens Pfs48/45 and Pfs230 in an area of seasonal transmission. *Infect. Immun.* 79: 4957-4964.
- Ogwan'g, R., Mwangi, J., Gachihi, G., Nwachukwu, A., Roberts, C.R., Martin, S.K. (1993) Use of pharmacological agents to implicate a role for phosphoinositide hydrolysis products in malaria gamete formation. *Biochem. Pharmacol.* 46: 1601-1606.
- Okamoto, N., Spurck, T.P., Goodman, C.D., McFadden, G.I. (2009) Apicoplast and mitochondrion in gametocytogenesis of *Plasmodium falciparum*. *Eukaryot. Cell* 8: 128-132.
- Önfelt, B., Nedvetzki, S., Yanagi, K., Davis, D.M. (2004) Cutting edge: Membrane nanotubes connect immune cells. *J. Immunol.* 173: 1511-1513.
- Ong, C.S., Zhang, K.Y., Eida, S.J., Graves, P.M., Dow, C., Looker, M., Rogers, N.C., Chiodini, P.L., Targett, G.A. (1990) The primary antibody response of malaria patients to *Plasmodium falciparum* sexual stage antigens which are potential transmission blocking vaccine candidates. *Parasite Immunol.* 12: 447-456.
- Parker, J.C., Dunham, P.B. (1989) Passive Cation Transport. In: Agre, P., Parker, J.C. (Eds.). Red blood cell membranes: Structure, Function, Clinical implications. Dekker, New York, pp. 507–543.
- Pasini, E.M., Kirkegaard, M., Mortensen, P., Lutz, H.U., Thomas, A.W., Mann, M. (2006) In-depth analysis of the membrane and cytosolic proteome of red blood cells. *Blood* 108: 791-801.

- Pasini, E.M., Lutz, H.U., Mann, M., Thomas, A.W. (2010) Red blood cell (RBC) membrane proteomics--Part I: Proteomics and RBC physiology. *J. Proteomics*. 73: 403-420.
- Paton, M.G., Barker, G.C., Matsuoka, H., Ramesar, J., Janse, C.J., Waters, A.P., Sinden, R.E. (1993) Structure and expression of a post-transcriptionally regulated malaria gene encoding a surface protein from the sexual stages of *Plasmodium berghei*. *Mol. Biochem. Parasitol.* 59: 263-275.
- Peatey, C.L., Skinner-Adams, T.S., Dixon, M.W., McCarthy, J.S., Gardiner, D.L., Katharine R. Trenholme, K.R. (2009) Effect of Antimalarial Drugs on *Plasmodium falciparum* Gametocytes. *J. Infect. Dis.* 200: 1518-1521.
- Pertoft, H., Laurent, T.C., Låås, T., Kågedal, L. (1978) Density gradients prepared from colloidal silica particles coated by polyvinylpyrrolidone (Percoll). *Anal. Biochem.* 88: 271-282.
- Pilch, P.F. (1990) Glucose transporters: what's in a name? *Endocrinology* 126: 3-5.
- Pinder, J.C., Fowler, R.E., Dluzewski, A.R., Bannister, L.H, Lavin, .FM., Mitchell, G.H., Wilson, R.J., Gratzer, W.B. (1998) Actomyosin motor in the merozoite of the malaria parasite, *Plasmodium falciparum*: implications for red cell invasion. *J. Cell Sci.* 111 : 1831-1839.
- Plagemann, P.G., Woffendin, C. (1988) Species differences in sensitivity of nucleoside transport in erythrocytes and cultured cells to inhibition by nitrobenzylthioinosine, dipyridamole, dilazep and lidoflazine. *Biochim. Biophys. Acta.* 969: 1-8.
- Ponnudurai, T., Lensen, A.H., Leeuwenberg, A.D., Meuwissen, J.H. (1982) Cultivation of fertile *Plasmodium falciparum* gametocytes in semi-automated systems. 1. Static cultures. *Trans. R. Soc. Trop. Med. Hyg.* 76: 812-818.
- Ponzi, M., Sidén-Kiamos, I., Bertuccini, L., Currà, C., Kroeze, H., Camarda, G., Pace, T., Franke-Fayard, B., Laurentino, E.C., Louis, C., Waters, A.P., Janse, C.J., Alano, P. (2009) Egress of *Plasmodium berghei* gametes from their host erythrocyte is mediated by the MDV-1/PEG3 protein. *Cell. Microbiol.* 11: 1272-1288.
- Poole, R.C., Sansom, C.E., Halestrap, A.P. (1996) Studies of the membrane topology of the rat erythrocyte H⁺/lactate cotransporter (MCT1). *Biochem, J.* 320: 817-824.
- Pradel, G. (2007) Proteins of the malaria parasite sexual stages: expression, function and potential for transmission blocking strategies. *Parasitology* 134: 1911-1929.
- Pradel, G., Frevert, U. (2001). Malaria sporozoites actively enter and pass through rat Kupffer cells prior to hepatocyte invasion. *Hepatology* 33, 1154-1165.
- Pradel, G., Hayton, K., Aravind, L., Iyer, L.M., Abrahamsen, M.S., Bonawitz, A., Mejjia, C., Templeton, T.J. (2004) A multidomain adhesion protein family expressed

- in *Plasmodium falciparum* is essential for transmission to the mosquito. *J. Exp. Med.* 199: 1533-1544.
- Pradel, G., Wagner, C., Mejia, C., Templeton, T.J. (2006) *Plasmodium falciparum*: Co-dependent expression and co-localization of the PfCCp multi-adhesion domain proteins. *Exp. Parasitol.* 112: 263-268.
- Preiser, P.; Kaviratne, M., Khan, S., Bannister, L., Jarra, W. (2000) The apical organelles of malaria merozoites: host cell selection, invasion, host immunity and immune evasion. *Microbes. Infect.* 2: 1461-1477.
- Premawansa, S., Gamage-Mendis, A., Perera, L., Begarnie, S., Mendis, K., Carter, R. (1994) *Plasmodium falciparum* malaria transmission blocking immunity under conditions of low endemicity as in Sri Lanka. *Parasite Immunol.* 16: 35-42.
- Przyborski, J.M., Wickert, H., Krohne, G., Lanzer, M. (2003) Maurer's clefts – a novel secretory organelle? *Mol. Biochem. Parasitol.* 132: 17-26.
- Quakyi, I.A., Carter, R., Rener, J., Kumar, N., Good, M.F., Miller L.H. (1987) The 230-kDa gamete surface protein of *Plasmodium falciparum* is also a target for transmission-blocking antibodies. *J. Immunol.* 139: 4213-4217.
- Quakyi, I.A., Matsumoto, Y., Carter, R., Udomsangpetch, R., Sjolander, A., Berzins, K., et al. (1989) Movement of a falciparum malaria protein through the erythrocyte cytoplasm to the erythrocyte membrane is associated with lysis of the erythrocyte and release of gametes. *Infect. Immun.* 57: 833-839.
- Quashie, N.B., Ranford-Cartwright, L.C., de Koning, H.P. (2010) Uptake of purines in *Plasmodium falciparum*-infected human erythrocytes is mostly mediated by the human equilibrative nucleoside transporter and the human facilitative nucleobase transporter. *Malar. J.* 9: 36.
- Raabe, A., Berry, L., Sollelis, L., Cerdan, R., Tawk, L., Vial, H.J., Billker, O., Wengelnik, K. (2001) Genetic and transcriptional analysis of phosphoinositide-specific phospholipase C in *Plasmodium*. *Exp. Parasitol.* 129: 75-80.
- Raine, J.D., Ecker, A., Mendoza, J., Tewari, R., Stanway, R.R., Sinden, R.E. (2007) Female inheritance of malarial lap genes is essential for mosquito transmission. *PLoS Pathog.* 3: e30.
- Ralph, S.A., van Dooren, G.G., Waller, R.F., Crawford, M.J., Fraunholz, M.J., Foth, B.J., Tonkin, C.J., Roos, D.S., McFadden, G.I. (2004) Tropical infectious diseases: metabolic maps and functions of the *Plasmodium falciparum* apicoplast. *Nat. Rev. Microbiol.* 2: 203-216.
- Ranjan, R., Chugh, M., Kumar, S., Singh, S., Kanodia, S., Hossain, M.J., Korde, R., Grover, A., Dhawan, S., Chauhan, V.S., Reddy, V.S., Mohammed, A., Malhotra, P.

- (2011) Proteome analysis reveals a large merozoite surface protein-1 associated complex on the *Plasmodium falciparum* merozoite surface. *J. Proteome Res.* 10: 680-691.
- Read, D., Lensen, A.H., Begarnie, S., Haley, S., Raza, A., Carter, R. (1994) Transmission-blocking antibodies against multiple, non-variant target epitopes of the *Plasmodium falciparum* gamete surface antigen Pfs230 are all complement-fixing. *Parasite Immunol.* 16: 511-519.
- Rees-Channer, R.R., Martin, S.R., Green, J.L., Bowyer, P.W., Grainger, M., Molloy, J.E., Holder, A.A. (2006) Dual acylation of the 45 kDa gliding-associated protein (GAP45) in *Plasmodium falciparum* merozoites. *Mol. Biochem. Parasitol.* 149: 113-116.
- Reininger, L., Billker, O., Tewari, R., Mukhopadhyay, A., Fennell, C., Dorin-Semblat, D., Doerig, C., Goldring, D., Harmse, L., Ranford-Cartwright, L., Packer, J., Doerig, C. (2005) A NIMA-related protein kinase is essential for completion of the sexual cycle of malaria parasites. *J Biol Chem.* 280: 31957-31964.
- Reininger L, Tewari R, Fennell C, Holland Z, Goldring D, Ranford-Cartwright L, Billker O, Doerig C. (2009) An essential role for the *Plasmodium* Nek-2 Nima-related protein kinase in the sexual development of malaria parasites. *J Biol Chem.* 284: 20858-20868.
- Reiss, M., Viebig, N., Brecht, S., Fourmaux, M.N., Soete, M., Di Cristina, M., Dubremetz, J.F., Soldati, D. (2001) Identification and characterization of an escorter for two secretory adhesins in *Toxoplasma gondii*. *J. Cell Biol.* 152: 563-578.
- Rener, J., Graves, P.M., Carter, R., Williams, J.L., Burkot, T.R. (1983) Target antigens of transmission-blocking immunity on gametes of *Plasmodium falciparum*. *J. Exp. Med.* 158: 976-981.
- Richard, D., MacRaid, C.A., Riglar, D.T., Chan, J.A., Foley, M., Baum, J., Ralph, S.A., Norton, R.S., Cowman, A.F. (2010) Interaction between *Plasmodium falciparum* apical membrane antigen 1 and the rhoptry neck protein complex defines a key step in the erythrocyte invasion process of malaria parasites. *J. Biol. Chem.* 285: 14815-14822.
- Ridzuan, M.A., Moon, R.W., Knuepfer, E., Black, S., Holder, A.A., Green, J.L. (2012) Subcellular location, phosphorylation and assembly into the motor complex of GAP45 during *Plasmodium falciparum* schizont development. *PLoS One.* 7: e33845.
- Roberts, L., Enserink, M. (2007) Malaria. Did they really say ... eradication? *Science* 318: 1544-1545.

- Rodríguez Mdel, C., Martínez-Barnetche, J., Alvarado-Delgado, A., Batista, C., Argotte-Ramos, R.S., Hernández-Martínez, S., González Cerón, L., Torres, J.A., Margos, G., Rodríguez, M.H. (2007) The surface protein Pvs25 of *Plasmodium vivax* ookinetes interacts with calreticulin on the midgut apical surface of the malaria vector *Anopheles albimanus*. *Mol. Biochem. Parasitol.* 153: 167-177.
- Roll Back Malaria Partnership. (2008) The global malaria action plan. World Health Organization <http://www.rbm.who.int/gmap/gmap.pdf>.
- Roudier, N., Verbavatz, J.M., Maurel, C., Ripoché, P., Tacnet, F. (1998) Evidence for the presence of aquaporin-3 in human red blood cells. *J. Biol. Chem.* 273: 8407-8412.
- Rudzinska, M.A. and Trager, W. (1968) The fine structure of trophozoites and gametocytes of *Plasmodium coatneyi*. *J. Protozool.* 15: 73-88.
- Rupp, I., Sologub, L., Williamson, K.C., Scheuermayer, M., Reininger, L., Doerig, C., Eksi, S., Kombila, D.U., Frank, M., Pradel, G. (2011) Malaria parasites form filamentous cell-to-cell connections during reproduction in the mosquito midgut. *Cell Res.* 21: 683-696.
- Russell, D.G., Burns, R.G. (1984) The polar ring of coccidian sporozoites: a unique microtubule-organizing centre. *J. Cell Sci.* 65: 193-207.
- Rustom, A., Saffrich, R., Markovic, I., Walther, P., Gerdes, H.-H. (2004) Nanotubular highways for intercellular organelle transport. *Science* 303: 1007-1010.
- Saeed, M., Roeffen, W., Alexander, N., Drakeley, C.J., Targett, G.A., Sutherland, C.J. (2008) *Plasmodium falciparum* antigens on the surface of the gametocyte-infected erythrocyte. *PLoS One.* 3: e2280.
- Saeed, S., Carter, V., Tremp, A.Z., Dessens, J.T. (2010) *Plasmodium berghei* crystalloids contain multiple LCCL proteins. *Mol. Biochem. Parasitol.* 170: 49-53.
- Saeed, S., Tremp, A.Z., Dessens, J.T. (2012) Conformational co-dependence between *Plasmodium berghei* LCCL proteins promotes complex formation and stability. *Mol. Biochem. Parasitol.* 185: 170-173.
- Saeed, S., Carter, V., Tremp, A.Z., Dessens, J.T. (2013) Translational repression controls temporal expression of the *Plasmodium berghei* LCCL protein complex. *Mol. Biochem. Parasitol.* 189: 38-42.
- Sanders, P.R., Gilson, P.R., Cantin, G.T., Greenbaum, D.C., Nebl, T., Carucci, D.J., McConville, M.J., Schofield, L., Hodder, A.N., Yates, J.R. 3rd, Crabb, B.S. (2005) Distinct protein classes including novel merozoite surface antigens in Raft-like membranes of *Plasmodium falciparum*. *J. Biol. Chem.* 280: 40169-40176.

- Sanders, P.R., Kats, L.M., Drew, D.R., O'Donnell, R.A., O'Neill, M., Maier, A.G., Coppel, R.L., Crabb, B.S. (2006) A set of glycosylphosphatidyl inositol-anchored membrane proteins of *Plasmodium falciparum* is refractory to genetic deletion. *Infect Immun.* 74: 4330-4338.
- Sanger, F., Nicklen, S., Coulson, A.R. (1977) DNA sequencing with chain-terminating inhibitors. *Proc. Natl. Acad. Sci. U.S.A.* 74: 5463-5467.
- Sannella, A.R., Olivieri, A., Bertuccini, L., Ferrè, F., Severini, C., Pace, T., Alano, P. (2012) Specific tagging of the egress-related osmiophilic bodies in the gametocytes of *Plasmodium falciparum*. *Malar. J.* 11: 88.
- Sattler, J.M., Ganter, M., Hliscs, M., Matuschewski, K., Schüler, H. (2011) Actin regulation in the malaria parasite. *Eur. J. Cell Biol.* 90: 966-971.
- Sauerwein, R.W. (2007) Malaria transmission-blocking vaccines: the bonus of effective malaria control. *Microbes and Infection.* 9: 792-795.
- Saul, A. (2007) Mosquito stage, transmission blocking vaccines for malaria. *Curr. Opin. Infect. Dis.* 20: 476-481.
- Saxena, A.K., Singh, K., Su, H.P., Klein, M.M., Stowers, A.W., Saul, A.J., Long, C.A., Garboczi, D.N. (2006) The essential mosquito-stage P25 and P28 proteins from *Plasmodium* form tile-like triangular prisms. *Nat. Struct. Mol. Biol.* 13: 90-91.
- Saxena, A.K., Wu, Y., Garboczi, D.N. (2007) *Plasmodium* p25 and p28 surface proteins: potential transmission-blocking vaccines. *Eukaryot. Cell.* 6: 1260-1265.
- van Schaijk, B.C., van Dijk, M.R., van de Vegte-Bolmer, M., van Gemert, G.J., van Dooren, M.W., Eksi, S., Roeffen, W.F., Janse, C.J., Waters, A.P., Sauerwein, R.W. (2006) Pfs47, paralog of the male fertility factor Pfs48/45, is a female specific surface protein in *Plasmodium falciparum*. *Mol. Biochem. Parasitol.* 149: 216-222.
- Schmitz, S., Grainger, M., Howell, S., Calder, L.J., Gaeb, M., Pinder, J.C., Holder, A.A., Veigel, C. (2005) Malaria parasite actin filaments are very short. *J. Mol. Biol.* 349: 113-125.
- Schmitz, S., Schaap, I.A., Kleinjung, J., Harder, S., Grainger, M., Calder, L., Rosenthal, P.B., Holder, A.A., Veigel, C. (2010) Malaria parasite actin polymerization and filament structure. *J. Biol. Chem.* 285: 36577-36585.
- Scholz, S.M., Simon, N., Lavazec, C., Dude, M.A., Templeton, T.J., Pradel, G. (2008) PfCCp proteins of *Plasmodium falciparum*: gametocyte-specific expression and role in complement-mediated inhibition of exflagellation. *Int. J. Parasitol.* 38: 327-340.

- Schüler, H., Mueller, A.K., Matuschewski, K., 2005. Unusual properties of *Plasmodium falciparum* actin: new insights into microfilament dynamics of apicomplexan parasites. *FEBS Lett.* 579: 655-660.
- Seithel, A., Eberl, S., Singer, K., Auge, D., Heinkele, G., Wolf, N.B., Dörje, F., Fromm, M.F., König, J. (2007) The influence of macrolide antibiotics on the uptake of organic anions and drugs mediated by OATP1B1 and OATP1B3. *Drug Metab. Dispos.* 35: 779-786.
- Severini, C., Silvestrini, F., Sannella, A., Barca, S., Gradoni, L., Alano, P. (1999) The production of the osmiophilic body protein Pfg377 is associated with stage of maturation and sex in *Plasmodium falciparum* gametocytes. *Mol. Biochem. Parasitol.* 100: 247-252.
- Shavit, N., Dilley, R.A., San Pietro, A. (1968) Ion translocation in isolated chloroplasts. Uncoupling of photophosphorylation and translocation of K^+ and H^+ ions induced by Nigericin. *Biochemistry.* 7: 2356-2363.
- Sidén-Kiamos, I., Vlachou, D., Margos, G., Beetsma, A., Waters, A.P., Sinden, R.E., Louis, C. (2000) Distinct roles for pbs21 and pbs25 in the in vitro ookinete to oocyst transformation of *Plasmodium berghei*. *J. Cell Sci.* 113: 3419-3426.
- Sidén-Kiamos, I., Pinder, J.C., Louis, C. (2006) Involvement of actin and myosins in *Plasmodium berghei* ookinete motility. *Mol. Biochem. Parasitol.* 150: 308-317.
- Sidén-Kiamos, I., Ganter, M., Kunze, A., Hliscs, M., Steinbüchel, M., Mendoza, J., Sinden, R.E., Louis, C., Matuschewski, K. (2011) Stage-specific depletion of myosin A supports an essential role in motility of malarial ookinetes. *Cell Microbiol.* 13: 1996-2006.
- da Silva-Nunes, M., Ferreira, M.U. (2007) Clinical spectrum of uncomplicated malaria in semi-immune Amazonians: beyond the " symptomatic " vs " asymptomatic " dichotomy. *Mem. Inst. Oswaldo Cruz.* 102: 341-347.
- Silvestrini, F., Alano, P., Williams, J.L. (2000) Commitment to the production of male and female gametocytes in the human malaria parasite *Plasmodium falciparum*. *Parasitology* 121: 465-471.
- Silvestrini, F., Bozdech, Z., Lanfrancotti, A., Di Giulio, E., Bultrini, E., Picci, L., Derisi, J.L., Pizzi, E., Alano, P. (2005) Genome-wide identification of genes upregulated at the onset of gametocytogenesis in *Plasmodium falciparum*. *Mol Biochem. Parasitol.* 143: 100-110.
- Simon, N. (2012) Molecular interactions of the malaria parasite *Plasmodium falciparum* during the sexual reproduction in the mosquito midgut. PhD thesis, University of Würzburg, Würzburg.

- Simon, N., Scholz, S.M., Moreira, C.K., Templeton, T.J., Kuehn, A., Dude, M.A., Pradel, G. (2009) Sexual stage adhesion proteins form multi-protein complexes in the malaria parasite *Plasmodium falciparum*. *J. Biol. Chem.* 284: 14537-14546.
- Simon, N., Lasonder, E., Scheuermayer, M., Kuehn, A., Tews, S., Fischer, R., Zipfel, P.F., Skerka, C., Pradel, G. (2013) Malaria parasites co-opt human factor H to prevent complement-mediated lysis in the mosquito midgut. *Cell Host Microbe.* 13: 29-41.
- Sinden, R.E. (1982) Gametocytogenesis of *Plasmodium falciparum* *in vitro*: an electron microscopic study. *Parasitology* 84: 1-11.
- Sinden, R.E. (1983) Sexual development of malarial parasites. *Adv. Parasitol.* 22: 153-216.
- Sinden, R.E. (1999) *Plasmodium* differentiation in the mosquito. *Parassitologia* 41: 139-148.
- Sinden, R.E. (1998) Gametocytes and sexual development. In Sherman, I.W (Ed.): Malaria: parasite biology, pathogenesis and protection. *Am. Soc. Microbiol. Press* 1998: 25-48.
- Sinden, R.E. (2010) A biologist's perspective on malaria vaccine development. *Hum. Vaccin.* 6: 3-11.
- Sinden, R.E., Billingsley, P.F. (2001) *Plasmodium* invasion of mosquito cells: hawk or dove? *Trends Parasitol.* 17: 209-212.
- Sinden, R.E., Butcher, G.A., Billker, O., Fleck, S.L. (1996) Regulation of infectivity of *Plasmodium* to the mosquito vector. *Adv. Parasitol.* 38: 53-117.
- Singh, H., Parakh, A., Basu, S., Rath, B. (2011) *Plasmodium vivax* malaria: is it actually benign? *J. Infect. Public Health.* 4: 91-95.
- Smalley, M.E., Abdalla, S., Brown, J. (1981) The distribution of *Plasmodium falciparum* in the peripheral blood and bone marrow of Gambian children. *Trans. R. Soc. Trop. Med. Hyg.* 75: 103-105.
- Smith, T. F., Gaitatzes, C., Saxena, K. and Neer, E.J. (1999) The WD repeat: a common architecture for diverse functions. *Trends Biochem. Sci.* 24: 181-185
- Smith, T.G., Lourenco, P., Carter, R., Walliker, D., Ranford-Cartwright, L.C. (2000) Commitment to sexual differentiation in the human malaria parasite, *Plasmodium falciparum*. *Parasitology* 121: 127-133.
- Sologub, L., Kuehn, A., Kern, S., Przyborski, J., Schillig, R., Pradel, G. (2011) Malaria proteases mediate inside-out egress of gametocytes from red blood cells following parasite transmission to the mosquito. *Cell Microbiol.* 13: 897-912.

- Staines, H.M., Powell, T., Thomas, S.L., Ellory, J.C. (2004) *Plasmodium falciparum*-induced channels. *Int. J. Parasitol.* 34: 665-673.
- Stephens, J.W.W., Christophers, S.R. (1908): The practical study of malaria, University Press of Liverpool, London.
- Stinchcombe, J.C., Bossi, G., Booth, S., Griffiths, G.M. (2001) The immunological synapse of CTL contains a secretory domain and membrane bridges. *Immunity* 15: 751-761.
- Stirnemann, C.U., Petsalaki, E., Russell, R.B., Müller, C.W. (2010) WD40 proteins propel cellular networks. *Trends Biochem. Sci.* 35: 565-574.
- Stokkermans, T.J., Schwartzman J.D., Keenan, K., Morrissette, N.S, Tilney, L.G., Roos, D.S. (1996) Inhibition of *Toxoplasma gondii* replication by dinitroaniline herbicides. *Exp. Parasitol.* 84: 355-370.
- Stowers, A., Carter, R. (2001) Current developments in malaria transmission-blocking vaccines. *Expert Opin. Biol. Ther.* 1: 619-728.
- Sturm, A., Amino, R., van de Sand, C., Regen, T., Retzlaff, S., Rennenberg, A., Krueger, A., Pollok, J.M., Menard, R., Heussler, V.T. (2006) Manipulation of host hepatocytes by the malaria parasite for delivery into liver sinusoids. *Science* 313: 1287-1290.
- Sturm, A., and Heussler, V. (2007) Live and let die: manipulation of host hepatocytes by exoerythrocytic *Plasmodium* parasites. *Med. Microbiol. Immunol.* 196: 127-133.
- Su, X.Z., Wu, Y., Sifri, C.D., Wellems, T.E. (1996) Reduced extension temperatures required for PCR amplification of extremely A+T-rich DNA. *Nucleic Acids Res.* 24: 1574-1575.
- Tachibana, M., Sato, C., Otsuki, H., Sattabongkot, J., Kaneko, O., Torii, M., Tsuboi, T. (2012) *Plasmodium vivax* gametocyte protein Pvs230 is a transmission-blocking vaccine candidate. *Vaccine.* 30: 1807-1812.
- Taechalertpaisarn, T., Crosnier, C., Bartholdson, S.J., Hodder, A.N., Thompson, J., Bustamante, L.Y., Wilson, D.W., Sanders, P.R., Wright, G.J., Rayner, J.C., Cowman, A.F., Gilson, P.R., Crabb, B.S. (2012) Biochemical and functional analysis of two *Plasmodium falciparum* blood-stage 6-cys proteins: P12 and P41. *PLoS One.* 7: e41937.
- Talman, A.M., Domarle, O., McKenzie, F.E., Ariey, F., Robert, V. (2004) Gametocytogenesis: the puberty of *Plasmodium falciparum*. *Malar. J.* 3: 24.
- Tanner, M.J. (1993) Molecular and cellular biology of the erythrocyte anion exchanger (AE1). *Semin. Hematol.* 30: 34-57.

- Tanner, M., Hommel, M., (2010) Towards malaria elimination—a new thematic series. *Malar. J.* 9: 24.
- Tardieux, I., Liu, X., Poupel, O., Parzy, D., Dehoux, P., Langsley, G. (1998) A *Plasmodium falciparum* novel gene encoding a coronin-like protein which associates with actin filaments. *FEBS Lett.* 441: 251-256.
- Tate, S.S., Yan, N., Udenfriend, S. (1992) Expression cloning of a Na(+)-independent neutral amino acid transporter from rat kidney. *Proc. Natl. Acad. Sci. U.S.A.* 89: 1-5.
- Tatem, A.J., Smith, D.L., Gething, P.W., Kabaria, C.W., Snow, R.W., Hay, S.I. (2010) Ranking of elimination feasibility between malaria-endemic countries. *Lancet* 376: 1579–1591.
- Tavares, J., Formaglio, P., Thiberge, S., Mordelet, E., Van Rooijen, N., Medvinsky, A., Ménard, R., Amino, R. (2013) Role of host cell traversal by the malaria sporozoite during liver infection. *J. Exp. Med.* 210: 905-915.
- Templeton, T.J., Kaslow, D.C. (1999) Identification of additional members define a *Plasmodium falciparum* gene superfamily which includes *Pfs48/45* and *Pfs230*. *Mol. Biochem. Parasitol.* 101: 223-227.
- Templeton, T.J., Keister, D.B., Muratova, O., Procter, J.L., Kaslow, D.C. (1998) Adherence of erythrocytes during exflagellation of *Plasmodium falciparum* microgametes is dependent on erythrocyte surface sialic acid and glycophorins. *J. Exp. Med.* 187: 1599-1609.
- Templeton, T.J., Kaslow, D.C., Fidock, D.A. (2000) Developmental arrest of the human malaria parasite *Plasmodium falciparum* within the mosquito midgut via CTRP gene disruption. *Mol. Microbiol.* 36: 1-9.
- Templeton, T.J., Iyer, L.M., Anantharaman, V., Enomoto, S., Abrahante, J.E., Subramanian, G.M., Hoffman, S.L., Abrahamsen, M.S., Aravind, L. (2004) Comparative analysis of apicomplexa and genomic diversity in eukaryotes. *Genome Res.* 14: 1686-1895.
- Templeton, T.J., Enomoto, S., Chen, W.J., Huang, C.G., Lancto, C.A., Abrahamsen, M.S., Zhu, G. (2010) A genome-sequence survey for *Ascogregarina taiwanensis* supports evolutionary affiliation but metabolic diversity between a Gregarine and Cryptosporidium. *Mol. Biol. Evol.* 27: 235-248.
- Tewari, R., Dorin, D., Moon, R., Doerig, C., Billker, O. (2005) An atypical mitogen-activated protein kinase controls cytokinesis and flagellar motility during male gamete formation in a malaria parasite. *Mol. Microbiol.* 58: 1253-1263.

- Tews, S. (2011) Multimere Proteinkomplexe in den Sexualstadien von *Plasmodium falciparum*. Bachelor thesis, University of Würzburg, Würzburg.
- Thompson J, Janse CJ, Waters AP. (2001) Comparative genomics in *Plasmodium*: a tool for the identification of genes and functional analysis. *Mol. Biochem. Parasitol.* 118: 147-154.
- Thompson, J.K., Triglia, T., Reed, M.B., Cowman, A.F. (2001) A novel ligand from *Plasmodium falciparum* that binds to a sialic acid-containing receptor on the surface of human erythrocytes. *Mol. Microbiol.* 41: 47-58.
- Thompson RF, Langford GM. (2002) Myosin superfamily evolutionary history. *Anat. Rec.* 268: 276-289.
- Thomson, J.G.R.A. (1935) The structure and development of *Plasmodium falciparum* gametocytes in the internal organs and peripheral circulation. *Trans. R. Soc. Trop. Med. Hyg.* 29: 31-34.
- Thorens, B., Mueckler, M. (2010) Glucose transporters in the 21st Century. *Am. J. Physiol. Endocrinol. Metab.* 298: E141-145.
- Tibúrcio, M., Niang, M., Deplaine, G., Perrot, S., Bischoff, E., Ndour, P.A., Silvestrini, F., Khattab, A., Milon, G., David, P.H., Hardeman, M., Vernick, K.D., Sauerwein, R.W., Preiser, P.R., Mercereau-Puijalon, O., Buffet, P., Alano, P., Lavazec, C. (2012) A switch in infected erythrocyte deformability at the maturation and blood circulation of *Plasmodium falciparum* transmission stages. *Blood.* 119: e172-80.
- Tomas, A.M., Margos, G., Dimopoulos, G., van Lin, L.H., de Koning-Ward, T.F., Sinha, R., Lupetti, P., Beetsma, A.L., Rodriguez, M.C., Karras, M., Hager, A., Mendoza, J., Butcher, G.A., Kafatos, F., Janse, C.J., Waters, A.P., Sinden, R.E. (2001) P25 and P28 proteins of the malaria ookinete surface have multiple and partially redundant functions. *EMBO J.* 20: 3975-3983.
- Tonkin, C.J., van Dooren, G.G., Spurck, T.P., Struck, N.S., Good, R.T., Handman, E., Cowman, A.F., McFadden, G.I. (2004) Localization of organellar proteins in *Plasmodium falciparum* using a novel set of transfection vectors and a new immunofluorescence fixation method. *Mol. Biochem. Parasitol.* 137: 13-21.
- Trueman, H.E., Raine, J.D., Florens, L., Dessens, J.T., Mendoza, J., Johnson, J., Waller, C.C., Delrieu, I., Holders, A.A., Langhorne, J., Carucci, D.J., Yates, J.R., Sinden, R.E. (2004) Functional characterization of an LCCL-lectin domain containing protein family in *Plasmodium berghei*. *J. Parasitol.* 90: 1062-1071.
- Tyan, Y.C., Jong, S.B., Liao, J.D., Liao, P.C., Yang, M.H., Liu, C.Y., Klauser, R., Himmelhaus, M., Grunze, M. (2005) Proteomic profiling of erythrocyte proteins

- by proteolytic digestion chip and identification using two-dimensional electro-spray ionization tandem mass spectrometry. *J. Proteome Res.* 4: 748-757.
- Vale, R.D. (2003) The molecular motor toolbox for intracellular transport. *Cell* 112: 467-480.
- Vanderberg, J.P., Frevort, U. (2004). Intravital microscopy demonstrating antibody-mediated immobilisation of *Plasmodium berghei* sporozoites injected into skin by mosquitoes. *Int. J. Parasitol.* 34: 991-996.
- Vavricka, S.R., Van Montfoort, J., Ha, H.R., Meier, P.J., Fattinger, K. (2002) Interactions of rifamycin SV and rifampicin with organic anion uptake systems of human liver. *Hepatology.* 36: 164-172.
- Vera, I.M., Beatty, W.L., Sinnis, P., Kim, K. (2011) *Plasmodium protease* ROM1 is important for proper formation of the parasitophorous vacuole. *PLoS Pathog.* 7: e1002197.
- Vermeulen, A. N., Ponnudurai, T., Beckers, P.J., Verhave, J.P., Smits, M.A., Meuwissen, J.H. (1985) Sequential expression of antigens on sexual stages of *Plasmodium falciparum* accessible to transmission-blocking antibodies in the mosquito. *J. Exp. Med.* 162: 1460-1476.
- Vermeulen, A.N., van Deursen, J., Brakenhoff, R.H., Lensen, T.H., Ponnudurai, T., Meuwissen, J.H. (1986) Characterization of *Plasmodium falciparum* sexual stage antigens and their biosynthesis in synchronised gametocyte cultures. *Mol. Biochem. Parasitol.* 20: 155-163.
- Vincenzi, F.F. (1989) The Plasma Membrane Calcium Pump: The Red Blood Cell as a Model In: Agre, P., Parker, J.C. (Eds.). Red blood cell membranes: Structure, Function, Clinical implications. Dekker, New York, pp. 481–505.
- Vogel, G. (2010) The 'do unto others' malaria vaccine. *Science* 328: 847-848.
- Volkman, K., Pfander, C., Burstroem, C., Ahras, M., Goulding, D., Rayner, J.C., Frischknecht, F., Billker, O., Brochet, M. (2012) The alveolin IMC1h is required for normal ookinete and sporozoite motility behaviour and host colonisation in *Plasmodium berghei*. *PLoS One.* 7: e41409.
- Wagner, C., Scholz, S.M., Abreu, A., Frank, R. (2006) Molecular interactions between PfCCP multiadhesion proteins during gametogenesis in *Plasmodium falciparum*. *11th Int. Congress of Parasitology. – ICOPA XI:* 631-635.
- Wallace, L.J., Candlish, D., De Koning, H.P. (2002) Different substrate recognition motifs of human and trypanosome nucleobase transporters. Selective uptake of purine antimetabolites. *J. Biol. Chem.* 277: 26149-26156.

- Waller, R.F., Keeling, P.J., van Dooren, G.G., McFadden, G.I. (2003) Comment on 'A green algal apicoplast ancestor'. *Science* 301: 49.
- Wesseling, J.G., Smits, M.A., Schoenmakers, J.G. (1988) *Extremely diverged actin proteins in Plasmodium falciparum*. *Mol. Biochem. Parasitol.* 30: 143-153.
- Wesseling, J.G., Snijders, P.J., van Someren, P., Jansen, J., Smits, M.A., Schoenmakers, J.G. (1989) Stage-specific expression and genomic organization of the actin genes of the malaria parasite *Plasmodium falciparum*. *Mol. Biochem. Parasitol.* 35: 167-176.
- Wirth, C.C., Pradel, G. (2012) Molecular mechanisms of host cell egress by malaria parasites. *Int. J. Med. Microbiol.* 302: 172-178.
- White, N.J. (2008) *Plasmodium knowlesi*: the fifth human malaria parasite. *Clin. Infect. Dis.* 46: 172-173.
- Wickham, M.E., Culvenor, J.G., and Cowman, A.F. (2003) Selective inhibition of a two-step egress of malaria parasites from the host erythrocyte. *J. Biol. Chem* 278: 37658–37663.
- Williamson, K.C., Keister, D.B., Muratova, O., Kaslow, D.C. (1995) Recombinant *Pfs230*, a *Plasmodium falciparum* gametocyte protein, induces antisera that reduce the infectivity of *Plasmodium falciparum* to mosquitoes. *Mol. Biochem. Parasitol.* 75: 33-42.
- Williamson, K.C., Fujioka, H., Aikawa, M., Kaslow, D.C (1996) Stage-specific processing of *Pfs230*, a *Plasmodium falciparum* transmission-blocking vaccine candidate. *Mol. Biochem. Parasitol.* 78: 161-169.
- Willmann, M., Ahmed, A., Siner, A., Wong, I.T., Woon, L.C., Singh, B., Krishna, S., Cox-Singh, J. (2012) Laboratory markers of disease severity in *Plasmodium knowlesi* infection: a case control study. *Malar. J.* 11: 363.
- Winter, G., Kawai, S., Haeggström, M., Kaneko, O., von Euler, A., Kawazu, S., Palm, D., Fernandez, V., Wahlgren, M. (2005) SURFIN is a polymorphic antigen expressed on *Plasmodium falciparum* merozoites and infected erythrocytes. *J. Exp. Med.* 201: 1853-1863.
- Wirth, C.C., Pradel, G. (2012) Molecular mechanisms of host cell egress by malaria parasites. *Int. J. Med. Microbiol.* 302: 172-178.
- Wu, Y., Ellis, R.D., Shaffer, D., Fontes, E., Malkin, E.M., Mahanty, S., Fay, M.P., Narum, D., Rausch, K., Miles, A.P., Aebig, J., Orcutt, A., Muratova, O., Song, G., Lambert, L., Zhu, D., Miura, K., Long, C., Saul, A., Miller, L.H., Durbin, A.P. (2008) Phase 1 trial of malaria transmission blocking vaccine candidates Pfs25 and Pvs25 formulated with montanide ISA 51. *PLoS One.* 3: e2636.

- Wu, X.H., Chen, R.C., Gao, Y., and Wu, Y.D. (2010) The effect of Asp-His-Ser/Thr-Trp tetrad on the thermostability of WD40-repeat proteins. *Biochemistry* 49: 10237-10245.
- World Health Organization. (2000) Severe falciparum malaria. World Health Organization, Communicable Diseases Cluster. *Trans R Soc Trop Med Hyg* 94 (Suppl 1): S1–S90.
- World Health Organization. (2012a) World malaria report 2012. World Health Organization
http://www.who.int/malaria/publications/world_malaria_report_2012/wmr2012_full_report.pdf.
- World Health Organization. (2012b) Malariamapr: http://gamapserver.who.int/mapLibrary/Files/Maps/malaria_003.jpg, accessed on 17.04.2013.
- Wu, Y., Sifri, C.D., Lei, H.H., Su, X.Z., Wellem, T.E. (1995) Transfection of *Plasmodium falciparum* within human red blood cells. *Proc. Natl. Acad. Sci. U.S.A.* 92: 973-977.
- Wu, Y. (2008) Transfection of *Plasmodium falciparum* within human red blood cells. In: Moll, K., Ljungström, I., Perlmann, H., Scherf, A., Wahlgren, M. (Eds.) *Methods in Malaria Research*. MR4 / ATCC Manassas, Virginia, pp. 267-271.
- Xu C, Min J. (2011) Structure and function of WD40 domain proteins. *Protein Cell*. 2: 202-214.
- Yeoh, S., O'Donnell, R.A., Koussis, K., Dluzewski, A.R., Ansell, K.H., Osborne, S.A., Hackett, F., Withers-Martinez, C., Mitchell, G.H., Bannister, L.H., Bryans, J.S., Kettleborough, C.A., Blackman, M.J. (2007) Subcellular discharge of a serine protease mediates release of invasive malaria parasites from host erythrocytes. *Cell* 131: 1072-1083.
- Yeoman, J.A., Hanssen, E., Maier, A.G., Klonis, N., Maco, B., Baum, J., Turnbull, L., Whitchurch, C.B., Dixon, M.W., Tilley, L. (2011) Tracking Glideosome-associated protein 50 reveals the development and organization of the inner membrane complex of *Plasmodium falciparum*. *Eukaryot. Cell*. 10: 556-564.
- Yu, L., Gaitatzes, C., Neer, E., Smith, T.F. (2000) Thirty-plus functional families from a single motif. *Protein Sci*. 9: 2470–2476.
- Yuda, M., Sakaida, H., Chinzei, Y. (1999) Targeted disruption of the *Plasmodium berghei* CTRP gene reveals its essential role in malaria infection of the vector mosquito. *J. Exp. Med.* 190: 1711–1716.

8 Appendix

8.1 Vector maps

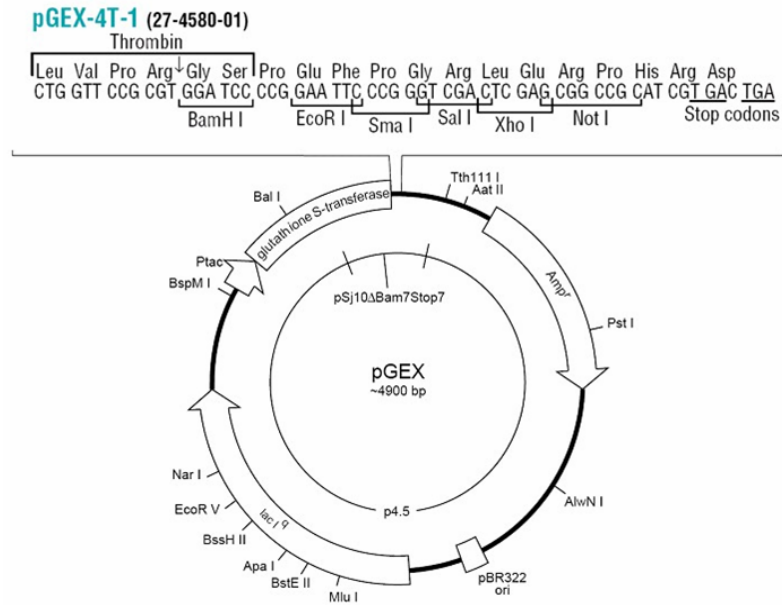


Fig. 8.1: Vector map of the expression vector pGEX-4T-1 used for the generation of GST fusion proteins.

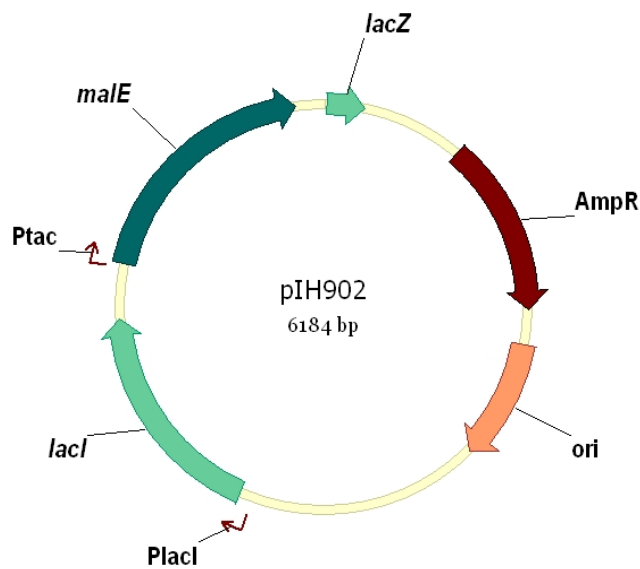


Fig. 8.2: Vector map of the expression vector pIH902 used for the generation of MBP fusion proteins (vector kindly provided by Prof. Kim Williamson, Chicago).

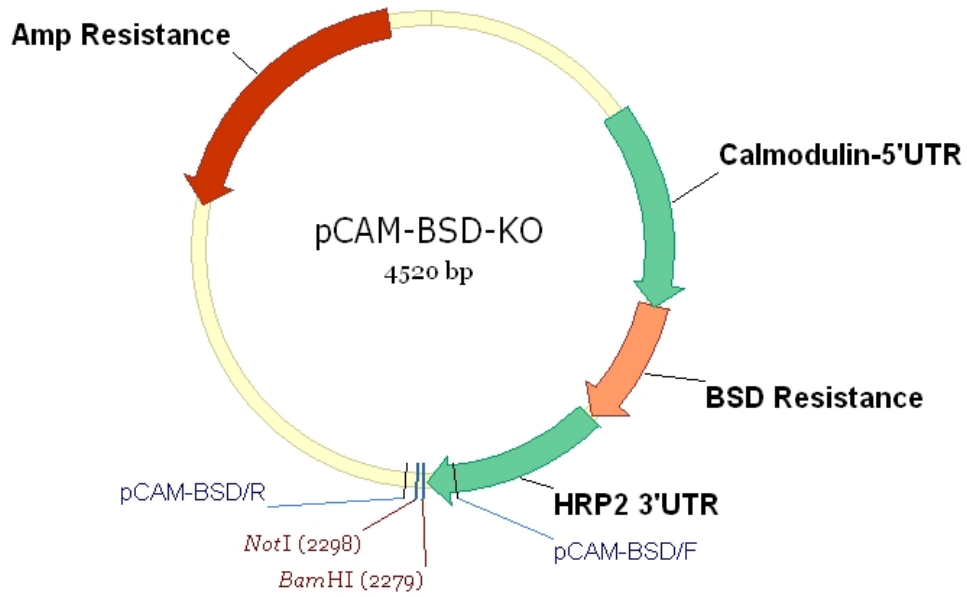


Fig. 8.3: Vector map of the vector pCAM-BSD (kindly provided by Prof. Christian Doerig, Melbourne).

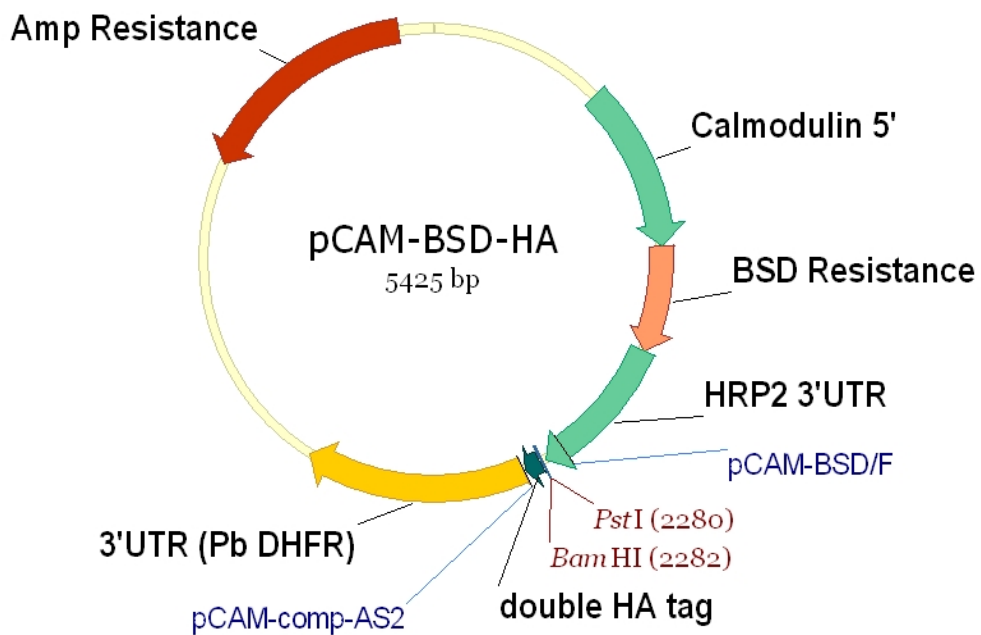


Fig. 8.4: Vector map of the vector pCAM-BSD-HA (kindly provided by Prof. Christian Doerig, Melbourne).

8.2 Substances employed in exflagellation assays

Tab. 8.1: Previously described inhibitors of transport pathways were tested on their potential influence on XA uptake by RBCs. The inhibitors were applied directly to gametocyte cultures during exflagellation assays (iRBCs). Secondly, non-infected RBCs were incubated with inhibitor and XA and the subsequently obtained XA-RBCF was tested in exflagellation assays (niRBCs). Thirdly, XA uptake by RBCs in the presence of XA was measured via LC/ESI/MS/MS.

Inhibitor	Target	Conc. Stock	Solvent	Concentration used			Concentration literature	Reference
				iRBCs	niRBCs	LC/MS/MS		
Adenine	hFNT1	148 mM	0.5 M HCl/PBS	1-2 mM	1 mM	–	0.1-3 mM	Domin <i>et al.</i> , 1988; Wallace <i>et al.</i> , 2002; Mahony <i>et al.</i> 2004
Hypoxanthine	hFNT1	10 mM	PBS*	1 mM	1 mM	–	1 mM	Mahony <i>et al.</i> 2004
NBTI	hENT1	10 mM	DMSO	0.005 mM	0.005 mM	–	0.001- 0.004 mM	Plagemann and Woffedin, 1988; Mahony <i>et al.</i> 2004
L-Leu	System L	20 mM	ICM	2 mM	–	2-10 mM	1 mM	Tate <i>et al.</i> 1992
	Non-saturable uptake of L-Trp			–	–	30-50 mM	30-50 mM	Lopez-Burillo <i>et al.</i> , 1985
L-Phe	System L/ System T	10 mM	ICM	2 mM	–	0.01-25 mM	10 mM	Lopez-Burillo <i>et al.</i> , 1985
L-Trp	System T	10 mM	ICM	2 mM	–	0.01-25 mM	2 mM	Lopez-Burillo <i>et al.</i> , 1985
Cytochalasin B	GLUT1/ GLUT5	20 mM	Ethanol	–	–	0.5-10 mM	0.0001-0.1 mM	Concha <i>et al.</i> , 1997; Kasahara <i>et al.</i> , 2009
Rifampicin	OATP	50 mM	DMSO	0.1-0.5 mM	0.5 mM	–	0.01-0.1 mM	Vavricka <i>et al.</i> , 2002
Erythromycin	OATP	50 mM	Ethanol	0.2-0.5 mM	0.5 mM	–	0.00001-1 mM	Seithel <i>et al.</i> , 2006

*Hypoxanthine was solubilized by heating of powder in PBS at 90°C

Tab. 8.2: Substances applied in exflagellation assays and their previously described effect.

Substance	Effect	Conc. Stock	Solvent	Conc. used	Conc. literature	Reference
BABTA-AM	Ca ²⁺ chelator, inhibition of Gc egress	10 mM	DMSO	25 µM	100 µM	Billker <i>et al.</i> , 2004; McRobert <i>et al.</i> , 2008
Chymotrypsin	proteolysis of band 3, inhibition of NPP	20 mg/ml	1 mM HCl/ 2 mM CaCl ₂	3 mg/ml	0.2-2 mg/ml	Baumeister <i>et al.</i> , 2006
Nigericin	egress of <i>T. gondii</i> from host cell	10 mM	Methanol	5-100 µM	2-10 µM	Fruth and Arrizabalaga, 2007
Proteinase K	digestion of glyco-phorin A, B, C	1 mg/ ml	PBS	500 µg/ml	6.7- 66.7 µg/ml	Poole <i>et al.</i> , 1996; Thompson <i>et al.</i> , 2001

8.3 Parameters used in LC/ESI/MS/MS analyses

Tab. 8.3: Parameters for HPLC and mass spectrometry.

HPLC Parameter	Specification
Column	Synergi MAX-RP 50 x 2.0 mm 4 μ m
Mobile Phase	A: 0.1 % Formic acid
	B: Acetonitrile
Flow rate	0.6 ml/min
Gradient	2.5–25 % B, 0–4 min (chromatography)
	100 % B, 4–6 min (rinsing of column)
	2.5 % B, 6–10 min (re-equilibration)
Injection volume	20 μ l
Column thermostat	30°C

MS Parameter	Specification
Source	ESI
Polarity	positive
Dry gas temperature	300°C
Dry gas flow	8.0 l/min
Nebulizer	45 psi
Capillary voltage	3500 V
Sheat gas temperature	300°C
Sheat gas flow	10.0 l/min
Nozzle voltage	500 V
Quad temperature	100°C
Scan type	MRM

Tab. 8.4: Parameters for detection of analytes.

Time Segment	Time (min)	Valve	Delta EMV (V)	Compound	Precursor Ion (m/z)	Product Ions (m/z)	Fragmentor Voltage (V)	Collision Energy (V)
1	0.0	to waste	–	–	–	–	–	–
2	2.0	to MS	100	XA	206.1	160.0 ^a	110	17
				XA	206.1	132.0 ^b	110	29
				KA (IS)	190.1	144.0 ^a	100	17
				KA (IS)	190.1	89.0 ^b	100	45
3	4.0	to waste	–	–	–	–	–	

a, quantifier ion, b, qualifier ion, IS, internal standard

8.4 Indirect IFAs investigating co-dependent expression

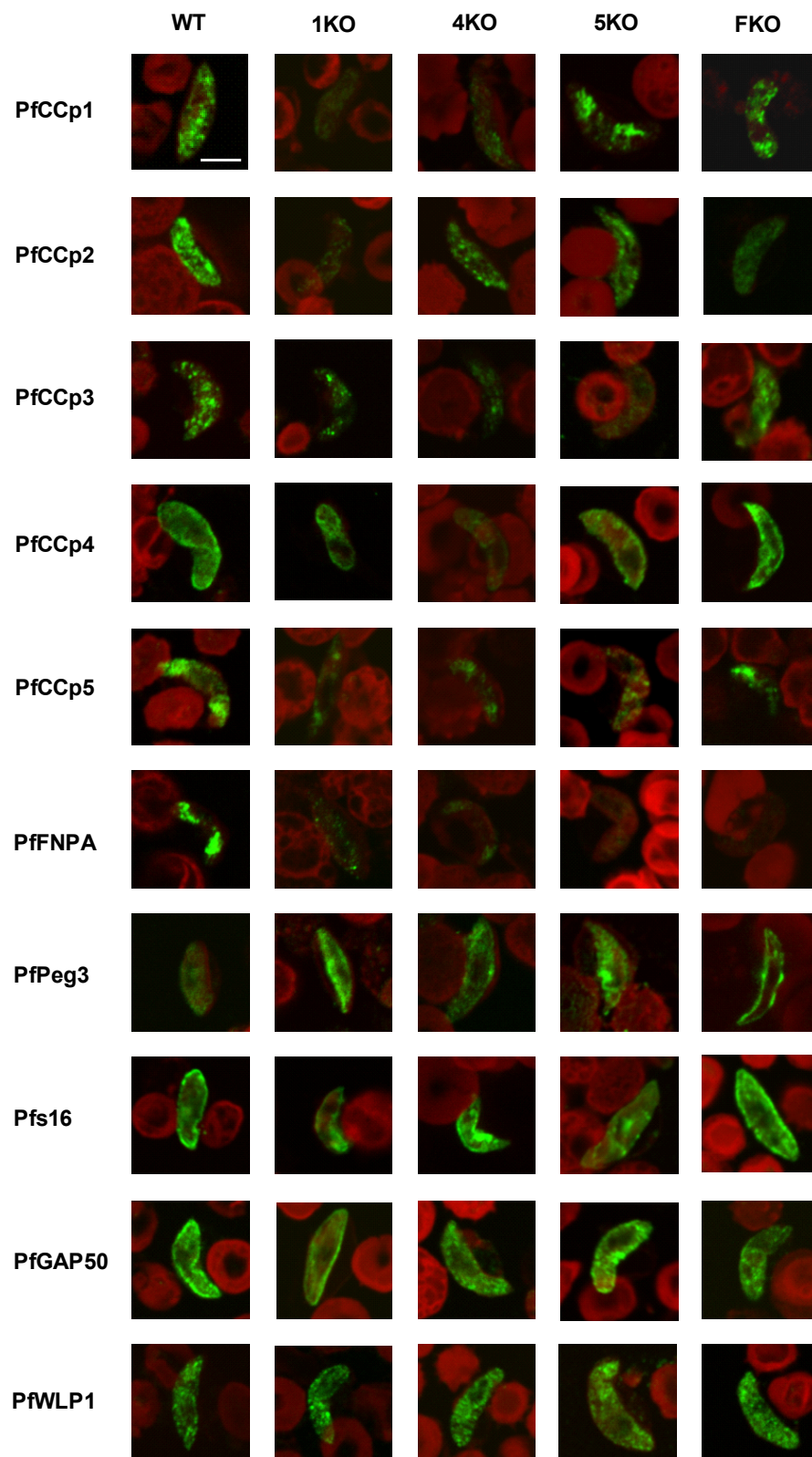
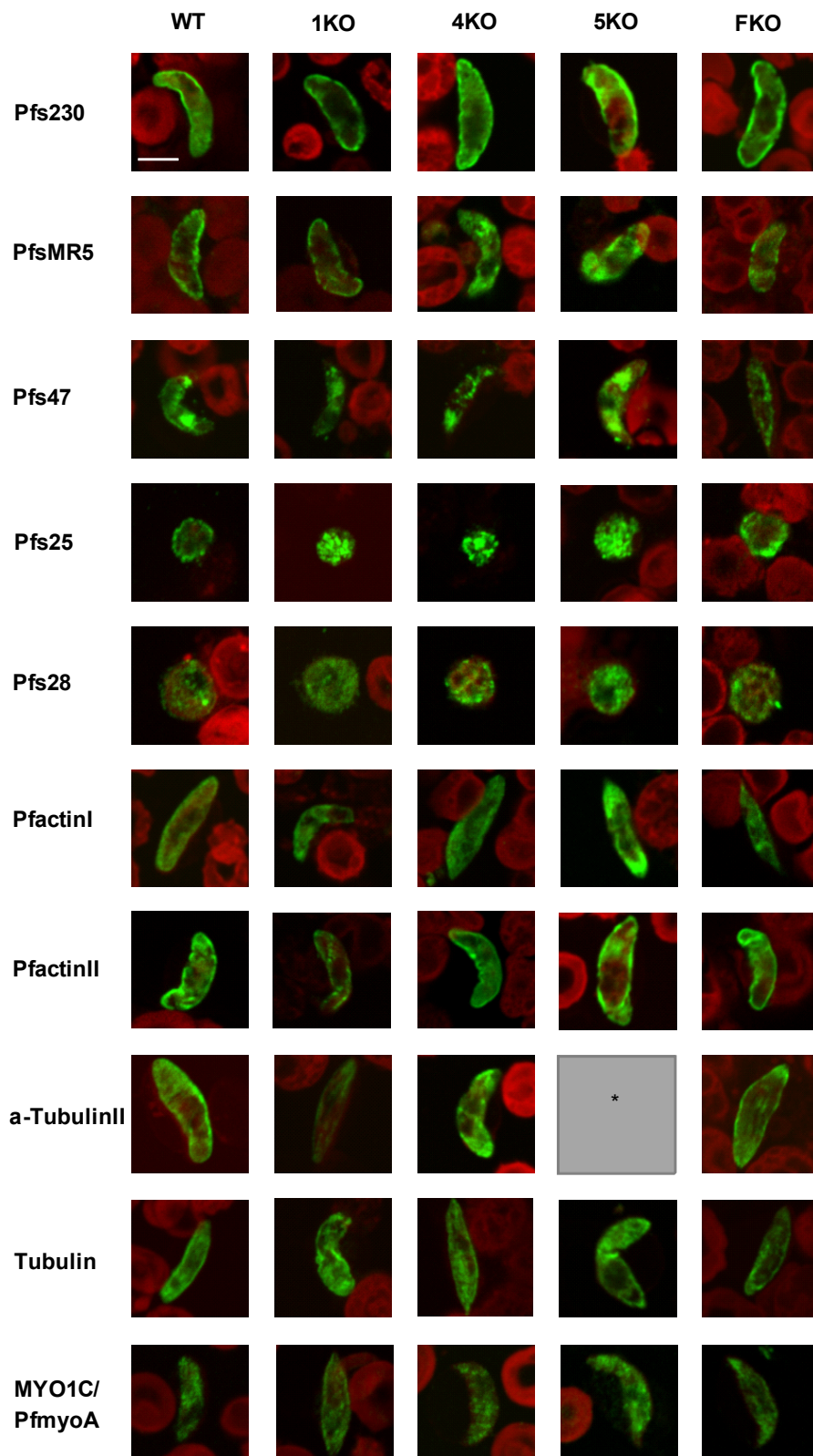


Fig. 8.5 (part 1)



* Combination was not investigated due to shortage of antiserum.

Fig. 8.5 (part 2)

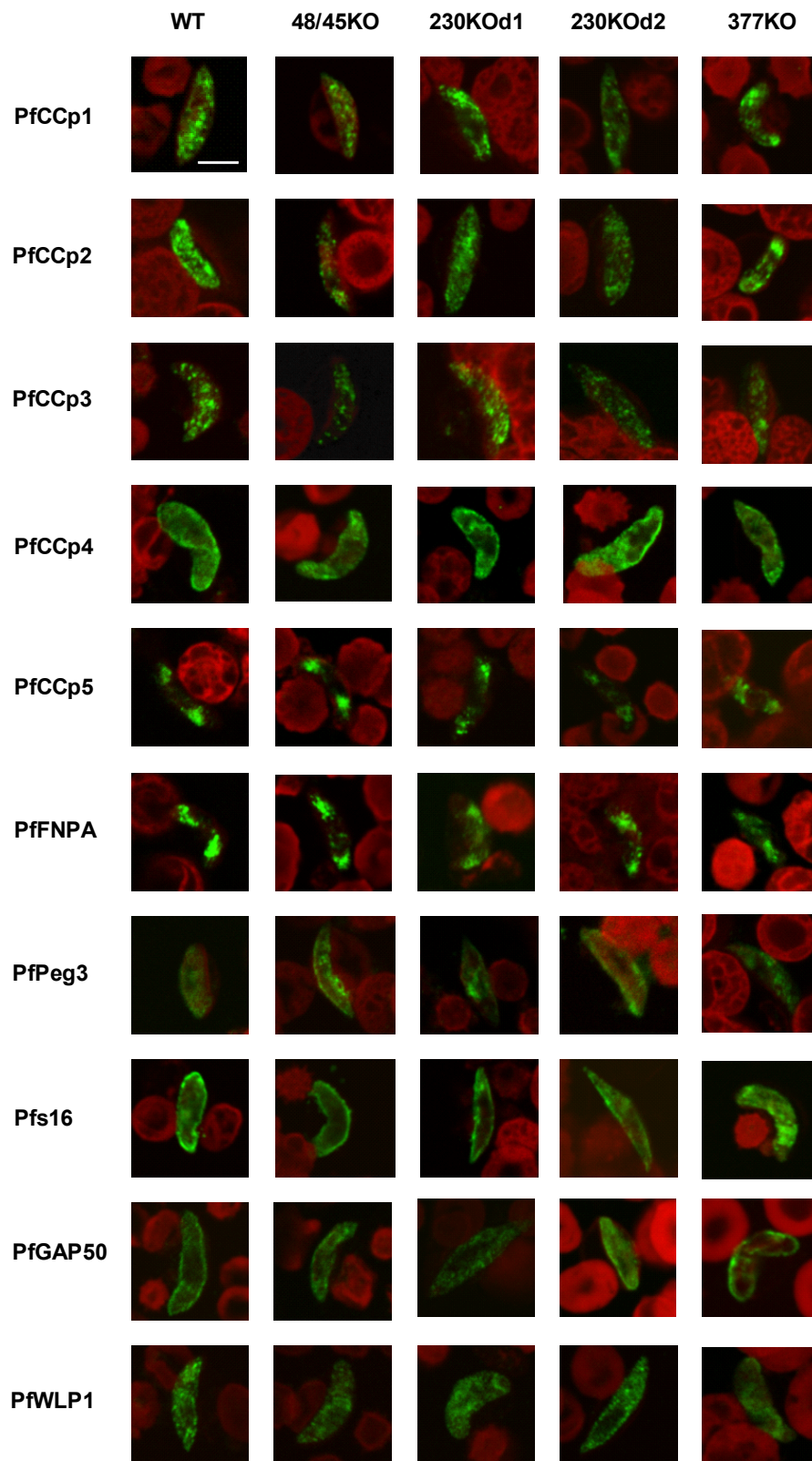


Fig. 8.5 (part 3)

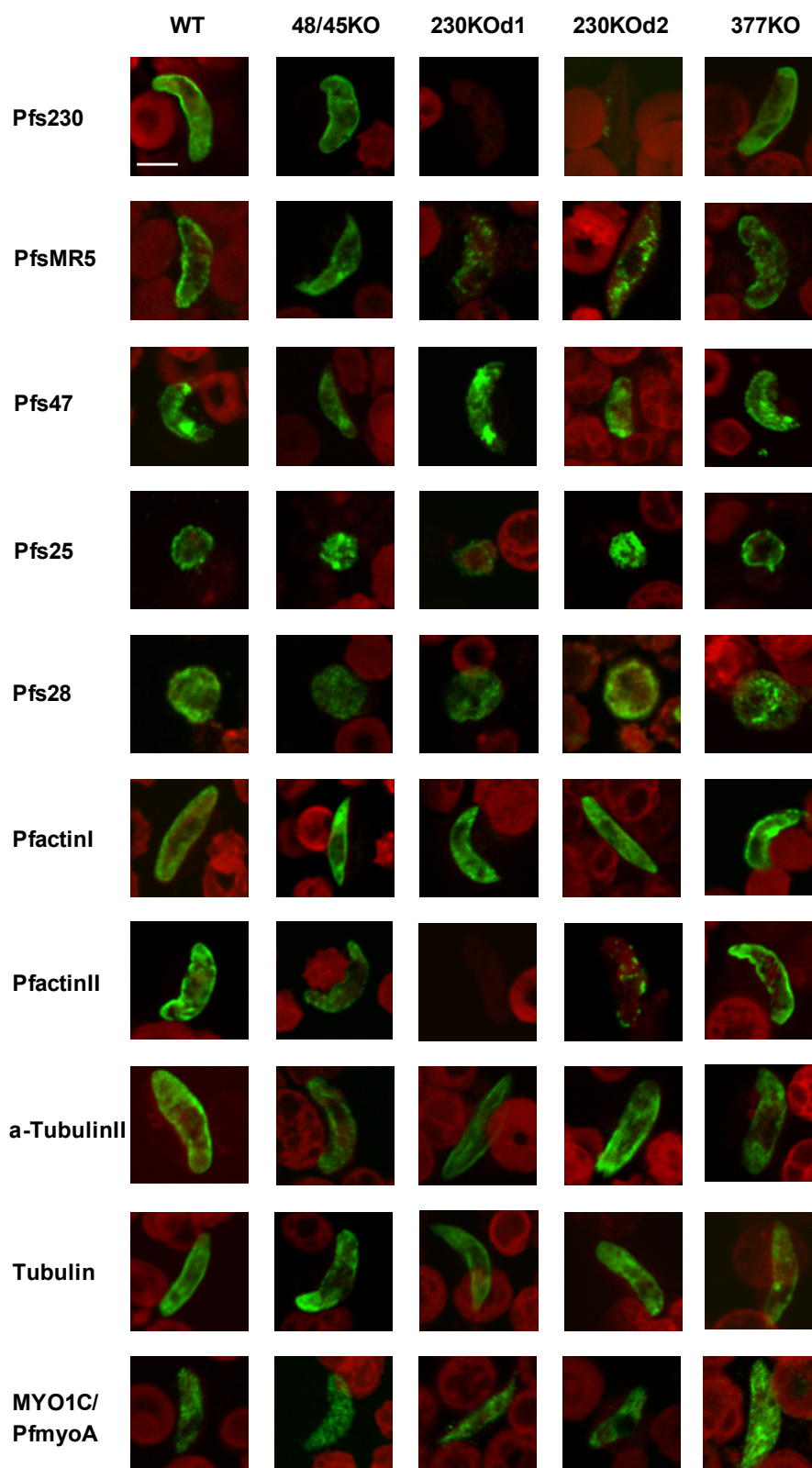


Fig. 8.5 (part 4): Indirect IFA investigating expression of 20 proteins in sexual stage parasites of eight gene-disruptant parasite lines. Genes of interest are labeled with Alexa Fluor-488, RBCs are counterstained with Evans Blue. 1KO, PfCCp1-KO, 4KO, PfCCp4-KO, 5KO, PfCCp5-KO, FKO, PfFNPA-KO, 48/45KO, Pfs48/45-KO, 230KOd1, Pfs230-KOd1, 230KOd2, Pfs230-KOd2, 377KO, Pfg377-KO, WT, wild-type Bar—4 μ m.

8.5 Abbreviations

aa	Amino acids
APAD	3-Acetylpyridine adenine dinucleotide
BAPTA-AM	1,2-Bis(2-aminophenoxy)ethane-N,N,N',N'-tetraacetic acid tetrakis(acetoxymethyl ester)
BCIP	5-Bromo-4-chloro-3-indolyl phosphate disodium salt
BSA	Bovine serum albumin
BSD	Blasticidin S
cGMP	Cyclic guanosine monophosphate
CIP	Calve intestinal phosphatase
Co-IP	Co-immunoprecipitation
DAG	Diacylglycerol
ddH ₂ O	Double-distilled water
dH ₂ O	Deionised water
DEPC	Diethylpyrocarbonate
Dipl.-Biol.	Diplombiologin
DIG	Digoxigenin
DNA	Deoxyribonucleic acid
dNTP	Deoxynucleotide
dsDNA	Double-stranded DNA
DTT	1,4-Dithiothreitol
Eds.	Editors
EDTA	Ethylenediaminetetraacetic acid
EGF	Epidermal growth factor
EGTA	Ethylene glycol tetraacetic acid
Epon	Epoxy resin
ER	Endoplasmatic reticulum
GlcNAc	N-Acetyl-D-glucosamin
GpA	Glycophorin A

GpC	glycophorin C
GPI	Glycosyl-phosphatidyl inositol
HA	Hemagglutinin
hENT1	Human equilibrative nucleoside transporter 1
HEPES	4-(2-Hydroxyethyl)piperazine-1-ethanesulfonic acid, N-(2-Hydroxyethyl)piperazine-N'-(2-ethanesulfonic acid)
hFNT1	Human facilitative nucleobase transporter 1
ICM	Incomplete medium
IFA	Immunofluorescence assay
IMC	Inner membrane complex
IPTG	Isopropyl- β -D-thiogalactopyranoside
IP ₃	Inositol 1,4,5-triphosphate
iRBC	Infected RBC
kDa	Kilodalton
KO	Knock-out
LB	Lysogeny broth
LCCL domain	Limulus coagulation factor C-like domain
LC/ESI/MS/MS	Liquid chromatography/ electrospray injection/ tandem mass spectrometry
MQH ₂ O	Milli-Q water
mRNA	Messenger RNA
NBT	Nitroblue tetrazolium
NBTI (NBMPR)	6-[(4-Nitrobenzyl)thio]-9- β -D-ribofuranosylpurine
NGS	Normal goat serum
niRBCs	Non-infected RBCs
NP-40	Nonidet™ P 40
NPP	New permeability pathways
OD	Optical density
p.a.	para analysum
p.act.	post activation

PAGE	Polyacrylamide gel electrophoresis
PBS	Phosphate buffered saline
PCR	Polymerase chain reaction
PDE	Phosphodiesterase
PFA	Paraformaldehyde
PIC	Protease inhibitor cocktail
PIP ₂	Phosphatidylinositol 4,5-bisphosphate
PI-PLC	Phosphoinositide phospholipase
PNK	Polynucleotide kinase
pp.	Pages
PPM	Parasite plasma membrane
PV	Parasitophorous vacuole
PVM	Parasitophorous vacuole membrane
RBC	Red blood cell
RBCM	Red blood cell membrane
RNA	Ribonucleic acid
rpm	Rounds per minute
RT	Room temperature
SD	Standard deviation
SDS	Sodium dodecyl sulphate
SOC	Super optimal broth with catabolite repression
spp.	species (plural)
Tab.	Table
TAE buffer	Tris-acetate-EDTA buffer
TBS	Tris buffered saline
TBSM	3 % milk powder in TBS
TBV	Transmission blocking vaccine
TEM	Transmission electron microscopy
TEMED	N,N,N',N'-Tetramethylethylenediamine

tRNA	transfer RNA
WHO	World Health Organization
XA	Xanthurenic acid
XA-RBCF	Filtrate of homogenized RBCs that had been incubated with XA and
XA-RBCH	Homogenized RBCs that had been incubated with XA followed by extensive washing

8.6 Curriculum Vitae

.....

.....

—

—

"

—

—

8.7 Acknowledgements

The present PhD study has been accomplished in the research group of PD Dr. Gabriele Pradel at the Research Center for Infectious Diseases, University of Würzburg from March 2008 to January 2012 and at the Institute for Molecular Biotechnology, RWTH Aachen University from February 2012 to July 2012.

I would like to acknowledge the following persons and institutions that contributed to completion of this PhD thesis:

First and foremost I would like to thank PD Dr. Gabriele Pradel for constant support and guidance during all those years in her lab. I am very grateful, for her taking time for discussions about the diverse projects of my thesis, which always have been helpful and resulted in new avenues. I am further grateful to her for not only enabling acquisition of laboratorial knowledge but also for many other scientific skills when attending courses, conferences and participating in scientific writing projects.

I am very grateful to my co-supervisors Prof. Dr. Klaus Brehm and Dr. Oliver Billker for fruitful discussions about my PhD projects that resulted in helpful ideas and suggestions that contributed to the successful completion of this work.

I thank Prof. Dr. Dr. h.c. mult. Jörg Hacker, Prof. Dr. Matthias Frosch, Prof. Dr. Jörg Vogel and Prof. Dr. Rainer Fischer for the possibility to accomplish my thesis at two very well-equipped institutes.

I would like to thank all former and present members of the Pradel lab for the great time working together. I especially thank Ludmilla for enabling such well organized work. I thank Matthias for his very helpful suggestions and advices. Thanks to Ludmilla, Nina and Selina for taking care of the animal work. I thank Nina, Selina and Andreas for proofreading of the thesis and for their suggestions. I would like to thank all the motivated undergraduate students who were working with me. Many thanks to all of you for all kinds of jokes and absurdities that are essential to survive the PhD work load and for helping out in diverse emergencies

Many special thanks to PD Dr. Matthias Unger and his PhD student Michael Völker who carried out the mass spectrometric analyses. I am grateful for all the helpful discussions unveiling new experimental possibilities.

I am grateful to Dr. Jude Przyborski for fruitful discussions and for providing antibodies.

I would like to thank Prof. Dr. Krohne and his team for the kind assistance with sample preparation for electron microscopy and for their technical support.

I am very grateful to all ZINF/IMIB members as well as all members of the Institute for Biotechnology for the nice atmosphere and good co-operation. I especially thank Hilke Merkert for support with IT and confocal microscopy and Josef Heger for fixing any kind of defect.

I would like to thank Dr. Stefano di Fiore of the Fraunhofer IME for assistance with confocal microscopy.

I would like to thank the BioMedTec International Graduate School of Science (BIGSS) coordinated by Prof. Paul Rösch and Dr. Stephan Schwarzinger for giving me the opportunity to get in contact with young, motivated scientist of Erlangen and Bayreuth and helpful discussion during reunions. Furthermore, I am very grateful for the financial support enabling the participation at the Molecular Parasitology Meeting in Woodshole, USA as well as my visit at Sanger Institute in Hinxton, UK.

I would like to thank the GSLS and its staff for administrative assistance and for their constant effort to provide a variety of courses mediating skills essential for a scientific career.

I am truly grateful to my friends and my family who supported me throughout the entire process of practical work and writing and who always believed in me. I especially thank my parents who did whatever possible to support me regardless the huge distance during writing of the thesis and who kindly agreed to accomplish printing and shipment of the thesis.

Finally I would like to thank everyone who contributed directly or indirectly to completion of this PhD thesis.